UNCLASSIFIED

AD NUMBER

AD887860

NEW LIMITATION CHANGE

TO

Approved for public release, distribution unlimited

FROM

Distribution authorized to U.S. Gov't. agencies and their contractors; Critical Technology; JUL 1971. Other requests shall be referred to Air5 Force Materials Lab., Wright-Patterson AFB, OH 45433.

AUTHORITY

AFML, per DTIC form 55

THIS PAGE IS UNCLASSIFIED

AFML-TR-71-38 Vol. I

AD888860

AD887860

MANUFACTURING PROCESS

FOR

SUPERALLOY CAST PARTS

Phase I—Fundamentals

AUTHOR
Bruce A. Heyer

ABEX CORPORATION

MAHWAH, NEW JERSEY

TECHNICAL REPORT AFML-TR-71-38 Vol. I
JULY 15, 1971

atter / T

AIR FORCE MATERIALS LABORATORY
AIR FORCE SYSTEMS COMMAND
WRIGHT-PATTERSON AIR FORCE BASE, OHIO

NOTICE

MANUFACTURING PROCESS

FOR

SUPERALLOY CAST PARTS

Phase I—Fundamentals

AUTHOR
Bruce A. Heyer

ABEX CORPORATION

MAHWAH, NEW JERSEY

TECHNICAL REPORT AFML-TR-71-38 Vol. I
JULY 15, 1971

This document is subject to special export controls and each transmittal
to foreign governments or foreign nationals may be made only with
prior approval of the Manufacturing Technology Division.

AIR FORCE MATERIALS LABORATORY
AIR FORCE SYSTEMS COMMAND
WRIGHT-PATTERSON AIR FORCE BASE, OHIO

FOREWORD

This Final Technical Report covers all work performed under Contract AF33(615)-2797 from 1 July 1965 to 31 December 1971. The manuscript was released by the author on 15 February 1971 for publication. This report is published in two volumes. Volume I covers the work performed in Phase I. Volume II covers the work performed in Phase II.

This contract with Abex Corporation Research Center, Mahwah, New Jersey, was initiated under Manufacturing Methods Project 8-297, "Manufacturing Methods for Superalloy Cast Parts." The initial work was performed under the technical direction of Lt. Agustin Lopez, and the remaining effort under the direction of Mr. William T. O'Hara, both of the Materials Processing Branch (AFML/LTP), Manufacturing Technology Division of the Air Force Materials Laboratory, Wright-Patterson Air Force Base, Ohio.

Work at the Abex Corporation Research Center was performed under the supervision of Dr. Hugo R. Larson, Director of Metallurgical Research, as Project Manager. Mr. Bruce A. Heyer, Research Metallurgist, was principal investigator for the program. Two major subcontractors supported the effort. The Flight Propulsion Division of General Electric Company was responsible for supplying the design and the testing of subscale and full-scale engine components manufactured under the program. This work was carried out under the supervision of Mr. H. J. Brands, Supervisor of Turbine Rotor Design, with the assistance of Mr. J. W. Heyser and Mr. W. Schweikert. LTV Aerospace Corporation, Vought Aeronautics Division, was responsible for the design of the cast airframe component. This work was carried out under the direction of Mr. G. W. Starr, Chief of Applied Research and Development, with the assistance of Mr. S. W. McClaren, Structures Design Engineer. This project was assigned Abex internal case number XC-1360. Volume I of this report has been given Abex internal report number XC-1360-9I. Volume II has been given number XC-1360-9II.

This project has been accomplished as part of the Air Force Manufacturing Methods Program, the primary objective of which is to implement, on a timely basis, manufacturing processes and techniques for use in economical production of USAF materials and components. The program encompasses the following technical areas:

Metallurgy   - Rolling, Forging, Extruding, Drawing, Casting, Powder Metallurgy, Composites

Chemical   - Propellants, Plastics, Textile Fibers, Graphite, Fluid & Lubricants, Elastomers, Ceramics

Electronic   - Solid State, Materials & Special Techniques, Thermionics

Fabrication   -   Forming, Material Removal, Joining, Components

Suggestions concerning additional Manufacturing Methods projects required on this or other projects will be appreciated.

This technical report has been reviewed and is approved.

George M. Glenn for

H. A. JOHNSON
Chief, Materials Processing Branch
Manufacturing Technology Division

ABSTRACT

This is Volume I of the final Technical Engineering Report covering Phase I of a two-phase program designed to establish procedures for the manufacture of large, high-integrity, superalloy castings with shipping weights near 100 pounds. Specifically, a main fin-beam structural component and a hollow, air cooled turbine rotor disc are to be produced during Phase II, with Phase I serving as the source of fundamental data required for their manufacture.

A literature survey covering the field of high-integrity and super-alloy castings is presented, and a survey of the current and future needs of the aerospace industry is used to document the need for the program.

Based on foundry characteristics and the mechanical properties and microstructure of separately cast specimens and specimens cut from cast components with section thickness up to 5 inches, alloy 713LC was selected from among 713LC, 718, and R-41 alloys for sub-scale spin testing and for the final components.

The methods of manufacturing a series of spin-test discs for evaluation of the alloy and process for the turbine rotor application are presented, together with the procedures adopted for overcoming a serious problem of residual stresses in the cast or heat treated disc.

The testing of the spin-test discs has established that the cast rotor can be designed using the same burst criterion as is currently used for forged discs.

The mechanical property minimums to which the air cooled turbine rotor disc will be designed are presented.

TABLE OF CONTENTS

TABLE OF CONTENTS (con't.)

LIST OF ILLUSTRATIONS

LIST OF ILLUSTRATIONS (con't).

ix

x

LIST OF ILLUSTRATIONS (cont.)

LIST OF ILLUSTRATIONS(con't.)

LIST OF TABLES

LIST OF TABLES (con't).

LIST OF TABLES (con't.)

I. INTRODUCTION

In recent years, significant strides have been made by the foundry industry toward meeting the requirements of cast components for aerospace application (1) high integrity, (2) precision, and (3) reproducibility of the first two categories. The products of the combined efforts of government and corporate sponsored research and development have come to be known as "Premium Quality" castings, and are well established in the fields of aluminum alloys and, more recently, high strength steels.

In the field of cast superalloy components, the greatest strides have been made by the manufacturers of small components for propulsion application. The progress in this area is exemplified by the technological advances in the casting of turbine buckets and blades, such as reproducible grain size control, controlled directional solidification, intricately cored hollow blades etc., together with a high degree of dimensional precision. These advances have been combined with vacuum melting and casting methods found to be a virtual necessity for the attainment of reproducibily high mechanical properties at room and elevated temperatures in the vast majority of superalloys.

Progress is equally evident in areas of alloy development for application at temperatures of 1800°F and higher. As the high temperature strength of these alloys increases, however, they become inherently more difficult to hot work and, as a result, the casting process moves closer to being the ideal method of fabrication. Other advantages of the casting process as compared to forging and machining are abundantly detailed in the literature and can be summarized by the recognition of the fact that casting is the shortest route from raw material to finished product. This factor takes on even greater significance as the complexity of the component increases.

Against this background, it is the purpose of the current program to develop methods for the manufacture of large superalloy castings with reproducibly high integrity and with dimensional tolerances within the category of "precision" castings. The size of the castings involved is in the category of 100 lbs. or somewhat larger, considering foundry shipping weight as the criterion. More specifically, the program considers two components for development as castings: (1) a full scale hollow, air cooled turbine disc with an operational aim temperature of 1000°F to 1200°F and (2) a full scale aircraft fin beam with an operational aim temperature of 1600°F. In order to place the end product of the program on a firm, realistic plane, the two components to be cast will be designed and tested by recognized manufacturers in the aerospace industry, the Flight

-1-

Propulsion Division of the General Electric Company and the Vought
Aeronautics Division of LTV Aerospace Corporation respectively.

The three nickel-base alloys, Inco 713C (or LC), Rene 41 and
IN-100, were originally specified for investigation in the program. Since
the initiation of the contract, IN-100 was dropped in favor of Inco 718
which is reported to exhibit more favorable mechanical properties (par-
ticularly ductility) in the temperature range of interest for turbine disc
application. While the superiority of IN-100 over Inco 718 at very high
temperatures is evident in the literature, it may be considered inferior
for operation in the lower temperature ranges due to an extremely
limited ductility.

With a choice of three alloys and an aim of two final components,
the program is divided into two major Phases. Phase I was devoted to
an alloy and methods evaluation together with a search of the appropriate
literature and a survey of the aerospace industry with regard to its
possible utilization of large, superalloy castings. Phase II was primarily
concerned with pilot production and testing of the fullscale cast components.

III. LITERATURE SURVEY

A. Castings for Aerospace - A General Discussion

While it is recognized that the current program is aimed at
the production of large, aircraft quality castings in nickel-base
superalloys, the dearth of literature on that subject not only testifies
to the originality of the effort, but also necessitates reviewing the
literature concerning similar castings in alloy or size categories
other than those specified. The most closely related field of endeavor
has been, for a number of years, the evolution of high integrity
steel castings for aircraft applications. Another area closely
related to the current effort, in a material and process sense, is that
of investment and ceramic shell cast superalloy components for hot
engine applications such as turbine buckets, etc. The component
size in this field is usually less than that of the turbine disc and
airframe components currently under consideration. The present
program may, in many respects, be considered an effort to marry
the technologies invloved in the production of large, precision, high
integrity steel castings and the concurrent manufacture of smaller,
investment cast superalloy components. It is for this reason that a
review of both fields was considered a necessary part of this program.

In 1952, Peterson [1] presented the view that the requirements of
the aircraft industry for sand castings were so small that they could
be met by sand foundry practice current at the time, and that the
prerequisites for the increased use of castings by the aircraft industry
were improved foundry techniques and greatly improved casting
reliability. Three years later, Papen [2] echoed this opinion by
venturing that airframe designers were making the optimum use of
castings and that further expansion of the use of castings in the air-
craft industries was dependent upon improved casting materials and
techniques. He also pointed out the need for high quality,
precision steel castings produced under greatly improved foundry
controls. In 1955, the largest investment casting in use in an
aircraft was 5 pounds, and the need for much larger precision
investment castings was recognized. [2] A complete summary of
the problem of precision cast steel components is provided by a
1956 report of the Materials Advisory Board of the National Academy
of Sciences. [3] Since 1956, a large number of articles and reports
have been published which attempt to detail the requirements of the
aerospace inductry and the foundry techniques necessary to fulfill
these requirements. While the approach of each of the authors frequently
differs, their conclusions are invariable similar. The following
represents a summary of these conclusions. (4-13)

  1. The need for cast components in engine and airframe
  fabrication is a current as well as a future one. Castings
  have the potential of solving many of the design problems

attendant to the increased complexity of components while, simultaneously, sharply reducing the high costs associated with machining extremely complex shapes unsuitable for forging. They have a potentially lucrative market in the aerospace field, providing their reliability can be thoroughly proven. (4, 6, 7, 8, 9, 13)

2. The requirements of a casting for aerospace application can be summarized as follows. (9)

   a. Accuracy and Precision of Configuration

   This requirement cannot be met by conventional casting techniques. Only through methods such as ceramic shell molding, or massive investment molding with permanent or disposable patterns can the required level be approached. Of particular value, it appears, is permanent pattern, massive investment molding. (4, 5, 9, 11, 12)

   b. Reproducibly High Integrity

   High integrity is undoubtedly the foremost requirement of a casting for application in space vehicles, airframes, or engines. It is this requirement which, by definition, obviates the presence of shrinkage or gas porosity, hot tears, and surface imperfections in critical areas. Equally important as the integrity itself, is the reproducibility of high integrity from casting to casting, and lot to lot. Inherent in this requirement are exceptionally stringent foundry controls over every phase of the casting process, from the designs and fabrication of the pattern to the final control inspection. (8, 9, 10) Inspection must go far beyond the normal procedures, particularly during pilot work but continuing on through the production stage. Destructive testing of castings on a statistical basis [13] should include microradiography, metallographic examination, and test specimens cut from specific areas where critical design criteria may dictate.

   c. Ability to Perform the Design Function

   Regardless of the amount of inspection and testing

which goes into the preparation of a casting, (or
any other fabrication) it is considered generally de-
dirable, wherever possible, to provide full scale
testing of the integral casting under conditions as
similar as possible to the final application. (6, 3)

d. Reliability of Delivery

The problem of delivery schedules is one which can
only be solved through the combined and cooperative
efforts of the aircraft buyer and the foundry supplier.
Too often, in the past, a casting has been ordered
only as a last resort when all other methods failed
and, as a result, unrealistic delivery times have
been required. (3, 9) The foundries are equally at
fault in this respect for accepting orders for high
integrity castings of difficult configurations without
insisting upon adequate lead time. Cooperation in
this area between the indistries can reduce the
problem to minor proportions. (10, 6)

3. Foundries must recognize that they cannot produce the
type of casting demanded by the aerospace industry with
ordinary casting techniques. An entirely new set of standards
is required, together with certain basic equipment and know-
ledge necessitated by the dimensional and high integrity re-
quirements of such castings. (3, 5, 8, 10)

4. On the other hand, the aerospace industry must recognize
the fallacy in the belief that a casting is a cheaper, weaker
substitute for a forged or machined part. A casting made to
the high standards required for aerospace applications will
seldom, if ever, be cheaper than a part fabricated by some
other means in original purchase price. (5, 8) Rather, the
advantage of a cast part appears dominant when one considers
the finishing required beyond the initial fabrication process.
Neither will a casting be significantly weaker than a forging
unless, by the nature of the alloy, the fundamental structure
developed by the casting process deviates considerably from
its forged counterpart, a reasonably rare circumstance. In
the opinion of many authors, the absence of anisotrophy in the
cast structure is a distinct design advantage, particularly
where complexity of shape is a factor. (10, 11)

Technological development in the findamentals of solidification
and in the manufacture of castings has, in recent years, placed in
the hands of the foundry industry the capability of meeting the demands

-6-

of the aerospace industry. M'.ding systems are now available which appear to be capable of producing the dimensional and surface finish control required. (3, 11, 15, 16, 17) Among these, the Shaw Process (15, 18) and other proprietary processes which involve the use of massive ceramic molds and permant patterns appear to show the greatest promise for the production of large steel and superalloy castings. The inorganic nature of these molds makes then of particular value for use in vacuum melting and pouring, found to be a fundamental necessity of the attainment of reliable properties in the majority of nickel-base and cobalt-base superalloys. (19, 20, 21)

The metal which goes into these molds has received the attention it deserves in recent years. Studies of the fundamentals of solidification (22, 23) as well as the more practical aspects of gating and risering of castings in specific alloys have been the subject of a large number of government, corporate and university sponsored research and development projects. Other subjects treated in recent literature which all bear on the problem of producing high integrity castings are grain refinement, (19, 24) the effects of unidirectional solidification, (14, 25, 26) and efforts to reduce to mathematical prodiction the complex variables associated with the casting process. (27, 28). Successful use of the knowledge gained by the foundry industry is evidenced by examples of actual production of high strength, high integrity steel castings. (29)

In summarizing the available literature in regard to the need for and the ability to produce large, high integrity castings, it appears apparent that both exist, and that the increased use of castings of this type in the aerospace industry depends, to a large extent, upon the degree of cooperation which can be attained between the aerospace and foundry industries.

Unlike the large castings, small, high integrity precision castings have been used in aircraft and space vehicle construction for many years. These castings, ranging in size from a few ounces to several pounds, are normally produced using disposable pattern materials (wax, plastic) and either monolithic investment molds or one of the more recently developed ceramic shell molding systems. (3, 30-34) Among the castings produced by these methods, the heat resistant alloys have received particular emphasis in the casting of engine components. In this area, significant strides have been made by the foundries toward dimensional accuracy and control of mechanical properties by contrdling grain size (34, 35, 19) and mode of solidification. (26) Freedom from the oxide films and high gas contents which originally plagued the attainment of uniform and reproducible properties in many of th.: superalloys has been obtained through vacuum melting and casting techniques. (36, 37, 21, 38, 20) Vacuum melting has also given the foundry a degree of control over final composition impossible to obtain using normal melting techniques.

-7-

Along with the improving technology in casting the superalloys, have come significant advances in the alloys themselves. New alloys capable of operating at higher engine temperatures are continually appearing. (39, 40, 41) Other alloys are being developed which have similar mechanical properties to existing alloys, but are intended to have better "castability" and thermal stability over long time exposures. (42) The difficulty in forging these materials due to their inherent hot strength, and the high cost of machining the, have made them particularly adaptable to casting as the most logical means of fabrication. (6, 26)

It is apparent that the requirements of the aerospace industries for small, high integrity, precision cast parts, particularly in the superalloys, have been met by one section of the foundry industry, the investment casting foundries. Obviously, continuing improvement of that technology is necessary if further developments in both industries are contemplated. (34)

As was pointed out previously, there appears to be a complete absence of literature on the subject of large superalloy castings. However, in 1959 and in 1962, respectively, two reports were issued which cited the need for such castings. (9, 12) If the difficulty of forging and machining of the superalloys is considered, and if the aerospace industry contemplates increases in complexity, as seems always to be the general trend, it appears that a real need for a program such as this one exists. It is the intent of the next section to determine the present and future requirements of the aerospace industry for such castings.

B.   Survey of Aerospace Manufacturers

In order to accurately determine the needs and requirements of the aerospace industry for large superalloy castings, both in the present and in the future, a survey of a significant cross section of engine, airframe and space vehicle manufacturers was conducted. As a first step, a letter of inquiry and questionnaire were sent to these manufacturers. The letter of inquiry and the questionnairre appear as Appendices i and ii at the end of this report.

A total of forty-nine inquiries were mailed to airframe, space vehicle, and engine manufacturers according to the distribution list which appears as Appendix (iii). In a number of cases, the distribution list includes several divisions of the same parent company. Of the forty-nine organizations surveyed, a total of 17 replies were received, representing about 35% response. Of these 17 replies, four are from engine manufacturers and the remaining thirteen are from airframe and space vehicle manufacturers. The following is a summary of the replies.

-8-

Question	Summary of Replies
1. Do you now utilize super-alloy castings?	Airframe: 13 No, 0 Yes Engine: 0 No, 4 Yes
a. Up to what size?	Airframe: - Engine: Up to 50 pounds.
b. What alloys?	Airframe: - Engine: Inco 713C, Inco 713LC, GMR 235, Udimet 500, HS 31, Hastelloy X, PDRL 162 and 163, Inco 718, Rene 41, X40.
c. In what applications?	Airframe: - Engine: Turbine wheels and nozzles, flanges, blades, vanes, shrouds, main bearing support housing, and other gas turbine components.
2. Do you utilize superalloy forgings?	Airframe: 12 No, 1 Yes Engine: 0 No, 4 Yes
a. Up to what size?	Airframe: Five Pounds. Engine: Up to 55 pounds.
b. What alloys?	Airframe: Inco 718 Engine: A286, D979, Rene 41, Udimet 700, Waspaloy, Inconel X 750, Inco 700, Inco 718.
c. In what applications?	Airframe: In areas adjacent to pro-pulsion units. Engine: Turbine discs, turbine blades, engine housing flanges, and other gas turbine components.
3. Can you envision applications for reliable superalloy cast-ings in the weight range of 1000 lbs. or higher?	Airframe: 6 No, 7 Yes Engine: 1 No, 1 Yes, 2 Yes, but in 50 to 100 lbs. category.
a. In what applications?	Airframe: Reentry vehicle primary structures, i.e., fuselage frame, wing pivots, rudder or elevator hinges, support fittings, primary beams.

		Others include thrust reverser frames, tail and engine support bulkheads for Mach 3 or higher sustained cruise vehicles.
	Engine:	Integral turbine wheels, nozzles, turbine casings, annular diffuser housings, flanges and shrouds, exhaust housings and rear main bearing supports; other applications might include cast parts for stationary power plants (non-aircraft).

b. At what service temperature?

Airframe: 1. 1000 to 1500°F
2. 1200 to 1700°F
3. -150 to 1800°F

Engine: 800 to 2000°F

c. In what environment?

Airframe: Oxidizing atmospheres, e.g. air.

Engine: Air and jet engine combustion products, e.g., oxidizing and sulphidizing atmospheres.

4. If an industrial capability for manufacturing large (100lb. and larger) superalloy castings was developed, would you envision an improved flexibility in high temperature service design?

Airframe: 4 No, 5 Yes, 4 No comment.
Engine: 3 Yes, 1 Possibly.

a. Would you consider redesigning existing superalloy forgings to any advantage?

Airframe: 5 No, 5 Yes, 3 No comment.
Engine: 0 No, 3 Yes, 1 No comment.

b. Assuming that reliability consistent with present requirements could be documented, would you consider large superalloy

Airframe: 4 No, 7 Yes, 2 No comment.
Engine: 0 No, 3 Yes, 2 No comment.
(2 of the "yes" answers were qualified to a casting weight of between 50 and 100 lbs.)

castings for future designs?

5. Please comment on your opinion of the future of large superalloy castings, assuming that a reliable industrial supply would become available in the future.

The comments concerning the future of large superalloy castings ranged from "very limited" to "definite and useful". For the most part, two major areas of usefulness were described; (1) propulsion systems and (2) hypersonic vehicles. Among the engine manufacturers, there appears to be a clear need for castings in a somewhat smaller weight category than 100 lbs. For example, one manufacturer suggested that castings in the 70 lb. category would have useful application in the near future. Another suggested that thin walled castings of high quality in the 25 to 50 lb. class would be of great interest. In most cases, emphasis was placed upon the need for quality or, in another definition, integrity as well as strength. Interestingly, none of the 17 respondents mentioned precision as a clear-cut requirement. Summarizing, the large majority of airframe and space vehicle manufacturers gave the opinion that there was no immediate future for large superalloy castings but that future craft designed for sustained hypersonic flight would introduce a market, the size of which would be determined by the properties of such castings when compared to forgings as well as the economic comparisons. Engine manufacturers, on the other hand expressed the general opinion that the need for superalloy castings for turbine discs etc. exists now, and that further development of the casting processes involved would be matched by increased use of these castings. The weight category, however, would be, presently, somewhat smaller than 100 pounds.

It appears obvious on the basis of the 17 replies the survey received thus far, that the development of procedures for the manufacture ot relatively large superalloy castings is a desirable end.

Two obvious sources of detailed information regarding the applicability of superalloy castings to engine and airframe design are the two sub-contractors involved in the program, Vought Aeronautics Division and the Flight Propulsion Division of the General Electric Company. The opinions of these two prominent manufacturers of engines and airframes match very closely the general tenor of the survey replies, i.e., the airframe manufacturer has no immediate application for large superalloy castings, but predicts a future for them in larger, hypersonic craft and reentry vehicles. The engine manufacturer considers the need for a cast turbine disc a very current and a very real need due, in particular, to increased complexity of design fostered by higher engine temperatures.

The industrial survey has apparently shown that both an immediate and long range need for superalloy cast parts of reasonably large sizes exists, and that it is up to the foundry industry to determine

-11-

whether these requirements can be met.

C. The Nickel-Base Superalloys, Their Physical Metallurgy and Mechanical Properties

While the current program is in the category of manufacturing process development, it is, nonetheless, necessary to obtain at least a working knowledge of the alloy systems under consideration. More specifically, it is necessary to gain some understanding of the physical metallurgy of the materials under investigation together with the mechanical properties to be expected under various conditions of testing. Toward this end, a substantial section of the literature survey being conducted for this program is in the area of the physical metallurgy and mechanical properties of the nickel-base superalloys, with particular emphasis on Inco 713C and LC, Rene 41, In 100, and Inco 718. Although In 100 has been dropped from the application stages of the program, the knowledge gained during the initial literature survey conducted prior to the change to Inco 718 is included for general information purposes.

(43) The nickel-base face-centered cubic atomic lattice typical of the alloys under study has considerable capacity to dissolve other elements and to hold them in solid solution. Some of this solubility is due to the direct substitution of the atoms of the solute element for the atoms of nickel. Chromium, added to this class of alloys in substantial amounts for corrosion resistance, is typical of this substantial type of solid solution. Other smaller atoms, such as carbon, can fit interstitially between the larger metallic atoms. Temperature has a profound controlling effect in determining whether such atoms are in or out of solution. Compound formation may also remove or cause rejection of certain atoms from the solid solution. These phenomena have powerful and important effects on the properties of the material. In a single phase, face-centered cubic matrix, the strengthening effect of other elements in solid solution is expected to be small, and, if the solute element is body-centered cubic by nature, it may have a weakening effect, even if no second phase is formed. Such is the case with chromium additions to the nickel-base alloys which while necessary to impart oxidation resistance, have a deleterious effect on high temperature properties. The major contribution to high temperature strength is made by precipitated phases, which are usually in the form of compounds.

Current theory of creep and plastic flow postulates that the slip or ductile behavior of alloys is due to movement of dislocations or imperfections in the otherwise regular geometrical arrangements of atoms in the lattice of the metallic crystals. If these dislocations are free to migrate under the influence of stress the metal deforms when such motion occurs. If a discrete particle is precipitated at the site of a dislocation, or if it blocks the motion of the dislocation along the plase of slip, there is a tendency to immobilize the

-12-

dislocation and thus prevent slip. This is perhaps oversimplified, but helps explain why very fine precipitates make a profound contribution to hot strength and creep resistance. This mechanism is usually referred to as "precipitation hardening". Even before a precipitating phase exists as a discrete particle, especially where both the solvent and the solute have the same crystal structure coherency or registry of the atomic lattices of the forming phase and the matrix cause atomic strain. This strain interferes with dislocation movement and thus the effect of a precipitating phase is evident before it can be seen with a microscope.

In these alloys this mechanism depends on solubility of the precipitating phase that changes with temperature. Simply stated, the phase or its ingredients are soluble at the high temperatures near the melting point of the alloy but at some lower temperatures the equilibrium phase volume exceeds the solubility in the matrix. At such lower temperature the solute can either remain in supersaturated solution or it can precipitate as a discrete phase. Since the sluggishness of the precipitation reaction depends on temperature, the thermal history of the alloy has a profound effect on the occurrence and the habit of the precipitating phase. Rapid cooling may maintain the supersaturated solution, and since at room temperature most of these alloys are too sluggish to permit reactions of this type the ambient temperature structure may be a clear austenite. Slower cooling or holding at an elevated temperature, where sluggishness does not restrain the reaction, can permit precipitation, as can reheating the supersaturated solution to a high enough temperature. Where this reheating is deliberate it is usually termed "aging".

The temperature at which precipitation occurs affects the size and number of the resultant particles. At a relatively high temperature they tend to be large and few, while at lower temperatures they are more numerous, smaller, and more potent in their strengthening effect.

If the form of the precipitate is modified by hot working, agglomerating the phase and producing fewer particles, or if a casting cools very slowly and thus precipitates the phases in coarse and relatively ineffective form the precipitation hardening mechanism may operate rather feebly. In such cases it is possible to redissolve the solute by a "solution heat treatment" at a suitably high temperature, cool rapidly, and then induce the desired fine precipitation by an aging treatment. This is the usual procedure for wrought high temperature alloys. While the lowest effective aging temperature may produce the greatest temporary strength, it is not advisable to age below the temperature of service, since time at the service temperature will tend to agglomerate the fine particles, reduce their number, and result in loss of some of their strengthening effect. This behavior is known as overaging.

-13-

Whereas for wrought alloys a solution heat treatment and aging may be necessary, for castings there are cases when either or both may be omitted. A rapidly cooled casting will hold the solute elements in solid solution and, aside from the fact that they will be somewhat sigregated in a dendritic solidification pattern, they can precipitate as expected. Also the first few hours or days of the service exposure may cause this precipitation. Only in case the distribution of the precipitated phase is unsatisfactory (from the as-cast status) is a special solution heat treatment considered necessary. Since it may be a cause of distortion of castings that have close dimensional tolerances this heat treatment stage should be avioded when feasible. Similarly the aging treatment is not necessary unless the alloy is too weak to properly withstand the service stresses for the time before service aging becomes effective. Aging, being at a lower temperature than solution, is less likely to cause distortion problems.

The intermetallic compound of the type Ni_3Al, also called the "gamma prime" phase, is especially effective for strengthening the nickel-base alloys and is a feature of all grades being included in this project. In the solid state this compound exists over a rather narrow range (about 3% variation in aluminum about the stoichiometric composition) in the pure nickel-aluminum alloys. (44, 45) The solid phase gamma prime is very close in composition to a eutectic at melting temperatures and there is some question about the exact behavior as an alloy in this composition range cools, solidifies, and perhaps reacts in the solid state. Floyd (46) investigated this, and concludes that the solid Ni_3Al phase is the product of a peritectic reaction between the melt and the beta NiAl phase that characterizes such alloys with slightly higher aluminum content than the gamma prime phase. Many of the nickel-base superalloys contain varying amounts of titanium, which may substitute for part of the aluminum in the Ni_3Al compound. (45) In alloys with high columbium contents as well as aluminum and titanium, the compound $Ni_3(Al, Ti, Cb)$ may be expected. (47, 48) Where the aluminum to titanium atomic ratio is such that less than three out of five aluminum atoms are replaced by titanium the precipitate on aging is the face-centered-cubic Ni_3Al phase. As the titanium content exceeds the solid solubility of both matrix and Ni_3Al, the precipitating phase will increase in amounts of the hexagonal phase, Ni_3Ti. Titanium rich gamma prime has been found to be superior for strengthening to either pure Ni_3Al or Ni_3Ti. (49)

Basically, Ni_3Al is an ordered face-centered-cubic structure in which the nickel atoms occupy the face centers and the aluminum atoms the cube corners, having a lattice parameter a=3.570 A. The effect of various alloying additions on the lattice parameter of the gamma prime precipitate has been studied by Guard and Westbrook. (50)

-14-

It is expected that the habit of the gamma prime phase and the effect of casting cooling rate on its behavior will play an important role in this project.

"The sigma Phase is a hard, brittle, intermetallic compound of complex structure which occurs in systems involving a body-centered cubic and a face-centered cubic transition metal. Apparently the phase is characterized by a constant number of (3d+4s) electrons per atom, calculated according to appropriate formulae. In addition, the difference in the atomic diameters of the two metals should be close to 8%, for if it is less, complete solid solution occurs, while if it is greater, compounds of simpler structure are formed. The crystal structure of the phase (in a large number of binary and ternary systems) has been indexed on the basis of a tetragonal cell having 30 atoms." (51) The lattice parameters of the tetragonal crystal structure of sigma are generally constant with a=8.80A and c=4.60A.

The most commonly occurring sigma phase appears in the iron-chromium system and generally forms from chromium rich ferrite, although it can also form from austenite.

Sigma appears in the cobalt-chromium (52) system in a range varying from approximately 56-to-61 at.pct.Cr., at temperatures ranging from about 1200°C to room temperature. However, the first precipitation of sigma occurs at 1310°C at 48 at.pct.Cr. A distinct sigma phase does not occur in either the molybdenum-chromium or the cobalt-molybdenum systems. It does appear in the molybdenum-cobalt-chromium isothermal ternary.

A sigma phase has been reported in IN-100 aged at 1600°F for 100 hours but is not present when specimens are aged at 1800°F for times up to 300 hours in the absence of stress. However, the presence of sigma in samples aged at 1800°F under stress, strongly suggests that this reaction is highly sensitive to slight variations in test conditions. Generally sigma nucleates at grain or second phase boundaries. In specimens aged under stress, the sigma phase appears either as an acicular distribution when present in small amounts, or as coarse Widmanstatten plates when present in large amounts. Cold work increases the amount of sigma present and extends the area of composition in which it develops. Increasing the nickel concentration decreases the temperature at which sigma forms and narrows the temperature range at which sigma is stable. (53) This phase generally has a damaging effect on the mechanical properties of heat resistant nickel base alloys.

-15-

The presence of columbium, titanium, vanadium, and chromium results in the precipitation of thermodynamically stable carbides. Iron, Nickel, Cobalt, and Molybdenum along with the previously mentioned potent carbide formers, result in the precipitation of complex carbides which may play some role in strengthening the alloys.

Inconel 713 C

This alloy was developed by the International Nickel Company and is covered by U. S. Patent No. 2,570,193. Inconel is an INCO registered trademark. The nominal composition and the ranges set for Aerospace Material Specification 5391 are:

Chemical Composition of Inconel 713C

C%	Mn%	Si%	Cr%	Co%	Mo%	Al%	Ti%	Cb=Ta%	Zr%	B%
0.08	0.25	0.50	12.0	1.0	3.8	5.5	0.50	1.8	0.05	0.005
0.20	max.	max.	14.0	max.	5.2	6.5	1.0	2.8	0.15	0.015

S%	Fe%	Cu%	Ni + Co%
0.015	2.5	0.50	remainder
max.	max.	max.	

This alloy is intended for use in the as-cast condition, therefore no heat treatment is specified. In rapidly cooled small castings most of the elements that contribute to precipitation hardening will be retained in solid solution at ambient temperature. Precipitation of carbides and intermetallic compounds (such as Ni_3 (Al, Ti) will occur at the service temperature or it may be induced by a deliberate aging treatment. As-cast INCO 713 exhibits a massive "white-etching" constituent which is probably massive "gamma prime", in the inter-dendritic regions. This "white etching" constituent is based on the binary eutectic $Ni + Ni_3Al$, although limit of solid solubility need not be exceeded to produce it. Further heat treatment can completely dissolve this eutectic, although incipient melting may be invloved. This micro constituent of eutectic composition can be absorbed into the solid solution phase which itself is, therefore, not completely saturated. The inclusion of Columbium, a potent carbide former, is a salient difference in comparison with Rene 41. It is likely that much of the carbon present will precipitate in the form of CbC, with excess Cb forming other compounds. With added columbium and less chromium this alloy may be less oxidation resistant that Rene' 41.

Heat treatments have been employed. Solution for two hours at 2150°F followed by aging at 1700°F (927.C) for 16 hours can increase the stress rupture life at 1700°F. However, if the aging treatment is omitted the rupture time at 1300°F (704°C) can be sharply reduced, though rupture time at 1700°F (927°C) is little affected.

By a comparison of the data included here, it will be recognized that Rene' 41 is considerably stronger than 713C at ambient temperature and that it maintains a superiority in short time strength up to about 1500°F (982°C).

The following values are presumably characteristic of IN-713C:

Temperature		Ultimate Tensile	Stress Rupture Properties PSI		
F°	C°	Strength PSI	100 hrs.	1000 hrs.	10000 hrs.
70	21	123,000			
1000	538	119,000-125,600			
1100	593				
1200	649	125,700			
1300	704				
1350			97000-90000	76000-83000	56000
1400	760	113,500-136,000			
1500	816	120,000-124,000	60,000	44,000	30000
1600	871	105,000-111,000	44000-42000	31000-28000	
1700	927	82,500- 90,000	30,000	18000-23000	12000
1800	982	68,400-72,000	20000-21000	15000-13000	
2000			6,400		

A more recent development is the low carbon grade of alloy 713C, designated as Inco 713LC. The alloy is chemically different only in carbon content (0.08 max.) and iron content. (less than 0.5%) Mechanical properties are reported to be somewhat improved over standard 713C alloy. (40)

IN 100

IN 100 was developed by the International Nickel Company and its composition ranges set by Aerospace Materials Specification 5397 are as follows:

				Chemical Composition of Superalloy IN-100					
C%	Mn%	Si%	Cr%	Co%	Mo%	Al%	Ti%	V%	Zr%
0.15	0.10	0.15	8.00	13.00	2.00	5.00	4.50	0.70	0.03
0.20	max.	max.	11.00	17.00	4.00	6.00	5.00	1.20	0.09

B%	S%	Fe%	Ti + Al%	Ni%
0.01	0.015	1.00	10.00	remainder
0.02	max.	max.		

This is intended for use as-cast. Compared with 713C it employs vanadium instead of columbium and has the highest level of titanium of the alloys under consideration.

-17-

The primary strengthening in this nickel base alloy is derived through the precipitation of gamma prime, most of which is a general precipitate and the remainder of which precipitates as large spherulitic particles located along the arms of the dendrites. There has been a tentative identification of a perovskite carbide $Ni_3(Ab, Ti)$ C within the massive $Ni_3(Al, Ti)$ particles. The solution of $Ti(C, N)$ and repreciptation of $M_{23}C_6$ begins at 1600°F but becomes more pronounced at a800°F. Only small amounts of M_6C are generally formed and these appear to be formed during solidification. The (Fe-Cr) sigma phase appears during aging at approximately 1600°F, in an acicular form and begins to nucleate at grain and phase boundaries. Stresses extend the range of sigma formation to 1800°F.

It is important to note that restrained castings are subject to hot tearing and that in such cases the zirconium and boron should be kept on the low side of the specification.

The following values are presumably characteristic of In-100:

Temperature		Ultimate Tensile	Rupture Strength PSI	
°F	°C	Strength PSI	100 hrs.	1000 hrs.
1000	538	158,400*		
70	21	147,100*		
1100	593			
1200	649	160,900*		
1300	704	142,900**		
1350		159,000*	88,000	77,000
1400	760	144,500**		
1500	816	144,300*	71,000	51,000
1600	871	110,400**	52,000	35,000
1700	921	106,600*	36,000*	24,000*
1800	982	69,100**	25,000	15,000
1900		63,800*	15,500*	8,400*

*Titanium addition 4.80 percent (as cast, vacuum melted, vacuum cast).
** " " 5.00-5.50

Rene' 41

Rene 41 was developed by the General Electric Company, and is covered by Aeronautical Materials Specification 5545, dated 1961, which includes the composition range in Table 1.

Chemical Composition Specification for Rene 41

C%	Mn%	Si%	Cr%	Ni%	Mo%	Ti%	Al%	Co%	B%	Fe%
0.12	0.10	0.50	18.00	bal	9.00	3.00	1.40	10.00	0.0030	5.00
max.	max.	max.	20.00		10.50	3.30	1.60	12.00	0.010	max.

$$\frac{S\%}{0.015}$$
max.

AMS 5545 is intended for sheet, strip and plate. Thus the material in its final form will have received considerable hot working. The processing details include heat treatment: Material shall be solution heat treated by heating to $1975°F \pm 25°F$, holding at heat at least for a minimum time based on 60 minutes per inch of thickness, followed by rapid cooling in air blast or quenching in oil or water.

There are two heat treatments usually suggested for use when dealing with René 41. The first (A) is designated to provide optimum short-time tensile properties while the second (B) is specified to provide optimum stress-rupture properties.

Heat treatment (A) invloves a solution treatment at $1950°F$ for 4 hours followed by air cooling plus a subsequent aging treatment at $1400°F$ for 16 hours followed by air cooling. The principal strengthening in René 41 nickel base alloy is derived through the precipitation of $Ni_3(Al, Ti)$ and Ni_3Ti. Carbides such as TiC, M_6C, $M_{23}C_6$ contribute to a lesser extent as do Laves type, mu and sigma phases*. The $1950°F$ solution treatment dissolves the gamma prime phase $Ni_3(Al, Ti)$ which is reprecipitated as a fine uniform dispersion of particles throughout the structure at $1400°F$. Aging at higher temperatures produces coarses gamma prime particles. The $M_{23}C_6$ carbide will dissolve at approximately $1900°F$, although most carbides will not dissolve at $1950°F$. If they are present at $1950°F$ in a supersaturated solution, they may precipitate; further precipitation would be expected at lower aging temperatures.

Heat treatment (B) entails a 2-hour solution treatment at $2150°F$ followed by an air cool plus a $1650°F$, 4-hour aging treatment.

The $2150°F$ treatment is expected to dissolve both the $M_{23}C_6$ carbides, but it may not completely dissolve TiC. All gamma prime is expected to go into solution. It is abundantly precipitated between $1600°F$ and $1900°F$. The $M_{23}C_6$ carbides tend to precipitate most abundantly near $1550°F$, but occur after aging between $1400°F$ and $1800°F$. The M_6C carbides may precipitate from $1400°F$ to $2150°F$ but are most abundant near $1900-1950°F$. The $M_{23}C_6$ carbides disappear near $1900°F$, but it is not certain if this is solution or change into the M_6C type. It is recognized that such a change to M_6C carbides does occur. On the premise that $M_{23}C_6$ is undesirable

*Note: Laves phases are $(Fe, Cr, ...)_2(Ti, Mo)$, mu is Co_7Mo_6, sigma is complex Cr-Mo-Fe-Ni.

-19-

because it may cause grain boundary brittleness, the solution temperature should not be too high, lest it dissolve all the carbides and thus facilitate the precipitation of the $M_{23}C_6$ type at the usual aging temperatures. If the solution temperature is above that necessary for gamma prime and $M_{23}C_6$ solution but below that for M_6C, the latter is expected to tie up the available carbon and minimize the lower temperature formation of $M_{23}C_6$. A lower solution temperature is also less likely to cause grain growth.

Comparing the two recommended treatments, 1900°F precipitates M_6C but dissolves gamma prime; while 2150°F dissolves both and may cause grain growth. Aging at 1400°F precipitates chiefly gamma prime, while at 1650°F both carbides may precipitate as well though the availability of carbon for this is low if most of it has already precipitated at 1900°F.

The following strength values are presumably characteristic of Rene 41 nickel-base alloys:

Temperature		Ultimate Tensile Strength	Rupture Strength PSI	
°F	°C	PSI	100 hr.	1000 hr.
70	21	143,000-206,000		
1000	538	203,000		
1100	593	200,000		
1200	649	194,000	110,000	102,000
1300	704	182,000		
1350			81,000	65,000
1400	760	127,000-150,000	68,000	50,000
1500	816	126,000	45,000	29,000
1600	871	90,000	28,000	17,000
1700	927	58,000	18,000	11,000
1800	982	15,000- 20,000*	10,000	

*Represents extrapolated values.

Inconel 718

Inco 718 was developed by the International Nickel Company for service at medium temperatures, up to about 1300°F. The alloy differs from the other nickel-base alloys under consideration in that iron is present in considerable quantity and columbium is substituted for much of the titanium and aluminum. The chemical composition of the alloys, from AMS 5596A is as follows:

Chemical Composition of Inconel 718

C%	Mn%	Si%	P%	S%	Cr%	Ni+Co%	Mo%	Cb-Ta%	Ti%	Al%
.03	max	max	max	max	17.0	50.0	2.80	5.00	0.65	0.40
.10	.35	.35	.015	.015	21.0	55.0	3.30	5.50	1.15	0.80

B%	Cu%	Fe%
.002	max	Rem.
.006	.10	

The alloy is originally intended for use as sheet, strip and plate. Its salient feature is its weldability compared to other superalloys. The material is not specifically intended for use in the as cast condition, and the heat treatments recommended include a high temperature solution anneal followed by a lower temperature aging treatment. A recent DMIC report (47) details the various recommended combinations of heat treatment and composition.

The major strengthening machanism operative in this alloy is the precipitation of a complex intermetallic compound identified as a gamma prime type with the formula $Ni_3(Al, Ti, Cb)$ or, possibley, $Ni_3(Al, Ti, Cb, Mo)$. Laves phases have been found in the alloys, the actual composition of which seems to be dependent upon the thermal history of the sample examined. These phases appear in the inter-dendritic areas of the cast product and may, if not properly modified by heat treatment, have detrimental effects on the mechanical properties.

The following strength values are presumably characteristic of alloy 718:

Temperature		Ultimate Tensile	Rupture Strength**	
°F	°C	Strength (PSI)*	100 hrs.	1000 hrs.
70		211,000-176,000		
1100			135,000	115,000
1200		168,000-140,500	105,000	85,000
1300		146,000-121,000	75,000	53,000
1400		116,000-113,500	44,000	25,000

*Alloy in wrought condition with various heat treatments.
**Varying heat treatment 1800°F/1+1325°F/8, F.C. 100°F/hr. to
1150°F + 1150°F/8
1800°F/1+1325°F/8, F.C. 20°F/hr. to 1150°F

Statistical Analysis of Literature Data

The mechanical property data given for the four alloys above, is taken from a large number of literature references and is not, necessarily, statistically dependable. Evaluation of the representative hot strength of the heat resistant alloys is always a problem. The first, or prototype heat of a given grade is frequently accepted as the base line for properties, though there is no assurance that it will be representative. Much more experience is necessary before the central tendency of the properties can be established with assurance.

For this reason, the literature was scanned carefully for single heat data which might occur in large quantities. In only one alloy was the search successful, Inconel 713C. (54)

Even within a single heat, where composition and processing are presumably not variables, experimental error can produce considerable scatter of the results. Replication is desirable to help define this experimental error. Fortunately there are available a number of parameters that can be plotted against strength to allow for the influence of temperature and time on a broad basis. One of the simplest and therefore the preferred parameter is that proposed by Larson and Miller. However, it must be used with discretion as it gives a linear plot only over a restricted temperature range and it requires use of a derived constant that differs for various alloys and processing history.

If the Larson-Miller parameter constant is derived carefully for a material, and the strength values derived from the parameter are confined to the conditions for which linear behavior is likely, the appropriate interpolations and extrapolations can be made with considerable assurance. This has been done here for a heat of alloy 713C that has been extensively tested. (54) The test data at 1500°F, 1600°F, and 1700°F, for a total of 18 points were fed to a computer, the constant derived to provide the best fit of the master rupture curve by the method of least squares, and the rupture stresses obtained for 10, 100, 1000, 10,000, and 100,000 hours life expectancy. Similarly, the 0.000001%/hr., 0.00001%/hr., 0.0001%/hr., and 0.001%/hr. limiting creep stress values were derived, though it should be recognized that the experimental error and scatter for creep rates are greater than those for rupture times.

The derived rupture stress and creep stress values of this (Heat No. X-4027) 713C alloy are shown in Table I. In general the values derived are slightly lower than those of the INCO published brochure on this alloy and those of the DMIC summaries prepared at Battelle Memorial Institute. Thus they seem conservative.

IV.   THE VACUUM FURNACE

Figure 1 shows an overall view of the vacuum melting and casting unit in use on this program.   The furnace was particularly designed for the melting and pouring of large castings under vacuum. The power unit provides 100 KW at 3000 cycles to an interchangeable (300 or 500 lb. capacity), alumina lined, induction melting furnace at the rear of the vacuum chamber.   Power controls for the melting operation are conveniently located on the control platform, as are the vacuum pump controls.   In the vacuum chamber, in front of the furnace, a large turntable arrangement permits the indexing of more than one mold for pouring while viewing through the large sight port just above the pouring station.

The vacuum system consists of a mechanical pump, a Roots-Connersville blower and two oil diffusion pumps in parallel.

Support equipment for the vacuum melting and pouring operation is shown in Figure 2.   This view of the equipment shows the facilities for removing metal samples during the melting operation, the thermocouple lance, the alloy hopper, valved to permit alloy additions during the melting operation, and the remote controls for indexing the mold table as well as the furnace tilting and power controls.   Sight ports for optical temperature measurements and general viewing of the melting and pouring are also visible in Figure 2.

Standard temperatures control practice has been established which only rarely requires the use of the immersion thermocouple. A bi-color pyrometer equipped with both a dial indicator and recording chart is used for most of the melting operations.   Absolute errors inherent in most optical type pyrometers are minimized in this type of instrument.   In addition, the absolute value of temperature is considered relatively unimportant if one follows the method of adjusting all temperatures relative to the upper freezing temperature (liquidus) as measured by the pyrometer in use.   Toward this end, the first step after obtaining a meltdown is, normally, to obtain this freezing temperature by detecting the upper thermal arrest with the bi-color pyrometer.   All operating temperatures are then based on "freeze plus X", where X is the degrees superheat for pouring or other considerations.

V. PROCUREMENT AND CONTROL OF MELTING STOCK FOR PHASE I

Early in the program, it was decided that the initial melting stock for the entire program would be in the form of vacuum melted ingot purchased from a recognized industrial supplier. This decision was based on the obvious desirability of eliminating the complex variables associated with vacuum refining of raw material charges from the program. The purchasing specifications for ingot are shown in Table II.

A typical analysis of incoming ingot is shown in Table III. All ingot and vacuum remelt heats for the program were analyzed completely. These representative ingot analyses are provided only for general information.

The materials were ordered as vacuum refined and chill cast ingot, approximately 3 inches in diameter and cropped from the top end to show an ingot pipe no greater than 3/8 inches in diameter. Chemical certification was required. For Phase I of the Program, alloy was ordered in 1000 lb. lots.

In order to establish X-Ray flourescent and emission spectrographic standards for analysis, the wet analyses were performed in triplicate. In addition, spectrographic standards for Inco 713LC alloy were obtained from the National Bureau of Standards.

VI. ESTABLISHMENT OF BASE-LINE (CONTROL) MECHANICAL PROPERTIES

A. Experimental Procedure

1. Specimen Design

In designing a specimen for the establishment of control mechanical properties, three major factors were considered: (1) section size (2) soundness of the final test bar, and (3) casting yield, i.e., the number of test specimens per pound of metal cast.

The most desirable section size was determined on the basis of the size of the final test specimens to be obtained for testing and, more importantly, the section sizes which would be involved in the end products of the program. On this basis, a one-half inch section size was chosen. The length of the specimen was set at five and one-eighth inches which accommodates the large variety of test specimens to be prepared from the cast bar, i.e., tensile bars, creep rupture specimens, impact specimens, etc. The final specimen blank to be obtained from the casting was, therefore, established with the rough dimensions of 1/2x1/2x5-1/8 inches.

Soundness of the test specimen, the most important of the three factors was established by incorporating a full length riser section above the basic test bar, appropriately tapering the side walls of both the test bar and riser to promote directional solidification, and assuring that the riser was approximately four times the volume of the test bar.

Casting yield at a relatively high level was obtained by equipping each test bar and riser assembly with an end gate and arranging several of these symmetrically on each side of a central runner, with all the assemblies in a single plane. The pattern designed from these concepts placed the entire assembly of sixteen test specimens, runner, etc. in the drag section of the mold, permitting stacking of any number of drags with connecting downsprue sections. This pattern is shown in Figure 3. A closer view of the pattern which illustrates the details of the specimen and riser connection to the runner and sprue well is provided by Figure 4. The pattern board shown is designed for a 14" by 18" by 4" or 6" deep flask with pin centers at the ends of the runner. What cannot be seen in Figures 3 or 4 is that the six riser-specimen assemblies most remote from

-25-

the downsprue may be removed from the pattern to permit molding of a ten-specimen drag in a 12" by 14" flask. The purpose of this feature is to permit the use of the same pattern for producing small molds to be cast with large castings in Phase II as qualifying separately cast test bars. Regardless of how the pattern is used, the cope section provides only the pouring basin and a short downsprue.

Figure 5 shows a ceramic molded drag made from the subject pattern. By stacking three of these drags with one cope, with two stacked molds in the vacuum chamber, 96 test specimens were obtained from approximately 250 lbs. of metal. Mold material was ethyl silicate bonded calcined kyanite.

In order to verify the characteristics of the multispecimen pattern described, prior to its use in the vacuum melting furnace, a heat of HW, an iron-base heat-resistant alloy was induction melted (in air) and cast into a single ceramic molded cope and drag assembly. The elevated temperature tensile and stress rupture properties of the test bars produced were compared with those of 1 inch diameter, center risered castings used as standard specimens for heat resistant alloy evaluation by the Abex Laboratory for many years. In addition, 0.020" thick slices were cut and ground from several of the test blanks produced. These slices were subjected to micro-radiography and macroetching and examined to determine the extent of microporosity present in the eventual gauge section of the test bar.

The properties obtained from the new specimen design were satisfactory compared to the standard specimen. No microporosity was found in any part of the test specimen blank. On the basis of these results, and the fact that no foundry difficulties were encountered in the molding or casting of the design, the pattern was accepted for use for the determination of control, base line properties for the program.

2. Molding, Melting and Casting Procedures

Heat 65-456, the first vacuum heat of the program, was designed to establish the base line mechanical properties of alloy 713L·C. Two stacked, ceramic molds were prepared from the multi specimen pattern previously des-cribed. Together, these molds would produce 96 test specimens from which the various test bars could be machined.

-26-

After molding and stripping the pattern, each cope and drag section was fired separately by gas-air torches to remove all traces of organic materials. The molds were then assembled and closed and placed in an oven at 450°F for a minimum of twelve hours in order to reach equilibrium from the firing temperatures and, simultaneously, to keep them moisture-free until cast.

The 300 lb., alumina lined vacuum induction furnace was charged with 280 lbs. of ingot from vendor heat 6-3900. After charging the furnace, the molds were arranged for pouring on the turntable in front of the furnace. Since no additions were to be made to the heat, the alloy addition hopper was not charged. The vacuum chamber containing the furnace and the molds was then closed and pumped down to 19 microns (single diffusion pump), at which point power was turned on low to preheat the furnace lining and then higher to promote meltdown. After meltdown, about five minutes of minor outgassing of the melt occurred at 20 microns pressure. It is believed that the bubbling observed was from the crucible and not the metal charge.

Since no vacuum refining was required, the melt was brought to an arbitrary level above the reported melting range of 2350°F to 2410°F and power was shut off. From the time the power was reduced, continuous chart readings of temperature from the bi-color pyrometer were recorded. The typical thermal arrest associated with solidification provided the "freeze point" of the alloy. The measured freeze point was 2475°F. Power was then turned on again and the melt raised to the specified pouring temperature, 200°F above the measured freeze point. When that temperature was reached, the forst mold was poured. The furnace was then returned to the melting position, the temperature readjusted to the desired level of 200°F above the freeze, and the second mold was poured, having been positioned by manipulating the turntable during the reheating period.

Due to outgassing of the mold, pressure in the melting chamber rose to 120 microns during the pouring of the first mold. There was little recovery of vacuum during the short time of reheating and the final pressure of the chamber after the second pour was 230 microns.

Two additional base-line property heats were cast, one of Inco 718 and one of Rene 41, for which identical procedures were used for specific items such as pouring temperature etc. which were controlled by the nature of the specific alloy. The melting and casting data for all three base-line property heats are shown in Table II under heats 65-456 (Inco 713LC),

-27-

65-506 (Inco 718) and 65-522 (Rene 41). The test
bars for each of these alloys were poured at 200°F above
the liquidus temperature as determined for each heat by a
bi-color pyrometer, thus eliminating superheat as a
variable in comparing the test bar properties of the three
alloys.

Attention is called to the melting pressure indicated in
Table II for the base line property (and other) heats to be
described. The pressures noted are those established
prior to meltdown and maintained for the entire melt until
the molds were poured. It will be noted that the pressures
during heat 65-623 and subsequent heats are considerably
lower than those shown for previous heats. This is not a
function of the vacuum equipment but, rather, of the Pirani
gauge used to record the chamber pressure. It has been
noted that the pressure reading generally increases with
successive heats due to contamination of the measuring
source. With no change in the vacuum system, but with
recalibration of the gauge against standard, the pressures
read normally in the 5 to 10 micron range. It may, there-
fore be assumed that the actual melting pressures en-
countered in heats 65-456 through 65-542 are considerably
lower than the indicated pressure, i.e., in the 5 to 10
micron range.

Heat 65-456 was melted with one diffusion pump in the vacuum
system. All the remaining heats were processed using
two identical diffusion pumps in parallel. Interestingly, only
a small difference was noted in the general operating press-
ures. However, a major difference was seen in recovery of
high vacuum after occasions such as mold outgassing during
pouring. In heat 65-456, mold outgassing resulted in a
pressure of 230 microns after pouring the second test bar
mold. In all subsequent heats, no pressure higher than about
150 microns was observed, and this was a maximum at pour.
The pressure was very quickly lowered to high vacuum levels
by the two diffusion pumps.

3. Shakeout Derigging and Cutoff

The test bar molds were removed from the vacuum chamber
within ten minutes after pouring. After a minimum of four
hours after casting, the test bar assemblies were shaken
out. The four hour minimum was set in order to insure that
each of the three alloys had cooled in the mold below 1000°F,
a temperature at which further precipitation could not be

expected in the microstructure. This procedure is representative of large castings which are rarely shaken out of the molds at temperatures higher than 1000°F.

After shakeout, the three layers of test bars from each mold were identified as A, B, C from top to bottom. The test bars within each layer were identified with the numerals 1 through 16 starting at the downsprue for each set of 8 specimens per side. From this point on, each test bar retained the identification which indicated the heat number, casting (mold) number, layer, and position in layer. For example, 65-456-2A13 represents a test specimen from heat number 65-456, casting 2, layer A (top), position 13 (fifth from the downsprue on the right side of the sprue). After identification, the test specimens with the integral risers still attached were cut from the runners. Downsprues, basins, and runners were returned to segregated barrels for subsequent use as revert. The test bar, with riser still attached is shown in Figure (7). A dimensional drawing of the specimen is shown in Figure (8).

After derigging, the risers were removed from the basic test bar by wet abrasive cutoff wheels. The basic test bar dimensions, after removal of the riser, are shown at the top of Figure (9).

4. Inspection

All test specimen blanks were subjected to conventional X-Ray inspection prior to machining into test specimens. Of the 288 specimens cast in three heats, only three were rejected on this basis. The cause of rejection was ceramic chip inclusion caused by mold corner breaking. In addition to conventional X-Ray inspection, one blank from each layer of one mold was selected for microradiographic analysis in order to reaffirm the total soundness of the test bar. The techniques applied in microradiographic analysis will be detailed in a subsequent section. In no case was evidence of microporosity found in any test bar section examined microradiographically.

The chemical and gas analysis of each of the base line property heats was determined from X-Ray spectrographic samples and drillings from sound portions of the runners.

Spectrographic standards were established by analysis in triplicate of each of the incoming ingot lots. The standards thus obtained were used for the analysis of subsequent heats of the same material.

Hydrogen, oxygen, and nitrogen were determined for each heat by vacuum fusion and analysis.

5. Initial Heat Treatment

Inco 713LC - Test bars of this alloy were tested in both the solution treated and "as cast" conditions. One set of tensile bars was aged at 1500°F for 16 hrs. per a GE requirement on cast 713 alloy parts. The solution treatment, where applied, was 2150°F, two hours, air cool. No special atmosphere was used in any heat treatment of test specimen blanks since final machining to the various test specimens used removed the surface layer affected by the high temperature and air atmosphere.

Inco 718 - Test bars of Inco 718 were tested in the as cast and solution treated conditions for information only. The majority of testing was performed on test bars which received the following feat treatments, depending upon the type of test. (56)

For optimum tensile properties: 1800°F, 2 hrs. air cool, followed by 1325°F, 8 hrs., cool at 100°F per hour to 1150°F, hold at 1150°F for 8 hours, air cool.

For optimum stress-rupture properties: 1900°F, 2 hrs., air cool, followed by aging treatment as above.

Rene'41 - Rene'41 test bars were also tested in the as cast and solution treated condition for information only. Tests were performed mainly upon specimens which received the following heat treatment, depending upon the type of test. (57)

For optimum tensile properties: 1950°F, 4 hr., air cool, followed by, 1400°F, 16 hrs., air cool.

For optimum stress-rupture properties: 2150°F, 2 hrs., air cool, followed by 1650°F, 4 hrs., air cool.

Triple solution treatments of Rene'41 test bars at 1950°F were also applied in an attempt to raise the 1200°F tensile properties. (58)

6. Final Test Specimen Preparation

After heat treatment, the test specimen blanks from each of the heats were machined to the appropriate test specimen dimensions. The number of specimens for each type of test was determined by the number of heat treatment variables to be investigated. The dimensions of all of the types of test specimens used in this investigation to date are shown in Figure (9). Figure (9) also shows the number of specimens machined from the specimen blank. Most of the test specimens are based upon standard practices of the Abex Research Center which can be traced to ASTM standards.

One group of Charpy impact specimens from each of the heats was precracked to an approximate depth of 0.2 inches at the root of the notch by a special machine which subjected the notch to bending fatigue. These specimens were used for the determination of fracture toughness of the alloys investigated.

The resistance heated hot tensile specimen shown in Figure (9) (F-51) was only used for a few tests to determine its applicability to the program. This type of test is much more rapid than conventional hot tensile testing and would have been of considerable value in lessening the amount of time devoted to hot tensile testing. However, it was found that the only property which could be dependably measured was the ultimate tensile strength. Yield strength could only be estimated, and the elongation and reduction in area were affected by a hot spot which formed during neck-down. This test was therefore abandoned and the more conventional externally heated test bar was used.

7. Testing Procedures

Room temperature tensile tests were performed on 0.252" gauge diameter, 1" gauge length threaded test bars per Figure (9). Cross-head speed was maintained at 0.05" per minute throughout the test. The strain-rate in the test bar gauge length was approximately 0.005 inch/inch/ minute through the yield strength, increasing for the remainder of the test. Yield strengths were determined at 0.2% offset.

Elevated temperature tensile tests were performed with the following critical parameters:

-31-

Time at temperature: 30 minutes
Temperature deviation over gauge length: less than 5°F
Cross-head speed: 0.05"/minute

Other test factors were the same as for the room temperature
tests. The specimen, thermocouple, and extensometer
arrangement for the elevated temperature tensile tests is
illustrated in Figure (10).

Impact and fracture toughness tests were performed on a
24 ft. lb. capacity Charpy impact machine designed for
precision impact testing. The machine, with a vernier
dial, is capable of realistically reading to 0.1 ft. lbs.
Room temperature and -40°F impact and fracture toughness
tests were performed in accordance with conventional stand-
ard practice. Delay time from the acetone-dry ice bath at
-40°F to fracture was less than 3 seconds. 1200°F impact
tests were accomodated by holding the specimens in a
furnace at 1200°F ± 10°F for two hours, and then trans-
ferring each specimen to the test machine within 5 seconds.
Time for furnace and specimen temperature recovery was
permitted between each test.

Fracture toughness values (59) were calculated by determin-
ing the average crack depth (visible as a discolored surface
compared to the clean new fracture) and, from this,
calculating the area of new fracture surface. The energy
to form this new fracture surface was calculated according
to the following equation.

$$\frac{G(\text{in.-lb.})}{(\text{sq. in.})} = \frac{\text{impact energy absorbed (ft.-lbs.)} \times 12}{\text{New fracture area (sq. inches)}}$$

Room temperature compression tests were performed on the
specimens shown in Figure 9. SR-4 type strain gauges were
used. After determining the compression yield strength
(.2% offset in a .25 inch gauge length), the specimen was
permitted to run to failure. The failure for all specimens
was in shear which occurred after considerable deformation.
Although the value is not particularly meaningful for ductile
materials such as the alloys tested, the maximum load
was recorded and the compressive strength calculated on the
basis of this load and the original cross sectional area.

Creep-rupture testing was performed in accordance with the
practices established by Fellows, Cook and Avery (60) and
using the same equipment discussed by them. No attempt
was made to establish statistically proven creep-rupture
data such as would be required in an alloy development
program. Rather, each of the alloys was tested at stresses

-32-

and temperatures chosen on the basis of literature and specifications available in order to determine if the current reported properties were being met by test bars produced in each of the alloys under investigation.

Thermal fatigue testing was performed on the apparatus shown in Figures 11 and 12. In this type of apparatus, an electrically heated specimen (F-45 in Figure 9) is clamped firmly at each end between two relatively immovable, water cooled blocks. Thermocouples are spot welded on two sides of the specimen to detect and control the temperature of the reduced test section. Due to inherent thermal expansion and contraction, the specimen is subjected to compressive stresses during heating and to tensile stresses during the cooling cycle, their magnitude being determined by the coefficient of thermal expansion and by the position of zero stress relative to temperature and initial clamping stresses. The time-temperature cycle is programmed by a gleeble type controller and consists of .5 seconds of heating to the pre-set temperature and 2.5 minutes of cooling to 300°F. The heating and cooling rate is determined by the current fed through the specimen by the "Gleeble "unit. Temperature and stress levels are recorded constantly by the recording instruments seen in Figure 12. Since total failure of the specimen may be preceded by partial cracking, an 8 mm movie camera is set to photograph a magnified image of the gauge length at the peak of each heating cycle. Subsequent examination of the film thus provided reveals the point at which the first crack occurred at the top of the guage section. It should be pointed out that maximum stresses are usually developed when the heating cycle brings the compressive stresses above the compressive elastic limit at the temperature involved. This results in visible "upset" of the gauge section and subsequent cooling builds rather high tensile stresses.

For the purpose of this program, the thermal fatigue test was used only to compare one alloy with the others and is not intended to be a thorough analysis of thermal fatigue properties. Therefore, if a specimen went for more than 1000 cycles, the test was discontinued. As might be expected, where visible "upset" occurred, failure occurred in less than 1000 cycles. Where no upset was detected, the specimen normally ran the full term.

-33-

Where appropriate to the context of the program, micro-specimens were cut from the various test specimens after testing to determine the mode of failure or, simply, to compare the properties obtained with the microstructural characteristics of the particular alloy or heat treatment.

B. Initial Results and Discussion

1. Chemical and Gas Analysis

The chemical analyses of the heats cast to determine the base-line mechanical properties of the three subject alloys are shown in Table V. The table lists all of the heats cast on Phase I of the program and only heats 65-456, 65-506, and 65-522 are of immediate concern. As can be seen by comparing the analyses in Table V with the representative ingot analyses in Table III, the analyses of the test heats reflect very closely the analyses of the ingot charged. Except for titanium in the Rene'41 heat, 65-522, all elements fall within the specifications to which the original ingot was ordered. The titanium level in heat 65-522 (Rene 41) is 0.07% over the 3.30% maximum permitted in AMS 5545 and GE B50T53-S7. The analysis of heat 65-542, however, melted from the same ingot, indicates 3.21% Ti, within both specifications. Based upon a 1965 report of the General Electric Company, the high titanium may be expected to lower the tensile properties of Rene'41 to some extent at room temperature and up to about 1300°F. At 1400°F, the effect would be reversed. (61) This effect will be noted again in the discussion of the mechanical properties of Rene'41.

The vacuum fusion gas analyses of the experimental heats are also shown in Table V. For the most part, the gas content or decrease in gas content compared to the original ingot analysis (Table III).

2. Base Line Mechanical Properties

Inco 713LC

In examining the mechanical properties of Inco 713LC, two basic comparisons are of interest - the properties obtained compared to those reported in the literature and the effect of the 2150°F solution treatment compared to "as cast" properties. Since no specification has been written for the low carbon grade of alloy 713, data comparisons were made mainly with AMS 5391A (Inco 713C) and other literature concerned with the standard grade of the alloy. (11)

-34-

The requirements of AMS 5391A include room temperature
tensile properties and stress-rupture requirements as
follows:

Room temperature tensile properties (Minimums):
    Ultimate tensile strength: 110,000 psi
    Yield strength at .2% offset: 100,000 psi
    Elongation, % in 4D: 3%

Stress-Rupture properties (Minimums):
    Temperature: 1800°F
    Stress: 22,000 psi
    Life: 30 hrs.
    Elongation   5% in 4D

The properties obtained from test specimens from heat
65-456 are listed in Table VI. Section A through F. As
can be seen in Section A, the room temperature tensile
properties required by AMS 5391A have been exceeded
by both the as cast and the solution treated test bars.
The creep-rupture properties shown in Section B also
exceed the requirements of the specification cited above,
again with an improvement in ductility attributable to
solution treatment.

The tensile data from Table IV-A have been plotted in
Figures 13 and 14 for as cast and solution treated test
bars respectively. It is apparent from these curves,
that there is a general improvement in yield strength and
ductility up to 1200°F as a result of solution treatment.
The tensile strength in the same temperature range is
somewhat higher for the as cast condition. At 1400°F,
the ductility and tensile strength of the solution treated
test bars is lower than that of the as cast, but the yield
strength is still significantly higher. The major ad-
vantage of solution treatment is gained at 1600°F and
higher, where the strength of the as cast material falls
off very rapidly. It should be pointed out at this juncture
that the suggested requirement for the cast fin beam
design is a 90,000 psi yield strength at 1600°F. Obviously,
this requirement could not be met by as cast 713LC, but
can easily be accommodated by solution treatment as
indicated.

The creep-rupture properties of Inco 713LC test bars from

heat 65-456 (Table VI-B) compare very favorably with literature data on 713C (54) and with values reported by the International Nickel Company (55). In general, the rupture life and ductility exceed literature data by a significant percentage. Of particular interest is the 50% improvement in 1600°F rupture life with solution treatment, as well as an improvement in the minimum creep rate.

Table VI-C lists the room temperature compression properties of Inco 713LC. The compressive yield strength values compare well with tensile yield strength again showing an increase in yield strength as a function of solution treatment. Very high ductility was exhibited by all specimens tested in compression, with the final mode of failure being shear after extreme distortion of the test specimen.

The Charpy "V" notch impact strength of Inco 713LC, Table VI-D showed little change as a function of test temperature from -40°F to 1200°F, but exhibited significantly higher values for the solution treated specimens at all test temperatures. Room temperature Charpy values of 14 ft. lbs., exhibited by the solution treated specimens, are considered reasonably good for alloys of this type. The fracture toughness of this material, shown in Table VI-E, shows the same reaction to solution treatment as the simple impact strength, i. e., a marked improvement over as cast values. The effect of test temperature is virtually nil. As a matter of comparison, the room temperature fracture toughness values (G) obtained for Inco 713LC compare very closely to values obtained on a precipitation hardenable martensitic alloy, 17-4-PH, which has been under investigation in the Research Center.

Solution treatment also improves thermal fatigue life according to the data in Table VI-F. In tests where the thermal cycle was 300°F-1600°F, solution treated bars yielded double to quadruply the life of as cast bars except where the tensile stress introduced during the cooling cycle was 123,000 psi, well above the room temperature yield strength of the material. Tests performed with a 300-1200°F cycle introduced tensile stress levels generally below the yield strength and compressive stresses at or slightly above the compressive yield strength. These tests yielded no failures after 1000 cycles and were discontinued. It should be noted that the "Cycles to Failure" reported for these and all other specimens represents total failure, or rupture, of the specimen. Reading of the

-36-

film strip to determine "cycles to first cracking" was discontinued after it was recognized that the initial crack was normally followed by relatively few additional cycles. For example, in five tests of Inco 713LC alloy, a maximum of seventeen of the cycles to failure occurred after initial cracking was observed. The average was 10.6 cycles to failure after initial cracking, while total cycles to failure averaged over 250 cycles.

In view of the data reported in the literature for alloy 713C and 713 LC, the base line mechanical properties developed in cast and machined test bars from heat 65-456 appear to be excellent in both the as cast and solution treated conditions. However, certain advantages are gained by solution treatment of the cast structure during the relatively slow cool in the mold from casting temperatures. It is, from the foundry's point of view, a credit to the alloy that more drastic effects of this slow cooling are not exhibited since it is reported that most of the superalloys are subject to property degradation with slower cooling rates.

Inco 718

Property specifications for cast Inco 718 were taken from a General Electric specification B50T68-S3. AMS 5596A lists property specifications for the wrought alloy which are considerably higher than the cast equivalent. GE B50T68-S3 specifies properties as follows:

Room temperature tensile properties:
Ultimate tensile strength	115,000 psi
Yield Strength, .2% offset	85,000 psi
Elongation, % in 4D	5%
Reduction of Area	10%

No stress rupture requirements are cited in the GE specification, nor did the literature survey turn up any references to the stress-rupture properties of cast Inco 718.

Since this alloy is intended for use below 1400°F, no tensile or creep rupture tests were performed above that temperature.

The mechanical properties obtained from Inco 718 test bars cast in heat 65-506 are listed in Table VII, Section A through F. The room temperature tensile properties of as cast and solution treated test bars are included in order to demonstrate the necessity of heat treatment. Interestingly, the as cast room temperature tensile and yield strengths are only slightly below the fully heat treated levels indicating considerable aging during cooling in the mold. The solution treated properties (1800°F solution treatment) show the expected high ductility

and low strength level. Test bars solution treated at 1800°F
and aged exhibit tensile and yield strength values which meet
the requirements of GE B50T68-S3, while the ductility is
considerably in excess of the required 5% El and 10% RA.
In comparing the aged properties and the solution treated
properties, a doubling of the yield strength and halving of
the ductility can be attributed to aging, while the tensile
strength is raised by a considerably smaller factor.

The tensile properties of Inco 718 test bars are plotted for
test temperatures up to and including 1400°F in Figure 15.
As can be seen, the tensile strength of Inco 718 drops off
very rapidly after 1200°F without the benefit of increasing
ductility. In the room temperature to 1200°F range, the
ductility of Inco 718 is excellent, consistently above 10%
and, in some cases, in the 15 to 20% range of elongation.
Reductions in area of over 30% were recorded at 1000 and
1200°F. In the same temperature range, however, yield
strengths are less than 80,000 psi with tensile strengths
barely over 100,000 psi.

The first creep-rupture tests performed on Inco 718
specimens were based upon wrought data from the lit-
erature. The results are shown in the first three tests
listed in Table VII-B. Obviously, the stresses listed
were far too high to yield reasonable life for the alloy in
the cast form. Since there were no literature references
available from which reasonable stresses could be obtained,
the stress levels chosen for the remaining test were arbitrary
and based on fundamental knowledge of the alloy. Consideration
of the potential end use of the alloy as a turbine disc operating
in the range of 1000 to 1200°F prompted the 1200°F test at
68,000 psi (calculated to yield between 50 and 100 hrs. life).
Although the creep rupture values are of little absolute value,
they do permit a comparison with the two other alloys in-
vestigated.

The room temperature compression properties of Inco 718
are shown in Table VII-C. As in the case of Inco 713LC, the
compression yield strength is very similar to the tensile
yield for both the solution treated and the solution treated
and aged condition. The strengthening effect of the aging treat-
ment is obvious. Compression failure were all in shear with
extreme ductile distortion prior to failure.

The -40°F and room temperature Charpy impact strength of
this alloy in the solution treated and aged condition is in the
same category as solution treated Inco 713LC, about 13 ft.
lbs. At 1200°F, however, the impact strength is considerably
higher. This is undoubtedly a reflection of the high ductility
of the alloy at 1200°F as seen in the tensile test data.

-38-

Fracture toughness data, Table VII-E, also place Inco 718 in the same category as Inco 713LC except somewhat higher values at 1200°F.

Two failures out of three thermal fatigue tests with a 300 to 1400°f. cycle occurred where cooling tensile stress was beyond the yield strength of the alloy. The results are shown in Table VII-F. In the third test, the stresses developed were below the yield strength and failure did not occur after 1000 cycles. Relative to the yield strengths of the two alloys, the thermal fatigue life of Inco 718 would appear superior to Inco 713LC. However, on an absolute stress vs. cycles to failure basis, the 713LC must be considered superior.

Thermal fatigue tests using a 300 to 1200°F cycle yielded no failures after 1000 cycles.

Tensile properties and creep-rupture properties of Inco 718 are considerably lower than Inco 713LC. This, however, is to be expected based upon available literature on the cast alloys. The single advantage exhibited by the 718 alloy is that of ductility in the 1000-to-1200 degree range, exhibited both as tensile ductility and increased impact strength and fracture toughness in that temperature range. The properties exhibited by cast Inco 718 fell far short of the values reported for the equivalent wrought material.

Rene 41

Property specifications for cast Rene 41 were taken from GE C50T53-S7. No room temperature tensile requirements are listed, but the 1200°F tensile property minimums are as follows:

Ultimate tensile strength:	100,000 psi
Yield strength at .2% offset:	90,000 psi
Elongation, % in 4D:	3%
Reduction in area:	5%

Stress-rupture properties are required as follows:

Temperature:	1650°F
Stress:	25,000 psi
Minimum Life:	25 hrs.

The base-line mechanical properties obtained from heat 65-522 are listed in Table VIII, Sections A through F.

The room temperature tensile properties of material solution treated at 1950°F are very similar to those of as cast material. This is a probable indication that the 1950°F solution treatment is dissolving very little of the constituents precipitated in the microstructure during solidification and cooling in the mold. This is supported by the evidence of greatly increased ductility in test bars solution treated at 2150°F. Aging at 1400°F of test bars solution treated at 1950°F raises the yield strength and lowers the ductility markedly. Aging at 1650°F of test bars solution treated at 2150°F also raises their yield strength, but to a lesser degree. The optimum room temperature yield strength was obtained with a 1950°F solution treatment followed by the 1400°F aging treatment. The ductility obtained at this strength level is, however, considerably lower than for either 718 or 713LC.

The tensile properties listed in Table VIII-A are plotted in Figure 16 for the temperature range from room temperature to 1800°F. Only test bars heat treated for optimum tensile strength are included in the plot. The 1200°F yield strength did not meet the requirements of GE C50T53-S7. The tensile properties are, in general, somewhat lower than would normally be expected for Rene' 41. Two possible reasons for this behavior have been pointed out by Glover. (61) It has been shown that, in general, Rene' 41 is quite section sensitive, i.e., it is subject to degradation of strength as a function of cooling rate in the mold as well as cooling rate from solution treating temperatures. It is quite likely that the test bar cast for the current program exhibits a considerably slower cooling rate than a cast-to-size test bar. An additional factor which may also be contributing to the somehwat lower strength of Rene 41 test bars is the high titanium level. Glover (61) has shown that the strength level of high titanium Rene 41 is lower than that of normal titanium levels.

Regardless of strength level, however, the limiting factor in Rene' 41 appears to be ductility. Except at 1200°F and 1600°F the tensile ductility of the alloy is considerably below the 10% aim point of the program. In addition, the aim of a 90,000 psi yield strength at 1600°F for fin-beam application obviously cannot be met by this alloy in the cast form.

As can be seen in Table VIII-B, test bars from heat 65-522 successfully passed the stress-rupture requirements of the GE specification and went 2.8 hours beyond the point (70

-40-

hours) at which the specification suggests discontinuing the
test. The rupture life at 1600°F and 40,000 psi, however,
is only a fraction of the life of Inco 713LC under the same
conditions. The 1400°F-60,000 psi rupture life appears to
have been relatively unaffected by heat treatment. The
creep-rupture properties of Rene'41 are superior to Inco
718, as would be expected for an alloy designed to operate
in a higher temperature range.

As with the two alloys previously discussed, the compressive
yield strength and tensile yield strength are very similar for
Rene'41. Compressive failures were all extremely ductile
with a final shear fracture after extreme distortion. The
distortion, however, was not as great as for either of the
other two alloys tested, reflecting the generally lower
ductility.

Charpy impact strength, listed in Table VIII-D, was lower
for Rene 41 than for either of the other two alloys at all
three test temperatures. Fracture toughness values are
also somewhat lower but with unusual scatter to occasionaly
high values.

The thermal fatigue properties of Rene'41 are listed in
Table VIII-F. In general, the performance of this alloys is
inferior to 713LC under similar conditions.

The tensile strength values of Rene'41 fall between the levels
obtained in 713LC and 718. Inspite of reasonable strength
through 1600°F and equally reasonable creep-rupture prop-
erties, the limited ductility of the alloy and its apparent sens-
itivity to cooling rate are significant drawbacks to be taken
into consideration.

3. Comparison of Base-Line Mechanical Properties

The relative property levels of the three alloys under in-
vestigations appear to be fairly straightforward. Inco 713LC
is a high strength alloy with excellent creep-rupture proper-
ties which retains yield strengths above 90,000 psi up to 1600°F.
Accompanying these properties is a reasonable ductility
and an apparently substantial immunity to the effects of slow
cooling in the mold from casting temperature. Inco 718, con-
versely, is a relatively low strength alloy exhibiting a sub-
stantial advantage in ductility and in impact strength and
fracture toughness at 1200°F. Although the alloy does exhibit
some sensitivity to mold cooling conditions, the effects appear
to be adequately diminished by heat treatment. The creep-
rupture properties of Inco 718 at 1300°F appear to be quite
adequate. The alloy is not, however, applicable at temp-
eratures above 1300°F due to rapidly decreasing strength
and creep-rupture properties.

-41-

The tensile and creep-rupture properties of Rene'41 fall midway between Inco 718 and 713LC, but with a significant sacrifice in ductility compared to either of the other alloys. The sensitivity of this alloy to cooling rate as a function of section size or mold conditions has been documented in the literature and is further verified by the difficulty encountered in properly solution treating to obtain optimum tensile properties.

Based upon the properties developed in this initial program, the best combination of strength, ductility, and other properties determined appears to be offered by Inco 713LC in the solution treated condition, although, for certain lower strength and temperature applications, the superior ductility of Inco 718 may provide certain advantages.

4. The Effects of Other Thermal Treatments on R-41, 718 and 713LC.

Rene' 41

One of the shortcomings of the base-line properties demonstrated by Rene 41 alloy is the low yield strength demonstrated by cast test bars tested at 1200°F. Two conventional heat treatments recommended for cast Rene'41 were unsuccessful in bringing the yield strength to the level demanded by GE C50T53-S7, 90,000 psi at 1200°F. (62) In order to determine the effect of a heat treatment recommended in the aforementioned GE specification, two test bars were subjected to a triple solution treatment and age as follows: 1975°F-3 hrs.-water quench, repeated three times, and followed by a 16-hour aging cycle at 1400°F. The 1200°F tensile properties of the test bars thus treated are shown in Table IX under Rene'41. As can be seen, the triple solution treatment did little to improve the yield strength of the alloy which still falls below the 90,000 psi called for in GE C50T53-S7. Virtually no effect on the other tensile properties was noted.

718

As seen in Table VII-B, one test bar of Inco 718 was creep-rupture tested at a load of 40,000 psi and at a temperature of 1300°F. The bar had not failed, nor had it elongated after 500 hours of exposure at which point the test was discontinued. Academic curiosity prompted the determination of the residual tensile strength after the long exposure to 1300°F under

load. The specimen was removed from the testing machine and tested as a conventional room temperature tensile specimen. The results are shown in Table IX under Inco 718. Apparently the long-time exposure at 1300°F has resulted in a marked strengthening of the alloy. Whether or not the strengthening would have occurred without the load is a matter for conjecture but it is most likely that the stress had some effect. The high strength obtained introduces the possibility, however, that some modified heat treating cycle of Inco 718 might offset the extremely low strengths obtained with the conventional heat treatments described in Section VIA-5 of this report.

A preliminary survey of the microstructure of 718 alloy gave evidence that the absence of reasonable strength in the alloy was probably attributable to microsegregation and the formation of massive laves phases which robbed the matrix of the elements required to strengthen by the normal precipitation hardening mechanism. It was determined, therefore, that some additional effort would be directed toward the possible correction of this solidification and cooling rate - dependent phenomenon by high temperature heat treatment. Normally, heat treatment of Inco 718 is sharply restricted to temperatures below which grain growth will occur. However, in the case of the material cast on this program, grain sizes were already quite coarse and there is, in fact, little risk of additional growth.

A second group of test bars of Inco 718 were vacuum cast according to procedures already described. Pouring temperature was adjusted to 300°F superheat for the current heat, as compared to 200°F superheat for the original heat of Inco 718 test bars. The ingot remelted to make the test bars was from the same lot as for the original heat, lot # 6-4220.

After casting and shakeout, the test bars were processed according to established practices previously described. Heat treatments were applied after removal of the riser but prior to machining to test specimen shape. The specific heat treatments are detailed in Table X. The basic high temperature treatment chosen was 2150°F for 2 hours, followed by an appropriate cooling method. The effect of the high temperature treatment alone was studied as well as the combined effect of additional treatment at 1850°F and aging. A control heat treatment at 1850°F with an air cool and followed by the standard aging treatment was used to compare the properties of this heat with those of

65-506. the original Inco 718 heat on the program.

Table X lists the room temperature tensile properties of the Inco 718 test bars from Heat 67-202 heat treated according to the schedule shown. Representative properties of Heat 65-506 are listed for comparison.

Obviously, the strength level of Heat 67-202 is generally higher than that of the original 65-506 with the same heat treatment. This lends support to an observation that the slower solidification rate introduced by the higher pouring temperature might improve the properties of the material. This is, however, difficult to accept in the face of the normal solidification rate-property relationships which are generally the reverse. As can be seen in Table V, there is no significant difference in chemical analysis between 65-506 and 67-202 which might account for the property difference.

Even more outstanding than the property difference between the two heats is the marked improvement in yield strength and ductility afforded by the high temperature heat treatment. In only one case did the use of the 2150°F heat treatment appear to be detrimental. The yield strength of the test bars air cooled from 2150°F and subsequently heat treated at 1850°F and aged is quite low. In fact, the overall property level compares with the properties obtained with the straight 1850°F solution treatment and age on the original heat 65-506. In all other cases, solution treatment at 2150°F raised the yield strength and in most instances, the ductility either remained the same as for the straight 1850°F plus age or was improved.

The difference between air cooling and oil quenching from 2150°F is apparently related to the superior retention of precipitating compounds in solution by the more rapid cool. This is illustrated by the lower yield strength and higher ductility of test bars oil quenched from 2150°F and tested without aging compared to those which were air cooled. Subsequent aging produces a significantly higher yield strength and lower ductility for the oil quenched bars, indicating the greater availability of the elements required for hardening.

The ideal combination of properties is obatined with an air cool from 2150°F followed by the conventional aging cycle, The high strength and ductility obtained easily place the alloy in a strongly competitive position with Inco 713LC for use as a turbine rotor material. However, there is much evidence within this heat treat study as well

-44-

as in previously reported work to indicate that the cooling rate sensitivity of this alloy is very high compared to Inco 713LC. This could be a major drawback for the manufacture of large castings with combinations of heavy and thin wall sections. With this new evidence of property improvement with heat treatment, however, Inco 718 may be considered as a back-up for Inco 713LC as the alloy of choice for the turbine rotor to be cast in Phase II of this program.

713 LC

While the results of the initial work indicated that solution treatment was beneficial to the properties of Inco 713LC, it was recognized that it would be considerably more convenient, when necessary, to relieve the stresses introduced which might be termed a "stress relief" treatment but which would, by the precipitation hardenable nature of the alloy, be an aging treatment as well. A 16-hour treatment at 1550°F was originally suggested as an appropriate treatment. The effect of such a treatment on the room temperature tensile properties was determined as shown in Table IX under Inco 713LC. The ductility of both "as Cast" and solution treated test bars was reduced by half by the 1550°F treatment. The remaining 5% ductility, while still useful, is somewhat lower than would be considered applicable to the turbine disc application. It is interesting to note that the solution treated test bar yielded a considerably higher strength after the 1550°F treatment than did the "as cast" bar, although the ductilities are similar.

After the results of the 1550°F treatment were seen to be unsatisfactory, several other "stress relief" treatments were applied to Inco 713LC test bars in an attempt to provide a heat treatment which would relieve machining stresses and, simultaneously, either improve upon solution treated ductility or, at least, not reduce the room temperature ductility to less than 8 or 9%. Sixteen hour treatments at 1200°F and 1700°F were applied to both solution treated and "as cast" test bars. The results of these heat treatments, shown in Table IX, indicate that only the 1200°F treatment would retain the ductility required for turbine wheel application.
In addition, these treatments also showed the greater increase in strength upon aging for the solution treated alloy with the ductilities equivalent to these obtained in bars aged from the "as Cast" condition.

While a 1200°F treatment would appear to be satisfactory
from the point of view of maintaining adequate ductility,
it is doubtful that any significant stress relief would occur
in the alloy at that temperature within normal heat treating
times. It was considered desirable, therefore, to determine
the effects of extended time exposures to a 1200°F environ-
ment, both for stress relief and for environmental per-
formance information. Table XI lists the room temperature
tensile properties of Inco 713LC test bars exposed to 1200°F
for 50 and 100 hours starting from both the as cast and from
the solution treated condition. As can be seen, no deleterious
effect is attributable to this exposure. Rather, a generally
beneficial effect of the 1200°F exposure on strength can be
observed here as in the case of the 16 hour treatment at 1200°F.
These tests indicate that the alloy will tend to strengthen
throughout at least the first 100 hours of exposure with no
loss in ductility. This is, of course, a most desirable trait.
It is doubtful that any further strengthening would occur with
additional exposure.

C. Additional Work - Properties of Cast-To-Size Test Bars (Lost
Wax - Ceramic Shell Process)

In order to provide a comparison between the base-line
properties obtained by the methods, previously described, and
those which might be obtained by molding methods more typical
of current superalloy practice, 12-pound vacuum heats of each of
the three alloys were ordered from a well known investment
caster. The ingot was supplied by Abex Corp., from the same
lots used to cast the baseline-property heats described previously.
Melting practice was left to the discretion of the caster. Each
heat was cast into pre-heated and backed-up ceramic shell molds
with no nucleant on the metal-mold interface. The test bars
produced were cast to size as 0.252" diameter, threaded and
tensile specimens, end gated per standard investment casting
procedure for the heat resistant alloys. A complete analysis of
the 713LC heat and the gas analysis of the 718 and René 41 heats
are shown in Table XII.

Where called for, the test bars cast on these heats were
heat treated according to the procedures already described in a
preceding section and tested according to established standards.
The tensile properties of the cast-to-size test bars are shown in
Table XIII.

When compared to the properties obtained in base-line-
property heat 65-456 (reported in IR-8-297-II), it becomes
obvious that the "as cast" properties of the cast-to-size test
bars exhibit a markedly lower strength and higher ductility in

-46-

Inco 713LC. After solution treatment, however, the cast-to-size bars exhibit properties similar to those of the base-line property test bars except for generally erratic behavior. In contrast to the data in Table XIII, the range of ultimate tensile strength for five machined test bars from heat 65-456 in the solution treated condition was from 131,200 to 137,200 psi. Erratic results were also obtained in yield strength and in ductility in the cast-to-size bars, although the variations are not as large.

The low "as cast" properties of the cast-to-size Inco 713LC test bars indicates that the cooling rate in the hot ceramic shell maybe considerably lower than in the cold, monolithic ceramic mold used for the development of base-line property data. This was confirmed by a cursory examination of dendrite arm spacing which was considerably coarser in the cast-to-size bars.

The room temperature tensile properties of cast-to-size test bars of Inco 718 tend to exhibit considerably higher strength and much lower ductility than those developed as base-line properties, particularly after solution treatment and aging. The same is true of the Rene 41 alloy test bars, but with the decrease in ductility less significant due to its low starting value of 3 to 8% in the base-line property test bars. Based upon the room temperature tensile data, it appears that the Rene'41 cast-to-size test bars would easily meet the required strength levels of GE C 50T53-S7 at 1200°F. As previously reported, the test bars cast in base-line property heat 65-522 were unable to meet the required level of yield strength, 90,000 psi.

Probably the most improtant fact to be gathered from the cast-to-size test bar data when compared to the data previously reported for the test bar more representative of the casting methods typical of large precision castings, is that Inco 713LC exhibited the smallest difference in properties among the three alloys tested. This again indicates the lower sensitivity of the alloy to section size, cooling rate, etc. when compared to the other alloys investigated.

-47-

VII.   SURVEY OF THE OPTICAL MICROSTRUCTURE OF CAST
         INCO 713 LC, RENE 41, AND INCO 718 ALLOYS

A.   Introduction

In order to gain a more thorough understanding of the role of section
size, cooling rate, heat treatment, etc., on the mechanical properties of
the alloys involved in the program, an investigation of microstructure was
undertaken. For the most part, the specimens for metallographic examination
were taken from test bars or castings used in the early stages of the base-
line property evaluation. Greater emphasis has been placed in Inco 713LC
alloy since it appears to be the likely candidate for use in Phase II of the
program.

Comprehensive phase studies in nickel-base superalloys require
electron microscopy and x-ray diffraction techniques since most of the
microstructural details are too fine to be resolved in the optical microscope.
However, extensive work using these advanced techniques has defined
various phase reactions in these alloys and is reported in the literature.
In this study, phase identification has been carried out by inference based
upon such published data.

The phases usually encountered in nickel-base superalloys and their
characteristics are summarized below.

1.   Gamma is the fcc nickel matrix.

2.   Gamma-prime is the major strengthening agent in all nickel-base
       superalloys containing appreciable amounts of Al, Ti, Cb or V.
       It is an intermetallic compound whose composition approaches the
       stoichometric ratio A_3B. resulting in ordering of the atomic positions
       and a slight distortion of the lattice. The "B" in A_3B stands for Al,
       Ti, Cb and V or their combinations and "A" stands for Ni. A_3B -
       type intermetallic compounds are classified according to the way
       atoms are ordered. (64) Depending on the stacking sequence of
       ordered layers, six different crystal structures result. Thus, for
       example, Ni_3Al is fcc, Ni_3Ti is hcp and Ni_3Cb assumes a meta-
       stable body centered tetragonal or a more stable orthorhombic
       structure depending on thermal history and composition of the
       parent alloy.

       The role of gamma-prime as a strengthening agent is not well
       understood. However, it is relatively well established that gamma-
       prime does not act as a simple hardening precipitate with associated
       coherency strain fields. It has been proposed that gamma-prime
       acts as a dispersoid and that the gamma/gamma-prime interfacial tension
       acts as a barrier to dislocation movement. (63)

-48-

Ni_3Al-type gamma-prime, when extensively overaged, can be seen as approximately cubic particles at about 1000X or even less. In the non-overaged condition it appears as an unresolvable general precipitate, under the optical microscope. Usually gamma-prime is precipitated directly from the solute-rich matrix upon cooling from high temperature.

3.   MC-type carbides are usually CbC, TiC, (Ti, Mo) C or their equivalents. Their solution temperatures exceed about 2200°F and are not dissolved in the usual solution-treatments. They appear as coarse, irregular particles, distributed according to the solidification segregation pattern.

4. $M_{23}C_6$ type carbides are $Cr_{23}C_6$ or $Cr_{21}Mo_2C_6$. Normally they are precipitated at grain boundaries direct from the matrix. However, Sims (63) points out that they can precipitate according to the following reaction:

$$Gamma + MC = Gamma\text{-}prime + M_{23}C_6 \text{--- } 1$$
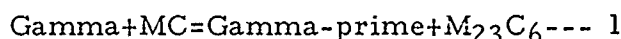
Thus even though MC-type carbides are normally stable, they can decompose according to Equation 1. In certain alloys like Rene'41, $M_{23}C_6$ transforms in situ to M_6C when the Mo content of the alloy is about 9% or higher.

$M_{23}C_6$ can precipitate at grain boundaries as films, globules, platelets, lammelae or a cellular growth (65). The globular morphology is considered the least detrimental to properties.

5. M_6C-type carbides are mainly Mo_6C, with some dissolved Cr. When precipitated direct from the matrix, they appear as randomly distributed, approximately spherical particles.

6.   TCP Phases or topologically close packed phases found in nickel-base alloys are laves, mu and sigma. They are extremely brittle, refractory, complex intermetallic compounds. Occasionally they form as layers aligned on the close-packed planes of the fcc matrix and manifest as Widmanstatten needles in the microstructure. When present in this type of morphology, TCP phases provide continuous fracture paths and embrittle the structure. Their formation results in a drain of solute elements and a weakening of the matrix.

7.   Minor Phases present in nickel-base alloys are borides and nitrides. Their contribution to the properties is relatively minor in most commercial alloys.

The metallography of cast nickel-base superalloys is less well documented than that of their wrought counter parts. The photomicrographs presented in this report should help as introduction to this area.

B.   Inco 713 LC

Alloy 713 LC is a low carbon, cast nickel-base superalloy, developed by the International Nickel Company. This alloy has been introduced recently and no definitive structure descriptions have appeared in the literature as yet. Private communication from the International Nickel Company indicates that the phases detected in this alloy are MC, $M_{23}C_6$, M_3B_2, gamma-prime and gamma. X-ray diffraction analysis conducted at the Laboratory on electrolytically extracted residues from as cast 713 LC indicates the presence of $M_{23}C_6$, CbC and gamma-prime.

Specimen Preparation Procedure

After several trials, the following two-step etching procedure was found to be satisfactory.

Step 1   Etch for 1 second in a mixture of 15cc of concentrated HNO_3 and 7 drops of concentrated HF.

Step 2   Etch by swabbing with a solution 25cc of conc HCl and 3.5 gms of $FeCl_3$. $6H_2$) in 100cc of distilled water.

As Cast Structure

Figures 17 and 18 show the as cast structure of 713 LC. The segregation due to dendritic solidification is clearly seen in Figure 17. The coarse, irregular particles, distributed according to the segregation pattern are thought to be the MC type columbium carbides.

The massive white-etching constituent, the structure of which can be clearly seen in Figure 18, is eutectic gamma-prime. This constituent was originally identified by Gregg and Piearcey (66).

The general precipitate in Figures 17 and 18 is gamma-prime formed during cooling in the mold from high temperatures. In this condition, the precipitate is too fine to be resolved at 500X (Figure 18).

The small irregular particles found at the grain boundary in Figure 18 are thought to be $M_{23}C_6$.

Effects of the Cooling Rate from Solution-Treating Temperature on Structure

Figures 19 through 26 illustrate the effects of water quench, oil quench, air cool, insulated cool and furnace cool on the structures of as cast 713 LC after a 2-hour solution-treatment at 2150°F. The insulated cool is representative of the cooling rate of a test bar cooled in Sil-O-Cel and is plotted in Figure 129.

-50-

It is surmised from figures 19 through 26 that:

1. The MC-type carbides are not dissolved at 2150°F.

2. $M_{23}C_6$, general and eutectic gamma-prime are dissolved at 2150°F.

3. Water and oil quenching of small sections result in an almost complete retention of dissolved solute elements (Figures 19 and 20).

4. The amounts of general and boundary precipitates increase with decreasing cooling rate from 2150°F.

5. The general gamma-prime becomes progressively coarser, with decreasing cooling rate from 2150±F. In the furnace cooled sample, this precipitate is readily resolved at 500X (Figure 26).

6. The "density" of the general gamma-prime precipitate follows a pattern similar to that produced by dendritic segregation. Hence it is deduced that complete homogenization is not effected by the solution treatment at 2150°F.

7. Coarse, irregular particles found at the boundaries in the insulated and furnace cooled specimens (Figures 24 and 26) are believed to be $M_{23}C_6$. These particles are much less abundant in the air-cooled specimen (Figure 22) and are not detected at all in the water and oil quenched specimens (Figures 19 and 20). It would appear that the circled areas in Figures 22 and 24 show MC carbides which have been partially converted to $M_{23}C_6$ and gamma-prime by the reaction shown in Equation 1.

Effects of Aging on Structure

Figures 27, 28 and 29 show the structures of cast 713 LC aged for 16 hours at 1200, 1550 and 1700°F, respectively. Effects of this aging treatment on the room temperature tensile properties are shown below.

Effect of Aging on the Room Temperature Tensile Properties of As Cast Alloy 713 LC

Aging Treatment	Y. S. (Ksi)	T. S. (Ksi)	%El	%R. A.
none	108/113	123/132	7/10	10/15
1200F-16 hr-A. C.	116	135	8	10
1550F-16 hr-A. C.	109	122	5	10
1700F-16 hr-A. C.	105/108	116/119	6/8	15/26

No significant differences can be detected between the as cast and 1200°F aged microstructures (Figures 18 and 27). The tensile properties are also comparable. At higher aging temperatures, the matrix precipitate coarsens and some evidence of $M_{23}C_6$ and gamma-prime precipitation at the grain boundaries can be seen. Apparently this results in some loss of tensile strength.

Figures 30, 31 and 32 show the structures of solution treated (2150°F - 2 hr-A.C.) 713 LC aged for 16 hours at 1200, 1550 and 1700°F, respectively. Effects of the aging treatment on the tensile properties are shown below:

Effects of Aging on the Room Temperature Tensile Properties of Solution Treated (2150F-2 hr-A.C.)713 LC

Aging Treatment	Y.S. (Ksi)	T.S. (Ksi)	%El	%R.A.
none	108/113	131/137	10/11	14/19
1200F-16 hr-A.C.	123	138	9	14
1550F-16 hr-A.C.	121	137	5	8
1700F-16 hr-A.C.	119/121	129/133	6/7	12

The aging treatment at 1200F, as shown above, results in a substantial improvement in yield strength of the solution-treated alloy. The matrix of the aged structure (Figure 30) appears to be much less resolvable that that of the solution-treated structure (Figure 22). This may be an evidence for the additional general gamma-prime precipitation on a fine scale which contributed to the yield strength improvement. Increases in the aging temperature result in some loss of strength. However, the structures remain approximately the same. (Figures 31 and 32)

Effect of Creep Rupture Testing

The structures of as cast and solution treated 713 LC specimens exposed to 1600F-40Ksi rupture testing are shown in Figures 33 and 36. The rupture properties are shown below.

1600F-40KSI Rupture Properties of 713 LC

Thermal History	Life Hrs.	MCR %/Hr.	%El	%R. A.
As Cast	161.0	0.016	6	5.5
2150F-2 hr-A.C.	243.7	0.005	6	5.5

The general gamma-prime precipitate in the solution-treated specimen(Figure 36) appears to be finer than that in the as cast specimen (Figure 34). This may explain the longer rupture life of the solution-treated specimen. Both specimens show evidence of gamma-prime and $M_{23}C_6$

-52-

precipitation at the grain boundaries, probably according to the reaction Gamma+MC= Gamma-prime+$M_{23}C_6$. The MC type columbium carbides in Figures 34 and 36 seem to have decomposed to a certain extent.

The structures of as cast and solution-treated specimens of 713 LC exposed to 1800F-22 Ksi rupture testing are shown in Figures 37 through 40. The rupture properties are shown below:

1800F-22KSI Rupture Properties of 713 LC

Thermal History	Life Hrs.	MCR %/Hr.	%El	%R. A.
As Cast	64.4	0.038	7	7
2150F-2 hr-A. C.	63.3	0.037	11	7

Inspection of Figures 37 through 40 reveals that

1. The specimens tested at 1800F-22 KSI (Figures 37 and 39) show more extensive grain boundary precipitation than those tested at 1600F-40 KSI (Figures 33 and 34).

2. The as cast and solution-treated specimens tested at 1800F-22 KSI show

    a) Almost continuous gamma-prime precipitate with $M_{23}C_6$ particles at the grain boundaries.

    b) MC carbide particles partly decomposed into gamma-prime and $M_{23}C_6$.

3. The general gamma-prime precipitate is readily resolved at 500X in both specimens, which is an evidence of agglomeration of gamma-prime at 1800F-22 KSI.

    C. Inco 718

INCO 718 was developed by the International Nickel Company for applications up to about 1300F. The physical metallurgy of Inconel 718 is well reported in the literature (64, 67).

The phases encountered in Alloy 718 along with their characteristic features are shown below.

Phases Detected in Alloy 718

Phase	Description	Solution Temperature	Metallographic Features
Gamma	Ni rich matrix	-	Matrix
Gamma-Prime	Metastable body centered tetragonal Ni_3 (Cb, Ti, Al)	1600°F	When overaged, appears as unresolvable matrix precipitate at 1000X
M_6C	$(NiCb)_6C$	1700°F	Globular particles
Laves	A_2B type Ni_2CB	2100°F	Irregular, blocky white etching phase
Ni_3Cb	Orthorhombic	1800°F	Dark etching, can assume Widmann-Statten morphology upon heat treatment
M (CN)	Cb, Ti, CCN	2100°F	Massive elongated particles. Also appears as a cellular grain boundary film.

The strengthening agent, gamma-prime, in alloy 718 is metastable body centered tetragonal Ni_3(Cb, Ti, Al) which transforms to orthorhombic Ni_3Cb upon long exposures at 1400 to 1700°F. This transformation results in overaging of the alloy. Hence to obtain maximum strengthening the alloy should be aged below the temperature ranges indicated.

Specimen Preparation Procedure

No difficulties were experienced during preparation of metallographic specimens. An electrolytic etch using 5% chromic acid at 15 volts and 3.2 amps/in^2 produced satisfactory results.

As Cast Structure

The as cast structure of alloy 718 is shown in Figure 41. Massive white etching laves phase and M(c, N) type carbide can be seen in the dark etching interdendritic region which is Ni_3Cb. Both Ni_3Cb and the gamma matrix are heavily cored.

Effect of Heat-Treatment

The effect of an 1800°F-2 hr-A.C. solution treatment on the structure of alloy 718 is shown in Figure 42. The Ni_3Cb has assumed an acicular

morphology.

The laves phase remains essentially unchanged. Also some un-dissolved carbide particles can be seen. The matrix is clear, solute-rich gamma.

Figure 43 shows the structure alloy 718 in the solution-treated and aged condition. The aging treatment was 1325°F-8 hrs-furnace cooled to 1150°F-8 hrs-air cooled. The object of the heat treatment was to precipitate gamma-prime without overaging. The gamma-prime precipitate manifests as a dark etching matrix in Figure 43.

D. Rene' 41

Rene' 41 was developed by the General Electric Company. The phases reported to be present in wrought Rene' 41 along with their characteristic features are shown in the following Table (68).

Phase Behavior in Wrought Rene' 41

Phase	Appearance	Solution Temp.
Gamma	Nickel rich matrix	-
Gamma-prime $Ni_3(Al, Ti)$	Fine uniform particles throughout the structure at 1400 F coarser at higher temperatures	1900 to 2000 F
Sigma	Irregularly-shaped Widmann-statten and grain boundary phase	1800 to 2000 F
MC Carbides TiC and (Cb, Ti) C	Uniformly dispersed irregularly shaped coarse particles	2250 F
$M_{23}C_6$ $(Cb, Mo, Cr)23C_6$	Irregular coarse particles at grain boundaries. Transform	About 1900 F
M_6C $(Cb, Mo, Cr)_6C$	Somewhat spherical particles. Before solution treatment they are randomly distributed. When forming from $M_{23}C_6$ they will remain in place.	2100 to 2250 F

Specimen Preparation Procedure

No excessive difficulties were encountered during specimen preparation. The etchant used consisted of 92cc of HCl, 5cc of H_2SO_4 and 3cc of HNO3 (68).

-55-

As Cast Structure

The as cast structure of René 41 is shown in Figures 44 and 45. The dendritic structure of the alloy is clearly seen in Figure 44. These figures show:

1. Coarse MC and M_6C type carbides, occurring in inter-dendritic regions.

2. Coarse general gamma-prime throughout matrix. The "density" of gamma-prime also follows the solidification segregation pattern.

Effects of Heat-Treatment on Structure and Properties

The effects of heat-treatment on the room temperature tensile properties of René 41 are shown in the following table.

Effects of Heat Treatment on the Room Temperature Tensile Properties of Cast Rene 41

Thermal History	0.2% Y.S. Ksi	T.S. Ksi	El%	R.A.%
As Cast	78.4/79.6	124.0/128.0	16	19/23
1950F-4 hr-A.C.	82.0/83.5	106.0/112.0	11/17	16/19
2150F-2 hrs-A.C.	81.6	126.0/129.6	33	30/32
1950F-4 hrs-A.C.+	98.0/101.2	111.6/114.0	3/5	7.7/9.3

The structures of heat-treated René 41 are shown in Figures 46 through 48. It is concluded from these figures that:

1. The solution-treatment at 1950F results in partial solution and reprecipitation of gamma-prime. However, the carbides at the grain boundary are essentially unaffected (Figure 46).

2. The solution-treatment at 2150F results in extensive solution and reprecipitation of gamma-prime. Almost all the M_6C carbides are dissolved, while MC carbides are not affected. The grain boundary precipitation upon air cooling from 2150F is light and probably consists of $M_{23}C_6$ or M_6C (Figure 47). These reactions would explain the superior strength and ductility of the solution treated specimen.

-56-

3.   As shown in the above table aging at 1400°F subsequent to solution-treating at 1900 embrittles Rene 41. The structure (Figure 48) showed heavy and continuous grain boundary precipitate and also rod like particles not seen in other structures. It is beli..ved that the new phase is sigma and accounts for the embrittlement.

E.   Summary

A representative microstructure of cast Inco 713 LC shows general and eutectic gamma-prime precipitates, MC-type columbium carbides and $M_{23}C_6$-type chromium carbides in a gamma matrix. The gamma-prime in this alloy is Ni_3 (Al, Ti, Cb) with a face centered cubic Ni_3Al structure. A solution-treatment at 2150F dissolves all constituents except the MC carbides. Cooling from 2150F produces a general gamma-prime precipitate, the particle size of which increases with decreasing cooling rate. In addition, at low enough cooling rates, a reaction represented by the following equation occurs.

$$gamma(matrix)+MC=gamma-prime+M_{23}C_6$$
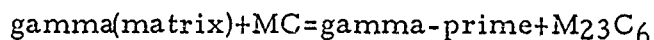
$M_{23}C_6$ appear at grain boundaries as irregular coarse particles, enveloped in gamma-prime. No topologically close-packed phases were detected in this alloy.

A representative microstructure of cast Inco 718 consists of laves phases embedded in Ni_3Cb in interdendritic regions, MC-type carbides and the gamma matrix. The gamma-prime in this alloy is metastable body centered tetragonal Ni_3Cb which transforms to ortho-rhombic acicular Ni_3Cb upon overaging. The bct Ni_3Cb is not resolvable with the optical microscope. Solution treatment at 1800F does not dissolve the laves phase.

A representative microstructure of as cast Rene 41 consists of general gamma-prime, MC and M_6C-type carbides and the gamma matrix. The gamma-prime in this alloy is Ni_3(Al, Ti) with a face centered cubic Ni3Al structure. Prolonged holding at 1400F results in sigma formation with a drastic embrittlement. The microstructures of Inco 713 LC are relatively less complex than those of Inco 718 and Rene 41. TCP phases, laves and sigma were found to occur in Inco 718 and Rene 41, respectively. These complex intermetallic compounds drain the matrix of alloying elements. Consequently, only smaller fractions of the alloying elements are available for gamma-prime formation and the strengthening effects gained from that formation. Inco 713 LC did not exhibit any TCP phases in the conditions investigated. Thus the alloying elements are beneficially utilized in gamma-prime formation. TCP phases are extremely brittle and could provide excellent fracture paths. Their absence provides 713 LC with superior resistance to embrittlement.

The grain boundary precipitate in Inco 713 LC consists of coarse particles of $M_{23}C_6$ enveloped by gamma-prime. This morphology is generally considered to be least detrimental to tensile and creep properties.

For the most part, the examination and classification of the microstructures of the three alloys indicates that the simpler Inco 713 LC shows less tendency for the formation of deleterious structures during solidification and slow cooling, a significant factor for consideration when heavy casting sections are inevitable. The low strength of Inco 718 illustrated in previous reports appears to be a function of segregation and the formation of massive phases which rob the matrix of the strengthening mechanisms. The low ductility of Rene' 41 is apparently due to the formation of grain boundary precipitates inherent in the alloy. In general, then, the choice of Inco 713 LC among the three alloys for use in large castings appears justified on the basis of microstructure as well as properties.

VIII. OTHER PROPERTIES OF INCO 713 LC

A. Low Cycle Fatigue Properties

1. Introduction

One of the properties of an alloy that is pertinent to its performance as a turbine rotor and structural material is its resistance to low-cycle fatigue failure. It was considered desirable, therefore, to determine the low cycle fatigue properties of Inco 713 LC since, at this stage of the program, it was established that Inco 713 LC would be the alloy from which both the turbine and airframe components would be manufactured in Phase II.

2. Procedure

Twenty-three test bars from several heats were shipped to Metcut Research Company for machining to low-cycle fatigue specimens of the type shown in Figure 49. The test bar identification was as follows:

Heat Number	Number of Bars Shipped
66-388	6
66-400	4
66-433	6
66-456	4
66-385	3 (spares)

All bars had been heat treated at 2150°F for two hours followed by an air cool. It should be noted that the test bars submitted for low cycle fatigue testing come from the same heats from which spin test discs were shipped or tested, except for the three spares. The bars were produced from the standard test bar pattern previously described. All were poured under essentially identical conditions.

All fatigue tests were conducted on a closed loop, servo activated, hydraulic test system. The apparatus is shown in Figure 50 with a specimen in position in the loading frame, to the left, rady for room temperature testing. Because the extensometer notches were outside the specimen uniform section, it was necessary to calculate an effective gage length. This was done under the assumption that all deformation outside the gage section was elastic. A summation of incremental elastic deformations over the changing cross-section in the specimen radii provided an effective gage length value.

The signals from the load cell of the test system and the extensometer transducers were fed into an x-y recorder which was calibrated in terms of load and strain. Mechanical load-strain hysteresis loops were

recorded periodically throughout each test. Schematic load-strain curves for the first one and one-half cycles were drawn to graphically illustrate the strain functions in Figure 51. The modulus was calculated on the initial load-strain slope. Subsequent recorded hysteresis loops were individually analyzed to determine the trend of load-strain behavior during each test.

Elevated temperatures were achieved by induction heating. A Lepel 5KW induction heater in conjunction with a stepless saturable core reactor control system maintained $1000 \pm 10°F$. Thermocouples mounted on the specimen fillets were used to establish uniform heat distribution across the gage length. In addition to thermocouple (t/c) recordings, an Ircon infrared radiation pyrometer monitored the temperature at the center of the gage section. Correlation between t/c and pyrometer readings indicated good temperature distribution.

The following conditions were maintained throughout the experimental program:

1. Longitudinal strain amplitude control.
2. Triangular wave form.
3 7.2 cpm frequency.
4. A-ratio of 1.0
5. Nominal room temperature of 77°F or elevated temperature of $1000 \pm 10°F$.

3. Results and Analysis

The fatigue data obtained are reported in Table XIV. Fatigue curves were drawn through the plotted points of alternating strain as function of cycles to failure in Figure 52. The plotted data exhibited very little scatter at elevated temperatures. At room temperature the observed scatter was fairly large at the high strain levels. This was probably a manifestation of the sensitivity of the crack detection system of the apparatus; that is, the number of cycles to failure mark the point in a test where a fatigue crack(s) had grown to a size sufficient to shut down the machine through a change in specimen compliance. Much of the scatter thus reflects the variation in fatigue crack size at the several shutdowns.

The data generated in this program suggested that the room temperature and 1000°F high cycle fatigue curves might converge. Extrapolation of the curves of Figure 52 indicated convergence would occur at about 10^5 cycles.

Comparison of the moduli reported in Table XIV to data reported elsewhere for cast Inconel 713 LC showed reasonable agreement within the limit of experimental errors. The arithmetic average of moduli measured in this program was 28.7 psi x 10^6 at room temperature and 24.4 psi x 10^6 at 1000°F.

-60-

The establishment of the low cycle fatigue behavior of Inco 713 LC will permit use of these data in the design of the final turbine rotor casting. In general, the data for cast 713 LC compare favorabley with materials currently in use for turbine rotors and other superalloy components.

4. Additional Comments

Fatigue behavior is observed to vary with microstructure, particularly grain size. Since cast metals can exhibit rather wide variations in grain size, it follows that the measured fatigue strength of a cast alloy should be referenced to the accompanying grain size to insure appropriate application of the data.

All fatigue specimens tested in the subject program were machined from castings of the given size with the specimen axis coincident with the length of the cast bar. One bar, not otherwise utilized, was sectioned, ground, polished and etched to disclose the grain structure. The most revealing structure was observed on a section normal to the bar (and specimen) axis. A photomacrograph of the transverse section is shown in Figure 53. It was evident from the solidifcation pattern that the thermal transfer characteristics of the mold resulted in a liquid-solid interface movement primarily inward from the outside bar surfaces. The resulting columnar grains were basically oriented in a fan-like distribution from a plane containing the bar center-line. The microstructure of the cast bars, therefore, was best described as consisting of elongated grains roughly parallel to the radial direction.

Two comments may be made with regard to the observed grain structure. First, the grain size dimension parallel to the loading axis in all specimens was rather small, typically about 0.40 in. Second, the planes parallel to the specimen axis would exhibit microstructures varying from equiaxed grains about 0.040 in. diameter to elongated grains about 0.25 in. by 0.040 in., depending on the angular relationship with the direction of elongation.

The ramification of the comments are as follows. The fatigue data may be associated with a medium grain size cast alloy since the uniaxial fatigue loading was parallel to the minor grain dimension. However, because the fatigue specimen reduced sections were cylindical, the outside surface of the reduced sections traversed the major grain axes at all possible angles and macroetched specimens could lead to an erroneous impression of a mixed grain size. A few failed specimens were macroetched and the reduced sections exhibited both equiaxed and elongated grains, confirming the anticipated behavior.

B. Coefficient of Thermal Expansion

The coefficient of thermal expansion for Inco 713 LC was determined on a Brinkmann-Netzsch Dilatometer for the temperature range from room temperature to 2000°F. The Brinkmann-Netzsch instrument provides a continuously programmed heating rate. During the heating cycle, the change in length of the specimen, a 1.5 inch long by 0.4 inch diameter bar, is continuously monitored by a sensitive recording instrument. After corrections for the expansion of instrument components is applied, the curve obtained represents an extremely accurate measure of the linear expansion of the specimen as temperature increases. The curve shown in Figure 54 is representative of the average of tracings obtained in three such trials. The values of the coefficent of thermal expansion for Inco 713 LC have been calculated from these average values of expansion from room temperature to 2000°F in increments of 200°F (room temperature is taken as 75°F), and are listed in Table XV. Intermediate values may be calculated from Figure 54.

It should be noted that the values listed in Table XV for the "LC" grade of 713 are somewhat higher than those listed for Inco 713 C in current literature.[69] It is not known at this time if this is a fundamental alloy difference between the high and low carbon grade or a difference reflecting the equipment and procedures of the tests.

C. Notched Tensile and Stress Rupture Properties of Inco 713 LC

In order to expand the knowledge of the behavior of Inco 713 LC further in the direction of turbine rotor design, it was suggested that the notched tensile and stress rupture properties of the alloy be investigated briefly.

Nine test bars were selected from extra stock cast during the course of the program. Bars from two heats were available. All nine bars were solution treated at 2150°F for 2 hours followed by an air cool. After heat treatment, the bars were machined to the standard test bar shape illustrated in Figure 9 (F42) with the addition of a notch located centrally in the gauge section. The notch dimensions had been previously calculated to give stress concentration factors (K_t) of 2.0, 3.0 and 3.7 in three sets of three bars each. Surface finish in all critical areas was maintained better than 16 micro-inches.

One test bar representative of each stress concentration factor was tensile tested at room temperature. Another set of three bars were stress rupture tested at 1800°F - 22,000 psi. A third set was tensile tested at 1200°F.

The results of the notched tensile and stress rupture tests on cast and solution treated Inco 713 LC are shown in Table XVI.

-62-

As shown at the bottom of Table XVI, the tensile tests result in an average notched-unnotched tensile ratio of 1.3 This falls into the category of materials with low notch sensitivity. The stress-rupture tests also provide sufficient evidence to indicate that the material is strengthened by the presence of a notch at the stress and temperature of the test.

The data provided by these tests will help the design engineers toward designing the full scale cast turbine rotor.

D. "Low" Temperature Creep Properties

In the effort to meet requirements for 0.2% creep property data for the General Electric turbine rotor design, a total of eleven creep tests at temperature of 1000°F and 1200°F were run on standard test bars. A summary of all tests is shown in Table XVII. Specimens were all solution treated for 2 hours at 2150°F.

The most significant data in Table XVII was obtained from specimen 67-506-2A, tested at a load of 105,000 psi and a temperature of 1200°F. This test bar provided the time for cast Inco 713 LC to reach 0.2% creep at the load and temperature values listed. By designing certain loads in the final turbine rotor to a value less than 105,000 psi, the designer can, on the basis of these figures be reasonably assured of a 100-hour life with 0.2% creep as failure, rather than catastrophic bursting.

This completed all 1000°F and 1200°F creep testing.

-63-

IX.   PROPERTIES OF SIMPLE PLATE CASTINGS

A.   Specimen Design

Of the several types of specimen which might be chosen to study
the effects of foundry variables on the mechanical and casting properties
of a metal, the simple, infinitely fed, feeding distance plate appears
to have the greatest advantage.

The feeding distance plates designed for this program are in the
form of a wing-block. The plate thicknesses are 1/2 inch at the ends
and they become thicker at a 6° taper toward a central riser which is large
enough to be considered infinite to the plates. One plate is three inches
in length from the riser and the other is six inches long. The plates and
the central riser are 5 inches in width. This is wide enough to provide
tensile and other specimens. The pattern built to produce this casting
for the study of feeding distance and other foundry variables is shown
in Figure 55. As can be seen in the photograph, each 14 x 18 inch cope
and drag produces two feeding plate castings. The two castings are fed
from a central downsprue in the cope which leads to the bottom extension
of the risers and is between the two risers. The casting weight in nickel
base superalloy is 113 pounds per mold, (2 castings). A sketch of the
casting is shown in Figure 56.

Using this casting as the specimen, the effects of several foundry
variables on the feeding distance and mechanical properties of the three
subject alloys can be studied. Feeding distance can be determined through
the liberal use of microradiographic slices cut from the plates. The effect
of microporosity on the alloy mechanical properties can be determined by cutting
test specimens from the plates alternating with microradiographic slices.

The following parameters were to be included in a factorially designed
experiment using this casting:

        a. pouring temperature,
        b. mold temperature,
        c. grain refinement (mold additives).

B.   Experimental Procedures

1.   Molding, Melting and Casting

Using the simple plate pattern described, two ceramic molds (4
plate castings) were prepared for casting in each of the subject alloys,
713 LC, 718 and Rene 41.[70] Prior to the final firing of the molds, one
cavity of each of the two molds scheduled for casting in each of the alloys
was painted with slurry of cobalt oxide and ethyl silicate. The slurry was
made in the ratio of 10g cobalt oxide to 100 ml ethyl silicate. No attempt
was made to alter this mixture. The two molds, each containing one
painted and one unpained plate casting cavity, were then fired with gas-

air torches to remove the final traces of organic material. After closing the cope and drag sections, the molds were permitted to reach ambient temperature prior to loading in the vacuum furnace chamber.

The melting stock and melting procedures used for the plate castings were identical to those described for the base line property test bar heats. After the freeze temperature (liquidus) of the heat had been determined by the bi-color pyrometer, the heat was brought to 100°F above the freeze and mold number one was poured. The furnace was then returned to the melting position and the heat brought to 200°F above the freeze temperature. The second mold was then poured. Unlike the test bar molds, the plates were permitted to cool in vacuum to emphasize the section size effect in the tapered plates. The melting and casting data for the initial plate heats are listed in Table IV under heats 65-511 (Inco 713 LC), 65-529 (Inco 718) and 65-542 (Rene' 41).

The evaluation of these initial plate heats, in combination with the results of the earlier test bar studies previously described, pointed to the choice of Inco 713 LC from the three alloys originally included in the evaluation. In order to complete the study of the effects of typical foundry variables on simple plate castings, two additional 713 LC alloy heats were cast. Heat 66-216 was cast under conditions and procedures similar to those described for heat 65-511 with one significant exception. Prior to loading the finished molds into the vacuum chamber, the riser cavities were fired to red heat with Selas gas-air burners. The riser openings were then covered with asbestos cloth to minimize initial convection and subsequent radiation losses while in the chamber during the melting cycle. The molds were positioned on the turntable and the chamber closed and pumped down immediately. The procedures for remainder of the heat followed exactly those described for heat 65-511.

Heat 66-167 was produced using procedures identical to those described for 65-511. The objectives of this heat were to determine the effects of pouring temperature, grain size as affected by nucleating agents (CoO), and microporosity, on the elevated temperature tensile properties of Inco 713 LC.

2. Shakeout and Derigging

The plate castings were normally shaken out the day after casting, having cooled to ambient temperature. After shakeout, the plates were cut from the risers, cutting as close to the risers as possible. The plates from each mold were identified as A(6-inch plate, CoO) B(6-inch plate, plain), C(3 inch plate, CoO), and D(3-inch plate, plain). The product of one mold prior to derigging is shown in Figure 57.

3. Inspection

All plates were radiographed after cut-off and sand blasting. No

plates were rejected on the basis of conventional X-ray, i.e., no macro-porosity was visible. It was interesting to note, however, that differences in grain size in the plates was quite apparent in the "mottling" effect on the radiographs. It was noted at this time that the plates from cavities coated with CoO were of a somewhat finer grain size than their uncoated companion plates.

4. Specimen Cutoff Procedure

After inspection, each of the plates was cut into sections for tensile testing and microradiographic examination according to the system illustrated in Figure 58. Beginning at the end of the plate furthest from the riser, a 1/2 inch slice was cut (wet abrasive cutoff wheel) followed by a 1/8 inch slice, then another 1/2 inch slice, etc. up to the riser end of the plate. Using this system, a six-inch plate yielded seven tensile specimen blanks and seven slices for preparation as microradiographic samples. The three-inch long plate yielded three tensile blanks and three radiographic slices. Each specimen was identified with is heat number, mold number, plate letter and spcimen number indicating its position relative to the riser, e.g., specimen 65-511-1B4 represents the fourth test bar from the chill end of the B plate in mold 1 of heat 65-511. The suffix A was added for the corresponding radiographic specimens.

5. Heat Treatment

Specimens from the plates scheduled for tensile testing were heat treated after sectioning and prior to final machining. The Inco 713 LC test bars were solution treated. Inco 718 and Rene 41 test bars were solution treated and aged for optimum tensile properties. The final test bar shape is shown in Figure 9 as the F-29 specimen, and is the same as that used for the base-line property tensile tests at room temperature.

6. Testing

The original layout of this initial foundry variable study called for a total of 120 microradiographic specimens, 40 per alloy. After initial attempts at grinding the 1/8" slices to the required thickness of 0.020" proved extremely difficult, the schedule was re-examined and pared to a more reasonable number of test bars and radiographic slices. The difficulty was introduced mainly by the exceptional tendency of the slices to "bow", even with the lightest passes of the grinding wheel, especially when the thickness approached about 0.050". The final method developed involved doing no more than six slices at a time down to 0.040", and finishing the slices one at a time to 0.020". In order to reduce the amount of work involved, only the 6-inch plates poured at $100°F$ superheat were fully examined from each heat. The remaining plates were scheduled for spot checking against the data from these plates. A greater number of tensile tests were scheduled since the time of preparation of the tensile specimens was considerably less than for the radiographic slices.

The sampling procedures were somewhat modified to limit the number of elevated temperature tensile tests on heat no. 66-267 to some

reasonable level. Referring to Figure 58, the sampling schedule was as follows. Specimens 1, 3, 5 and 7 from the six inch plates were tested at 1200°F after cutting, solution treating and machining to standard hot tensile test bars. Specimens 2, 4 and 6 from the six-inch plates were tested at 1600°F. To verify the quality and controlled behavior of the heat, all specimens from the three inch plates were tested at room temperature, and compared with the properties obtained for the identical specimen locations from heat 65-511. No microradiographic samples were prepared since the foundry variable levels for the heat were identical to those from 65-511, which had already been thoroughly evaluated from that viewpoint. Testing procedures for elevated temperature tensile tests have already been described in a prior section.

The method of preparing and evaluating microradiographic specimens was similar to that used by Larson et al.[71]

The radiographic test specimens were exposed one at a time using 135 KV and 10 milliamperes, for 1 min. 15 seconds at a distance of 48 inches. The film type is particularly recommended for this type of high sensitivity work, Kodak type R, single emulsion film. The resultant radiographs were examined at 20 diameters magnification using a zoom type binocular microscope with high-intensity back lighting.

Since there are no microradiographic standards such as exist for conventional radiographic comparison, a set of standards were developed on a descriptive basis. The system was accepted when three individuals read a total of 22 microradiographs and differed in no more than three readings and by only one classification difference. The standards are as follows:

Class	Description
0	No porosity visible at 20 diameters magnification.
1	Some microporosity resolvable at 20 diameters.
2	Considerable porosity resolvable at 20 diameters.
3	Minor porosity resolvable to the unaided eye.
4	Considerable porosity resolvable to the unaided eye.
5	Heavy porosity resolvable to the unaided eye.

The system of reading each microradiograph was to place it in a category such as 0-1, or 3-4, etc., meaning that, in the judgment of the observer, the best it could be categorized would be the lower number

-67-

and the worst would be the higher number. As empirical as this might seem, it appears to have worked quite well.

After reading the microradiographs, the specimens were macro-etched to reveal the grain size corresponding to the location in the plate.

Tensile tests were performed using procedures identical to those described for the base-line property heats.

C. Results and Discussion

As a preface to discussion of the results of microradiographic examination of the cast plates, it might be well to point out that the porosity described is far smaller than would be normally detected by conventional radiographic techniques. For example, if one were to consider the limit of detection as 2% of the cross section, with the 0.020" thick sections examined, a pore of 0.0004" diameter would be detected by the technique. This is a conservative estimate, and the actual sensitivity is probably superior to this. This high sensitivity is the reason that examination of the radiographs with a microscope is a necessity. The eye is incapable of resolving the extremely small discontinuities observed.

1. Room Temperature Properties of Plates Cast In Cold Molds at 100°F Superheat

Using the techniques described in the Experimental Procedure section, the microporosity levels of the 6 inch long tapered plates cast at 100°F superheat were first determined for the three alloys under investigation. The results are plotted in Figure 59 for plain ceramic molds and in Figure 60 for molds. coated with cobalt oxide slurry. The most outstanding factor which emerges from these plots of porosity vs. distance from riser is that the Inco 713 LC alloy exhibits the highest porosity levels among the three alloys cast, i.e., the alloy shows the poorest feeding distance characteristics. In nucleated molds, Inco 718 ranks second and René 41 shows virtually no microporosity over the entire length of the six inch plate. For the most part, the plates cast in the mold coated with cobalt oxide exhibited somewhat better feeding characteristics than their uncoated counterparts. The exception is Inco 718.

The choice of the plates poured at 100°F superheat for initial examination was based upon the fact that the lower pouring temperature would promote the worst possible conditions for feeding, recognizing that, with hot metal risers, higher pouring temperatures promote steeper thermal gradients toward the riser and thereby more directional solidication and better feeding. Early spot checks of several radiographic samples from the nucleated mold cast at 200°F superheat in Inco 713 LC confirmed this as a fact. In general, the microporosity rating

was one classification lower for the equivalent distance from the riser in the plate poured hotter. This is detailed in subsequent paragraphs.

Recognizing that the properties of Inco 713 LC obtained in test bars were the most favorable of the three alloys, the unfavorable position of the alloy from the feeding distance point of view made it imperative that the effect of the observed porosity on the mechanical properties be examined carefully. The most appropriate test for a first estimate of the effects is the tensile test, since it is recognized that porosity effects the tensile strength and ductility of most alloys.

Tables XVIII, XIX and XX show the room temperature tensile properties of Inco 713 LC, Inco 718 and Rene'41 test bars cut from the same plates as the radiographic specimens in accordance with the procedures previously described. The data for the Inco 713 LC 6 inch plates, plain and nucleated, are plotted in Figure 61. The test bars are all in the solution treated condition.

The tensile strength of Inco 713 LC decreases from the chill end of the plate toward the riser for both the nucleated and non-nucleated plates. However, the highest tensile strength obtained at the chill end, 6 inches from the riser, is more than 12,000 psi higher than the highest base line tensile strength of 137,000 psi. In the nucleated plate, only one value, at 1.5" from the riser, falls below the base line property data, and that value is still well above the requirements of AMS 5391A. It should be noted that this point on the plate also exhibits the lowest ductility, 9% El, 16% RA and nearly the highest porosity rating of the plate (See Figure 60). The non-nucleated plate exhibits a generally lower tensile strength and a more severe drop in tensile strength and ductility at the point of highest porosity rating. The reduction in area, however, is still 14% with an elongation of 6%.

The yield strength of Inco 713 LC is much less affected by position in the plate and porosity. As can be seen in Figure 61, the yield strength of the non-nucleated plate drops somewhat more than that of the nucleated plate. However, all values of yield strength in both plates exceed 100,000 psi, and are generally, higher than the base line yield strengths toward the chill end of the plate and equivalent to base line values nearer the riser.

Reduction in area is not significantly affected by position in the plate for either nucleated or non-nucleated plates. Except for two points, one in the nucleated and one in the non-nucleated platem ductility is consistent in keeping with that obtained from base line property test bar castings. The data for the tensile properties of the three inch long plates is shown in Table XVIII. As would be expected when compared to six-inch plates, the properties are excellent. Particularly high ductilities were obtained in the nucleated three-inch plate.

Table XIX and Figure 62 show the tensile data for the nucleated 6-inch plate and the nucleated and plain three inch plates from heat 65-529, Inco 718. In this alloy too, a degradation of tensile strength with increasing distance from the chill end of the plate is obvious. Also, as in Inco 713 LC, the tensile and yield strengths near the chill end are superior to the baseline properties established on test bar castings. The tensile data from the three inch plates indicates a slight superiority of the non-nucleated plate in tensile and yield strength. The effect of porosity on the tensile properties appears to be masked by a section size effect which will be discussed at length in a subsequent section.

As can be seen in Table XX and Figure 60, virtually no microporosity was detected in the cast René 41 plates. Therefore, differences in tensile properties as a function of distance from the riser must be attributed to solidification and cooling rates attendant to the plate section size which increases from 1/2" to 1 1/8" from chill end to riser. This effect is undoubtedly active in the 713 LC and the 718 data as well. Unlike the 718 and 713 LC plates, the tensile properties of the René 41 nucleated plate cast at 100°F superheat show little, if any, superiority to the base-line property data obtained from test bar castings (ret. Table VIII and Figure 63). Elongation, tensile strength, and yield strength all diminish toward the riser. As with the base line properties, the limiting factor for cast René 41 plates appear to be ductility in spite of the virtually total absence of microporosity. One might expect that if porosity was present in any significant amount, the ductility could be reduced to still lower values. Nucleated six-inch plates appear to show some advantage in yield strength and ductility, but of no great significance.

In order to more closely examine the role of section size on the tensile properties obtained from plates cast in the three subject alloys, as well as to determine the effect of cobalt oxide nucleation of the macro-structure, the radiographic slices were macroetched to reveal the grain size and other features of the plate cross sections from chill end (1/2" thick) to riser end (1 1/8" thick). Inconel 713 LC sections were etched in a cold solution of 2 parts water, 2 parts HCl, and 1 part 33% H_2O_2. The other two alloys did not react satisfactorily to this etch and were etched with HCl to which 33% H_2O_2 was added until a reaction was visible. The macroetched specimens, arranged in order of increasing distance from riser from top to bottom, are shown in Figures 64 for 713 LC alloy and in Figures 65 and 66 for alloys 718 and René 41 respectively.

As can be seen in Figure 64, the mode of solidification of the Inco 713 LC cast at 100°F superheat is strongly columnar with or without nucleation. The effect of the cobalt oxide, however, is obvious in the decreased width of the columnar grains in the appropriate plate, indicating a distinct nucleating effect produced by the presence of cobalt oxide at the metal-mold interface. The effect is particularly noticeable in the heavier end of the plate. Observation of the increasing grain size from the chill end of the plate to the riser end provides a strong clue to the behavior of the tensile properties from chill to riser, aside from the effects of

-70-

microporosity observed.

Inco 718 plates cast at 100°F superheat tended to solidify almost entirely equiaxially per Figure 65. The increase in grain size from chill to riser is quite obvious, although not as much so as in Inco 713 LC. In addition, the grain refining effect of cobalt oxide, if it exists for this alloy, is masked by a generally fine grain throughout the plate.

René 41 plates also exhibit an increase in grain size from the chill end to the riser end as a function of the section thickness. The effect of the cobalt oxide is, in this alloy, to promote a sharply columnar growth consisting of very fine columnar grains, compared to the tendency of the unnucleated plate to be equiaxed with increasing grain size as section size increases. This may be observed in Figure 66.

Up to this point, it appears obvious from observations of the macro-etched plate slices that the tensile property degradation observed in all three alloys from chill end to riser end is a function of the increasing grain size, which is a section sensitive parameter, as well as microporosity.

Considering, in particular, Inco 713 LC, the effects of small amounts of microporosity and grain size on the room temperature tensile properties are small compated to the base line properties established in test bar castings.

Considering Inco 718 and René 41, the section size effects appear to be somewhat greater than for 713 LC, but not so great as to rule out the use of the alloys in large castings. In the case of René 41, in plates or test bars, the usefulness of the cast material is restricted by minimal ductility.

2. Room Temperature Properties of Inco 713 LC Plates Cast In Cold Mold at 200°F Superheat

Following the procedures previously outlined, the room temperature tensile properties of Inco 713 LC plate castings were evaluated for material cast at 200°F over the liquidus for comparison with the data reported for same heat, 65-511, cast at 100°F over the liquidus. Plates were poured into both nucleated and plain molds at this higher pouring temperature. The results are shown in Table XVIII together with the results originally reported for the lower pouring temperature. Figure 67 graphically illustrates these data. The effect of the higher pouring temperature on the level of microporosity in the six-inch plates is shown in Figure 68.

In general, the effect of the higher pouring temperature is to reduce the amount of microporosity in the tapered plate casting, as would be expected with a hot-metal-riser system which tends to increase the desirable thermal gradient with an increase in pouring temperature.

There is, however, a marked increase in grain size which accompanies this increase in feeding capability. The macrostructures of microradiographic slices taken from the plates poured at 200°F above the liquidus are shown in Figure 69. The increase in grain size accompanying the increase in pouring temperature may be seen by comparing Figure 69 with Figure 64. These macrostructures also illustrate the marked increase in the beneficial effects of nucleation by cobalt oxide on the metal-mold interface as pouring temperature is increased. To put this another way, it appears that, if small grain size is taken as the criteria, nucleation becomes far more important as the pouring temperature is increased from 100°F above the liquidus to 200°F above the liquidus and higher.

The tensile properties of test bars cut adjacent to the microradiographic specimens shown in Figure 5 exhibit somewhat lower levels of tensile and yield strength than those cut from plates poured at 100°F above the liquidus. This may be seen by comparing Figure 67 with Figure 61, or by referring to Table XVIII. The ductility, if anything, is somewhat better for the plates poured at the higher temperature, a secondary indication of reduced microporosity. In general, the nucleated plates, with the finer grain size, show an advantage over the unnucleated plates in tensile and yield strengths. Elongation and reduction in area, show considerable cross-over between the nucleated and unnucleated plates, indicating no particular advantage.

The nucleating (or "grain refining") effect of the cobalt oxide is still more evident in 713 LC plates cast at 200°F superheat, as seen in Figure 69. In this case, the unnucleated material tends clearly toward large, equiaxial grains, although the directionality of the solidification was still noted in the dendrite growth. The presence of cobalt oxide at the mold metal interface clearly provides many more sites for initial crystal growth and, thereby, produces a relatively fine grain size throughout the cross section. Further evidence of the ability of cobalt oxide to "throw" across a relatively heavy section was found in the riser bases from the Inco 713 LC plates cast at 100°F superheat. Figures 70 and 71 show the grain size of cross sections of the heavy keels located below and between the six inch and three inch plates from heat 65-511. The only difference between the keels, since they were poured from a mutual downsprue, is that one was coated with cobalt oxide as previously described. Obviously, a refining effect exists, not only at the surface, but throughout the entire 3 inch cross section. It should be noted, however, that this effect was wiped out completely at higher pouring temperatures, i.e, 200°F superheat.

3. Room Temperature Properties of Inco 713 LC Plates Cast in Pre-heated Molds at 100°F and 200°F Superheat

The tensile properties and microporosity levels of the plates cast in heat 66-216 are listed in Table XXI. The tensile data for the six inch plates are presented graphically in Figures 72 and 73. Microporosity levels are plotted in Figures 74 and 75. Macrostructures appear in Figures 76 through 79. The macrostructure of the three inch plates has been included.

As might be expected, the effect of preheated risers on microporosity levels is quite favorable, particularly in the heavier plate sections near the risers. The considerable advantage offered by higher pouring temperature in molds with unheated risers appears to be masked by the more significant effect of riser preheat. For the most part, as in previously reported results, nucleation appears to aid somewhat in reduction of microporosity. Examination of all of the microporosity data presented in the current work indicates that the following conditions are generally favorable to reduced microporosity (increased riser feeding distances) in Inco 713 LC cast under the conditions described:

(1) Nucleation by cobalt oxide at the metal-mold interface

(2) Preheating of mold riser cavities

(3) Increased pouring temperature

Riser preheat had virtually no effect on yield strength. One unusually high yield strength value was obtained in specimen number 66-216-2A3, but this does not appear to be representative of the general trend in the plate. The effect of microporosity or section size on yield strength as influenced by distance from the riser is apparently minimal. Some slight trend downward with increasing proximity to the riser may exist, but the unusually high level previously noted for specimen 66-216-2A3 has distorted the plot for the yield strength of the unnucleated plate too dratically to be able to recognize a trend of minor proportions. Theoretically speaking. such a trend as a function of section size is possible, but it is most unlikely that it could occur as a function of porosity.

In general, preheating of the riser has had a favorable influence on tensile strength. This may be assumed to be a function of improved feeding distance and lower microporosity levels. Th behavior of tensile strength is generally to improve, as in the pa ., with the presence of a nucleant in the mold. One exception to this behavior can be seen in Figure 72. The low tensile strength shown for the specimen just past two inches from the riser is matched by a low elongation and reduction in area together with a normal yield strength. This combination of factors points to microporosity as the cause of low tensile strength in this specimen. Lower pouring temperatures (again with the exception of the low tensile strength of the specimen discussed above) appear to generally improve tensile

strength, with the most pronounced improvement occurring in the unnucleated plates. This stands to reason, particularly if it is assumed that grain size is exerting a strong influence on tensile strength in cases where microporosity may be ignored. This effect of grain size, as well as other factors influenced by solidification rate is illustrated by a general downward trend in tensile strength as section size increases. The section size increases toward the riser due to the six-degree taper designed into the plates.

An overall improvement in ductility, both elongation and reduction in area, is affected by riser preheating. The effect is again attributable to the decrease in microporosity. As in this discussion of tensile strength, one exception to this general behavior can be seen in Figure 72.

With the preheated risers, the effect of nucleation is to yield a slightly improved ductility at the higher pouring temperature, with no clearly definable trend at the lower temperature. This may be attributable to the grain size differences which are shown in Figures 76 and 78. The improvement in grain size with nucleation is quite obvious in the alloy poured with 200°F superheat. However, the overall grain size for the plates poured with 100°F superheat is much finer, even with no nucleation.

With cold risers, the ductility improved somewhat with increased pouring temperatures. This is not the case with preheated risers. Apparently the improvement in feeding distance afforded by the higher pouring temperature with cold riser cavities is masked by the similar improvement imposed on the system by riser preheating. If anything, the lower pouring temperature appears to afford some very slight advantage.

No separate effect of section size on ductility could be ascertained for the plates poured with preheated risers. This may be noted to be similar to the plates poured with cold riser cavities.

In Figures 76 through 79, the effects of the variables imposed on the system on the macrostructure may be observed. Comparing these structures with those presented previously for plates cast without preheated risers, little difference may be noted except at the higher pouring temperature with no nucleation. Under these conditions, it appears that the grain size of the plate with the heated r'ser is slightly larger than that of the cold-riser plates. Figures 77 and 79 illustrate the grain size of the three inch long plates, not previously shown. As can be seen, the effects of the variables are the same as can be observed in the six-inch plates.

4. 1200°F and 1600°F Properties of Inco 713 LC Plates
   Cast in Cold Molds at 100°F and 200°F Superheat

Test bars cut from the three inch long plates from heat 66-167 were tested at room temperature in order to provide a controlled level for comparison against elevated temperature properties. The results of these tests are listed in Table XXII and are plotted against distance from the riser in Figures 80 and 81. Three cases of low ductility were observed

-74-

in the three-inch long plates from this heat. Test specimens 1D2, 2C3 and 2C4 exhibited 6, 8 and 7 percent elongation respectively. All three bars also exhibited low tensile strengths compared to the bars surrounding them in their respective plates. It may therefore be assumed that porosity was the probable limiting factor in those locations. Unfortunately, micro-porosity measurements were not made for these specimens as they had been for preceding heats in the foundry variable program. Except for these particular cases, the room temperature properties for heat 66-167 compare relatively well with those of 65-511 and 66-216, the first two Inco 713 LC plate heats.

The $1200°F$ tensile properties of plates cast from heat 66-267 are listed in Table XXIII and plotted in Figures 82 and 83. Compared to the base-line control properties of separately cast test bars the general trend is for tensile and yield strength to be lower, with approximately equivalent ductility, i.e., about 10 percent elongation. Exceptions to this appear in the plates cast at $100°F$ superheat, in the test bars from the locations most remote from the riser, and therefore in the thinnest sections. These locations exhibit tensile and yield strengths at least equivalent to those of separately cast test bars and, in the cast of tensile strength, two bars exceed the control strength levels by a significant margin. The ductility of these bars also meets or exceeds the control levels. Although the remaining locations, which are more susceptible to microporosity and which have a larger grain size, exhibit lower strength levels, these are still quite adequate. The $1200°F$ tensile strength for all locations under all conditions exceeds 100,000 psi. Similarly, the yield strength exceeds 90,000 psi and ductility, except in one test bar, varies from 8 to 17%, depending upon location.

The effect of higher pouring temperature on the $1200°F$ tensile properties is similar to the effect on room temperature properties. Tensile strength is lowered, while the remaining properties exhibit considerable cross-over. Tensile strength is favored by nucleation while yield strength and ductility show mixed reactions, depending upon location in the plates. Reduction in area is markedly higher for the unnucleated plate cast at $200°F$ superheat than for any other condition.

In general, room temperature tensile strength has shown a tendency to decrease with increasing proximity to the riser, both as a function of increasing microporosity in areas about 2 inches from the riser, and as a function of the sections size changes introduced by the plate taper. While this trend appears in the $1200°F$ tensile strength to some degree, it is not as clearly defined as in the former case, particularly in plates which were not provided with the cobalt oxide nucleating coating. Yield strength at $1200°F$ exhibits less variation with location but, in some circumstances, also exhibits a trend toward decreasing values with increasing proximity to the riser and the resulting heavier sections and coarser grain size. For the most part, the ductility values at $1200°F$ tend to remain in

-75-

a fairly narrow band except where located in areas where previous examinations have indicated that porosity will be at a maximum. Normally, the highest values of elongation and reduction in area are exhibited by the locations most remote from and those adjacent to the riser.

The 1600°F tensile properties of the same plates from which the 1200°F properties were obtained are shown in Table XXIV and plotted in Figures 84 and 85. Since the bars were selected for test temperature on an "every other bar" basis, the properties most remote from the riser and closest to the riser are now shown for 1600°F. In the centrally located bars listed, the properties appear to show significant variation only with pouring temperature. Generally, the tensile and yield strengths for the plates poured at 200°F superheat are superior to those poured at the lower value, an effect which is the opposite of that noted for the room temperature and 1200°F values. Nucleation appears to have very little effect on the strength properties at 1600°F and, within the distance covered by the specimens tested, distance from the riser also has little effect. Ductility, however, varies considerably over the distance from the riser measured by the three bars tested for each plate. For example, elongations from 1% to 7% occur in Plate 1A from 1 to 6% in Plate 1B. The 1600°F ductility measured in separately cast test bars was from 5 to 6%. Since it seemed unlikely that merely changing the shape of the casting to a plate would reduce the ductility to 1%, the two test bars which yielded this value were examined metallographically. In both cases, the fracture was found to be associated with microporosity. The amount of porosity, however, was not so high as to be interpreted as greater than the amounts observed in test bars which yielded 10 percent elongation or higher at room temperature. It would appear, then, that the 1600°F ductility of this alloy is far more sensitive to microporosity than the room temperature or 1200° F properties.

D. Summary of Results on Simple Plate Castings of Inco 713 LC

In attempting to summarize the results of all of the testing done on the simple plate program, the most important factor to emerge appears to be that there is no untenable degradation in room or elevated temperature tensile properties when proceeding from separately cast test bars to plates. Granted, there is some degradation of properties with the increasing section size designed into the plates. The 1200°F and 1600°F properties are not invariably equivalent to the separately cast test bar levels. However, the overall results show that the room temperature properties of the plates are entirely in excess of the requirements of AMS 5391A, regardless of parameter level (within the confines of the experiment) that the 1200°F properties exceed 100,000 psi ultimate strength, 90,000 psi yield strength and with a minimum of 6% elongation even where porosity is known to exist, and that the 1600°F tensile properties, under known, controllable conditions, exceed 100,000 psi ultimate strength, 90,000 psi yield strength. Under adverse conditions, the yield strength at 1600°F still exceeds 80,000 psi. The one major problem appears to be in the dangerously low ductility associated with the 1600°F tests where microporosity is present in measurable amounts. Based upon the data from separately cast test bars, the 1600°F level appears to exhibit minimum ductility. Apparently, a

-76-

general rule concerning the more drastic effect of microporosity on low-ductility materials as opposed to high ductility materials holds true even when that low ductility is a function of test temperature. It is obvious, therefore, that a very critical inspection and evaluation of castings to be utilized at 1600°F will be necessary before it can be finally stated that ductility levels of 4 to 5% can be met at 1600°F in castings with reasonably heavy sections. It will be additionally necessary to determine if the 4 to 5% is adequate for the particular application.

The data from the experiments are far more encouraging concerning the application of this alloy at temperatures other than 1600°F, where inherent ductility is significantly higher.

Scanning of the data found in the tables and figures which have been presented has yielded certain fundamental knowledge concerning the behavior of Inco 713 LC under various conditions which are met in the foundry which produces large castings. Except for 1600°F tensile properties, it has been found that an increase in pouring temperature generally reduces the tensile strength probably due to the observed increase in grain size, although that same increase in pouring temperature reduces microporosity by improving hot metal riser feeding ability. Very significantly, it has been found that the increase in grain size produced by increased pouring temperatures can be counteracted to a large degree by the presence of a known nucleating agent, such as cobalt oxide, at the metal-mold interface. Tensile strength has been found to be affected by section size (and its accompanying change in grain size) while the other properties remain fairly constant. In some cases, other properties show trends with section size, but, in no case, as consistently as does tensile strength. Microporosity has detrimental effects on both tensile strength and ductility, but with little or not effect on the yield strength, as would be expected. Significantly, Inco 713 LC appears able to accommodate a considerable amount of microporosity and still maintain adequate ductility except at 1600°F (as has been described previously). Preheating of the riser cavity had its expected beneficial effect of microporosity, consistently reducing it to lower levels than had been obtained without the preheat. Nucleation at the metal-mold interface also aids in the reduction of micro-porosity under the conditions examined.

In final summary, with the results which have been generated by the simple plate casting program the manufacture of a large Inco 713 LC casting by the methods applied in the program would be guided as follows:

(1)   All critical sections would be nucleated by applications of cobalt oxide to the metal-mold interface.

(2)   All critical plate-like sections would be tapered a minimum of 6° with the big end toward the riser.

-77-

(3)   Pouring temperature would be adjusted to grain size requirements.

(4)   Riser cavities would be preheated prior to casting.

(5)   Riser spacing, with the taper described, would be approximately 12 inches, possibly slightly more, for plate-like sections.

Obviously, _many_ other factors enter into the final establishment of casting parameters. However, the above factors have been suggested by these experiments.

X. FOUNDRY PROCESS DEVELOPMENT

A. Fluidity Tests

1. Procedures

In attempting to determine the relative fluidity of the three alloys under investigation, the basic test specimen was a fluidity spiral used in the past by Schaefer and Mott to determine the fluidity of cast alloyed steels and irons, as well as copper base alloys.[72] Unfortunately, due to the space and complexity problems introduced by the vacuum chamber and turntable pouring, not all of the requirements for accurate fluidity testing could be met. In heat 65-623, 65-652 and 65-666, fluidity spirals of each of the three alloys were cast, two spirals per heat. An example of one of the fluidity spirals cast in a ceramic mold is shown in Figure 86.

One of the prime requisites for obtaining accurate fluidity data is that the exact freezing temperature and the exact pouring temperature be know. Another is that the metal enter the spiral under the same pressure head for each spiral. The thermocouple seen protruding from the pouring basin of the spiral casting in Figure 86 illustrates one of the attempts at providing precise thermal data. The pouring basin itself is the solution to the constant head problem, i.e., it is equipped with a dam which leads to a sharply tapered sprue which permits a metallostatic head only as great as the length of the sprue for the entire pour.

The major problems were introduced by the thermocouples. In order to obtain an exact pouring temperature in the mold basin (pouring temperatures out of the furnace are inadequate due to cooling effects of the furnace wall and lip), a fast thermocouple is required. This type of couple, however, will not stand up long enough to obtain a freezing temperature. It is necessary, however, to know both of these values in order that the superheat may be calculated, superheat having been shown to have the most significant effect on the fluidity of molten metal.[72] The pouring temperatures for several of the spirals was adequately obtained. However, exact liquidus temperature measurements were not obtained, thereby rendering the data virtually of no value.

A method was then established with which the required temperature measurements were accurately obtained. The method involved obtaining the pouring temperatures of the spirals using thin, fast response thermocouples in the pouring basins, and determining the liquidus temperature of the heat using a separate casting containing a sturdy, well protected thermocouple. It appeared redundant, however, to go back and determine the fluidity of all three alloys in the program for two reasons: (1) available literature indicates that fluidity is mainly controlled by the temperature above the liquidus at which the metal is poured, i.e., superheat,[72] almost without regard to alloy composition and (2) data indicated that the alloy Inco 713 LC would be chosen for further investigation to the exclusion of

-79-

Inco 718 and René 41. However, both on the basis of the literature and the tests already run, vacuum casting does appear to have a significant effect on fluidity when compared to air melted materials, due to the absence of oxide films and inclusions. It was proposed, therefore, that additional fluidity tests be run only on Inco 713 LC and that fluidity vs. superheat data be established for that alloy and compared with fluidity data already available on a large variety of air melted materials.

Two heats were therefore cast in connection with the determination of fluidity of Inco 713 LC melted and cast in vacuum. On each heat, two fluidity spirals were cast in cold, ceramic molds at two different degrees of superheat. A quick-response thermocouple was located in the pouring basin of each of the fluidity spirals. The thermocouple utilized a very thin glass protection tube enclosing extremely thin platinum-platinum 10% rhodium thermocouple wires. The response of this thermocouple to the pouring temperature was faster than the instrument to which it was connected; the instrument had a response of 1 second for a temperature range from 2200°F to 3200°F. Casting temperatures for each of the spirals were determined from these couples during pouring.

On each heat, a third mold was included in addition to the two fluidity spirals. This mold is shown in Figure 87 and will be referred to as an "octabar" mold. Two purposes were served by the inclusion of an octabar mold in each of the fluidity heats: (1) a relatively slow response, heavy duty thermocouple could be included in the mold to determine the freezing range of the heat and (2) a rather heavy test bar section could be obtained for which the cooling rate after casting could be determined. The latter purpose will be discussed under heavy section properties.

After casting and shakeout, the length of each of the spirals was determined and plotted against the temperature above the liquidus at which the spiral was poured as measured by the quick response thermocouple in the pouring basins. The bi-color pyrometer was used only as a guide to temperature during melting and casting.

2. Results and Discussion

The data obtained from the two fluidity spiral heats are listed in Table XXV. These data are plotted as spiral length, the fluidity parameter, against casting temperature taken as the degrees above the liquidus temperature or, in another manner of description, superheat at pour. The data obtained for vacuum melted and cast Inco 713 LC are superimposed upon a band of data obtained by Schaefer and Mott [72] for a large number of air melted alloys including steels, FE-NI-CR heat resistant alloys and copper base materials (see Figure 88). Approximately 100 data points were included in the work on air melted materials and the conclusions, based upon the close agreement shown in the data band, were that the most effective parameter in controlling fluidity was the pouring temperature as related to the liquidus of the alloy, i.e., the degree of superheat in the metal as it enters the mold. Except as related to changes in the liquidus temperature, the chemical compositions had no direct effect on fluidity

except for one minor deviation, maganese steels which showed a slightly lower fluidity for a given superheat than the other alloys tested.

Compared to the data for air melted alloys, the fluidity of Inco 713 LC exhibits a clear trend toward higher fluidity for a given degree of superheat, particularly at the higher superheats tested. This is in agreement with the findings of Ollif et. al. [73]. In Oliff's study of the fluidity of air vs. vacuum melted alloys, vacuum melting was seen to increase the fluidity of a given alloy. This phenomena was explained as due to the abscence of oxide films on the surface of the molten metal entering and flowing through the mold. This is probably the most active parameter acting between the vacuum and air cast materials, although the abscence of air and other gas pressures in the mold held under vacuum may have a smaller but significant influence. In any case, the current work appears to substantiate the general opinion that alloys melted and cast under vacuum exhibit greater fluidity than their air-cast counter-parts.

B.   The Effect of Charging Gates and Risers

1.   Procedures

During the conduct of Phase I of the program, there were several opportunities to study the effects of charging gates and risers in varying percentages up to 100% of the charge. Most of these opportunities came as adjuncts to pilot casting, fluidity testing, etc. In one case, however, test bars were specifically cast of 100% revert material for the express purpose of comparing the properties obtained with the base line properties reported for virgin ingot charges.

In addition to the fluidity spirals cast in heats 65-623, 652 and 666, a set of twenty test bars, using the same pattern described for the base-line property heats, were cast. The bars were ceramic molded in smaller flacks with the last three pair removed from the standard pattern, resulting in a set of ten bars per drag as opposed to 16 in the molds already described. Two such drags were stacked to produce two layers of ten bars each. The lower, or "B", layer was entirely painted with the cobalt oxide ethyl-silicate slurry previously described in Section IX-B and the upper layer was left plain. The three heats involved in this facet of the program were made up entirely of reverted gates and risers from previous heats of the same alloys. The test bars cast on these heats therefore provided the opportunity to determine the effect of both revert and grain refinement on standard test bar properties. The casting data are shown in Table IV. Procedures such as cutoff, identification, etc. are similar to those described in section VI-A. Basic casting procedures were identical to those used for base-line property heats. The molds were cast at 200°F above the liquidus for the particular alloy.

2. Results and Discussion

After the choice of Inco 713 LC was made, the work on the revert test bars of Inco 718 and Rene 41 was discontinued. Test bars from heat 65-623, Inco 713 LC, were, however, processed and tested. The results are shown in Table XXVI. The chemical analysis of the heat is shown in Table V.

Comparison of the properties of this heat with the base-line properties previously reported indicates that the gates and risers in the charge may have had some influence in only one area, that of rupture ductility. All other properties either meet or exceed those of the base-line test bars. Further work would be necessary to determine whether or not the reduction in rupture ductility from a base line of 11% under the conditions of testing. to 4% is a direct function of the revert in the charge or whether some other phenomenon is interfering, such as grain size.

The cross section and surface macrostructures of the test bar castings from heat 65-623 are shown in Figure 89. In this figure, the top left section of each of the groups is representative of the appearance of the metal at the metal-mold interface, i. e., the casting surface. As can be seen, the appearance of the structure from the surface can be quite d ceiving in that none of the columnarity of the grains is visible. Only by cross sectioning can one be sure of the effect of the nucleation by cobalt oxide. In general, while the structure shows a fairly obvious refinement of the columnar grain in cross section, no strongly significant difference in tensile or stress-rupture properties may be attributed to this difference in grain size.

3. Final Disposition of Gates, Risers and Other Scrap

It was shown above that foundry returns can be directly vacuum remelted and cast as test bars with no detrimental effects on properties. The one area, however, where the direct charging of revert becomes a problem is in the presence of ceramic from the molds and other dirt which finds its way into the charge in spite of careful cleaning and classification. This dirt has been found to be one of the fundamental causes of many small surface defects which appear on casting surfaces. Since weld repair of surface defects is forbidden in most cases, these defects can lead to scrapping of large castings in spite of all other factors being satisfactory.

Design of pouring basins and other components of the mold prove quite successful in minimizing this type of defect. However, it does appear that the convenience offered by clean vacuum melted ingot remelt stock has distinct advantages.

Foundry returns were therefore, handled as follows for the remainder of the program.

(1) Direct charging of clean foundry returns will be permitted where the design of the pouring and gating system has proven to be 100% effective in removal of dirt from the pouring stream, or, where surface condition is unimportant as in test bar heats.

(2) Ingot will be manufactured in the research foundry vacuum furnace using ceramic molds to produce tapered three and on-half inch diamter by eighteen inch high ingots, the tops of which will be cropped to remove floated contaminants.

(3) Where large quantities of foundry returns are involved, the virgin ingot supplier will be requested to melt and refine a large master heat at commercial charges.

Item (2) has been used to produce about 800 pounds of ingot. The large amount of foundry returns currently on hand will be largely handled according to item (3).

Item (3) has been used to produce 2000 lb. heats with a cutting and handling loss of roughly 500 lbs., including cropping of ingots.

C.   Heavy Section Properties of Inco 713 LC

1.   Standard .505" Test Bars

Procedures

As pointed out in Section X, an "octabar" casting was poured with two fluidity heats; heats 66-106 and 66-153. This relatively heavy section casting provided the liquidus temperature of the heat through the expedient of a thermocouple located at the center of one of the eight test bar sections provided by the pattern (see Figure 87). The octabar pattern is one which is used frequently in the non-investment foundry for alloy evaluation and for research and development work for which test bars are necessary. The mold cavity (riser section removed) shown in Figure 87 shows the heavy central section, which functions as a reservoir of hot metal, surrounded by the eight one inch thick and six inch long test specimen sections which give the casting its name. Not shown in the photograph of Figure 87 is the riser section which fits above the heavy central section and which provides both a pouring location and a hot metal riser for the test bar castings.

In the experiments under discussion, four of the test bar cavities in the ceramic octabar molds were coated with a cobalt oxide slurry to determine if the already established grain refining effect of the cobalt oxide could exert an influence across a standard one inch test bar cross

section. The remaining four cavities were left uncoated.

As can be seen in Figure 87, the ceramic octabar mold was placed in a fourteen by eighteen by six inch deep flask and backed up with a coarse sand in order to prevent runnout in the vacuum furnace. After firing, the molds were permitted to cool and were then loaded in the vacuum chamber for casting cold. The mold included in heat 66-106 was cast at 200°F above the liquidus. The mold in heat 66-153 was poured at 100°F superheat.

After casting, the molds were allowed to cool under vacuum while a recorder outside the vacuum chamber recorded the cooling rate at the center of one of the eight test bar sections. After shakeout, the castings were cut into test bar sections and test specimens were prepared for testing according to procedures already described. The final test bars, however, were of the standard 0.505" gauge diameter, 2" gauge length type, rather than the smaller 0.252" gauge diameter test bars used up to this point in the program.

It should also be noted, that the charge material for heat 66-106 and 66-153 was 100% revert, i.e., gates and risers from previous heats which had been thoroughly cleaned and carefully selected.

Results and Discussion

The chemical analysis of heats 66-106 and 66-153 are shown in Table V (as are the analyses of all heats made in Phase I). It is worthy of note that the analyses of these heats do not vary significantly from the norm shown in Table V, the charge was entirely revert. (This may also be seen to be true of all the revert heats so marked in Table V).

The cooling curve recorded for the test bar section (see thermocouple location in Figure 87) is shown in Figure 89a. If 18°F is taken as the temperature at which significant precipitation may begin in the micro structure of Inco 713 LC and if 1000°F is taken as the temperature below which little precipitation will occur, the cooling rate through this critical temperature zone may be averaged at approximately 3.2°F per minute. Althought this figure means very little when taken alone, future work in the program will compare this cooling rate with the rate obtained in one-half inch test bar sections and then in actual castings. Subsequent comparison of the properties obtained with these various cooling rates should give a better understanding of the effect of section size on the properties of this alloy.

The macrostructure obtained in the octabar test bar sections with differences in pouring temperature and with and without nucleation are shown in Figures 90 and 91. At 200°F superheat, the grain refining effect of the cobalt oxide is obvious. However, as can be seen by comparing the one inch sections with their one-half inch counterparts, the effect is

-84-

diminished in the heavier section. With a reduction to 100°F superheat
at pour, a marked change in the macrostructure is apparent. As can be
seen in Figure 9, there is a marked tendency toward a fine, equiaxial
grain type with and without nucleation. The effect of nucleation, however,
is to promote the formation of a very fine, columnar-grained zone near the
metal-mold interface. This trend toward fine, equiaxial macrostructures
has been found tobe typically associated with pouring temperatures below
100°F above the liquidus, with some dependence upon section size. The
structure is indicative of shallow thermal gradients and uniform nuclea-
tion, neither of which condition is conducive to castings predictably free
of microporosity.

The tensile properties obtained from the one inch octabar test
bars are shown in Table XXVII.

Comparison of the properties shown in Table XXVII with the
base line properties of the alloy as established in heat 65-456 (see section
VI-B) indicates that the heavier section has little effect on the room temp-
erature properties and exhibits a higher ductility at 1200°F if the proper-
ties obtained at the higher pouring temperature are considered. If, however,
the properties of the heavy sections cast at 100°F superheat are considered,
the detrimental effects of the change in macrostructure become obvious parti-
cularly in ductility.

It may also be seen from these data that nucleation had little effect
in changing the properties obtained from the one-inch octabar section.
This is contrary to effects seen in one-half inch sections. It does, however,
follow from the small effect observed in the macrostructure of the one inch
section compared to a much greater net grain refinement in one-half inch
sections (see Figure 10).

Based upon these data, sections up to one inch, cooled in the mold
at about three degrees per minute from 1800°F to 1000°F present no parti-
cular problem in meeting the high properties associated with one-half inch
sections up to now providing that pouring temperatures are not permitted to
slip low enough to promote the formation of a fine, equiaxial structure
due to the absence of a steep thermal gradient. It is not the fine structure ,
per se, which is detrimental, but is, undoubtedly, the fine, dispersed
microshrink engendered by the thermal conditions in the mold which promote
the equiaxial structure.

2. Properties of a Five Inch Cast Section on Inco 713 LC

Procedures

In a later section of this report, a series of large castings in
Inco 713 LC will be described as "TEST FIXTURE CASTINGS FOR THE
LTV FIN BEAM" (see Section XI). During the production of one of these

castings, the sagging of a slot core made it useless for its intended purpose and thus provided the ideal opportunity to examine the properties of Inco 713 LC cast in very heavy sections. Figure 92 shows the scrap casting after shakeout. Its gross weight was 500 pounds. The 5 1/4-inch thickness of this casting makes it one of the heaviest sections of superalloy casting known to this writer intended for use without forging or rolling to some thinner configuration. A 1 1/2-inch thick slice was cut directly through the casting, roughly located on a plane with the vertical centerline of the riser and 90° to the longitudinal centerline of the casting. This cross section was macroetched in hot hydrochloric acid with hydrogen peroxide added. The grain size found is illustrated in Figure 93. The illustrated section was heat treated at 2150°F for two hours in argon and cooled in the furnace bell to 1200°F, then air cooled.

After macroetching the cut section, test specimens were cut according to the sketch shown in Figure 94. Test bars were machined and tested according to the procedures described in VI-A.

Results and Discussion

The results of tensile, impact and creep-rupture testing are shown in Table XXVIII. The major effects of the heavy section compared to previously reported properties appears to be a reduction in yield and tensile strengths, together with a rather poor showing for rupture life at 1800°F, 22,000 psi. Fortunately, tensile ductility appears to be effected very little by the heavy section. Rupture ductility is markedly increased. Charpy impact strength is virtually unchanged from the levels determined on separately cast test bars.

While the reduction in room temperature tensile properties in the very heavy section is undesirable, it is not unduly detrimental. In fact, it is remarkable, in the opinion of the writer, that this alloy has the ability to retain this much strength and ductility in a section over 5 inches thick. An average tensile strength of over 105,000 psi and an average yield strength of over 95,000 psi can apparently be maintained in some of the heaviest sections currently imagined in superalloy castings while simultaneously maintaining over 7% average tensile ductility. Based on data which will be reported in a subsequent section, it is quite likely that these properties could be improved considerably by a 1200°F aging treatment following solution heat treatment.

Somewhat disturbing, however, is the loss of rupture life compared to separately cast 1/2 inch section test bars. The average of the values obtained represents roughly a 50% loss in rupture life by direct (non-statistical) comparison. It is possible, however, that additional heat treatment could bring the values over the 30 hours minimum set down by AMS 5391A.

-86-

Figure 95 shows the unetched microstructure of the heavy section taken near the center of the 5 1/4 inch thickness. The porosity seen in the photomicrograph is not representative of the entire section, but was selectively photographed to illustrate the difficulty in feeding a truly heavy section 100% sound.

In general, the heavy section properties of Inco 713 LC are satisfactory.

D. Grain Refinement

1. Economical Cobalt Oxide

In cases where grain refinement is considered desirable, cobalt oxide has been shown to be extremely effective when applied to the mold surface in a slurry form. Until recently; the grade of cobalt oxide used for this purpose on the current program has been obtained from E. H. Sargent & Co., a chemical supply firm, as "technical grade". If used in very large quantity, the cost of this material could present a problem to the foundry. Three much less costly grades of cobalt oxide (mixed cobaltous and cobaltic) are available from African Metals Corporation. These are listed by African Metals as "Gray Co Oxide, Black Co Oxide and Met-Grade Co Oxide". Some general information concerning these materials is listed in Table XXIX.

In order to determine the relative grain-refining effectiveness of the three cheaper grades of cobalt oxide, a heat of Inco 713 LC scrap was made in the vacuum furnace and cast into a ceramic test bar molds of the type described in Figure 5. One mold was left uncoated as a control. The test bar cavities of the second mold were coated with the subject cobalt oxide slurries (alcohol and ethyl silicate as the vehicle) in sets of four. Both molds were subsequently fired and then cast under vacuum at $250^\circ F$ above the liquidus.

After casting, the test bars from the treated and the untreated test bar mold cavities at identical locations were cross sectioned and macroetched to determine the effect of the presence of each of the grades on the cast grain size. It was found that the four grades of cobalt oxide had identical effects and that no difference of significance could be determined among them. Figure 96 shows the macroetched cross sections of the nucleated and the control test bars with representative samples of all four grades illustrated.

From these results, it was determined that the less expensive grades of cobalt oxide would be used for grain refinement wherever larger quantities might be required.

-87-

2. Inclusion of Cobalt Compounds in the Ceramic Slurry

It was found during parts of the Phase I work, that the application of a slurry of cobalt oxide in an alcohol-ethyl silicate vehicle presented a possibility of introducing surface defects where applied too thickly. In order to avoid this possibility, it seemed advantageous to mix the grain refining addition in the ceramic mold slurry prior to pouring around the pattern. This is known to be an accepted practice in the area of investment casting where the pre-dip, the first coating to be applied to the expendable pattern, contains cobalt oxide as a grain refiner where such refinement is desired. Attempts have been made to accomplish a similar mixing in the ethyl silicate bonded ceramic molds of the type used in the preceding stages of the current program. Mixtures of ceramic grain containing from two to five percent cobalt oxide (by weight of ceramic grain) were successfully molded and gelled according to standard practice with ethyl silicate molds. However, the step of burning off of the alcohol from the gelled mold, no matter how it was tried, resulted in severe spalling and general degradation of the mold. The reaction is difficult to describe, but may be best compared with "fireworks" with respect to the manner in which tiny, discrete particles popped from the mold surface as glowing sparks. These particles were collected and identified spectrographically as cobalt oxide. The most likely mechanism for the observed phenomenon appears to be the formation of a cobalt carbonyl compound during the evolution of the strongly reducing atmosphere by the burning mold. The carbonyl compound subsequently reacts to form cobalt oxide and releases the combustible gas, CO. Whatever the mechanism, however, the fact remains that incorporation of cobalt oxide directly in an ethyl silicate bonded mold appears to be impossible. With the probable mechanism in mind, some effort was devoted to the incorporation of a cobalt compound other than the oxide in the slurry. It was proposed that the compound be chosen such that it avoids the formation of the carbonyl but oxidizes to cobalt oxide during firing.

The following cobalt compounds were chosen for availability and the probability that they would convert to the oxide during firing: (1) cobalt (ous) carbonate, (2) cobalt (ous) acetate, and (3) cobalt (ous) nitrate. Solubility in ethyl-silicate or alcohol was an additional consideration.

Standard molding slurries were prepared using 250cc of hydrolized ethyl silicate and 0.98 pounds of calcined kyanite as the ceramic. To three such slurries, 2% (by weight of kyanite) of each of the three cobalt compounds was added. After thorough mixing, accelerator was added (triethylammine) and the slurries poured into separate molds. The slurries containing the carbonate and the acetate gelled normally. The nitrate-containing slurry however, would not gel over any reasonable time span. The cobalt nitrate was eliminated from the experiment at this juncture due to interference with the gelling action of the ethyl silicate.

After gelling of the remaining slurries, excess alcohol was burned off and the molds were fired with gas-air torches to red heat. The success of conversion of the carbonate or acetate to cobalt oxide was judged on the basis of color change in the mold. In the case of the acetate, no color change was detected after firing. The cobalt carbonate mixes, both 2% and 5%, turned gray during firing and remained gray on cooling. The 5% mix was, as might be expected, a darker gray due to the presence of a greater amount of the cobalt oxide after firing.

The apparent successful manufacture of a mold containing cobalt carbonate and the equally apparent conversion of the carbonate to cobalt oxide lead to an attempt to grain refine Inco 713 LC using a mold containing the carbonate and mixes as described above. Three test bar mold sections (Figure 5) were prepared. The top section was made from the standard kyanite-ethyl silicate mix with a slurry of cobalt oxide, ethyl silicate and alcohol, brushed on the mold before firing. The bottom section was made identically, but without the cobalt oxide slurry. These sections served as controls for the experimental center section which was prepared from a mix containing the normal ratios of ethyl silicate and kyanite, but with 5% (0.05 x weight of kyanite) cobalt carbonate powder. All three sections plus a standard cope section containing the downsprue were fired after gelling and burning off the excess alcohol. The type of stack-molded set up used is illustrated in Figure 6.

After firing, the gray appearance of the carbonate-containing section was obvious. The three sections were assembled with the cope and vacuum cast using Inco 713 LC vacuum remelt ingot. The metal was poured at 300°F superheat. After casting, representative test bars from each of the three sections were cross sectioned and macroetched to determine the grain refining effect of both the control cobalt oxide coating and the cobalt carbonate-containing section. As can be seen in Figure 97, the effect of the brushed-on coating was normal in that it resulted in marked grain refinement as evidenced by comparison to the untreated bottom section. The carbonate-containing section, however, had no effect whatsoever on the grain size in spite of the apparent conversion to oxide.

It is possible that the 5% carbonate by weight of kyanite did not produce a sufficient number (or the required kind) of sites at the metal-mold interface for nucleation to occur. Additions of carbonate at much higher fractions will however, undoubtedly have some effect on the characteristics of the mold material.

In order to insure that the apparent conversion of the carbonate did, in fact, occur in the mold, samples of pure cobalt carbonate and mixtures between 3% and 50% cobalt carbonate and 100 mesh kyanite were subjected to firing times from 15 minutes to 8 hours at 1600°F. The pure carbonate samples showed essentially complete conversion to crystalline cobalt oxide, both CoO and Co_3O_4, after as little as 15 minutes at 1600°F.

With increasing time, the fraction of Co_3O_4 increased, with the sample baked for one hour showing more Co_3O_4 than CoO, and the sample baked for eight hours showing complete conversion to Co_3O_4.

The diffraction patterns for the mixtures of kyanite and cobalt carbonate could not be read directly since the lines for the compounds in question interfered with one another. However, an interesting color change occurred during firing. An initial color change from white to grey occurred at very short firing times. This is undoubtedly a result of the formation of CoO and Co_3O_4 from the decomposition of $CoCO_3$. After three hours, however, a change in color from grey to blue occurred, with the blue becoming more intense with increasing time up to eight hours. It is probable that this change in color is a direct result of the formation of cobalt aluminate ($CoAl_2O_4$) from the reaction of cobalt oxide (Co_3O_4) with kyanite, which is basically an alumino-silicate. Unfortunately, a positive diffraction identification of this compound could not be made since its "d" spacing is also the same as for the oxides and the kyanite. Cobalt aluminate is reported to have a grain refinement potential similar to that of cobalt oxide. Earlier observations in this program confirm this.

In any case, however, it appears that the conversion of cobalt carbonate to one of the compounds with a grain refining potential (CoO, Co_3O_4, $CoAl_2O_4$) can be assured by any reasonable firing time over fifteen minutes. On this basis, it must be concluded that the 5% addition of cobalt carbonate was inadequate provide a sufficient grain refining potential at the metal-mold interface. If a 100% conversion to CoO is assumed, the available CoO after conversion is 3.15%. This may not have been adequate.

No further work was done along these lines.

A second approach to developing a system which would permit the inclusion of a grain refining compound in the ceramic slurry was to retain the cobalt oxide and eliminate the triethylammine accelerator based on suspicions that the thermal energy provided by the simple burning of the alcohol is not nearly sufficient to promote direct formation of the cobalt carbonyl believed to be at the root of the problem. It was suggested that the cobalt oxide in the mold acts as a catalyst for the decomposition of the ammonia radical introduced by the triethylammine accelerator and that it is the subsequent burning of hydrogen which provides the thermal energy required for the formation of the cobalt carbonyl with its destruction of the mold bond. If this is the case, elimination of the ammine radical may serve to permit use of cobalt oxide directly in the slurry. This was investigated by the incorporation of a non-ammonia containing base as the accelerating agent in the slurry.

A mold was made containing 3% cobalt and using sodium carbonate as the gelling agent for the ethyl silicate. Gelation occurred normally.

During the burnoff, however, the same reaction as had been initially observed occurred. It may be concluded from this that the presence of the ammine radical is not required for the destructive reaction to occur, although the exact nature of the reaction may still remain in doubt.

Cobalt Oxide in Sand Molds

Work was initiated on the possible inclusion of cobalt oxide (or othernucleating agent) in zircon sand molds bonded with sodium silicate. The first mold samples produced as standard AFS two-inch diameter rammed cylinders contained three weight percent cobalt oxide. No degradation of the molding characteristics were noted. However, these first experiments are not far enough advanced to permit conclusions regarding the usefulness of the cobalt oxide as a grain refiner in this sand system. No further work is contemplated.

E. Sand Molds in Vacuum Casting

1. Initial Work - Zircon Sand

While ceramic molds are obviously satisfactory for casting large superalloy castings in vacuum, one of the obvious drawbacks is cost of the mold in both material and man-hours. With this in mind, a considerable effort was devoted to the development of an acceptable molding system which would be more "conventional" to large sand foundry operations and would, in addition, provide considerable savings in time and materials compared to ceramic molds. The requirements for such a system are that it be adaptable to conventional foundry molding methods such as ramming, jolting, squeezing, etc., that it does not require firing at high temperatures (greater than about 1000°F), that it can meet dimensional and surface finish requirements, and most important of all, that it produce a mold which is compatible with the vacuum environment in which it will be cast.

One heat of Inco 713 LC scrap was cast into 10" x 6" x 2" thick plates, risered at one end and poured down the riser. The molds were rammed from a mix of zircon sand and 2% and 3% by weight sodium silicate. The molds were not gassed, but were baked for one hour at 450°F to set the mold for storage. On the day of the heat, the molds were heated to 800°F and held for four hours, removed from the oven and closed, then loaded into the vacuum chamber and cast according to previously reported practics. Pouring temperatures for four molds was 200°F above the liquidus.

-91-

The appearance of the plates was excellent. Surface quality approximated that which would be obtained in an air melted and cast plate in a similar alloy system except, of course, for the absence of oxidation products. No evidence of a mold reaction was found, nor was any unusual out-gassing of the molds observed during the pump down period or during casting. This first heat was considered the starting point of the molding materials investigation and, as such, showed considerable promise.

The initial success with a molding system consisting of zircon sand and pure sodium silicate was followed with additional molds for castings weighing up to 500 pounds with rigging. The details of the casting will be presented in a subsequent section. The details of the development of molding materials and methods are as follows.

Zircon sand was chosen for most of the work done to date for several reasons, the most important of which are relative inertness to attack by reactive alloy systems and thermal stability. The latter is most important since it is the nature of the vacuum casting system that the molds must be baked or fired at temperatures high enough to remove all traces of free and chemically bonded water and organic materials.

Two grades of zircon sand were initially investigated. The first of these has an average grain fineness of 105. The second, and preferred grade, is from a new deposit and has a grain fineness of 155. There is reason to assume that similar properties could be obtained from tailored mixes of zircon sand and zircon flour. However, no work along these lines was pursued because of the high cost of such a mix compared to a "ready mixed" grade shipped as it is mined.

The basic binder under investigation is essentially pure sodium silicate with no additions normally associated with collapsibility, etc. Obviously, these could not be tolerated in vacuo. Binder levels from 1% through 5% have been investigated for green, gassed, baked and fired strength. A binder level of 3% by weight has been found to be ideal in most cases. With no gassing, the green strength of the mold material is inadequate for handling. A light gas with CO_2, however, permits handling of the mold with only the normal precautions observed in the foundry. Heavy gassing of the molds is considered undesirable due to the formation of excess sodium carbonate which could be troublesome in the vacuum casting system.

Although it is unnecessary from the viewpoint of mold strength, etc., it has been found desirable to bake the molds at 400°F to 450°F briefly to give the mold a higher strength for subsequent handling into the high temperature baking ovens, setting of cores, and other general

-92-

handling. After the low temperature bake, the molds are quite stable and they may be permitted to stand for several days before the final high temperature bake and casting.

The final baking cycle may be between 800°F and some unestablished maximum, with 1000°F currently being applied with marked success. The suspected maximum for baking (or firing) the molds is the softening point of the sodium silicate bond, about 1500°F. The 800°F minimum is set by the lowest temperature at which chemically bonded water is driven from the system. The time at temperature must be adjusted to the thickness of the mold and the intricacy of the mold cavity. After baking, the mold sections and cores are permitted to cool to handling temperature, cleaned and closed for casting. It has been found that the molds may not be permitted to return to room temperature after the high temperature baking cycle due to a reabsorbtion of atmospheric water and the problems introduced in vacuum processing. Therefore, the molds are brought to high vacuum while still above 200°F.

Sodium silicate is an excellent binder up to the temperature at which softening occurs. This limitation is most readily observed in areas where the mold cavity is such that a small amount of mold is surrounded by a large volume of molten metal, e.g., a slot core in a heavy section, etc. The softening will, under these circumstances, permit mold movement or sagging and, as a result, a casting scrapped due to dimensional deviations. In the current work, several attempts made to improve the high temperature strength of the basic sodium silicate mold. Additions of colloidal silica in several ratios with the sodium silicate showed considerable promise except for one problem. During exposure to about 400°F collodial silica rapidly releases water which has, in turn, a deleterious effect on the sodium silicate bond. Under the worst circumstances, the mold material becomes extremely weak and friable. Other factors which appear to affect the successful combination of colloidal silica and sodium silicate are the order of addition and of course, the ratio of the materials.

The concept of the use of zircon sand molds in the casting of large superalloy parts is restricted to application of the zircon-sodium silicate sand as a facing which may vary from 1/2 inch thick to 2 or 3 inches thick, depending on location, configuration, etc. Two factors, weight and cost, determine this restriction. Zircon is both one of the most expensive and one of the highest density sands used in the foundry. The procedures for molding with a facing sand are not new to this program. First, the facing sand is hand molded to the pattern in the thickness desired. The flask is then filled with the back-up sand, and rammed, jolted or squeezed as required. Certain configurations required that this be done in steps, but the principal remains the same. The back-up sand used for all of the experimental and production molds has been Calamo 20 (Harbison-Walker) bonded with pure sodium silicate.

-93-

2. Other Work - Zircon and Kyanite

Work has been done in one other area effecting the use of sand molds for the manufacture of superalloy castings. The original work used only one grade and type of aggregate, zircon sand of approximately 168 mesh. The surface finish of the large castings made using this aggregate and 3% sodium silicate binder was nearly up to the standards of a ceramic slurry mold casting, but the high thermal diffusivity of the zircon promoted the formation of a large number of small surface cold laps which, on a casting requiring a fine surface finish, would be unacceptable. Therefore, as a first step toward establishing other aggregate combinations which might be used for large superalloy castings, a series of molds were made and cast in an air melting alloy using a truncated fin beam pattern shown in Figure 98.

The binder was a pure sodium silicate containing no organic additions for collapsibility. After ramming, the molds were lightly gassed with CO_2 and baked at 400°F briefly. Final baking was at 1000°F for four hours. The percent binder, by weight of aggregate, was determined on the basis of the best workable mix. Additional work would be required to establish optimums (except for the zircon mixes). The aggregate blends and the percent sodium silicate binder (by weight of sand mix) for each are shown in Table XXX.

The castings were poured from a single ladle of AMS 5355A at a superheat of 330°F above the liquidus. After shakeout, the castings were sand blasted and examined for surface appearance. Figures 99 through 104 show some representative surface. Figure 104 is representative of the surface obtained with current ceramic molding using ethyl silicate as the binder and 100 mesh calcined kyanite as the aggregate.

Obviously, the surface finish produced from molds containing the coarse 35 mesh kyanite are totally unacceptable, except of course, if surfaces are to be machined. Figures 99 and 100 illustrate this. Similarly, the surface obtained using straight 105 mesh zircon is rougher than would normally be considered for a precision casting, but is acceptable for other requirements. Figures 101 and 103 show surface finishes which come reasonably close to the control surface in Figure 104. These were produced by straight 168 mesh zircon and a combination of 168 zircon and 100 mesh kyanite. Another mold produced an excellent surface finish, but ran out shortly after pouring and was scrapped before being photographed. That was a mold made from 100 mesh kyanite only, casting 68-014-4.

3. Summary

Large castings up to 500 pounds casting weight were made in molds made with 168 GFN zircon sand facing bonded with pure sodium silicate

-94-

and backed with sodium silicate bonded calamo. The molds were lightly gassed with CO_2 for green strength, baked briefly at 400°F to improve handling characteristics, and, finally, baked at 1000°F for several hours, cooled to about 250°F, cleaned, closed and placed under vacuum in the casting chamber while still over 200°F. After normal melting under vacuum, molds have been poured in Inco 713 LC both under high vacuum and under 100 mm of argon with absolutely no evidence of outgassing or other "metal-mold" reactions. The surfaces produced were excellent, comparing favorably with those produced on ceramic slurry molds used for the majority of the program thus far. Dimensional stability appears to be excellent except where the mold is unsupported and reaches temperatures of 1500°F or higher, e.g., in a slot core.

The results of other experiments indicate that sodium silicate bonded molds may be able to produce surfaces almost equivalent to those produced by ceramic slurry molding for the production of superalloy castings. Of particular interest are the results with molds using kyanite or a fraction of kyanite. The use of this aggregate would certainly aid in preventing the surface cold laps associated with the use of an all zircon rammed mix, since the thermal diffusivity of kyanite is considerably lower than that of zircon. Further work would be necessary however, to determine if the kyanite mixes are adaptable to large molds.

F. Exothermic Materials in Vacuum Casting

In several circumstances, it became obvious that the heat losses from exposed riser surfaces are considerably greater in vacuum than would be expected in air. This, added to the fact that the isolation of the vacuum chamber prohibits the addition of the normally applied "hot top" or insulating material to the riser surface after filling the mold, led to a series of experimental heats designed to evaluate the adaptability of exothermic compounds to vacuum casting of large shapes. The advantages in promoting directional solidification are obvious.

The first of these heats was cast into 10" x 6" x 2" thick plates risered at one end with a 4-inch diameter riser. Four molds were cast, both of which were made of rammed zircon sand bonded with sodium silicate per the previous section. (Note: The evaluation of the behavior of the exothermic material and the first evaluation of the silicate bonded mold were simultaneous on this one heat.) Two molds were equipped with pre-formed exothermic riser sleeves specifically for use in the vacuum application. The molds and sleeves were baked at 800°F prior to loading into the vacuum chamber for casting.

The first mold was poured at 200°F above the liquidus and at a pressure of less than 16 microns. The reaction of the exothermic riser sleeve was violent enough to eject at least half of the metal volume in the riser out into the chamber. To insure that the behavior was not an isolated case, the second mold was cast under similar circumstances, but at somewhat higher pressure. The reaction was identical. The two molds without exothermic sleeves were poured at 200°F superheat and

-95-

20 microns pressure without incident.

After shakeout, the plates were sectioned to determine the riser feeding distance. Although the violent reaction of the exothermic sleeve had created secondary problems, it was obvious that the feeding distance had been markedly improved. On the basis of the beneficial effect observed, additional work was undertaken.

Actually, very little experimentation beyond that already described was required to show that exothermic materials could easily be adapted for use in manufacturing large superalloy castings in vacuo. Two materials were evaluated, both manufactured by the same company. One of the materials is sold mainly for use in the air casting of steel and, as such, proved inconvenient for vacuum casting of the superalloys, mainly due to excessive outgassing and generation of dust, etc. The second material evaluated was formulated especially for use in vacuum with ignition temperature specifically designed for the nickel-base alloys. This vacuum exothermic is received in a dry powder form and, according to the manufacturer's instructions, it is mulled with 10% pure sodium silicate and 4% water. After molding to the shape required it is baked for one hour per inch at 450°F to 500°F.

The actual ignition temperature (in air) of the vacuum exothermic material was determined by molding a small sample around the bead of a chromel-alumel thermocouple, baking and placing in a furnace set to heat continuously. The temperature of the thermocouple was monitored and a sharp increase in the heating rate at 1100°F signalled ignition of the exothermic. A temperature of about 1050°F was then considered as the maximum for baking of the molded exothermic compound. This temperature is ideal since it fits into the processing of the zircon sand molds and permits baking of the mold assembled with exothermic components at 1000°F.

The same casting shape was used for the additional evaluations of exothermic materials, i.e., a 6-inch wide by 10-inch long by 2-inch thick plate fed by either one or two 4-inch diameter risers. The mold material was the zircon sand-sodium silicate bonded system described in the previous section.

Table XXXI summarizes the results of the first heat and two additional heats. The "violent outgassing" alluded to in the table refers to the reaction which was violent enough to eject molten metal from the riser and, therefore, is totally unacceptable for routine vacuum castings. As can be seen from the results listed, the only satisfactory performance of the vacuum exothermic riser sleeves was when the pressure was increased in the chamber by introducing argon. 500mm of argon was, in fact, introduced into the chamber through a misunderstanding and it is not suggested that this pressure be considered, particularly considering the cost of argon gas added

to the other costs of producing a superalloy casting. 100mm of argon proved to be quite adequate to prevent the violence of the exothermic reaction and, simultaneously to insure a leak-tight system during pouring.

The advantage of the exothermic lining in the risers of the plate castings examined was obvious in that the unlined riser exhibited gross shrink in the plate directly under the riser and the lined riser exhibited shrink only in the riser itself. This indicates that the exothermic lined riser was forced to feed almost the entire plate with little help from the unlined riser. The plate was, however, sound through the center indicating that the exothermic riser had indeed fed the entire section.

Through these experiments, a tentative standard practice for the use of exothermic compounds in vacuum casting was developed. The material is a specially blended, moldable vacuum exothermic compound. The material is mulled with 10% sodium silicate and 4% water until moldable and then rammed either as a riser lining in the mold or as a separate shape for special application. After ramming and before the compound sets hard, a large number of vents are forced into the walls to relieve the gas pressure after ignition. After venting, the exothermic is baked at 450°F for one hour per inch, either as part of the mold or as a separate shape, after which it may stand for an indeterminate time prior to final baking. The final baking cycle, again either as part of a mold or as a separate shape, is 1000°F for one hour per inch. The exothermic is normally brought to high vacuum while still above 200°F to avoid moisture pickup. The melting procedures for casting the shape are not changed except at the moment before pouring. After reaching pouring temperature, the chamber is isolated and argon is valved up to a pressure of 100mm as <u>measured by a gauge separate from the vacuum gauges</u> which are calibrated only against air pressure. When the chamber reaches 100mm of argon, the casting is poured.

If a ceramic slurry mold is considered, a somewhat different system must be adopted. First, the mold and the exothermic shape must be made separately in order that the mold may be fired without igniting the exothermic. After cooling the mold to any temperature below 1000°F, however, the exothermic sleeve, etc., may be cemented into place by an appropriate ceramic cement. The exothermic shape is however, baked at 1000°F separately.

It appears reasonable that the exothermic material cannot be located too close to a critical casting section because of the possibility of damage to the casting by gas pickup, oxidation, or other factors related to the exothermic reaction. It is suggested that riggings be designed such that the exothermic is, in all locations, one inch or more removed from the actual casting dimensions.

-97-

XI.   TEST FIXTURE CASTINGS FOR THE LTV FIN BEAM

A.   Introduction

In order to perform the elevated temperature flexural tests scheduled for the final LTV fin beam casting at LTV, fittings and fixtures for holding the beam and applying the test load must be constructed of materials capable of retaining high strength at the test temperature, 1600°F. With this in mind, LTV requested that Abex supply basic cast shapes of Inco 713LC in the solution treated condition which were to be machined into a set of test fixtures. The final shapes after machining serve the following functions.

> (1) Three 25-inch long by 4-inch diameter bars will be used as push rods for load transmission from the test equipment to the fin beam in the 1600°F environment.

> (2) One connector yoke, roughly triangular in shape, will serve to make the primary load-bearing connection to the fin beam in the test chamber.

> (3) Twelve 7-inch long by 2-inch diameter bars will be used as connector pins and other parts in the system.

In manufacturing these fittings for LTV, it was decided that advantage would be taken of the opportunity to apply the principles of sand molding and use of exothermic compounds described in preceding sections. This work would then serve as a primary "pilot program" for the casting of the final fin beam configuration.

B.   Wedge Bar Casting for 4 Inch Diameter Bars

The pattern equipment for the 4-inch diameter bars is shown in Figure 105. The wedge or keel bar shape was chosen as one of the most dependable methods of producing centerline soundness in the final shape, although it is obvious that considerable machining is required to produce the final circular cross section. The taper angle from the bottom to the top of the pattern is 15° per side. This favorable increase in section size with increasing height from the bar was combined with a 2 inch thick cover core molded from the vacuum exothermic material described in the preceding section. It was justifiably predicted that this combination would result in largely directional solidification from the bottom to the top of the wedge bar and, as a result, a sound bar on the first try. A hole in one end of the cover core permitted pouring of the casting from the top without a gating system.

The one-piece mold for the wedge bar was molded in an 18 inch by 30 inch flask using 168 zircon sand bonded with 3% pure sodium silicate as a facing sand roughly 1 inch thick all over. This facing was backed with sodium silicate bonded coarse calamo and hand rammed. The rammed mold was lightly gassed by venting from the bottom and then stripped from the pattern. Figure 106 shows one of the three molds made for this program after stripping. The exothermic cover core is also visible in Figure 106. This cover was rammed from the vacuum exothermic mix described in the preceding section. The hole for pouring the casting from the top is clearly visible in Figure 40. After molding, both the cover core and the mold were baked at 450°F to impart strength for additional handling. Finally, the cover core and mold were baked for four hours at 1000°F.

After cooling the baked mold to approximately 400°F, the cover core was placed in position, a pouring basin was supplied, and the mold was loaded into the vacuum casting chamber and the previously prepared chamber was pumped down to high vacuum. The metal charge was 500 pounds of vacuum cast ingot previously prepared in the same furnace by remelting and casting foundry returns into vertical ingot molds. The tops of these ingot are cropped prior to remelting to remove all traces of oxide, etc. The charge was melted, superheated to clean the surface, cooled to obtain the liquidus temperature, and then reheated to the pouring temperature, all under high vacuum. After reaching pouring temperature, the chamber was isolated from the pumping system and back-filled with argon gas to a pressure of 100mm. Immediately upon reaching the desired pressure, the casting was poured. Shortly after filling, the cover core was seen to ignite. The casting was permitted to solidify and cool in the argon atmosphere.

Chemical analyses and foundry details for the wedge bar castings (as well as all other fixture castings are shown in Table XXXII. Casting weight for the wedge bar was 500 pounds with the metal to within 1/2 inch of the cover core. A representative casting is shown in Figure 107 prior to cutoff. The wedge was cut off approximately 4 1/2 inches from the bottom (the casting is upside down in Figure 107) to yield a half-round bar from which the 4-inch diameter is machined.

C. Connector Yoke Casting

The pattern equipment for the connector yoke is only slightly more complex than the wedge bar pattern. Figure 108 shows the cope and drag pattern boards with core prints for two thin slots at the

wide end of the triangular configuration and one heavy slot at the narrower end, or apex. As can be seen, provision was made for a 9-inch diameter side riser through which the casting was both poured and, of course, fed during solidification. The pattern for the yoke casting required a 28 x 32 inch flask.

The connector yoke was molded in the same materials and using the same procedures as for the wedge bar described in the preceding sub-section, with one exception. The yoke casting riser was supplied with a molded-in-place exothermic riser sleeve rammed around a 9-inch diameter riser stick in an oversized riser cavity. This was done prior to the 1000°F bake, but after the 450°F bake.

For the first yoke casting, no backup sand was used for the two slot cores, i.e., they were molded solid in the sodium silicate bonded zircon sand with 1/8 inch diameter steel rods molded in place for support. The cope and drag mold halves with the cores in position are shown in Figure 109. This first casting gave the first evidence of having exceeded the softening temperature of the sodium silicate bond. The slot cores seen on the left side of the drag mold section in Figure 43 sagged or drooped roughly 1/2 inch during casting and solidification resulting in a casting scrapped for dimensional discrepancy in that area. The replacement casting was molded identically, but the cores were made from the conventional ethyl silicate bonded kyanite slurry (ceramic). No sagging occurred in these ceramic cores.

Casting procedures for the connector yoke were identical as those used for the wedge bars. The castings were poured down the riser through a ceramic pouring basin. The exothermic sleeve was seen to ignite shortly after filling of the riser.

Figure 92 shows the first casting after shakeout and prior to cutoff. The gross weight of the casting is 500 pounds. The riser was cut off within 1/2 inch of the casting dimensions. The casting scrapped for the sagged slot cores presented the ideal opportunity for studying the heavy section properties of Inco 713LC. The results of that study were reported in Section X-C of this report.

D. Hexabar for 2 Inch Diameter Pins

The twelve 2 inch diameter, 7 inch long bars required by LTV were cast as two six-bar (hexabar) castings as illustrated in Figure 110. Figure 110 shows the "drag" half of the pattern only. The cope side was simply a 5 1/2 inch diameter oversize riser, made over-

sized to accept a 4 inch I.D. rammed exothermic sleeve. This pattern was molded in a 12"x14" flask in the same materials and with the same procedures as the wedge bar and the connector yoke preciously described. It may be seen that the pattern shown in Figure 110 is also equipped to be molded in circular steel flasks which slip into a slot in the pattern board. Two castings were made on one heat of inco 713 LC vacuum remelted ingot according to procedures already described.

E. General

In making the patterns for the fixture castings, a 5/16" shrink rule was used with reasonably good results. Since the patterns were designed for the simplest production of the parts rather than ideal non-turbulent flow, etc., machine stock of 1/8 inch of all dimensioned surfaces was allowed to permit removal of surface defects where required.

After cutoff and sand blasting, all castings were radiographed to detect internal defects. None were found. However, a considerable occurrence of surface defects similar to folds and cold shuts were noted, particularly on the cope side of the connector yoke casting. It is likely that machining will remove all of these defects but their occurrence served to point up the importance of non-turbulent metal flow, pouring temperature control, and, most importantly, keeping furnace dross out of the pouring stream as it enters the mold cavity.

After inspection, all castings were solution treated at 2150°F for 1 hour per inch of thickness in an argon atmosphere. After a time at temperature determined by the maximum thickness of section in the atmosphere bell of the furnace, the bell was spray quenched to room temperature.

After heat treatment, the castings were shipped to LTV for machining to the required shape.

F. Results and Analysis

The most significant part of the production of the fixture castings is the success of the sand mold and the exothermic material in the vacuum casting of the superalloy configurations produced. On the basis of this success, it may be assumed that serious consideration will be given to utilization of these procedures either entirely or in part for the manufacture of the two full scale components required for this program. The fin beam casting appears to be adaptable somewhat more readily than the turbine rotor casting.

XII. PRODUCTION OF SPIN-TEST DISCS FOR BURST CRITERIA EVALUATION OF CAST ALLOY 713LC

A. Introduction and Disc Design

The fundamental objective of producing and testing a series of "spin-test discs" was to establish a "burst criterion" for the full scale cast 713LC alloy rotor. By definition, the "burst criterion" is a fraction or percentage of the ultimate strength of a material which the designer will not permit the stress in a rotating component to exceed, thus negating catastrophic bursting as a possible failure. The criterion which has been used by the Advanced Component Technology Department (of General Electric Co.) is that the average tangential stress in the disc must not exceed 70% of the ultimate strength of the material. For forged materials, this has been shown to be conservative, but for cast materials, the validity of a 70% criterion has never been established.

The General Electric Company in cooperation with the Abex Research Center, designed a burst test disc for testing prior to the casting of the full scale rotor in the second phase of the program. Stress and distortion values obtained from these tests will be included in the design information for the final turbine wheel. The machine drawing of the test disc is shown as Figure 111. This machine drawing was marked with recommendations for casting and returned to G.E. The recommendations were accepted and the final casting drawing is shown as Figure 112. Machine stock has been added all over the part, and tapers of 6° toward the heavy sections have been added. The castings have been dimensioned such that all critical areas, i.e., areas of high stress during the test, will occur off the centerline of the cast dimensions, thus, if porosity does appear, it will be machined out of the final test piece. Gating and risering of the test disc will be discussed in the next section.

B. General Foundry Practice

1. Basic Rigging Design

A rigging sketch for casting of the sub-scale burst test discs is shown in Figure 113. As can be seen in this sketch, the pattern for the disc required five pieces. (1) a drag pattern which produce the lower half of the disc and the core prints for the hub and mounting flange areas, (2) a cope pattern which produces the upper half of the disc and the O.D. of a ring riser, (3) a corebox for a ring core which fits in the drag print and forms the outside dimensions of the hub and forms the undercut for the mounting flange, (4) a second corebox for the lower center core which forms the inside diameter of the hub and disc and part of the ring riser and contains eight symmetrically located three-quarter inch

-102-

square ingates and a two inch diameter by one and one-quarter inch deep sprue well, and (5) a third corebox for the upper center core which forms the inside diameter of the ring riser and provides a central downsprue of one and one-half inches in diameter leading to the sprue well in the lower center core.

The cope and drag patterns were mounted on boards with pin centers to accomodate twenty four inch square flasks eight inches deep.

The location of the ingates is such that any "hot spots" formed by their presence will be well out of the dimensions of the final product and up in the riser section, thus promoting the hot metal riser conditions to be desired during solidification of the casting.

No fundamental changes were made to the original gating and risering of the burst test disc casting. However, certain minor changes were found to be necessary to produce sound castings free of major surface and other defects that would intrude within the final-machined dimensions.

The first of these changes was to equip the mold cavity with a ring run-off which encircled the perimeter of the casting and provided, through small connecting exit gates, opportunity for some sun-off of metal from the rim of the casting during filling of the cavity. The intent was to eliminate the small cold shuts which constantly appeared at the O.D. without raising the pouring temperature. In this respect, the run-off proved quite satisfactory and was adopted for regular use. Three more castings were made using this ring design before it was discovered that the rapid solidification of the ring prior to the perimeter of the castings was introducing local strains at the intersection of the exit gates and the casting and, consequently, hot tearing. Fortunately, two of the three castings involved were experimental and there was no interference with their performance in that respect. Modification of the run-off system to make the ring discontinuous between each exit gate was successful in entirely eliminating the danger of hot tearing while maintaining the benefits of metal run-off.

Two castings were made to determine the height of the riser necessary to feed the section under the riser and effectively eliminate porosity. This was necessitated by initial underestimates of radiation losses from exposed riser surfaces. The castings were poured with the annular risers four inches and eight inches high, respectively. The casting with the four-inch riser contained shrinkage porosity under the riser to a depth that may have entered into the final casting dimensions.

The casting with the eight-inch riser was completely sound under the riser. In both of these cases, and in all subsequent castings made after the riser cavity was preheated prior to loading the mold into the vacuum chamber. On the basis of this experiment, it was determined that the riser would be poured to the full eight inch height to insure casting integrity.

A pouring basin designed for use with the burst test disc molds was adopted as a standard for all the discs cast.

The design of the basin provides a "cushion" of metal prior to the actual beginning of entry of metal into the mold cavity, provides a "dam" which skims the stream surface as the metal enters the mold cavity, and permits, if desirable, primary choking of the metal in the down-sprue. Since the basin was designed to accommodate other castings as well as the burst test disc, the basin pattern is provided with sprues of several diameters between one-half and one and three-quarter inches. The positions of the sprue relative to the pouring point is also adjustable from about eight inches to seventeen inches, a condition which is most desirable since the furnace tilting position cannot be altered.

2. Molding

As was pointed out in the preceding section, the casting dimensions were selected relative to the final machined dimensions such that the machined product would not be located at the centerline of the casting, thus avoiding the area most likely to contain microporosity. Based upon previous experience with the tapered plates in the foundry variable experiments, very little microporosity was expected. However, due to the critical nature of the application involved, still one more step was taken to insure freedom from microporosity in the final machined burst test disc. In addition to the offset from the geometrical centerline closer to the drag than to the cope surface, a further offset of the solidification centerline was obtained by utilizing molding materials of different chilling capacity in cope and drag surfaces. Specifically, the drag and ring core were molded using zircon-ethyl silicate, and the cope and other core sections were molded using kyanite-ethyl silicate. The chilling capacity of zircon is known to be considerably higher than that of kyanite.

-104-

The overall effect of this selection of molding materials
was to move the solidification centerline of the casting
closer to the cope and still further from the centerline
to the machined product.   The effect on macrostructure
will be discussed in a subsequent section.

Figure 114 shows the zircon ceramic drag section of a spin-
test disc mold after firing to remove the last traces of
alcohol and moisture.   (The particular mold illustrated
was involved in an experiment to determine the most
effective manner of applying the cobalt oxide as a grain
refining agent. Each quadrant marked on the mold has
the cobalt oxide applied in a different manner - this will
be discussed in a subsequent section.) In Figure 114, the
ring core (coated with cobalt oxide) is in place and the
drag is ready to accept the upper and lower center cores.
Figure 115 shows the method by which the cope and drag
sections of the disc molds were fired.   In this illustration,
the bottom flask is a drag section and the upper flask of
the same dimensions is simply a roof rammed in sodium-
silicate-bonded calamo.   A cavity cut in the inside of this
roof and holes molded in its top for gas in and out make it
an ideal method for obtaining very high temperatures on
the mold surfaces without placing the entire mold in a
large furnace.   About one hour of firing by this method was
found to be quite adequate.   Cores are fired separately in
a furnace.   The grain refining coating of cobalt oxide (40g),
ethyl silicate (100g), and alcohol (100g) was applied prior
to firing by brushing on all critical surfaces.

Figure 116 shows the same drag section as in Figure 115.
now with the upper and lower center cores in place so that
the ingates are visible.   Figure 117 shows the complete
mold with the cope in place.   Prior to making this closing,
however, the ring riser opening in the cope was fired for
15 minutes with a gas-air torch in order to establish as
thermal gradient in the mold which would be favorable to
the desired gradient during solidification.

After assembling the mold as shown, the pouring basin
previously described was provided to lead the metal from
the pouring lip of the vacuum furnace into the downsprue.
This pouring basin almost entirely covered the opening of
the riser and thus minimized radiant heat losses from the
riser during the time between firing and casting.

3. Casting

Depending upon the intent of the particular heat, the furnace

-105-

was charged with either all revert, all virgin ingot, or some combination thereof such as 50% of each. After charging the furnace, the molds were loaded into the vacuum chamber (one disc mold and one standard test bar mold on each heat), the chamber was closed, and the mechanical pumps turned on. At a pressure of 500 microns, the diffusion pumps were cut into the system and at a pressure of 50 microns, a small amount of power was applied to the charge to preheat the system. The charge was then permitted to become uniformly red, but not melt, usually about 30 KW was sufficient, and held for one hour. After the hour, the optimum vacuum had normally been reached and the power was turned up for meltdown. After meltdown, the surface of the melt was examined. Frequently, if revert had been charged, a small amount of an unidentified material could be seen floating on the surface of the melt. If this was the case, the temperature was raised to 2850°F and held for ten minutes, after which time the substance normally dissolved completely. With or without this treatment, the melt was then permitted to cool to the liquidus temperature which was recorded on the bi-color pyrometer strip chart. The melt was then re-heated to the desired superheat and poured in the manner specified by the instructions for that particular heat.

In all, a total of 16 spin-test discs were cast for experimental purposes, pilot casting, and final spin-testing. A summary of the objectives and disposition of each of these castings is given in Table XXXIII.

4. Inspection

During the time the spin-test disc castings were piloted, radiographic techniques were developed to give the best inspection possible for the casting shape and alloy with available equipment. The following procedure represents the culmination of a number of methods tried and is the method by which the three final castings were inspected.

All radiography was done parallel to the axis of rotation of the disc. The outer portions of the disc were radiographed in four segments using the 250 volt X-Ray machine. Parameters were 10 milliamperes with a 1 minute, 30 second exposure time on Ansco HD film. The hub was radiographed using a multiple film technique with EKC A-A film and Ansco B in the same cassette. The exposure was 20 minutes with a thirty six inch source-to-film distance using an iridium source originally rated at 50 curie.

Several attempts were made to minimize mottling by varying

-106-

film or technique. In each case, however, the loss in sensitivity was too great to permit the change, even though the mottling was diminished. Inquiry into the subject of mottling in the superalloys has yielded little information other than the fact that it is well known and is virtually impossible to eliminate. A relationship between the radiographic mottling and grain size was observed. It was noted that the fineness or coarseness of the mottling may be directly related to grain size in the cross section.

Except in the specific discs in which porosity was known to exist as a function of short risers, no porosity was revealed in any of the radiographs. In all readiographs, including those of the final castings, surface defects show up readily.

Surface defects, both those revealed by dye-penetrant inspection and those visible without aid, were the major foundry-related problem associated with the casting of the burst test discs. These small defects are related to foreign material trapped in the pouring stream, spalling of the mold, dirt falling into the mold after closing, and other, mostly avoidable sources. The occurence of these defects and their effect on the overall program will be discussed in a subsequent section. In the initial castings, they were handled as follows. After radiography, the castings were dye-penetrant inspected for surface defects. Surface defects, normally in the form of small ceramic or oxide inclusions, were lightly ground out and rechecked with dye-penetrant. The procedure was repeated until one of two possibilities occurred: (1) The defect was ground to a depth which exceeded the finish stock allowance in the particular location or, (2) the defect disappeared. In the latter case, of course, the casting was considered to be satisfactory for shipping.

After radiography and dye-penetrant inspection, the castings were prepared for heat treatment by the methods to be discussed in a subsequent section concerning residual stresses.

The heat treatment was in an argon atmosphere to prevent alloy depletion or oxidation in the areas where the surface defects have been ground out to near the finished part surface.

Part of the inspection of the discs is the determination of the properties of test bars cast with the disc on the same heat. As a control device, each disc mold was accompanied by a single test bar mold which produced ten test bars of the same type cast for the base-line property program. Of these ten test bars one was designated for tensile testing and one was designated for tensile testing and one for stress-rupture testing according to the requirements of AMS 5391A. The bars were heat treated prior to machining. In order to more

accurately reflect the properties of the casting, the test bars were poured at the same temperature as the disc, i.e., with 300°F super-heat. All test bar mold cavities were nucleated with cobalt oxide. The properties obtained on test bars cast in this manner will be presented in a subsequent section.

C. <u>Macrostructure of Disc Cross Sections</u>

Casting 66-123-1 was selected prior to casting to be utilized in a study of the effects of cobalt oxide grain refinement on the macrostructure of the burst test disc and the effect of various methods of application of the nucleating agent to the mold surface. (Note: The casting was also used in a study of residual stresses - this will be discussed in a subsequent section).

In addition, the cut cross sections gave the ideal opportunity to study the effect of the combination of the zircon drag and Kyanite cope (see Section XII8-2') an the location of the solidification centerline.

As can be seen in Figure 114, the cope and drag mold sections of this disc mold were divided into four quadrants. Each of these quadrants was treated differently with respect to the coating method by which the cobalt oxide was applied to act as a nucleating agent for grain refinement.

Quadrant 1 -   No coating applied.

Quadrant 2 -   Brush coated with Slurry No. 1 as follows:
                Nalcoag 1030 (colloidal silica)   500cc
                Water   250cc
                Zircon flour (300 mesh x down)   0.5 lb.
                Cobalt (ic, ous) Oxide (powder) 0.4 lb.

Quadrant 3 -   Brush coated with Slurry No. 2 as follows:
                Synasol Solvent   500cc
                Cobalt (ic, ous) Oxide (powder) 0.5 lb.

Quadrant 4 -   Brush coated with Slurry No. 3 as follows:
                Ethyl Silicate   500cc
                Cobalt (ic, ous) Oxide (powder) 0.25 lb.

The coatings were made by brush. Attempts at spraying all types of coating were successful, but more difficult to control with regard to thickness and uniformity. After coating, the mold sections were permitted to stand overnight and then fired. The cores were coated entirely with slurry no. 2 and fired the following day.

After casting, the surface condition of the disc was observed and found to be generally satisfactory with some super-

iority in the quadrant coated with slurry no. 1, containing colloidal silica and zircon flour. The disc was sectioned and each of the sections macroetched to determine the effect of each of the coatings on the grain size. Figures 118 and 119 show the macroetched cross sections.

Examination of these etched structures shown in Figure 118 and 119 indicates that, while cobalt oxide clearly has the ability to refine the cast grain size, no particular method of application appears to have an advantage. Another, and perhaps more important, observation concerns the location of the centerline of solidification. As has been previously described, the drag mold section is made of zircon while the cope is of kyanite with the intent of chilling toward the cope. Examination of the macro-structures shown indicates that the effort has been quite success-ful in that the meeting plane of the two sets of columnar grains is considerably offset toward the cope. This structure provided a high degree of integrity in the final machined part which is offset considerably toward the drag.

D. Analysis and Treatment of Residual Stresses

1. Initial Discovery and Analysis

Spin test disc casting Number 66-097-1 was scheduled for sectioning for test specimens. According to the section-ing layout, the first cut was to be along a diameter result-ing in two equal and symmetrical halves. To make this cut, the disc was arranged horizontally on an abrasive cut-off wheel table with the hub up. The hub had been cut through and the web was cut less than one-eighth inch through when the disc fractured along the line of the cut with a loud report. The broken disc is shown in Figure 120. Upon fitting the two halves together, as much as three sixteenths inch clearance was found at the hub with the O. D. touching, indicating a relatively high level of residual stress. Due to the highly critical nature of the stress field calculations to be applied to the testing of the discs, it was deemed necess-ary to determine the level of residual stresses in both the "as cast" and the solution treated conditions.

Procedures

Casting 66-123-1 and casting 66-110-1 were designated for testing to determine the precise level of residual stress in both the as cast and the solution treated conditions. 66-110-1 was solution treated by holding at 2150°F for two hours and then cooling by blowing air down on the disc such that the flow of air was parallel to the rotational centerline, and flowed through the hub as well as over the remainder of the disc surface. Both castings were then prepared for stress analysis by lightly grinding a smooth area from mounting

-109-

flange to O. D. and glueing rosette type SR-4 strain gauges to the ground surface as shown in Figure 121. At 180°F from the four gauge locations shown in Figure 121, another four gauges were glued to act as replicates.

After the gauges had been thoroughly dried, they were read to obtain the tare reading on each gauge and waxed to prevent damage during cutting of the disc. After waxing, each gauge area was sectioned out of the disc, leaving no more than one-half inch of metal surrounding the gauge, thus assuring relief of the majority of the stresses existing prior to cutting. After cutting, the gauges were again read and the change in value from the tare recorded for each gauge as strain in inches per inch.

Stresses were calculated from the values recorded from the rosette gauges according to the method described by Hetenyi. (74) The location, value, and direction of all stresses measured on these first discs are shown in Figure 122.

Results and Discussion

As can be seen in Figure 122, the residual stress levels in the as cast disc are totally unacceptable from any point of view. Tensile stresses as high as 61, 000 psi were detected and a compressive force of almost 82, 000 psi exists in the thin area of the O. D.

Even if there was no other reason for heat treating castings made in this alloy (there are the level of the residual stresses would provide reason enough. It is suspected that it would be literally impossible to machine this casting in the as cast condition due to severe warping, and quite possibly, catastrophic failure.

Solution treatment provides considerable relief from the extremely high tensile values of residual stress found in the as cast condition, but little is accomplished in regard to the high compressive values in the O. D. It is most likely that the disc would still be extremely difficult, if not impossible to machine with this high compressive stress level at the O. D. and with tensile stresses nearing 25, 000 psi in the web area.

At this point, it might be well to consider exactly why residual stresses of this magnitude are unacceptable in the burst test discs or on other parts which may be considered in this program. First of all, the problem of machining has already been mentioned. Secondly, even if the part were nursed through the machining to the final shape, the problem of stress relief would again be foremost due to

-110-

the precise calculations of the active stress field which the success of the spin test is co. tingent upon. If, for example, a spin test is set up based upon a stress field calculation which indicates that a given area of the casting will be under a tensile stress of 80,000 psi, and if that area is already under 40,000 psi of residual tensile stress, the total stress value will exceed the yield strength and plastic deformation will occur under uncontrolled conditions, possibly leading to premature failure. This would not be too bad except that the existence of the residual stress and its magnitude would never be known and could not be included as a part of the calculations which would determine the performance of the casting. It is, therfore, considered necessary that the residual stresses in the cast and heat treated part be low (less than 25,000 psi in any direction) in order that machining may proceed without too much difficulty. It is further considered to be necessary that the residual stress of the final machined part be equally low in order that the stress field functioning during spinning by fully understood and under control.

The reasons for the high residual stresses are based upon two main factors. One is the shape and contour of the disc casting which promotes, during cooling from the casting or from the heat treating temperature, steep thermal gradients. These gradients are to be desired from the point of view of casting integrity, but result in unusually high stress buildups in the mold during solidification and cooling. The retention of these high stresses to room temperature is due to the second factor, the high strength of the alloy at elevated temperature. Alloys with low high-temperature strength are self-relieving and in a sense, tend to relieve their highest internal stresses by microscopic plastic flow at high temperature. Inco 713LC, however, with its extremely high elevated temperature strength has a minimum opportunity to relieve itself in this manner and therefore, retains markedly higher stress levels down to room temperature.

In an alloy designed for use in the aged condition adequate stress relief could probably be attained during aging and the problem would be much simplified. Inco 713LC, however, is designed for use in the as cast or the solution treated conditions and, as such, suffers a fair loss of ductility at temperatures where aging proceeds rapidly enough to promote simultaneous stress relief.

The factors discussed up to now lead to the conclusion that stress free part may only be obtained in this alloy and in the configuration of the disc in question by control of the thermal

-111-

gradients which exist in the part during cooling from the
solution treating temperature.

2. Measurement of Thermal Gradients

It was concluded that the best way to attack the problem
of residual stresses was to depend upon a high temperature
solution heat treatment (shown to be beneficial to properties)
combined with control of the thermal gradients in the cast-
ing while cooling from the high temperature. The
erature, 2150°F, serves to relieve the stresses shown to
exist in the "as cast" condition, and the controlled thermal
gradients would serve to minimize the buildup of stresses
during cooling to room temperature. Therefore, the ob-
jective of the first several experiments was to provide a
means of accurately measuring the thermal gradients in the
burst test disc cooling from solution treating temperature.

Procedures

One limitation to be placed upon the experimental procedure
for determining the thermal profile of the burst test disc
during cooling was solution treating temperature. No equip-
ment is available in the experimental foundry for heat
treating castings of the size involved at 2150°F. It was,
however, considered impossible to properly perform the
experiments required outside of our local facilities. The
The compromise was to assume that, for the purposes of
studying thermal profile only, 1900°F would suffice. The
principal objection to this procedure is that the actual
thermal gradient will be somewhat greater when cooling from
the higher temperature. However, so long as the experimen-
tal objective remains the minimum thermal gradient pract-
ically obtainable with continuous cooling at some established
minimum rate, the 250°F difference in starting temperature
will only enter into the picture when the final stress analysis
is performed. Therefore, it was decided that thermal
profile studies would be performed using available equipment
with 1900°F as the solution treating temperature. After
establishing methods to minimize the gradient, final stress
analysis would be performed on a disc solution treated at
2150°F according to the practices established in earlier
phases of this program.

The furnace used for these experiments was a resistance
heated car bottom furnace. Uniform heating is assured

by heating elements in walls, roof, and door. The remote controlled car bottom facilities handling of large parts by overhead crane. The maximum operating temperature is 1900°F.

The first experiments were run with six chromel-alumel thermocouples buried in certain locations in the disc. It was later found that spot-welding of the thermocouple beads yielded equivalent data while offering the advantage of simplicity. Figure 123 shows spin-test disc number 66-198-1 fully rigged with spot welded chromel-alumel thermocouple wires protected with ceramic insulators. The thermocouple locations are labeled 1 through 6.

In order to prevent failure of the couples near the bead, each couple was reinforced with a spot-welded bridge of a high temperature alloy sheet. These reinforcing bridges may be seen in Figure 123, as can the spot welding equipment used to apply the couples etc. In spite of the care taken, however, early experiments were plagued by breakage of the thermocouples. It was not until the stiff ceramic-insulated couples were replaced with glass fiber insulated flexible wire couples that all couples were in operation by the time the cooling thermal profile was to be read. In final form the burst test disc used for successful determinations of thermal profile was equipped with six fiberglass insulated, flexible wire chromel alumel thermocouples. The arc-welded beads of beads of each couple were flattened and resistance spot welded to specific locations of the hub side of the disc. The locations are pinpointed in Figure 124. These locations remained constant for all succeeding tests.

After a number of false starts, the final procedures for obtaining the cooling curves from the six thermocouples were as follows. The disc, with thermocouples attached, was loaded onto the furnace car, moved into the furnace chamber, and the heating cycle begun. Occasionally it became necessary to load the casting with the furnace at temperature. Although this was inconvenient, it was accomplished without excessive difficulty. Prior to loading the casting into the furnace, the thermocouples were hooked to a six-point recorded with the position identity of the couple maintained on the recorded, i.e., position 1 was hooked to indicator point 1, etc. The system was considered ready for test when the six thermocouples indicated 1900°F ± 10°F, and had been held at that point for 30 minutes to insure adequate soaking. The loading operation is shown in Figure 125.

After holding at 1900°F for the required time, the furnace

-113-

door was opened and the car rolled out. The disc began cooling immediately, but the heat of the brick on the car held cooling to less than 25°F in the time it took to lift the disc by overhead crane. After lifting from the fire brick placed on the car to hold the disc, cooling began at the normal air-cooling rate for the casting. The car was rolled immediately back into the furnace and the door shut while the six point recorder traced the cooling curves for each of the six positions.

After determining the cooling rates for the casting with no special treatment, one of the first efforts to reduce the gradients obtained way the application of a ceramic insulator in the areas which had been shown to cool most rapidly. This initial effort was so successful that other possible systems, such as air flow over the heavy sections, etc., were abandoned in favor of a concentrated effort on the insulating system. The ceramic was applied in slurry form and consisted of calcined kyanite (100 mesh) and ethyl silicate as a binder. After applying to the specific areas designated, the slurry was permitted to gel and the excess alcohol burned off. The ceramic was not fired prior to heat treatment.

Results and Discussion

The cooling curves obtained in three representative trials are shown in Figures 126 and 127 and 128. Figure 126 represents the cooling cirves obtained when no steps were taken to minimize thermal gradients. As can be seen, the maximum thermal gradient occurs after about 200 seconds of cooling between thermocouple 1, at the thin perimeter of the disc, and thermocouple 4, located at the heaviest section under the riser pad. The gradient at this point is about 456°F. Examination of this curve suggested that the objective of the control mechanisms to be investigated be to reduce the cooling rate of positions 1 and 2 so that they fell within the group formed by positions 3, 4, 5 and 6. The maximum thermal gradient at any time after cooling began is just over 125°F among these four latter positions and occurs at about 100 seconds. It was anticipated that this reduction in gradient involving the thin perimeter of the disc would reduce the residual stresses in that area to satisfactory levels.

Figure 127 shows an intermediate step in the program to accomplish the above objective. The disc which produced this curve was covered with about 3/8 of an inch of ceramic (as described above) at the perimeter, tapered to less than 1/8 inch just beyond thermocouple 2. Obviously, the effect on the cooling rate of positions 1 and 2 was exactly what was

-114-

required. In fact, the rate of position 2 had been corrected to fall within the much narrowed band containing positions 3 through 6. It remained to similarly adjust the cooling rate of position 1 and additional amount required to bring it into that same band.

Figure 24 represents the cooling rates obtained with a thick ceramic insulator which entirely covered the outer portion of the disc from just inside of position 3 to the perimeter, and tapered from about three quarters of an inch at the perimeter to less than one-eighth of an inch at position 3. As can be seen from the curve, the cooling rates of the more rapid cooling areas of the disc were brought well into line with the heavier sections and the objective of the experiments were apparently accomplished. A maximum thermal gradient of 125°F was reached at 200 seconds after cooling began.

The simplicity of the procedure and the success with which it had minimized the thermal gradients during cooling from 1900°F led to the decision to accept the system for final application on the spin-test discs, pending the results of stress analysis and test bar studies of the effects of the specific cooling rates generated in the disc.

3. Evaluation of the Effect of Cooling Rate from Solutioning Temperatures on Properties

In order to determine if the cooling rates established by the ceramic insulation system described above had any detrimental effect on the mechanical properties of the alloy involved, Inco 713LC, a program of testing was performed which was designed to determine the effect of cooling rate from solution treating temperature (2150°F on these properties.

For this program, separately cast test bars were selected from heats for which properties had already been established within the base-line property range. The test bars were of the standard configuration developed for base-line property evaluation. All bars were brought to 2150°F and held for two hours, after which they were selectively water quenched, oil quenched, air cooled, cooled in silocel (Insulating medium), and furnace cooled to 500°F at a rate which averages at about 1.8°F per minute. The bars cooled in air and those cooled in silocel were equipped with spot welded thermocouples with which the cooling rates for those conditions were recorded.

Figure 129 shows the cooling curves obtained for the test bars cooled in air and in silocel. The most significant

-115-

observation to be made concerning these curves is that
the silocel-immersed bar cooled at a rate considerably
slower than that of the heaviest portion of the burst test
discussing the heavy ceramic insulator (see Figure 128).
If this information is combined with the fact that the air
cooled bar, representative of the cooling method used
throughout the entire evaluation of base-line data, exhibits
a cooling rate faster than any obtained in the burst test
disc, it can be seen that the properties of these test bars
will represent cooling rates which bracket those obtained
in the disc.

The properties obtained from test bars cooled by the
methods described are listed in Table XXXIV. If discuss-
ion is initially restricted to the air and silocel cooled test
bars, it will be seen that the properties are approximately
equivalent except for some advantage for the slower cool
in 1200°F tensile strength and ductility. The rupture
strength and ductility resulting from the slower cool is
also equivalent to that obtained with an air cool (see base-
line property data . On this basis, it may be assumed that
cooling rates in the disc may be varied over a reasonably
wide range with little effect on properties. The insulating
practice for heat treating the discs has therefore been
proven acceptable from the point of view of cooling rate
from solution treating temperature.

The properties of the water quenched test bars exhibit
an interesting reduction in 1800°F rupture life and duct-
ility compared to air cooled or silocel cooled bars (air
cooled data from base-line properties). It is most like-
ly that this reduction is due to an undesirable form of
precipitate which forms as a result of initial retention
in solution by the rapid quench followed by the exposure
to the 1800°F environment of the S-R test. The room
temperature and 1200°F tensile properties are not part-
icularly affected by the water quench, lending support to
the above hypothesis.

The room temperature properties of furnace cooled Inco
713LC reaffirm the low degree of sensitivity of the alloy
to cooling rate. While tensile strength and yield strength
are somewhat reduced, they still exceed the values re-
quired by AMS 5391A. Ductility is excellent in the furnace
cooled bars.

Apparently, except for the combination of very high cool-
ing rates and application under stress at 1800°F or

-116-

other temperatures where undesirable precipitation may be expected, Inco 713LC has an unusually high (for a superalloy) range of cooling rates over which it will continue to function satisfactorily. The advantages of this attribute are obvious in the ability to adjust the local cooling rate of a part in heat treatment with little fear of reducing the mechanical properties to dangerous levels. The advantages in reduced section size sensitivity are also obvious. It is suggested, however, that the aim should generally be toward a slower cooling rate in order to avoid reduction of stress-rupture life and ductility if the final environment requires these at high levels.

4. Development of Final Controlled Cooling Practice

Procedure

While the simple application of ceramic insulation was adequate for the purposes of determining cooling rates under controlled laboratory conditions, the system was found to be lacking in the mechanical strength necessary to permit reasonably rough handling in production heat treatment. Obviously, the ceramic was not bonded to the metal and, consequently, it took very little in the way of mechanical shock to crack sections out of the insulator. The system finally developed to con ensate for this shortcoming. provided a reinforcing grid of heat-resistant wire on the surface of the disc prior to application of the ceramic insulator, similar to the manner in which a coarse wire mesh is used for reinforcement of poured concrete slabs. The grid was applied in two steps. First, short lengths of 14 gauge chromel wire were spot welded vertically to the disc surface to be insulated, then a "spider web" grid of 28 gauge chromel wire was constructed using the 14 gauge wire as anchor points. The entire operation took approximately 15 minutes.

After the reinforcing grid was completed, the disc was placed, hub down, into a bed of sand and surrounded with a galvanized steel strip about 4 inches high and touching the perimeter. This sheet acted as a dam for the ceramic slurry. The ethyl silicate-kyanite slurry was then mixed according to standard molding practice, accelerator added, and poured onto the disc surface to the level of the rough machined riser stub. After gellation of the slurry, the excess alcohol was burned off and the disc was ready for heat treatment. Figure 130 shows a spin-test disc prepared in the manner described. The disc shown in Figure 110 was subsequently heat treated at 2150°F for two hours and cooled in air. The reinforced

ceramic insulator was still perfectly intact after cooling
to room temperature. Embrittlement of the chromel at
2150°F permits the reinforcing grid to be snapped off at
the casting surface without a trace adhering to the casting.

Three spin-test discs were heat treated using the insulating
technique described. Discs 66-388, 400, and 433 were
originally intended for shipment to the General Electric Co.
for spin testing per subcontract arrangements. A fourth disc
was similarly heat treated and then destroyed in connection
with the determination of residual stress levels after heat
treatment. The three discs were heat treated as a unit
in an argon atmosphere in an Inconel retort lowered into
a vertical chamber furnace. The retort was water
quenched from 2150°F. The cooling rate obtained averaged
110°F per minute at the center of the load. This falls
between the two curves established in Figure 129 and may,
therefore, be considered as completely satisfactory.

Results and Discussion

Casting 66-456-1 was heat treated according to the practice
described above but in an air atmosphere and cooled in air.
After heat treatment and cleaning, rosette type SR-4 strain
gauges were arranged on the disc surfaces in a similar manner
to that previously described. Procedures for the determination
of residual stresses were also as previously described.

The residual stress levels in the disc heat treated in the
prescribed manner are listed in Table XXXV. These data
cannot be compared point for point with those shown in Figure
122, since the location of the strain gauges was changed to more real-
istically represent the entire disc rather than certain select
locations. The gauges for these current data were approximately
evenly spaced between just under the mounting flange on the hub
and about one-half inch from the perimeter as shown in Figure
131.

Position 3 is located approximately half way from the hub fillet
to the perimeter of the disc. While the radial stresses in this
area are at satisfactorily low levels, the circumferential tension
is at an unacceptably high level on one side of the disc, and near
the maximum acceptable level of 25,000 psi on the other.

Position 4 is located within one-half inch of the disc perimeter.
The radial stresses are again at low levels, but the residual
compressive stresses in a circumferential direction are more
than twice the maximum value of 25,000 psi. Compared to the
data for the disc cooled without benefit of the ceramic insulator,
there is an improvement of about 20,000 psi. However, it is not

-118-

enough to make the residual stresses acceptable for purposes of low distortion during machining.

Other locations in the disc exhibit residual stresses that are well below the desirable level of 25,000 psi.

Although the ceramic insulating system had reduced the highest peak stresses found in a conventionally solution treated disc by more than 20%, the reduction is insufficient. In addition, an area of high tensile stress, not previously measured, was found in the web mid-section. Obviously, an additional reduction in the thermal gradient across the web section is required to reduce these stresses to the acceptable maximum. The discs which have been heat treated in the Inconel retort as described in the previous section would probably exhibit lower stresses due to the thermal environment of the chamber during cooling. However, in the face of the high stresses exhibited by the insulated disc cooled in air, it appeared risky to proceed with the final machining of those discs. Taking advantage of the recently established knowledge of the minimal effect of cooling rate on properties in this alloy, the three final discs scheduled for shipment to the General Electric Company were re-heat treated, along with another scrap casting for analysis of residual stresses, in a similar manner to the first treatment except that the cooling rate from 2150°F was reduced by cooling the retort in the furnace to 1200°F, after which the retort was water quenched to room temperature. The cooling rate was measured by a load thermocouple located in the center of the load in the retort. The initial cooling rate was 32°F per minute and the overall rate between 2150°F and 1200°F was 12°F per minute. This represents a somewhat more rapid cooling rate than the slowest investigated on separately cast test bars and may, therefore, still be considered as satisfactory based on the properties obtained.

Disc number 66-456 was the scrap casting heat treated as above and subsequently equipped with strain gauges as shown in Figure 131 and sectioned according to previously presented procedures for the determination of residual stresses. The results of the analysis are presented in Table XXXVI which includes a summary of all of the discs tested since the first discovery of the high residual stress problem. As can be seen, the stress levels throughout the disc have been lowered to acceptable values, i.e., less than 25,000 psi.

E. Mechanical Properties of Spin-Test Disc and Control (Separately Cast) Test Bars

-119-

1. Separately Cast Control Bars

The properties of standard test bars cast from the same
heats as a large number of the spin test discs are shown in
Table XXXVII. As expected, the properties of these bars
are excellent.

2. Test Bars Cut From Spin Test Discs

While separately cast test bars lend control to the quality
of the particular heat, the properties of the disc itself must
be known in order to properly conduct the final spin test.
Therefore, an initial casting, 66-097-2, was sectioned
for the determination of tensile properties. The casting
was first cut along a diameter and the resulting halves
marked "A" and "B". The "A" half was left to the as cast
condition and the "B" half was solution treated at 2150°F
for two hours and air cooled using a fan. (Note: It was
during this cutting operation that the extremely high
residual stresses were first discovered.) Test bars were
then cut from the two halves, machined, and tested.

The results of these tests, together with the locations
of the test bars, are shown in Table XXXVIII. It should be
noted that all test bars were of the 0.252 inch gauge diameter
with threaded ends except the four test bars (two from each
half) representing the radial web properties near the O.D.
The dimensions of the casting in this location is such that
only a flat test bar with rectangular cross section may be
obtained. The ASTM recommended dimensions for such a
test bar were followed. The gauge length of this test bar is
1 inch and the cross section for testing is 0.250" x 0.125".

For the most part, the properties of the test bars cut from
the burst test disc casting compare favorably with the base-
line properties, except for a somewhat lower average duct-
ility. However, where the test bar type is the same as used
for obtaining base-line properties, and where no defect
appears as in bar B10, even the ductility compares favorably
with base-line properties.

Further testing of this nature was performed on other discs
prior to the final testing in the General Electric spin test
pit.

Figure 132 shows the location of tensile test specimens cut
from spin test discs 66-456-1 and 66-485-1. 66-485-1 is

-120-

the disc which was air cooled from 2150°F with the ceramic insulator described in a preceding section. 66-456-1 accompanied the three discs destined for testing at General Electric Co. during their heat treatment at 2150°F, followed by cooling in the retort in the furnace to 1200°F. The properties obtained at the locations shown in Figure 132 are listed in Table XXXIX. It will be noted that not all locations are represented in both discs.

The properties of test bars cut from the discs follow, with few exceptions, a similar pattern to those of test bars cut from the plates cast for the foundry variable study reported previously. In the latter case, the plates were tapered from riser to outer limits similarly to the manner in which the discs are tapered from I.D. to O.D., with the riser in a corresponding position. As in the plates, the tensile strength of the disc decreases with increasing section size. This may be best observed by isolating the data from Positions C, E, G, J and L in disc 66-456-1, which represent increasing section size in identical test bar configurations. A similar, although less pronounced effect, may be observed in the data from Positions C through L in disc 66-485-1.

As in the case of the plates, yield strength is somewhat less sensitive to location in the disc. The one low value of 98,880 psi in disc 66-456-1 appears to be a maverick and the general minimum appears to be about 100,000 psi.

As might be expected, the ductility of test bars cut from the discs is lower than that obtained in separately cast test bars from the same heats. Tensile and yield strengths are also lower than those of the separately cast bars. Based on the knowledge gained thus far, these reductions in properties are functions of section size and cooling rate from solution treating temperature. This is supported by the data from Position A in disc 66-485 1 which represents a section size similar to the separately cast bars and which was cooled relatively rapidly from 2150°F (too rapidly to lower residual stresses to acceptable levels). In this location and the one adjacent to it, strength and ductility values approach the values obtained in separately cast bars from the same heat.

While the tensile properties of test bars cut from the spin test disc representing the condition of discs for G.E. for

testing are lower than obtained in separately cast test bars
due to both section size effects and slow cooling rates
necessitated by stress-relief requirements, they still
appear to be quite adequate for the purposes of the program.
The final evaluation depended, of course, upon the results
of the spin testing program by the General Electric Company
as the final step in Phase I of the program.

F. Final Inspection and Shipment of First Three Spin-Test Discs

The three discs scheduled for testing by the General Electric
Company were shipped to machining to final test shape. Prior to
shipment, and after the final heat treatment for the relief of
residual stresses previously described, the discs were reinspected
as follows.

a) Dye penetrant inspection, followed by grinding out of any
small surface defects which may have been missed during
the original inspection. A photographic record of each of the
defect areas, together with its ground-out depth was made
and placed on file.

b) A second set of radiographs were shot after surface grind-
ing. These were shipped to G.E. together with notification
of the transmittal of the discs to the machining vendor.

A full report of the properties of separately cast test bars,
chemical analysis, inspection results, etc., was sent to G.E. in
a manner which approximated the normal customer-vendor relation-
ship. Other, more detailed information was supplied in separate
correspondence.

G. Machining and Stress Relief

1. Procedures

As reported, three discs were shipped to a machining source
for turning to the final test shape for the General Electric
Company. The discs shipped were identified as follows:

66-388-1
66-400-1
66-433-1

Instructions for machining of the discs were supplied to the
machining source by the General Electric Company and in-
cluded the removal of relatively small volumes of metal from
cope (aft) and drag (forward) sides alternately in order to
minimize or prevent warping due to surface stresses generated

-122-

by machining. (The cast and final machined cross sections were shown in Figures 111 and 112). The machining procedures included a stress relief heat treatment to be performed with an envelope of 0.060 inch remaining on the parts. After reviewing all of the available data concerning the properties of Inco 713LC in general and the discs in particular, it was decided that some advantage might be gained by stress relief treatment at 1200°F. The discs had, of course, already been solution treated at 2150°F and cooled in a manner described in preceeding reports to insure no residual stress greater than 25,000 psi. A subsequent treatment at 1200°F exhibited a beneficial effect on yield strength with little change in the other properties of the alloy. Although the 1200°F treatment suggested could never be expected to relieve high overall stresses in the cast part, a partial relief of the surface stresses put into the part during machining might be expected. These surface stresses are known to run as high as 75,000 psi (75), but fall off to zero only 0.003 to 0.004 inches below the surface. Knowing that the overall residual stress level is well below 25,000 psi, a partial relief of these limited-depth machining stresses appeared to be adequate for the purposes of the test. In order to prevent warping during the stress relief cycle due to thermal gradients in heating and cooling, the following specification was set on the treatment.

> "Stress relieve by heating to 1200°F at a rate such that the maximum temperature difference between any two points on the disc does not exceed 50°F. Disc temp-temperature must be monitored by a minimum of 6 thermocouples located on flange, bore (6.00 DIA REF.), both sides of outer web at minimum radius of 8.30 and on both sides of inner web at 5.20-5.70 R. Hold at 1200°F for 16 hours and cool at the same conditions used during heating by again maintaining a maximum temp-erature difference of 50°F.

In addition to the above specification for maintaining a thermal gradient of less than 50°F, a further precaution against warping was provided by supporting the disc on the cope (aft) face and placing a heavy steel weight on the drag (forward) face during the stress relief cycle. The steel weight used covered the drag (forward) face of the disc from a radius of 5 1/2 inches to a radius of 8 1/2 inches. It was matched by a support under the weight which covered the exact corresponding area on the cope (aft) face. A sketch of the set-up is shown as Figure 133.

Disc 66-388-1 was machined and stress relieved according to

the above procedures. After stress relief, the disc
was fluorescent penetrant inspected. A crack was found
at a location which corresponded roughly to the outer
limit of the heat treating fixture. The location of the crack
and its configuration are shown in Figure 134. The dis-
covery of the crack in Disc 66-388-1 resulted in the immediate
cessation of all further machining operations on additional
discs until the cause of the cracking could be determined.
Disc 66-433-1 and 66-400-1 were both fluorescent penetrant
inspected as received from Abex and were found to contain
a large number of indications on their surfaces which were
not detected by ordinary dye penetrant methods used in the
Abex Research Foundry. The course of action from the
point of discovery of the crack and the zyglo (fluorescent
penetrant) indications was as described in the following
sections.

2. Evaluation of Cracking in First Machined Disc

The procedures for determining the cause of the cracking
in the machined and stress relieved spin-test disc were in
three general categories:

(1) Radiographic and zyglo examination.
(2) Macro and microstructural examination, and
(3 Stress analysis.

Immediately upon learning of the presence of surface
indications revealed by fluorescent penetrant inspection
which were not revealed by dye penetrant methods used in
the Abex Laboratory, facilities were installed and materials
acquired for zyglo inspection of all castings for this
program according to the requirements set forth in GE P50T10B
and GE P3TF2-S2, Class E. Discs Numbers 66-388-1 (cracked)
and 66-433-1 were returned to Abex by the machining source.
Disc 66-400-1 was held at the machining source for future
disposition.

The first point to be established was whether or not the crack
existed prior to machining and/or stress relief and, as such,
was not discovered by the final inspection prior to shipment
to the machining source. The final radiographs of the disc
were carefully reexamined for any sign of the crack or an
indication which might provide a point of initiation for a
crack. No indications whatsoever were found. Next, the
cracked disc was re-radiographed. The crack showed up
quite clearly. No other indications were found. Finally,

-124-

a separate section of Inco 713LC was machined to a thickness which, when added to the cross section of the machined disc, would bring the total section in the cracked area to the exact dimension it was prior to machining. The disc was radiographed again, this time with the additional metal section covering the crack. The crack again showed quite clearly in the radiograph of the thicker section. These steps proved to the satisfaction of those concerned that the crack did not exist in the casting prior to machining and stress relief; at least not in its final form.

After the radiographic work was completed, a quadrant of the disc was isolated with wax strips for protection of the remaining surface and the quadrant was etched with HCl activated with H_2O_2. The structure revealed by the etching showed no unexpected anamolies or defects and followed exactly the pattern to be expected from previously macroetched cross sections. The macroetched section is shown in Figure 135.

After macroetching of the separate quadrant (the cracked area was not macroetched at this time), rosette type SR-4 strain gauges were mounted to the disc in a manner identical to that illustrated in Figure 131. After reading the gauges, the disc was sectioned to relax any residual stresses and the gauges read again. Residual stresses were measured from a minimum of less than 300 psi to a maximum of 7,229 psi. These stress levels gave excellent testimony to the efficiency of the stress relief afforded by the controlled cooling from solution treating temperature. Surface stresses of very limited depth, however, are not measured by this method. This examination of the stresses remaining in the machined and stress relieved disc served to show that no permanent high stress level had been permitted to build up in the disc during processing up to that point. There is no question, however, that a locally high stress would not be detected by this method after cracking had effectively relieved that stress.

During the sectioning of the disc for measurement of residual stress, the cracked area was carefully cut away from the main body of the disc and treated in the following manner. First, a section of disc was cut which contained only part of the crack at one of the crack termini. This section was fractured through the crack and examined to determine the characteristics of the crack interface and the fresh fracture continuing from it. Secondly, a microspecimen was cut and mounted to represent a cross section of the crack. Another was cut and mounted

-125-

to represent the surface appearance of the crack. A third section was cut from an area near the crack and was forcibly fractured. The fresh fracture surfaces were exposed to 1200°F for several hours and then examined for color, etc.

The nature of the crack interface may be characterized as generally smooth with curved contours and apparently grain boundary in nature. The color of the crack interface was a light moss green. New fracture surfaces were characterized by a more "dendritic" appearance than the crack interfaces. However, on exposure to 1200°F for an extended period, the new fracture surfaces exhibited both a blue oxide and a green coloration, the latter an exact match for the crack interface color. The microstructure of the crack exhibited an inter-granular character viewed in both cross section and plan view. Evidence of a thin oxide film was found at the inter-faces. Polarized light revealed a green flourescence which satisfied the observer that the thin film contributed the green color observed on the interfaces, and that the probable identification was chromium oxide. In one area in the micro-structure near the crack, a scattering of non-metallic inculsions atypical of those normally found in vacuum melted metals indicated that there was some possibility that the origin of the crack could have been an unobserved defect in the form of an exogenous non-metallic inclusion from the mold surface or other source.

From these examinations it was concluded that the cracking occurred during either machining or the 1200°F stress relief and could have originated as a tiny defect in the cross section not detected by the inspection techniques used. Later work, reported in succeeding paragraphs, pointed to the existence of a st:ep thermal gradient in the disc during stress relief heat treatment which may have been the main contributing factor to the cracking. However, it is impossible to state conclusively that the cracking would have occurred whether or not some point of nucleation were provided by a discontinuity in the cast structure.

3. Reinspection and Replacement of the Spin Test Discs

Spin test disc 66-400-1 had been left at the machining source for later disposition while the analysis of the cracking was conducted. After determining that the cracking _may_ have been due to the presence of sub-surface oxide inclusions related to the zyglo indications found on the cast surfaces, machining of 66-400-1 was begun in steps of roughly 0.020" with alternate zyglo inspection after each machining step. As the machining

proceeded in this manner, it was noted that the surface zyglo indications disappeared within about 0.060 inch of the surface. The disc was machined to the 0.060 inch stress relief envelope and shipped to Abex for the 1200°F stress relief treatment. The heat treating fixtures were shipped with the disc. Upon receiving the disc, it was re-zyglo inspected and re-radiographed. No interpretable indications were found. The stress relief heat treatment specification followed for Disc 66-388-1 was adhered to exactly with one addition. It was assumed that the coolest spot on the disc during heating (or the hottest during cooling would be the area located under the massive heat treating fixture. This was the one area which, in the original system, was not monitored for temperature during the heat treating cycle. For disc 66-400-1, all of the original 6 thermocouples were placed in their positions and one additional couple was placed through a 1/8 inch hole drilled from the top of the upper fixture to the disc surface. The bead of the thermo- couple was held in contact with the disc surface. Using the same 50°F maximum thermal gradient as for the first disc, it became obvious immediately on beginning the stress relief treatment that the area under the fixture lagged far behind all other areas in temperature. No attempt was made to determine what the gradient would have been if this additional thermocouple was ignored, but it was obvious that several hundred degrees would not be an exaggeration, particularly in view of the fact that it took 28 hours to bring the disc up to 1200°F and another 28 hours to cool it to 200°F under the new conditions.

After stress-relief, the disc was reinspected and found to be perfectly sound. It was shipped back to the machining source for final machining. Disc 66-400-1 received its final post machining inspection consisting of a hot acid etch followed by zyglo inspection, and was found perfect.

Disc number 66-433-1 was returned to the Abex Laboratory along with the cracked 66-388-1. After re-radiography in- dicated that no deep defects were present, a band was mach- ined from the cope surface which encompassed most of the most severe zyglo indications. The band was machined to a depth of 0.070" and re-zyglo inspected. It was found that all of the zyglo indications in the band had been removed by the machining. It was assumed, then, that the final configuration would be free of similar defects.

In addition to the salvage work done on 66-400-1 and 66-433-1,

two additional discs were cast to replace 66-388-1 and
either one of the others which might have proven defective.
There was a strong suspicion that the zyglo indications on the
casting surfaces were due in part to the cobalt oxide grain-
refining coating used on the molds for the discs. The coating
was eliminated from the molds for the two replacement discs.
In addition, the castings were poured under 100mm of argon
rather than high vacuum. However, all other procedures
including melting etc. under high vacuum were identical to
those reported for the first discs.

Inspection of the two replacement discs, 67-268-2 and 67-284-2,
revealed a markedly larger grain size that in the previous
discs accompanied by a significant decrease in the number and
size of the surface zyglo indications. Unfortunately, a center
core shift in 67-284-2 resulted in dimensional discrepancies.
However, the casting has been dimensioned and still appears
capable of producing the final shape. The increase in grain
size was predicted to have only a minor effect on the properties
of the disc according to studies of test bars made with and
without the grain refining benefit of the cobalt oxide coating.

Three discs were shipped to the machining source in addition
to the one already machined and shipped to General Electric
for testing. After examining the two replacement castings
67-268-2 and 67-284-2, it was decided that the former (67-
268-2) would be accepted as a replacement for the cracked
66-388-1. The decision was based entirely on dimensional
considerations rather than any metallurgical or quality diff-
erence between the two castings. The "spare" casting,
67-284-2, was returned to the Abex facility to be held against
additional contingencies. Disc number 66-433-1 was chosen
as the third disc. The machining and testing schedule for the
spin-test discs was finally resolved to the following order:

> (1) disc 66-400-1,
> (2) disc 67-268-2,
> (3) disc 66-433-1.

The machining of disc 66-400-1 proceeded with no dimensional
problems, although surface finish after the final lathe operation
was inadequate to permit spin testing without additional work.
The final finish was obtained by rotating the disc slowly on the
lathe and polishing with aluminum oxide paper on a disc sander.
Blemishes which were deeper than 0.003 inch to 0.004 inch were
locally polished with a hand grinder. Examination of the
surface blemishes produced by the lathe turning operation in-

-128-

dicated that the tool was literally "tearing" surface grain boundaries to a very limited depth. The blemishes on the surface were not, in fact, defects, but were introduced to the surface by the tool. In retrospect, it appears quite possible that this type of blemish, combined with the high thermal stresses developed in the first relief treatment given disc 66-388-1 might have contributed to the cracking. The notch effect of a torn grain boundary is obvious.

After polishing with the aluminum oxide paper, as described above, the surfaces of the disc were completely free of blemishes caused by the lathe tool and were accepted for testing. The machining of disc number 67-268-2 proceeded satisfactorily through rough machining to the 0.060" envelope. Stress relief treatment at 1200°F was carried out according to the procedures developed by Abex on disc 66-400-1. The casting was defect free after stress relief. Unfortunately, during the final machining, one of the last lathe cuts was taken too shallow. It has been found that a shallow cut in this (and other) superalloy creates a condition where no cutting occurs, but the tool severely smears (cold works) the immediate surface. In this case, the result was the creation of an asymmetrical stress distribution in the thin disc section and an 0.080" warp toward the effected face of the disc. After consulting with the General Electric Company Engineers, it was decided that disc 67-268-2 would be put aside for testing last, and that 66-433-1 would be moved up to second position. The schedule adopted was as follows. If the tests of 66-400-1 and 66-433-1 were successful and indicated reliability and repeatability, the warped disc 67-268-2 would be tested to determine the capability of the casting to conform to uneven stress distribution during spin testing. If, however, repeatability was not inferred by the two preceeding tests, then the spare disc held by Abex would be substituted for the third and final test.

As will be discussed in the next section on spin-testing, the first two tests were quite successful and disc number 67-268-2 was final polished and tested.

The machining, stress relief, final machining and polishing of the third disc 66-433-1 proceeded according to the prescribed methods with no difficulty other than those apparently inherent in the cast alloy.

In general, machining of the three cast Inco 713LC spin-test discs was found to be difficult, particularly with respect to surface finish.

-129-

4. Analysis and Discussion

Several important factors came to light during the investigation of the first disc cracking and the subsequent replacement through salvage and remaking. It appears obvious that a steep thermal gradient during the stress relief heat treatment at 1200°F engendered the cracking observed in the first spin test disc. However, there is no conceivable way of discounting the possibility that one of the zyglo indications later observed on the cast surfaces of other discs was deep enough to provide a nucleating site for the crack.

The presence of the surface defects detected by post emulsion type fluorescent penetrant inspection was totally unsuspected based on the less sensitive dye penetrant inspection performed by the Abex Research Foundry prior to shipment. This led naturally to two distinct courses of action. Facilities were immediately installed to perform the more sensitive inspection method and an investigation was begun into possible sources of the indications. The first part of the process to come under suspicion was the cobalt oxide slurry brushed on the mold surfaces prior to firing. This suspicion proved to be partly justified based on the much improved surfaces of discs cast without the coating on the mold.

Just as important to the program as the discovery that the cobalt oxide produces a large proportion of the zyglo indications is the fact that elimination of the oxide does not eliminate all of the surface indications. Metal turbulence and other metal and mold parameters obviously enter the problem.

H. Summary of Spin-Test Discs Cast

Table XXXIII summarizes the objection and disposition of the total of sixteen spin-test discs cast.

While certain problems were associated with casting of the burst test discs which were not anticipated at the inception of the program, a great deal more has been learned about the casting of large superalloy castings than would have been if the discs had been extremely simple in form as had been originally anticipated. In its final form, the burst test disc required 250 pounds of metal to produce a 66 pound casting after the riser and gates are removed. Unavoidably, about 50 to 60 pounds of the total heat weight is left in the pouring basin as a heel. This leaves a casting which, with gates and risers complete, weighs approximately 120 pounds. Yield is about 50% if the pouring besin heel is ignored.

-130-

Pouring temperature for the final castings was 300°F above the liquidus, the minimum temperature at which the casting could be poured and be reasonably free of cold shuts near the O. D., even with the run-off system operating.

Chemical analyses and change materials for all spin-test discs castings appear in Table V.

XIII. TESTING OF SPIN-TEST DISCS AND ESTABLISHMENT
OF BURST CRITERIA

A. Equipment and Objectives

The General Electric vertical spin-test pit together with some
of the associated control and monitoring equipment, is shown in Figure 136.
While the nature of the instrumentation and the mechanics of design are
somewhat sophisticated, the basic principles of the apparatus are simple.
The objective of the equipment is to provide a means of evaluating the
behavior of various materials and designs under conditions of high rotational
speeds, such as those that are encountered in turbine engine operation.
The specific objectives of the tests performed for this program were to
provide criteria for the design of the final turbine rotor to be cast on
Phase II of the program and to provide information regarding the mode
of failure (i.e., ductile, brittle) for the material. The testing of three
discs provided a measure of the repeatability and, therefore, the reliabil-
ity of the material and process under examination.

Figures 137 and 138 provide a closer view of the spin-test pit
during the loading of one of the discs from the current program. The
scars of previous bursts are easily visible on the interior surfaces of
the pit.

B. General Procedures

Prior to testing, each of the spin-test discs was macroetched
in a solution of hydrochloric acid and hydrogen peroxide. This served
two functions. Mainly, it served as a means of removing any metal which
might have been smeared over a minor defect during machining and
finishing. A subsequent fluorescent penetrant inspection would then reveal
these defects. Secondly, the cast macrostructure was revealed for
examination and record. After penetrant inspection, one side of the disc
was painted in a patchwork fashion as shown in Figure 139. The colors
red, yellow, gray, green, black, white and orange were used. This color
code was recorded for subsequent use in re-assembling the disc after burst.
After painting, the disc was mounted on the testing arbor, the entire
assembly balanced, and placed in the spin-test pit, as shown in Figures
137 and 138.

The general procedure for testing was to lad the disc incrementally
from zero to a target of 20,000 rpm. This rotational speed corresponds
to a calculated tangential stress which is 90% of the estimated, minimum
ultimate strength of Inco 713 LC as determined from test bars cut from
earlier cast discs (see Table XXXIX, etc.). This will be discussed in
greater detail under "Discussion of Spin-Test Results".

-132-

If the disc did not burst before 20,000 rpm, the speed would be increased until failure occurred.

All spin tests were carried out at room temperature.

C. Test Results

Test 1: Disc No. 66-400-1

Figure 140 shows disc 66-400-1 after macro-etching and mounting on the spin-test arbor. Careful examination of this photograph shows that an area of radial columnar crystals appears in the disc near the O.D. in one quadrant. This columnar area is shown in more detail in Figure 141. Although this structure appears unusual, it would not, except under very special and restricted conditions, be considered detrimental. The formation of a columnar structure such as this is the result of the accidental setting up of a certain thermal gradient, together with a selective heat flow toward the O.D. of the casting during solidification. This is a very likely result of the tapered cast section and fits in well with the observed rate of heat loss from the thin O.D. compared to the heavier section nearer the I.D. of the casting. In essence, the area over which the columnar grains exist solidified unidirectionally. Based on recent literature, it would be interesting to know the properties of a disc with all of its structure solidified unidirectionally from O.D. to I.D.[76], [77]. For the moment, however, it is sufficient to recognize that the properties of the columnar zone may, in fact, be superior to the areas containing equiaxial crystals.

The first efforts to spin-test disc number 66-400-1 were unsuccessful due to an excessive vibration which was set up in the equipment at 14,000 rpm. The disc and arbor assembly was rebalanced and the test repeated, but the same phenomenon occurred, and at the same speed. At first, it was suspected that the disc itself had a natural frequency which was being excited by unbalance. Past experience had shown that discs become resonant when the frequency of a backward traveling wave in some particular mode shape drops to zero. Analysis showed that the rotor speeds where this mode occurs for this disc design are at 8,300 rpm, 9,000 rpm and 17,700 rpm for the 4, 3 and 2 nodal diameter modes, respectively. The first two critical speeds actually occurred at about 8,000 rpm and 10,000 rpm, but the third one was never reached since vibrations became excessive at about 14,000 rpm.

The only disc vibration which could occur in this speed range is what is known as a minor resonance. The frequency of a backward traveling wave in a one nodal diameter mode never drops to zero. However, there is a speed where it becomes resonant with a one-per-revolution stimulus. This is a minor resonance. For this disc, the calculated speed is 13,100 rpm. Since this was close to the speed at which the serious vibrations were occurring, it was strongly suspected that this was the cause. However, this suspicion was lessened after several vibration experts at the General

Electric Company facility were consulted and they agreed that this mode of vibration is extremely difficult to excite and has never been known to occur except when intentionally excited or induced.

With the disc itself basically cleared of being at fault in the 14,000 rpm vibration problem, attention was focused on obtaining the shaft critical speed. Considering the disc to be rigid, the first calculated shaft resonance did not occur until 25,000 rpm and, obviously, was not contributing to the 14,000 rpm vibration. Two possibilities remained. One was that the flexibility of the disc was reducing the value of shaft response to a lower speed. The second was that the size and shape of the disc could promote gyroscopic instability. Both of these problems were considered difficult to identify analytically.

Rather than spend additional time on analysis of the system, it was decided that the facility design would be modified in a manner which would compensate for either of the two remaining possible causes. This was accomplished by changing the shaft system from pinned at one end and free at the other (pinned/free) to fixed at both bends (fixed/fixed). This was done by replacing two large clearance "catcher" bearings with close tolerance bearings at different locations on the shaft. This modification entirely eliminated the 14,000 rpm vibration and permitted full testing of the disc.

Additional, but minor, facility problems caused a shut down of this first test at 22,000 rpm and 23,200 rpm. At the time of these brief shutdowns, the disc bore radius was measured. A permanent set of 0.006 inch and 0.022 inch, respectively, were measured. While there is no specific design criteria that can be developed from this incidental information, it is no less important to note that the ductility of the alloy permitted this permanent set to occur without failure in the bore.

The final burst of disc 66-400-1 occurred at a rotational speed of 23,800 rpm which is representative of 117,000 psi tangential stress, or 96.7% of the estimated tangential ultimate strength. The burst of 66-400-1 was into both large and small pieces. However, there were a sufficient number of small pieces to frustrate any attempt to reconstruct the disc using the color coded paint. The test pit containing the remains of this first disc tested is shown in Figure 142. Several large pieces of disc can be seen in the pit bottom, but the impracticality of reconstruction is made obvious by the scattering of many pieces less than 1/4 inch in any dimension. Figure 143 shows the arbor after testing. As can be seen, a sizable portion of the disc has remained attached to the arbor, although it and the fasteners show considerable distortion.

Test 2: Disc No. 66-433-1

After repairing of the spin-test pit, the second spin test was initiated on disc number 66-433-1. This second test proceeded without incident to a speed of 23,189 rpm which produced a tangential stress of 111,000 psi. This is 91.7% of the estimated ultimate tangential stress. The test was not carried out to bursting. By stopping short of the final bursting, damage to the test facility was averted and the third test could be performed immediately. There was ample justification for not carrying the second and third tests through to the burst. It is not anticipated that any disc would ever be designed to have an average tangential stress greater than 90% of its ultimate strength. It was felt, therefore, that adequate design criteria had been established by simply exceeding the 90% level during the test, particularly in light of the high bursting stress recorded for the first disc. An unexpected dividend was discovered upon post-testing examination of disc 66-433-1. The odds against stopping a test at a point where failure has begun, but has not propagated to bursting are quite high. However, in this case, a small crack was found to have formed in the highly stressed bore area. Figure 144 shows the location of the crack in the disc after removal from the test arbor. The same crack is shown at roughly twice normal size in Figures 145 and 146, the latter exhibiting the macroetched structure in the bore area.

Test 3: Disc No. 67-268-2

It was assumed that sufficient data had been generated by the first two spin-tests to establish a design criterion for the cast turbine disc to be designed for the Phase II effort. However, an ideal opportunity to evaluate the ability of the cast Inco 713 LC discs to conform to symmetrical stresses was presented by a 0.080 inch warp which appeared in disc 67-268-2. In addition, since this disc was made without the benefit of the grain refinement afforded by the cobalt oxide coating on the mold surface, the grain size was considerably larger than its two predecessors (see Table XXXIII). Therefore, it seemded advisable to test this disc to at least 90% of the estimated ultimate tangential strength to determine the effect of these parameters on an actual spin-test result.

Spin test number three proceeded without incident to a terminal speed of 23,230 rpm which produced a tangential stress of 111,100 psi which is 92% of the estimated ultimate strength. The disc did not burst. Post-test examination indicated that the disc had conformed to the unequal stresses induced by the warp by plastic deformation of the surface in tension. Further gratification for proceeding with this test in spite of the warp was obtained from the fact that this disc also exhibited pre-burst cracking. In the words of a report originating at the G.E. Co.,

"Upon examination of the disc, it was
noted that considerable yielding had
occurred in the bore and in the web.
As in the case of (test) number two,
cracks were found at the bore, but on
this disc, cracks were also discovered
in the web. It would appear that the
failure point of these discs has been
well established and with good repeat-
ability. "

D. Discussion of Test Results

In general terms, the results of the spin testing of the three
cast Inco 713 LC discs was considered successful beyond the
expectations of General Electric Company personnel involved in the
program. A summary of the data appears in Table XL. The best
possible summary of the results however, is provided by the words
of the design engineer in charge of the project at G. E. Co.

"To permit evaluation of the results of
the burst test (s), it was first necessary
to determine the ultimate strength of the
material. Since the average tangential
stress is the stress in question, the tan-
gential test bars from disc number 65-456-1
(see Table XXXIX) were considered and
the ultimate strengths of these test bars
were averaged. (These bars are labeled
in Figure 132 as A, B, C, E, G, J, and L)
Disc number 66-456-1 was selected
since its heat treatment most closely
duplicated that of the (final) burst test
discs. The average ultimate strength
was determined to be 121, 000 psi. "

This value of 121, 000 psi was then used for all comparisons of
the actual stress in the test discs. Again quoting from the General
Electric reports to Abex,

"The criteria(on) which is presently used
by Advanced Component Technology Dept.
turbine rotor designers to insure that burst
does not occur in a disc is that the disc
average tangential stress must not exceed
70% of ultimate strength. For forged
materials, this has been shown to be con-
servative, but for less ductile cast
materials, the criteria(on) has not been
established. "

-136-

The G. E. design engineer then goes on to discuss the specific results of the spin-test discs supplied by Abex under the current contract and tested by the General Electric Co.

"The possiblity of shutting down a spin test just at the point where failure begins is quite remote. To accomplish such a thing on two successive tests is much more unlikely, but we have done just that on spin test numbers two and three. This would seem to be a sign of excellent repeatability of the casting process, ... good luck, or a combination of both. "

"As a result of the spin test phase of the program, it has been established that disc castings having ductilities as good as Inco 713 LC can be designed for an average tangential stress of 90% of the material's ultimate strength. Good design practice of course, requires that some margin safety be factored into disc design, but there should be no question about using 70% of ultimate as is currently used for forged discs. In designing the full scale disc for this program, 70% of ultimate will be used...."

Little can be added to the discussion and conclusions reached by General Electric engineer. However, from the foundry metallurgists point of view, credit must be given to the fundamental soundness of the casting supplied as well as to the inherent ductility of the material. It is doubtful that the presence of any major areas of microporosity in the highly stressed disc would have permitted the performance recorded for the test discs. The factors of stress, etc., learned from the spin tests will be used by the G. E. designers to design the final turbine rotor. In a similar manner, the details of feeding distance of risers, tapered sections, etc. applied to these discs will be applied by the foundry to the casting of the final shape.

XIV. DESIGN PROPERTIES FOR THE G. E. TURBINE ROTOR CASTING

At the request of the General Electric Company, all of the mechanical and physical property data obtained during the Phase I effort wꞁre reviewed and the anticipated minimum values for certain properties determined. Naturally, the predicted properties were to be based on the cast rotor rather than separately cast test bars, therefore, heavy section properties were considered as well as thin section properties.

Table XLI lists the anticipated <u>minimum</u> property levels and certain physical properties of Inco 713 LC based, except where indicated, on the data generated in the current program. Physical data, such as density, was obtained from literature sources.

It may be observed that some of the property levels appear considerably lower than those determined as base-line properties from separately cast test bars, and lower than the properties obtained from cast plates. However, the properties listed are based on a conservative estimate of the properties in the bore of the proposed rotor which will be cast almost entirely solid and result in a section thickness approaching four or five inches. Other areas of the rotor will have consistently higher property levels than those listed.

While the figures shown in Table XLI will serve as design values, the actual properties of the cast rotor will be determined by test bars cut from a representative casting after heat treatment. These will be reported at an appropriate time.

XV. CONCLUSIONS AND RECOMMENDATIONS - PHASE I

1. Under the conditions of manufacture and testing detailed in this report, the base-line mechanical properties of alloy 713 LC are generally superior to those of either R-41 or alloy 718 at room temperature, 1200°F and 1600°F, the temperature of interest. Special heat treatment can raise the properties of alloy 718 markedly, but section size and cooling rate sensitivity could be quite troublesome compared to the low sensitivity of 713 LC to these factors. R-41 has no value for this program due to extremely limited ductility.

2. The foundry characteristics (i.e., section size sensitivity, feeding characteristics, fluidity, sensitivity to microporosity, etc.) of alloy 713 LC are satisfactory for the manufacture of large castings with section sizes up to at least 5 inches. Heavier sections may be possible, but the investigation did not go beyond 5 inches. Of particular benefit is the low degree of sensitivity to section size and cooling rate noted in the alloy. This is documented by the microstructure as well as the mechanical behavior of the alloy.

3. Alloy 713 LC was designated for use throughout the remainder of the program based on the above conclusions.

4. The following conclusions and recommendations were based upon investigations of foundry practices and procedures for alloy 713 LC.

> a. Direct charging of foundry returns (gates, risers, etc.) is permissable only under special circumstances, and then, only the cleanest select revert should be permitted. Ideal practice would be to convert the foundry returns to virgin ingot for remelting, all under vacuum melting and casting procedures.

> b. The use of cobalt oxide (chemically pure as well as lower purity grades) as a coating brushed on the mold surface prior to firing provides significant grain refinement which appears to have some ability to "throw" across a cast section. The advantages of the finer grain size, however, are minimal under the conditions tested and may be offset by the contribution of the oxide to a surface defect problem. The cobalt oxide cannot be combined with the aggregate in an ethyl silicate bonded mold due to a severe mold degradation.

> c. Rammed sand molds bonded with sodium silicate can be used in the casting of alloy 713 LC in vacuo. Zircon sand may be used as a facing and a coarse calamo as a backing sand. Baking of the molds at temperatures above 800°F is required.

d. Exothermic materials may be used in vacuum casting providing two precautions are observed: (1) the exothermic components must be baked at temperatures above 800°F, and (2) the castings must be poured at a pressure of 100 mm of argon (or other inert gas).

5. The following conclusions are based on the manufacture and testing of several spin-test discs designed to establish burst criteria for the alloy and the casting.

a. The development of steep thermal gradients in a large 713 LC component during cooling from casting or heat treatment at high temperature (2150°F) can introduce extremely high residual stresses which must be either accounted for or eliminated prior to application in service. The simplest means of elimination of these stresses in heat treatment is by reduced cooling rates combined with methods of minimizing section size differences by padding with insulating material.

b. The final turbine rotor casting will be designed with a 70% burst criterion, the same criterion currently used for forged discs.

6. In general, it is concluded from the work performed during the first phase of this program that the alloy 713 LC can be used to manufacture the large superalloy castings required, i. e. , a main fin-beam casting and a turbine rotor disc for application at 1600°F and 1200°F respectively.

XVI. OUTLINE AND OBJECTIVES FOR PHASE II

The work which will follow in Phase II will be directed exclusively toward the manufacture and testing of the required full scale superalloy components. The knowledge gained in Phase I will be applied fully to the production of these components. A general outline of the effort is as follows.

I. Design of the Turbine Rotor Disc and Main Fin Beam

II. Design of the rigging (gating and risering) for each component.

III. Tooling Manufacture

IV. Pilot Casting

V. Production Casting

VI. Machining

VII. Testing.
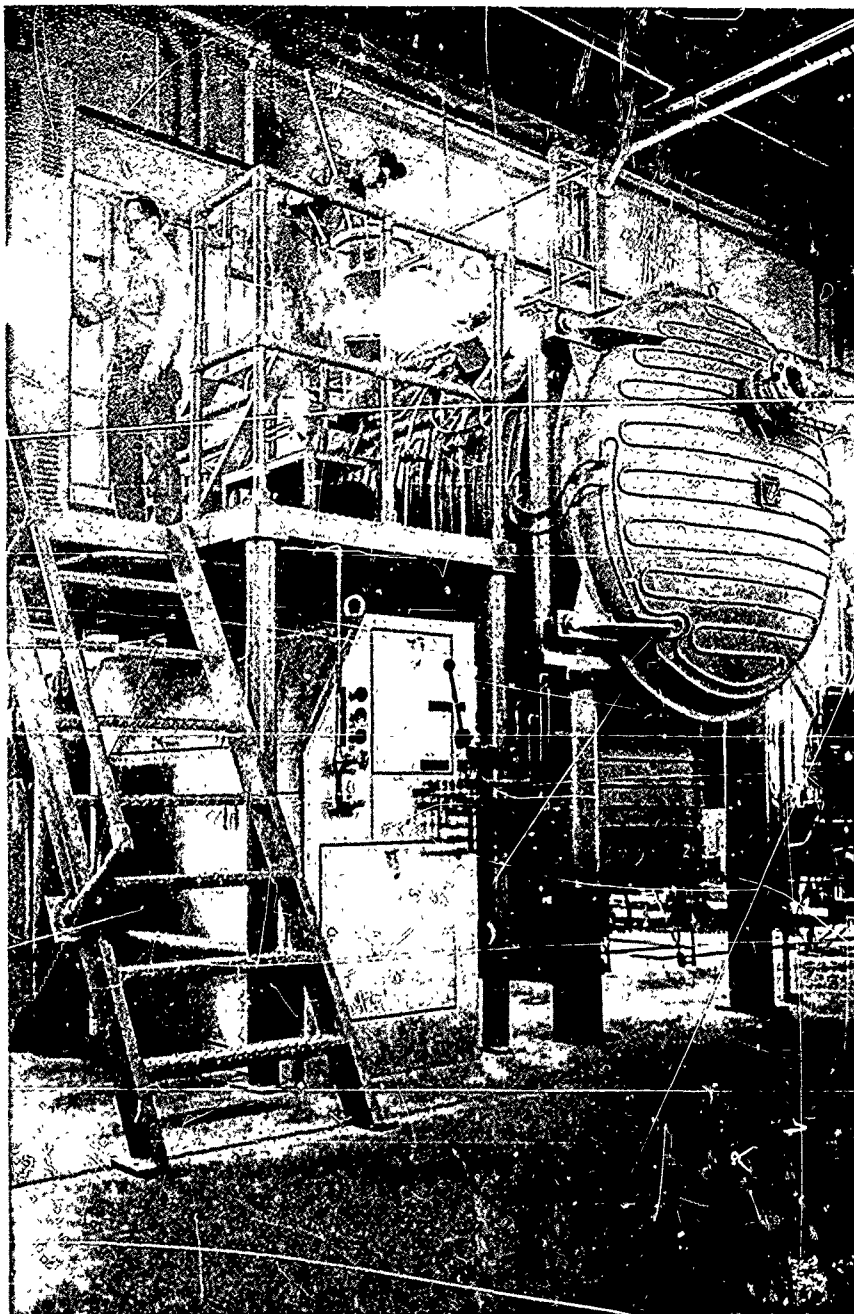
Figure 1

Overall View of Vacuum
Melting and Casting
Furnace
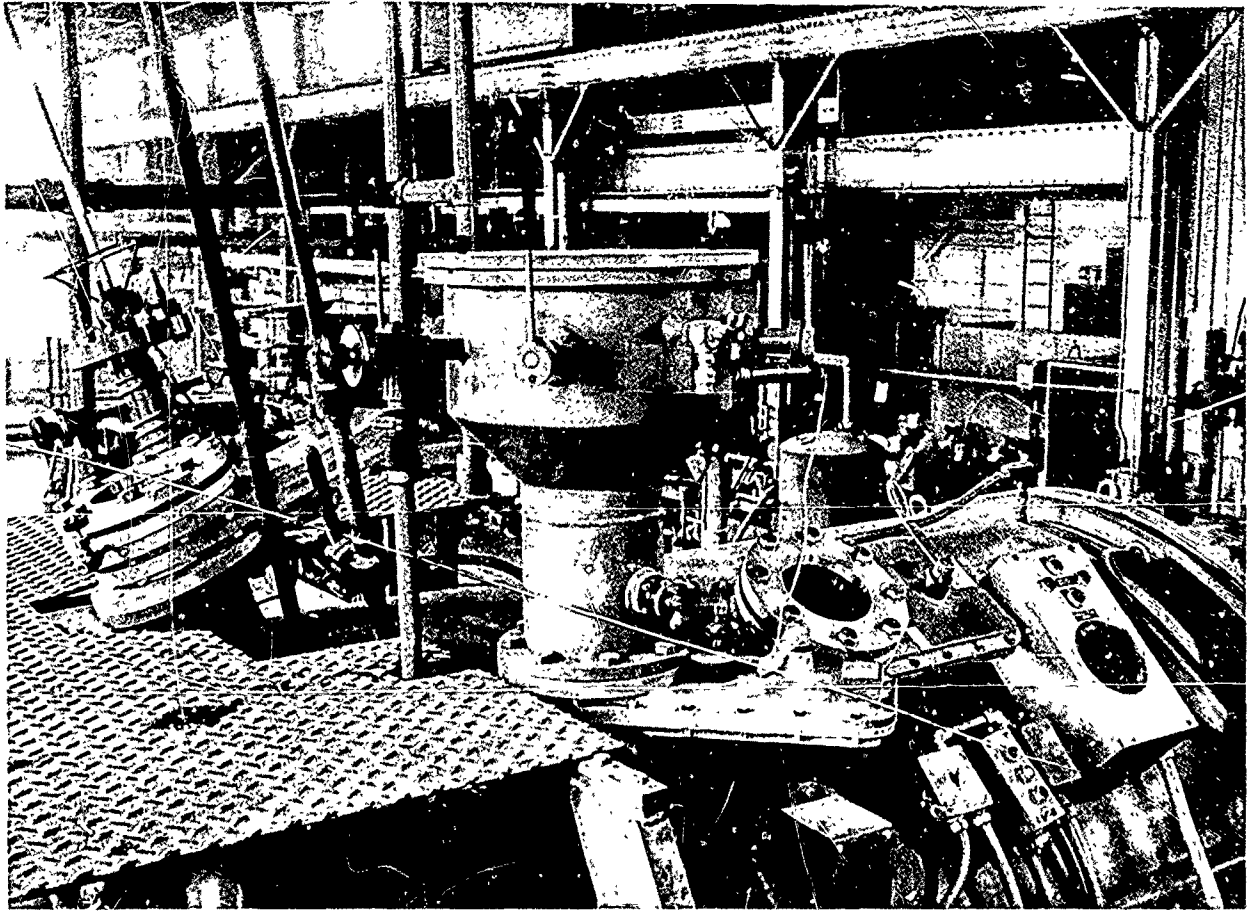
Figure 2

Vacuum Melting Furnace
Support Equipment
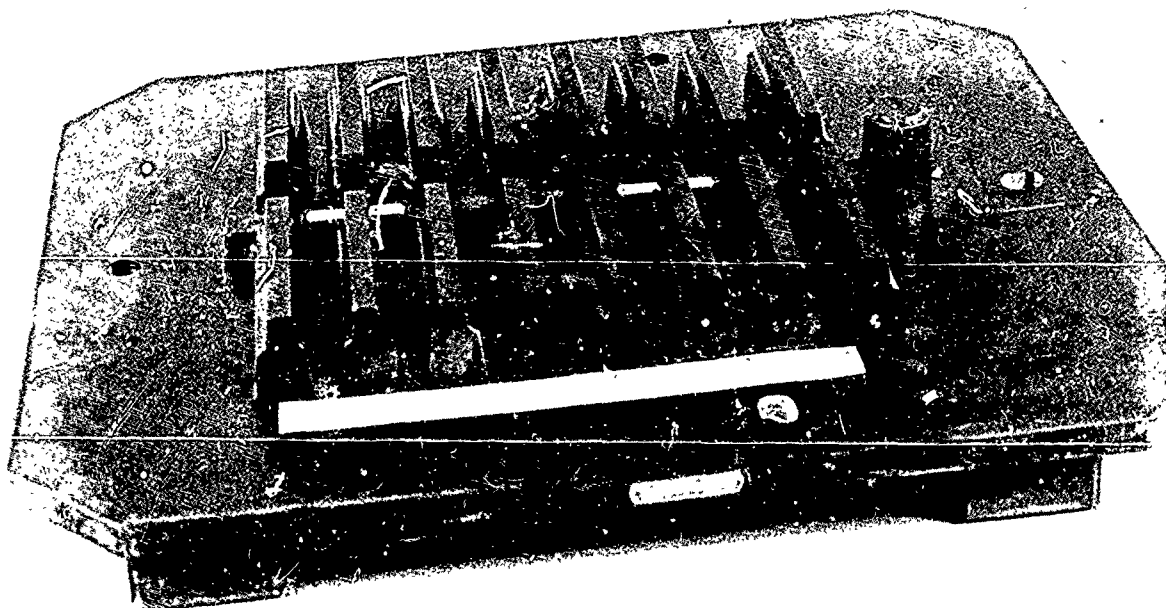
Figure 3

Drag Pattern For Production
of Test Bars

Each drag contains 16 individually
risered specimens. Drags may be stacked
three-high to produce 48 specimens per mold.
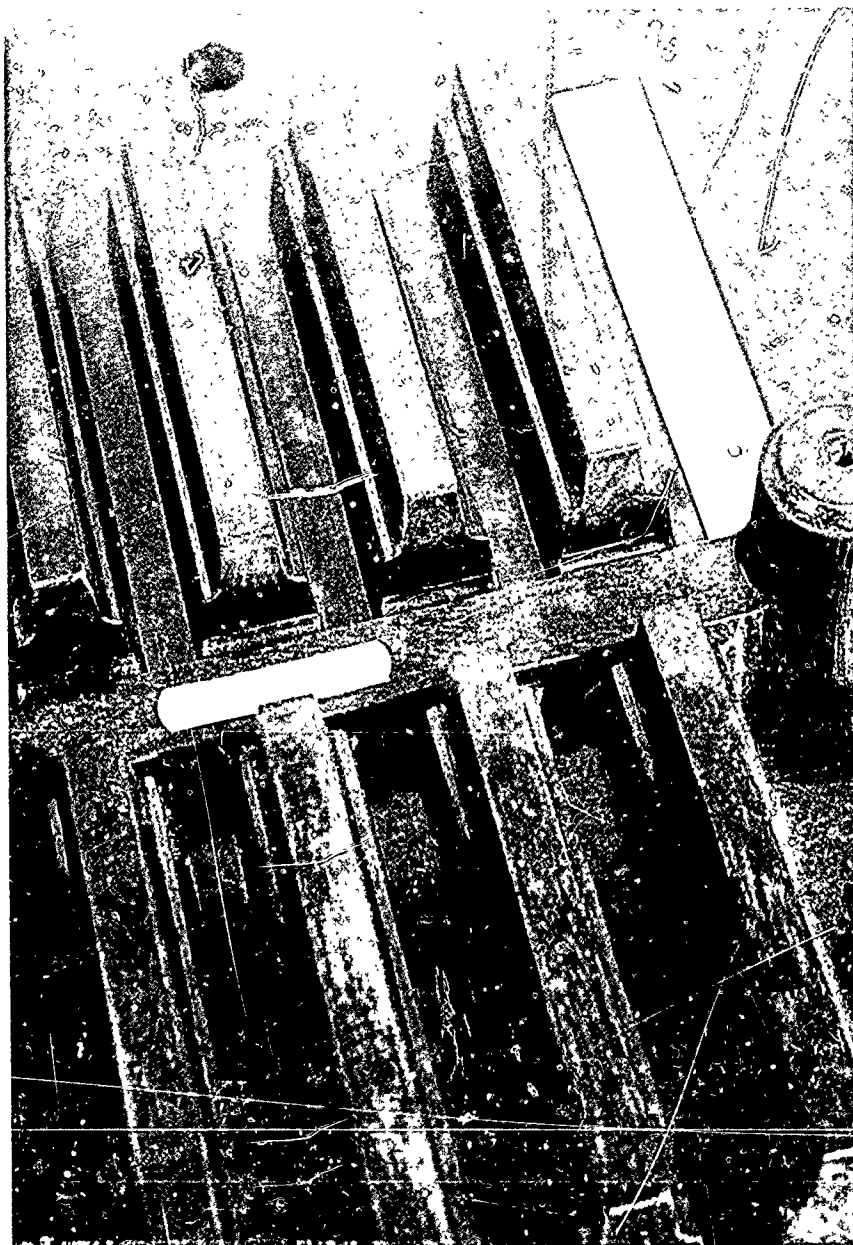
Figure 4

Same As Figure 3

Details of specimen, risers,
and central runner are shown.
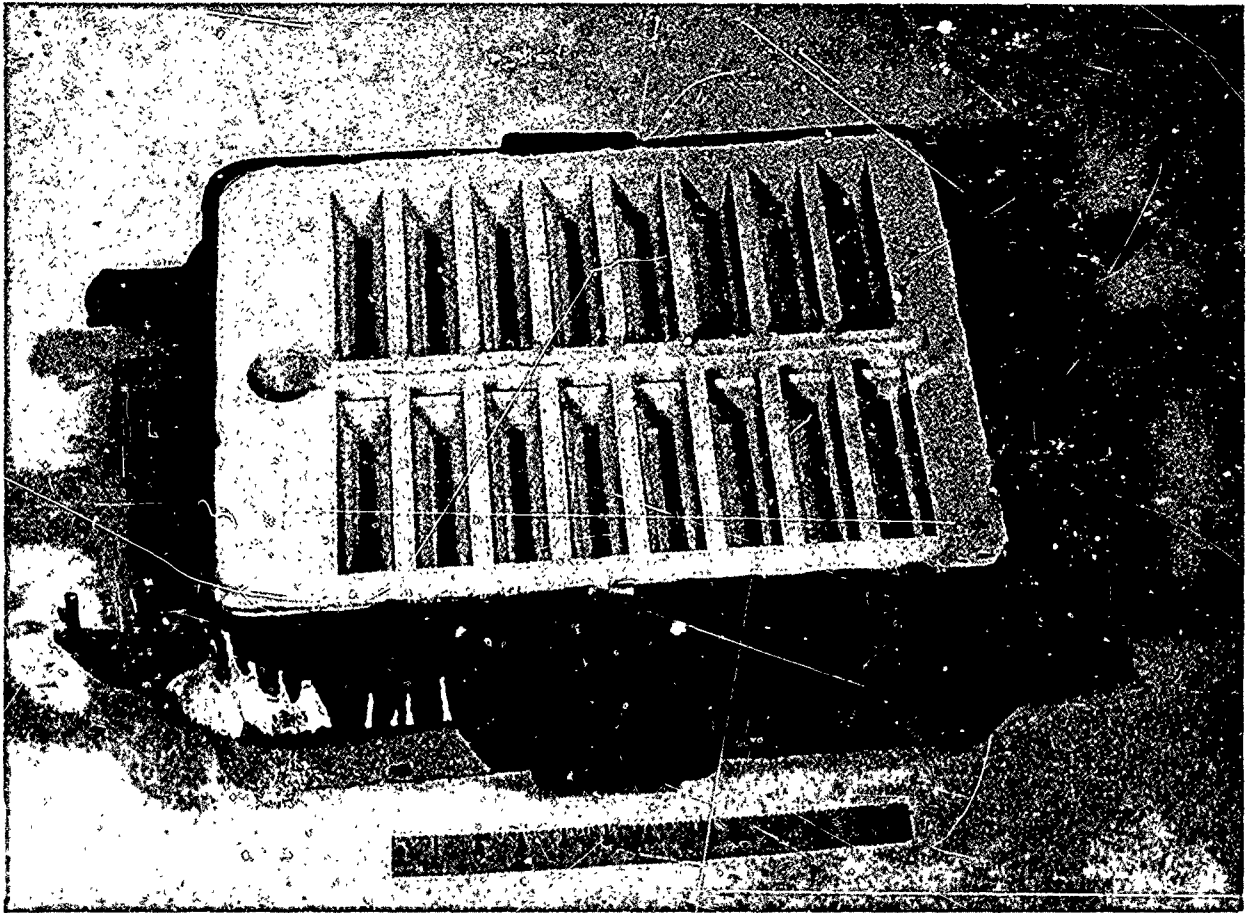
Figure 5

Ceramic Molded Drag Section
Made From Pattern Shown in
Figures 3 and 4.
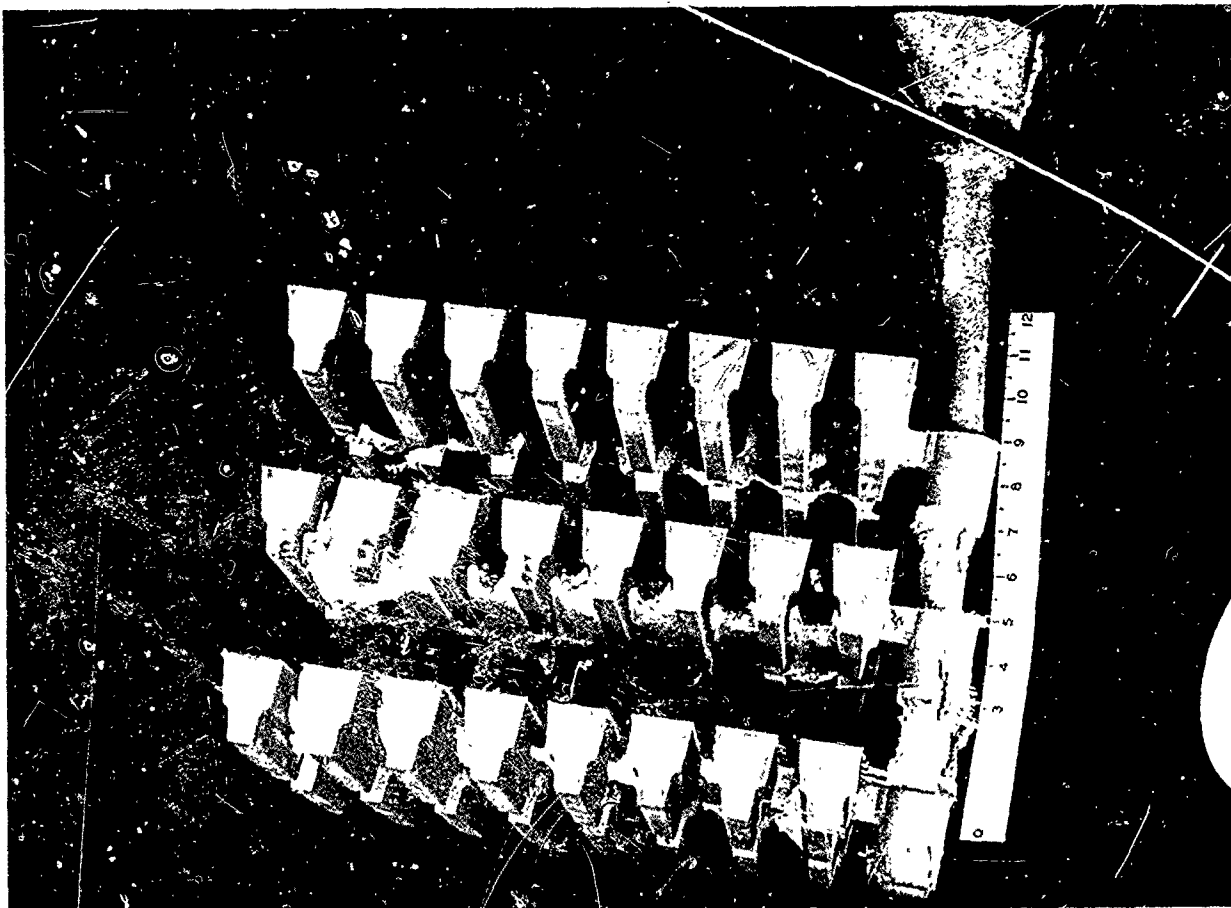
Figure 6

Alloy 713LC Casting Made
From Stacked Drags As Shown in Figure 5.
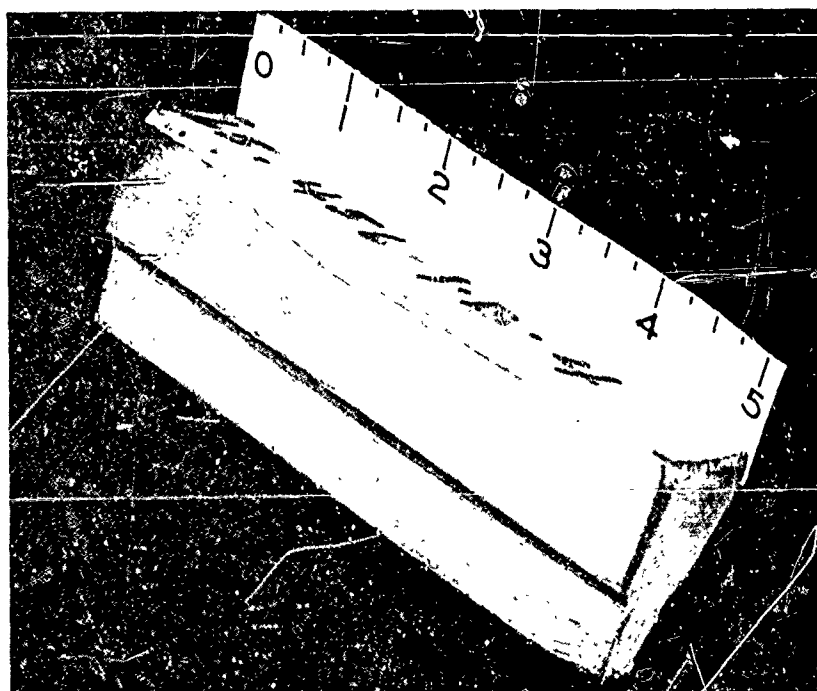
Figure 7

Test Specimen
and Riser After
Cut-off from
Runner.
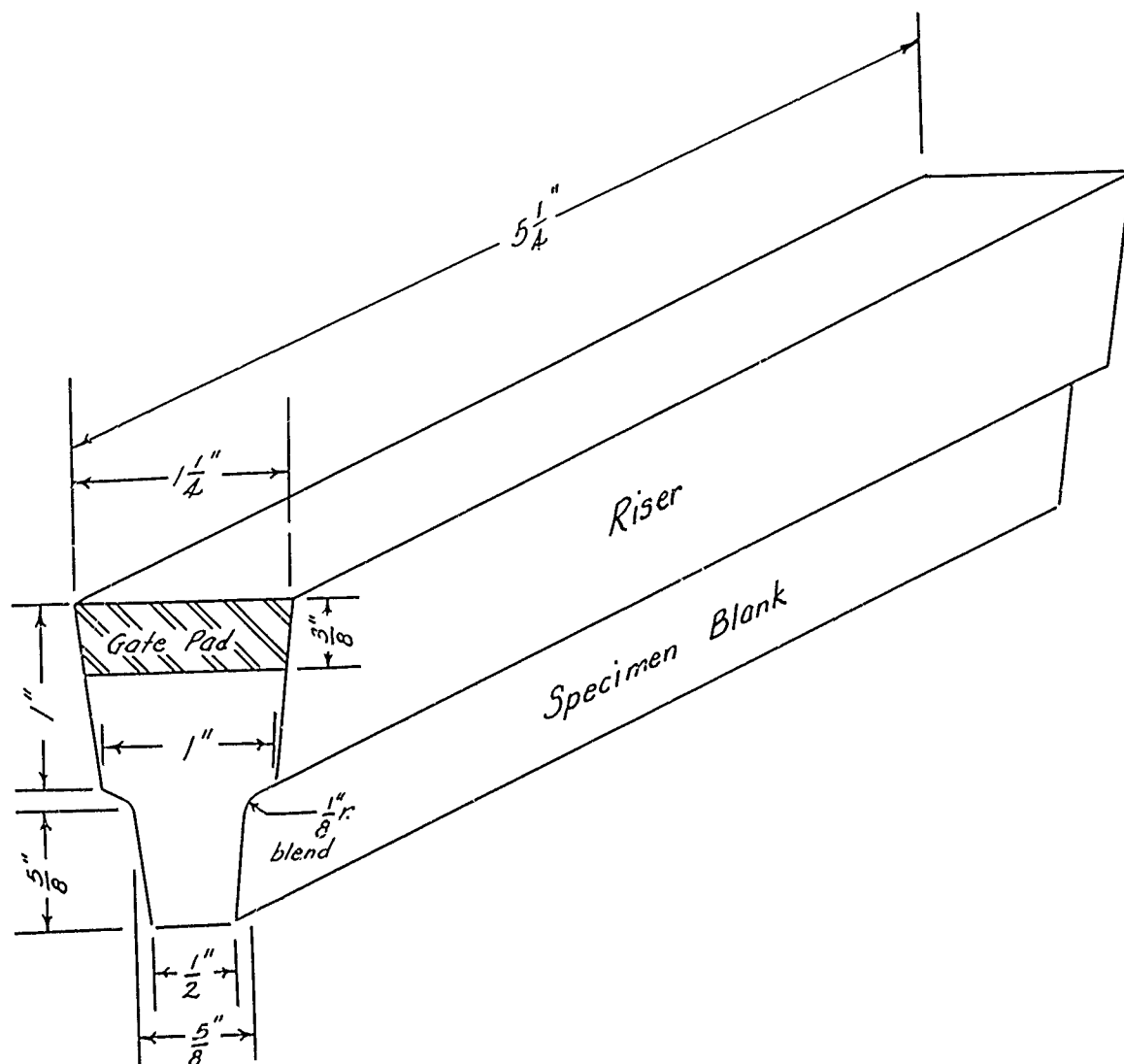
Figure 8

CAST TEST SPECIMEN
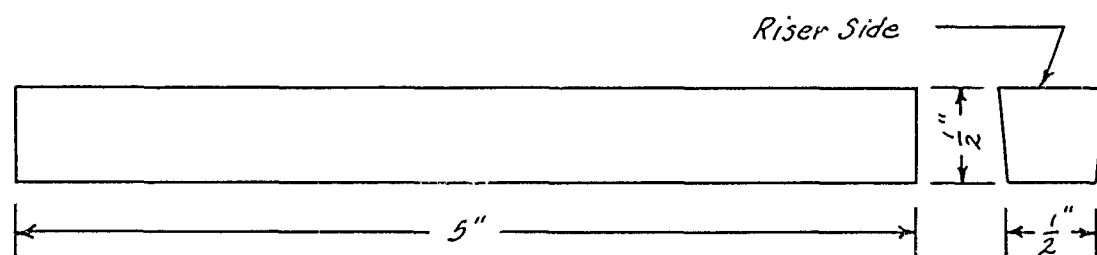
Specimen Blank
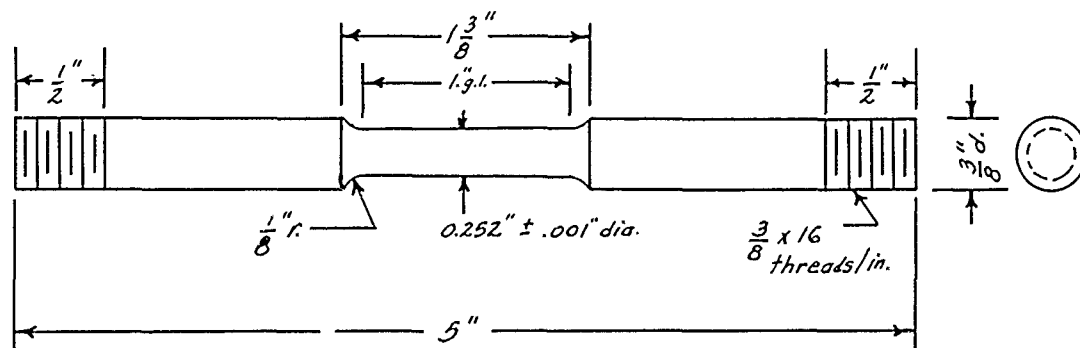
F-42   Hot Tensile and Creep Rupture
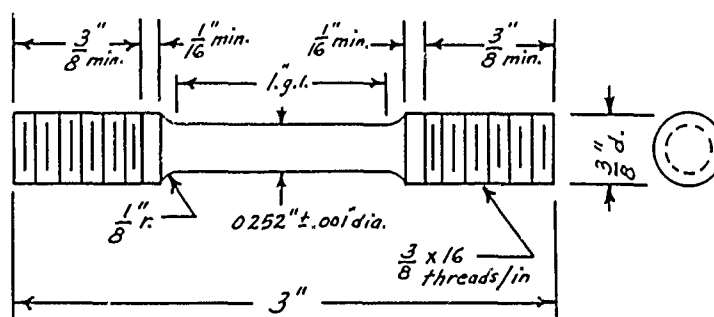
F-29   Room Temperature Tensile
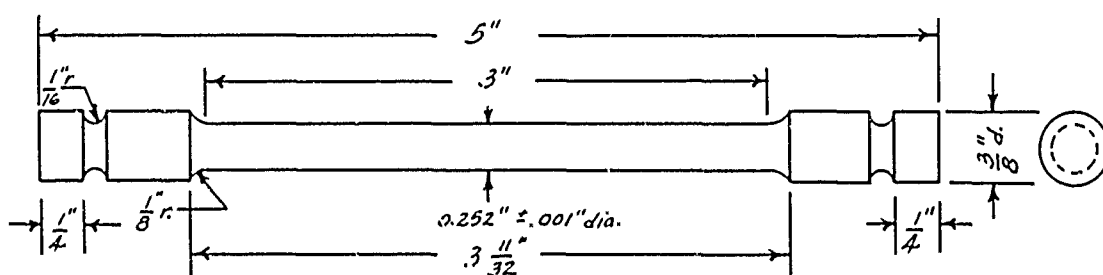
F-51   Resistance Heated Hot Tensile

Figure 9

TEST SPECIMENS UTILIZED IN PROGRAM
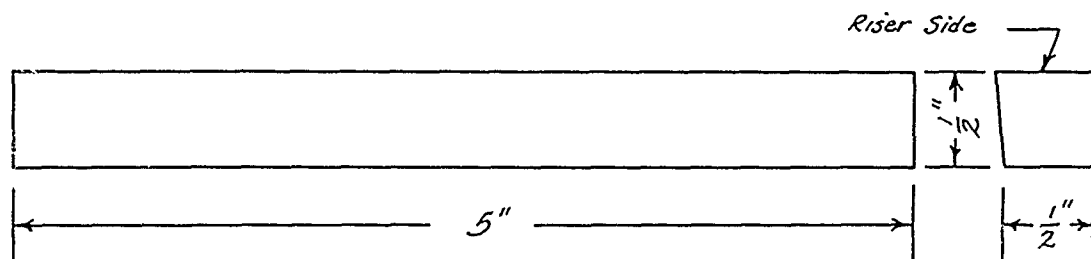
Specimen Blank
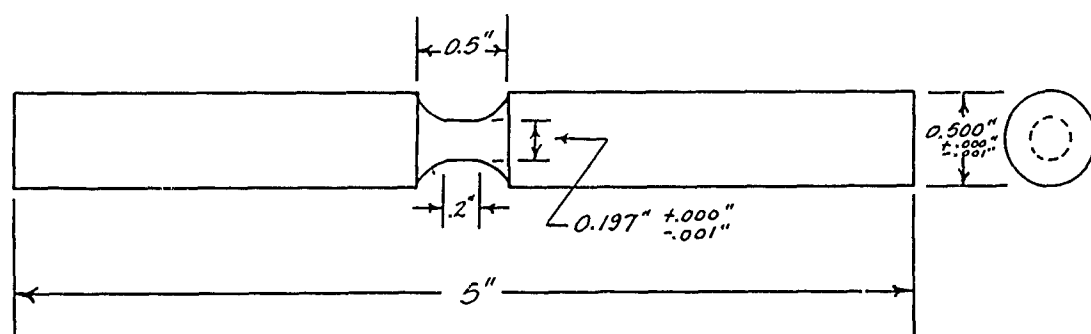
F-45 Thermal Fatigue
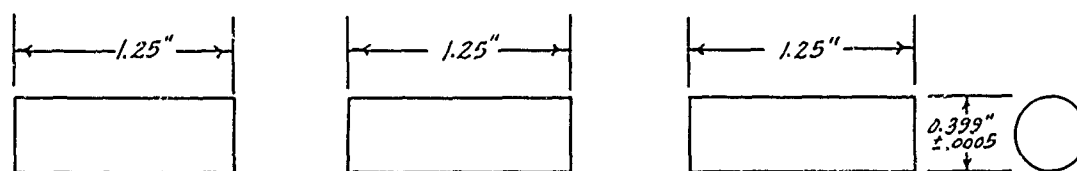
F-50 Compression
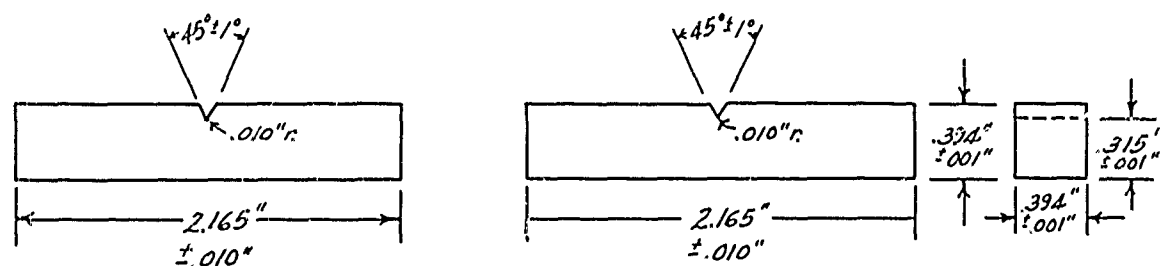
F-11 Charpy Impact

Figure 9 cont.

TEST SPECIMENS UTILIZED IN PROGRAM
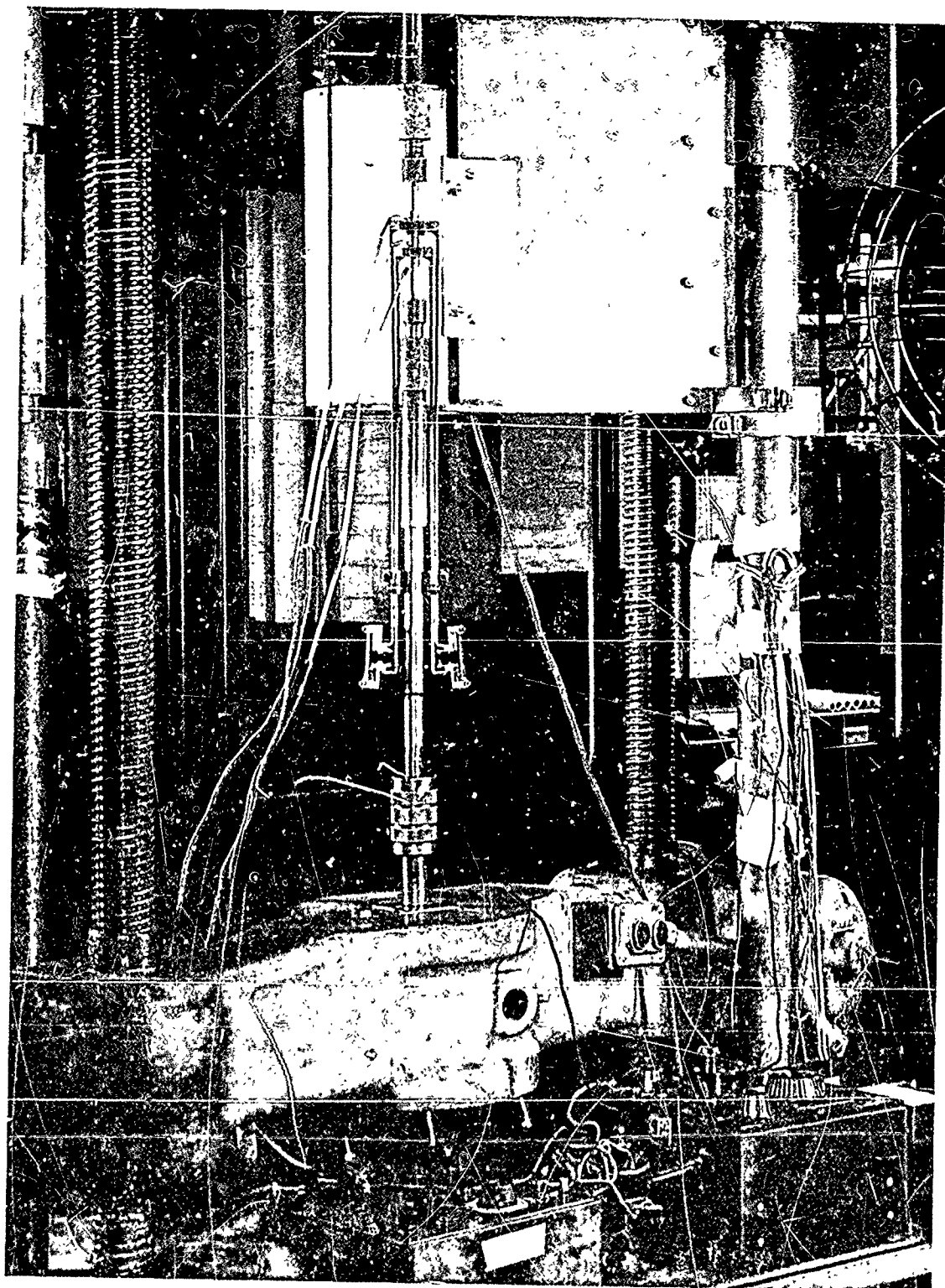
FIGURE 10

ELEVATED TEMPERATURE TENSILE TEST SETUP

Thermocouples are located at the top, center, and bottom of the test bar to insure a minimum deviation in test bar temperature.

-151-
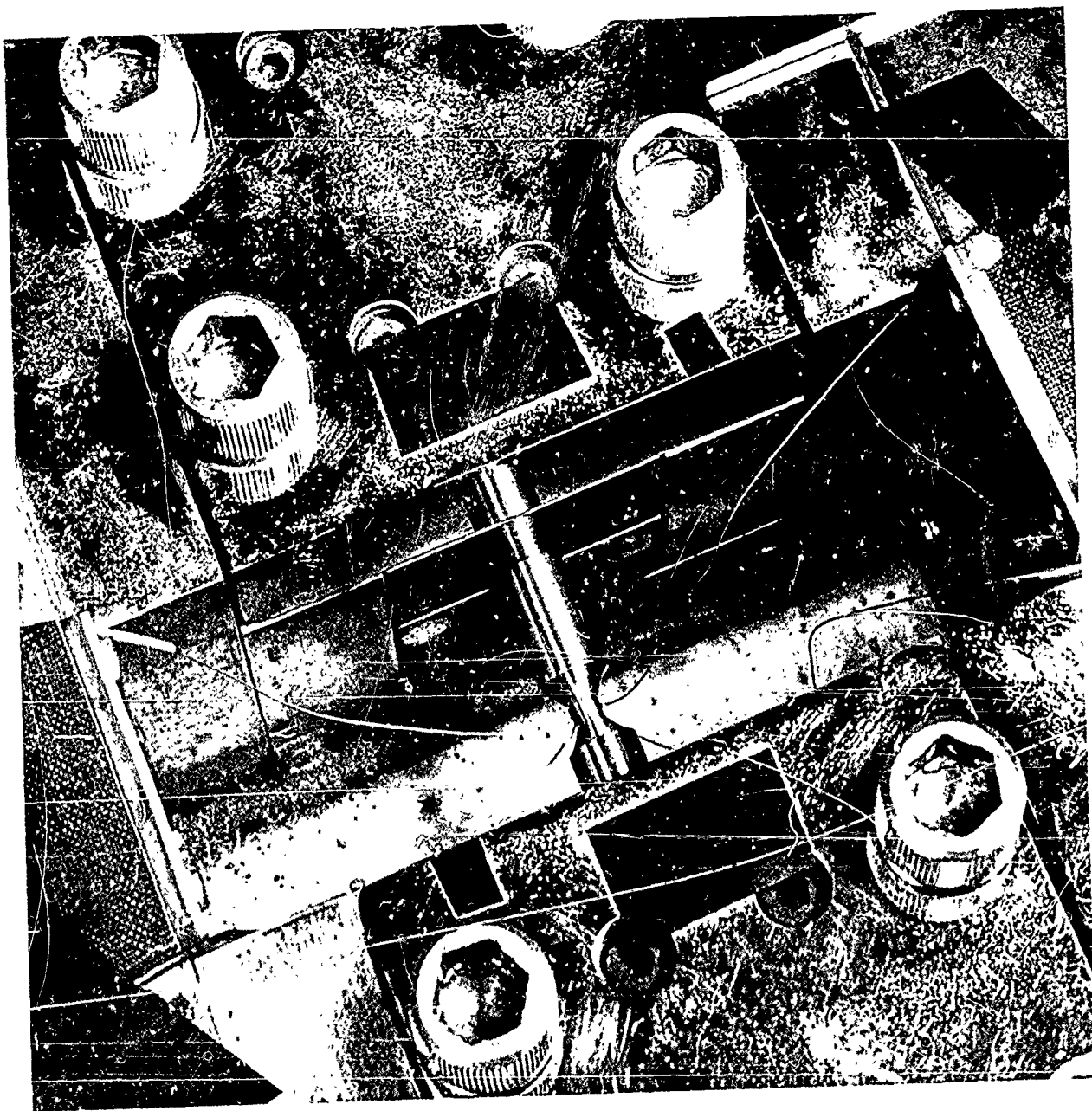
FIGURE 11

THERMAL FATIGUE SPECIMEN MOUNTED FOR TESTING

Two thermocouples provide measuring and control of temperature during cycling.
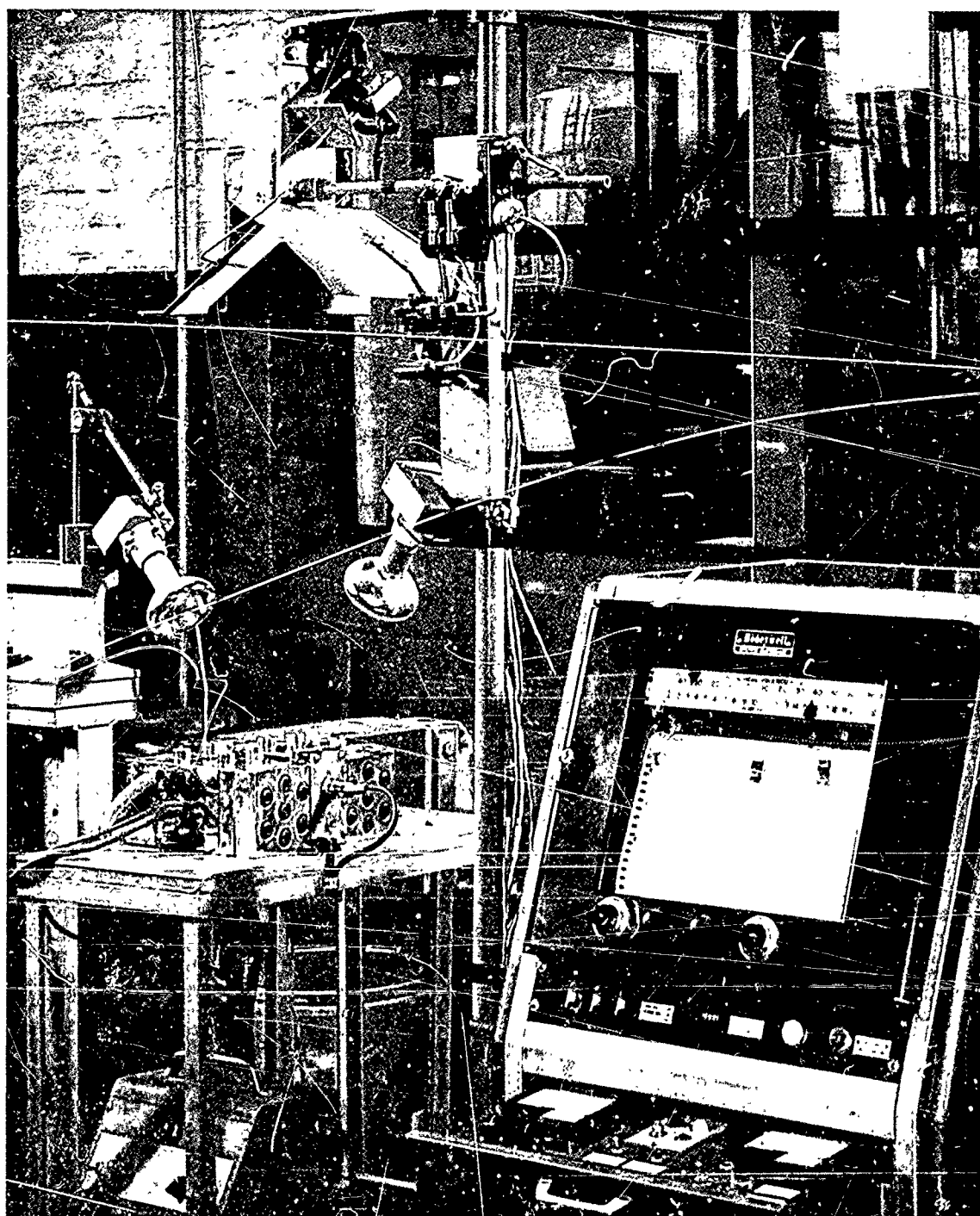
FIGURE 12

THERMAL FATIGUE APPARATUS SHOWING
STRESS – TEMPERATURE RECORDER AND FAILURE RECORDING CAMERA

-153-

FIGURE 13
ELEVATED TEMPERATURE TENSILE PROPERTIES

IN-713 LC   Heat No. 65-456

As Cast
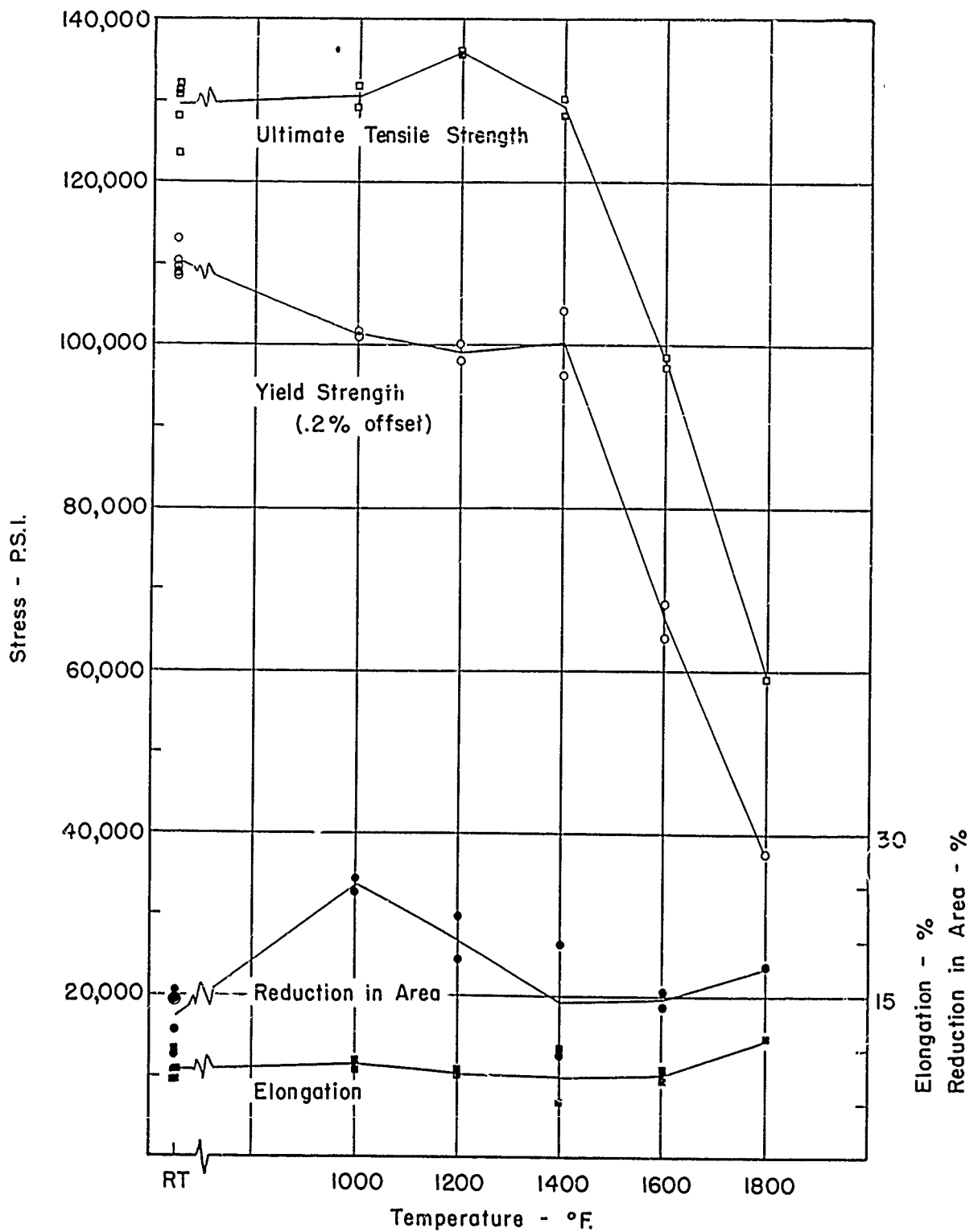
Test speed .05 in/min

-154-

FIGURE 14
ELEVATED TEMPERATURE TENSILE PROPERTIES

IN-713 LC   Heat No. 65-456

2150°F - 2 Hours - Air Cool
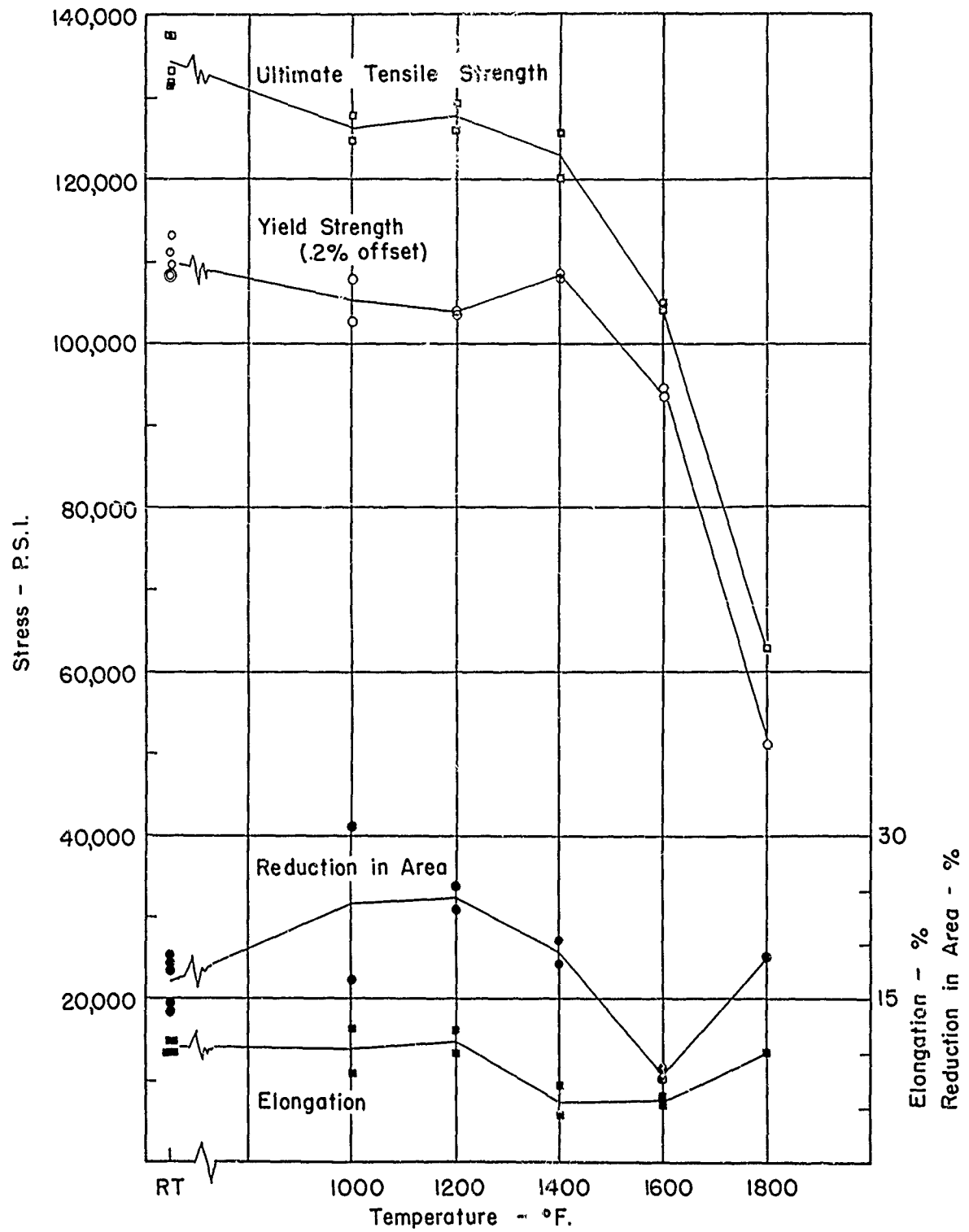
Test speed 05 in/min   -155-

FIGURE 15

ELEVATED TEMPERATURE TENSILE PROPERTIES

IN-718   Heat No. 65-506
Solution Treated: - 1800°F. - 2 Hours - Air Cool
Aged: 1325°F. - 8 Hours - Furnace Cool to 1150°F.
Hold for 8 Hours - Air Cool

Test speed .05 in/min   -156-
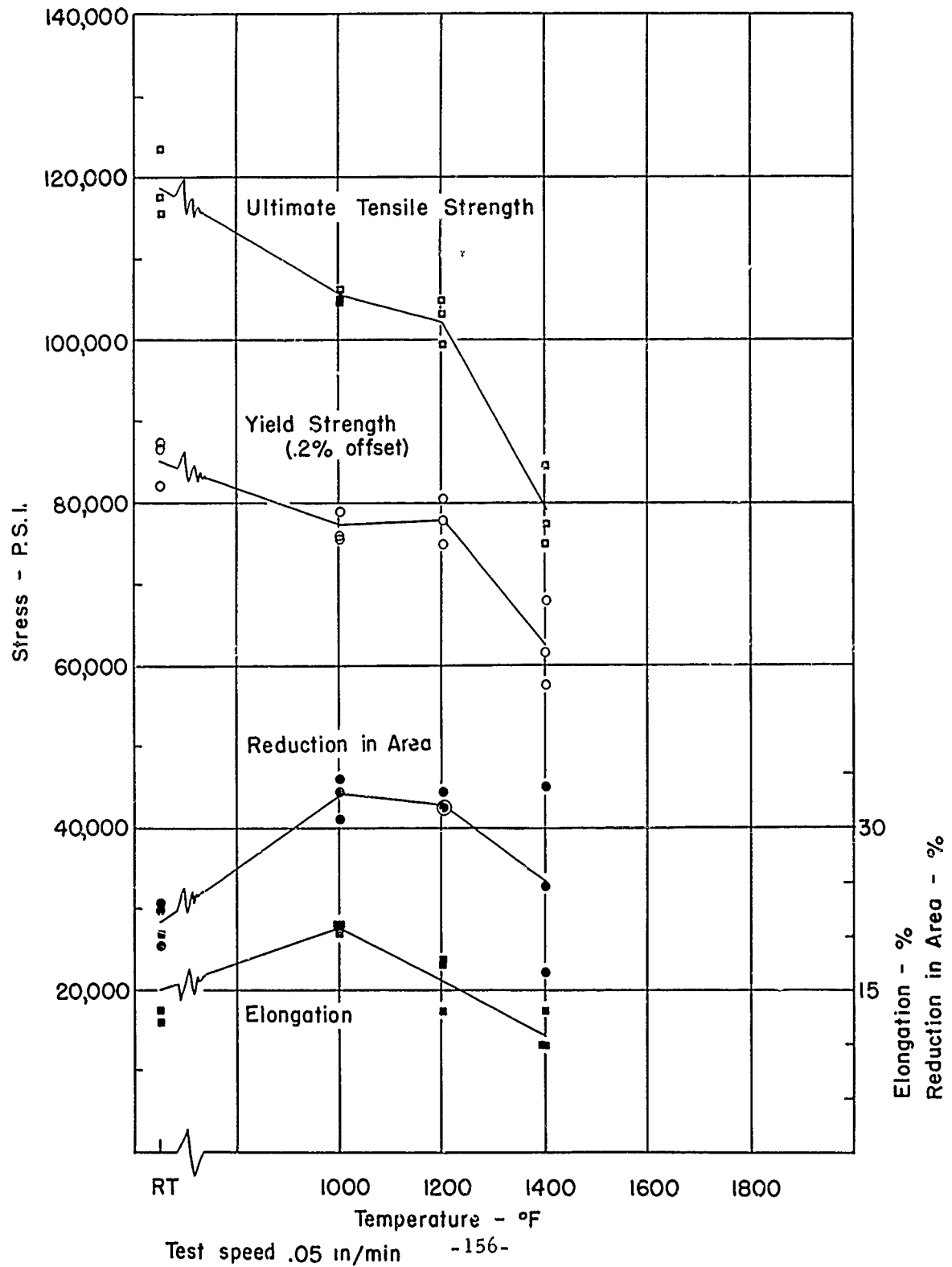
FIGURE 16
ELEVATED TEMPERATURE TENSILE PROPERTIES

Rene' 41   Heat No. 65-522
Solution Treated - 1950°F. - 4 Hours - Air Cool
Aged: 1400°F. - 16 Hours - Air Cool
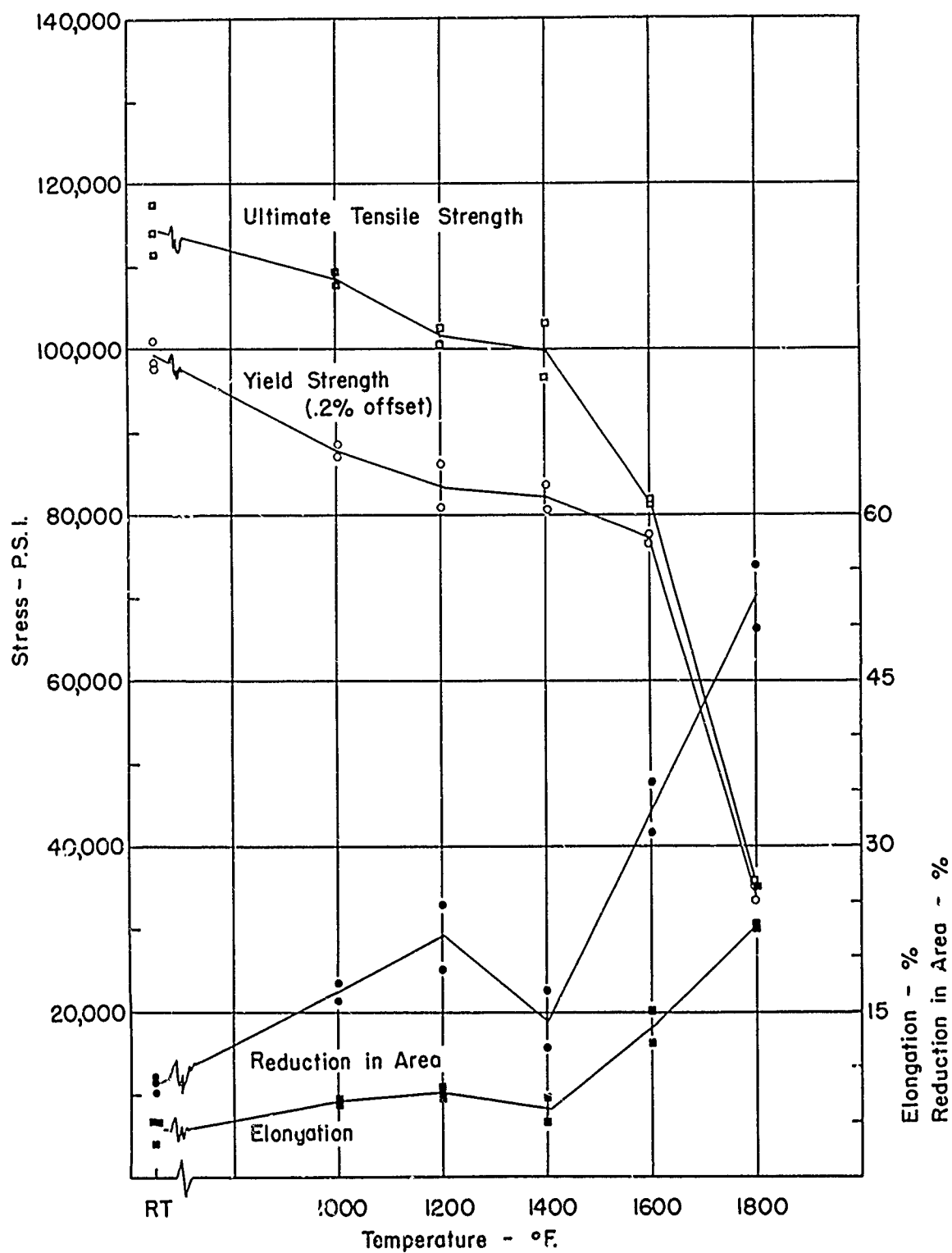
Test speed .05 in/min   -157-

CAST INCO 713 I.C

Photomicrograph
No. AK 172605

Room Temp. Tensile Data

Y.S. (KSI)	T.S. (KSI)	El (%)	R.A. (%)
$\frac{108}{113}$	$\frac{123}{132}$	$\frac{7}{10}$	$\frac{10}{15}$

Chemical Analysis

Heat No.	C%	Cr%	Mo%	Cb+Ta%	Ti%	Al%	B%	Zr%	Ni%
65-456	0.06	12.50	4.32	2.30	0.83	6.06	0.0074	0.094	Bal.

The unresolvable general precipitate is gamma-
prime. Areas A show massive white etching eu-
tectic gamma-prime. Coarse, irregular MC-type
columbium carbides can be seen in areas B.
Matrix is gamma.

CAST INCO 713 LC

Photomicrograph
No. AK 172604

Room Temp. Tensile Data

Y.S. (KSI)	T.S. (KSI)	El (%)	R.A. (%)
$\frac{108}{113}$	$\frac{123}{132}$	$\frac{7}{10}$	$\frac{10}{15}$

Chemical Analysis

Heat No.	C%	Cr%	Mo%	Cb+Ta%	Ti%	Al%	B%	Zr%	Ni%
65-456	0.06	12.50	4.32	2.30	0.83	6.06	0.0074	0.094	Bal.

Areas A indicate MC-type columbium carbides.
The substructure of eutectic gamma-prime is
clearly seen in area B. The coarse particles
at boundary C are $M_{23}C_6$ surrounded by gamma-
prime. The unresolvable general precipitate
is gamma-prime. Matrix is gamma.

-159-

CAST INCO 713 LC

Photomicrograph
No. AL 64802
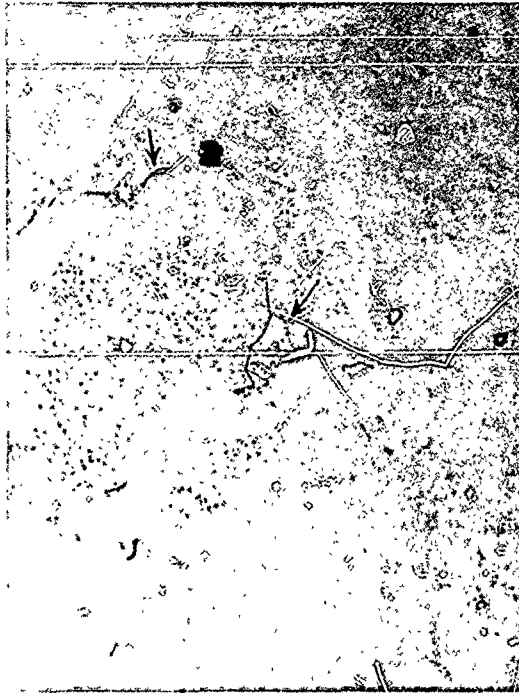
2150°F - 2 hrs.
Water Quenched

Etchant: $HF-HNO_3$,
$HCl-FeCl_3$

Chemical Analysis

Heat No.	C%	Cr%	Mo%	Cb+Ta%	Ti%	Al%	B%	Zr%	Ni%
66-198	0.06	12.20	4.15	2.14	0.83	6.50	0.012	0.091	Bal.

Arrows indicate undissolved MC-type columbium
carbides. The dot-like precipitates are gamma-
prime. These areas were rich in solute elements
due to segregation. Matrix is clear, solute-rich
gamma.

CAST INCO 713 LC

Photomicrograph
No. AL 64902
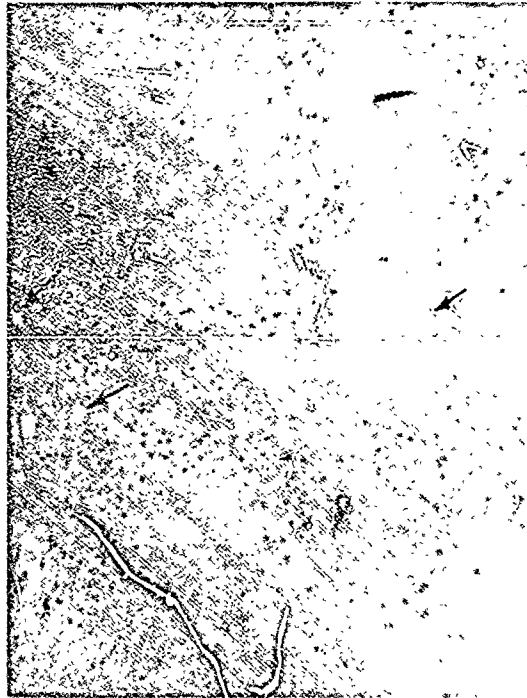
2150°F - 2 hrs.
Oil Quenched

Etchant: HF-HNO$_3$,
HCl-FeCl$_3$

Chemical Analysis

Heat No.	C%	Cr%	Mo%	Cb+Ta%	Ti%	Al%	B%	Zr%	Ni%
66-198	0.06	12.20	4.15	2.14	0.83	6.50	0.012	0.091	Bal.

Arrows indicate undissolved MC-type carbides.
The unresolvable general precipitate, outlining
original interdendritic areas is gamma-prime.
Matrix is gamma.

CAST INCO 713 LC

Photomicrograph
No. AL 65001
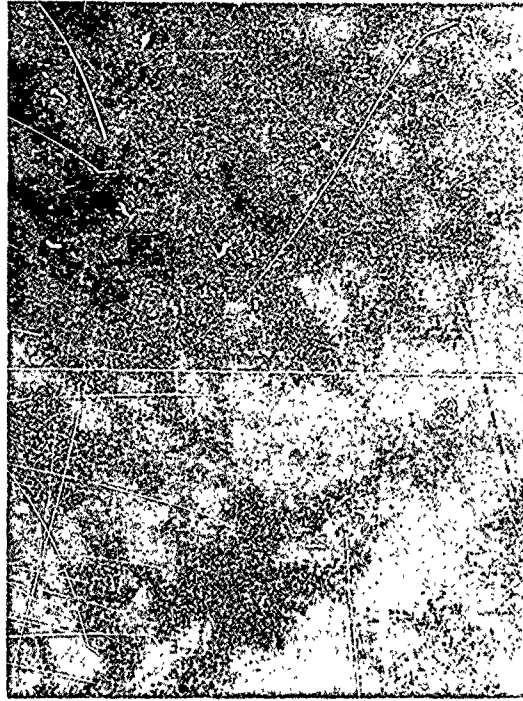
2150°F - 2 hrs.
Air Cooled

Etchant: $HF-HNO_3$,
$HCl-FeCl_3$

Room Temp. Tensile Data			
Y.S.	T.S.	El	R.A.
(KSI)	(KSI)	(%)	(%)
108	131	10	14
113	137	11	19

Chemical Analysis

Heat No.	C%	Cr%	Mo%	Cb+Ta%	Ti%	Al%	B%	Zr%	Ni%
66-198	0.06	12.20	4.15	2.14	0.83	6.50	0.012	0.091	Bal.

The white irregular particles are MC-type carbides.
The general precipitate is gamma-prime. The "density"
of gamma-prime is greater at original interdendritic
regions. Matrix is gamma.

CAST INCO 713 LC

Photomicrograph
No. AL 65002

Figure 22
500X

2150°F - 2 hrs.
Air Cooled

Etchant: HF-HNO$_3$,
HCl-FeCl$_3$

Room Temp. Tensile Data

Y.S. (KSI)	T.S. (KSI)	El (%)	R.A. (%)
$\frac{108}{113}$	$\frac{131}{137}$	$\frac{10}{11}$	$\frac{14}{19}$

Chemical Analysis

Heat No.	C%	Cr%	Mo%	Cb+Ta%	Ti%	Al%	Zr%	B%	Ni%
66-198	0.06	12.20	4.15	2.14	0.83	6.50	0.091	0.012	Bal.

Arrows A indicate MC-type columbium carbides. The
particles indicated by arrows B are thought to be
$M_{23}C_6$. Circled areas could be MC carbides partial-
ly transformed to $M_{23}C_6$ and gamma-prime. The gen-
eral precipitate is gamma-prime and the matrix is
gamma.

<u>CAST INCO 713 LC</u>

Photomicrograph
No. AL 65201

<u>Figure 23</u>
200X

2150°F - 2 hrs.
Insulated Cool

Etchant: HF-HNO$_3$
HCl-FeCl$_3$

<u>Chemical Analysis</u>

<u>Heat No.</u>	<u>C%</u>	<u>Cr%</u>	<u>Mo%</u>	<u>Cb+Ta%</u>	<u>Ti%</u>	<u>Al%</u>	<u>Zr%</u>	<u>B%</u>	<u>Ni%</u>
66-198	0.06	12.20	4.15	2.14	0.83	6.50	0.0591	0.012	Bal.

Coarse gamma-prime general precipitate and carbides
(white).

<u>CAST INCO 713 LC</u>

Photomicrograph
No. AL 65202
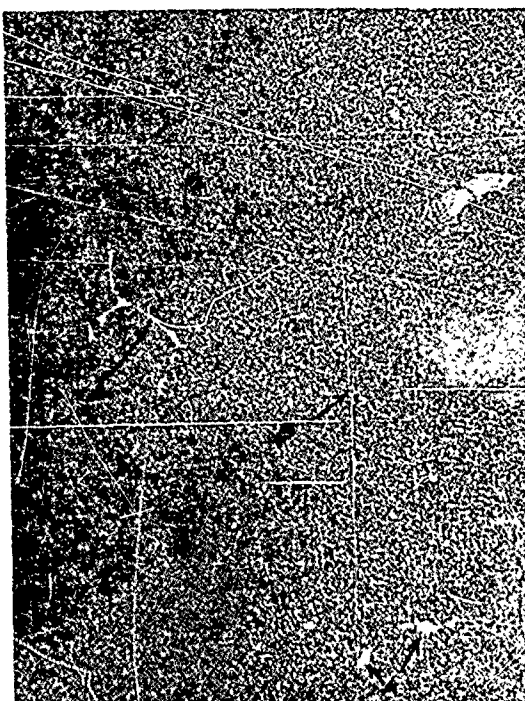
2150°F - 2 hrs.
Insulated Cool

Etchant: HF-HNO$_3$,
    HCl-FeCl$_3$

<u>Chemical Analysis</u>

<u>Heat No.</u>	<u>C%</u>	<u>Cr%</u>	<u>Mo%</u>	<u>Cb+Ta%</u>	<u>Ti%</u>	<u>Al%</u>	<u>Zr%</u>	<u>B%</u>	<u>Ni%</u>
66-198	0.06	12.20	4.15	2.14	0.83	6.50	0.0591	0.012	Bal.

Arrows A indicate MC-type columbium carbides.
Boundaries B show M$_{23}$C$_6$ carbide particles sur-
rounded by gamma-prime. The circled area is
thought to be a MC-type carbide particle, par-
tially transformed to gamma-prime and M$_{23}$C$_6$.
The general precipitate is gamma-prime in a
gamma matrix.

-165-

CAST INCO 713 LC

Photomicrograph
No. AL 65101

200X

2150°F - 2 hrs.
Furnace Cooled to 500°F
and Air Cooled

Etchant: HF-HNO$_3$,
HCl-FeCl$_3$

Chemical Analysis

Heat No.	C%	Cr%	Mo%	Cb+Ta%	Ti%	Al%	Zr%	B%	Ni%
66-198	0.06	12.20	4.15	2.14	0.83	6.50	0.0591	0.012	Bal.

The general gamma-prime precipitate is relatively
coarse. Substantial grain boundary precipitation
is readily seen. Original dendritic segregation
pattern persists, indicating lack of homogenization
at 2150°F.

-166-

CAST INCO 713 LC

Photomicrograph
No. AL 65102

2150°F - 2 hrs.
Furnace Cooled to 500°F
and Air Cooled

Etchant: HF-HNO$_3$,
HCl-FeCl$_3$

Chemical Analysis

Heat No.	C%	Cr%	Mo%	Cb+Ta%	Ti%	Al%	Zr%	B%	Ni%
66-198	0.06	12.20	4.15	2.14	0.83	6.50	0.0591	0.012	Bal.

The general gamma-prime is heavily agglomerated
and is readily resolved. Arrows A indicate MC-
type carbides. Boundary B shows an array M$_{23}$C$_6$
particles enveloped by gamma-prime. Matrix is
gamma.

-167-

CAST INCO 713 LC

Photomicrograph
No. AL 46601
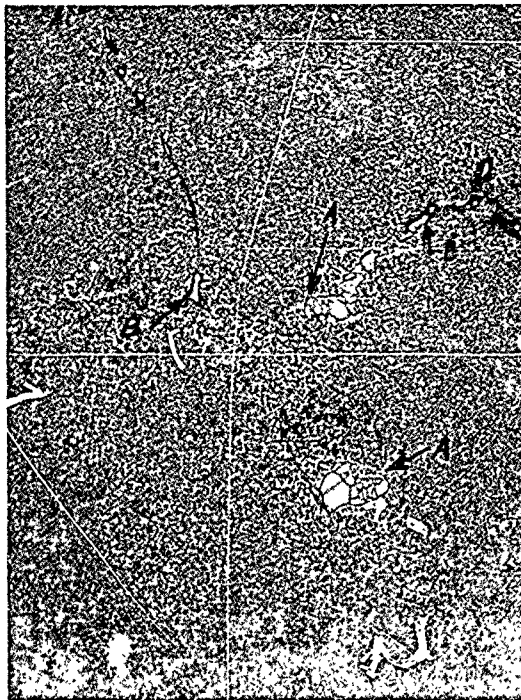
Aged 1200°F - 16 hrs.
Air Cooled

Etchant: HF-HNO$_3$,
HCl-FeCl$_3$

Room Temp. Tensile Data

Y.S. (KSI)	T.S. (KSI)	El (%)	R.A. (%)
116	135	8	11

Chemical Analysis

Heat No.	C%	Cr%	Mo%	Cb+Ta%	Ti%	Al%	B%	Zr%	Ni%
65-456	0.06	12.50	4.32	2.30	0.83	6.06	0.0074	0.094	Bal.

Eutectic gamma-prime is indicated by arrows A and
MC-type carbides by arrows B. The general precipi-
tate is gamma-prime in a gamma matrix.

-168-

CAST INCO 713 LC

Photomicrograph
No. AL 46301

Aged 1550°F – 16 hrs.
Air Cooled

Etchant: HF–HNO$_3$,
HCl–FeCl$_3$
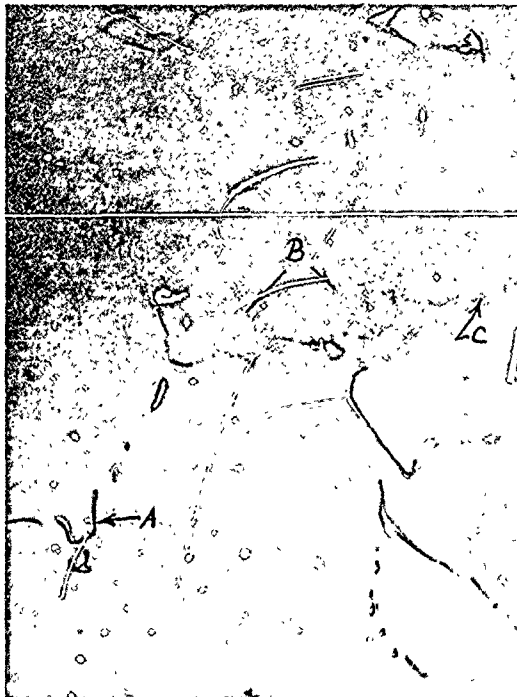
Room Temp. Tensile Data			
Y.S.	T.S.	El	R.A.
(KSI)	(KSI)	(%)	(%)
109	122	5	11

Chemical Analysis

Heat No.	C%	Cr%	Mo%	Cb+Ta%	Ti%	Al%	B%	Zr%	Ni%
65-456	0.06	12.50	4.32	2.30	0.83	6.06	0.0074	0.094	Bal.

MC-type carbides (A) show script like shapes.
Eutectic gamma-prime is indicated by arrow B.
The boundary C probably consists of gamma-
prime and M$_{23}$C$_6$. The general precipitate is
gamma-prime in a gamma matrix.

-169-

CAST INCO 713 LC

Photomicrograph
No. AL 46401
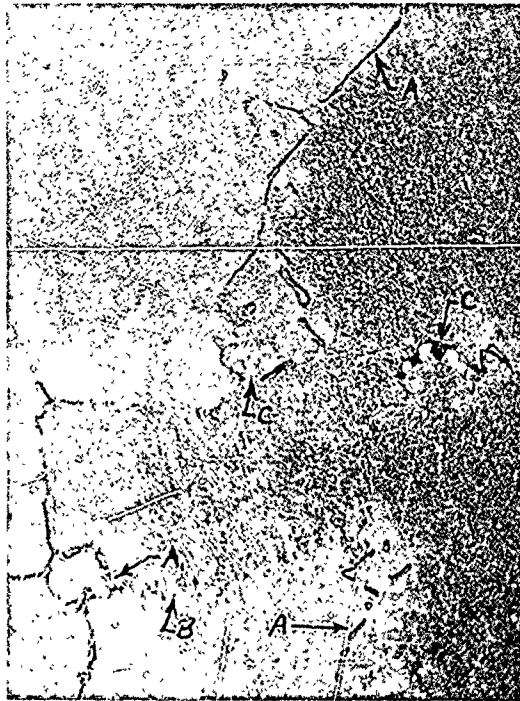
Figure 29
500X

Aged 1700°F – 16 hrs.
Air Cooled

Etchant: HF-HNO$_3$,
HCl-FeCl$_3$

Room Temp. Tensile Data

Y.S. (KSI)	T.S. (KSI)	El (%)	R.A. (%)
$\frac{105}{108}$	$\frac{116}{119}$	$\frac{6}{8}$	$\frac{15}{16}$

Chemical Analysis

Heat No.	C%	Cr%	Mo%	Cb+Ta%	Ti%	Al%	B%	Zr%	Ni%
65-456	0.06	12.50	4.32	2.30	0.83	6.06	0.0074	0.094	Bal.

MC-type carbides are indiated by arrows A, some
of which (A$_1$) are partially transformed. Bound-
ary B shows M$_{23}$C$_6$ and gamma-prime. Eutectic
gamma-prime, arrows C, show evidence of agglom-
eration. The general gamma-prime precipitate is
also relatively coarse.

CAST INCO 713 LC

Photomicrograph
No. AL 46201
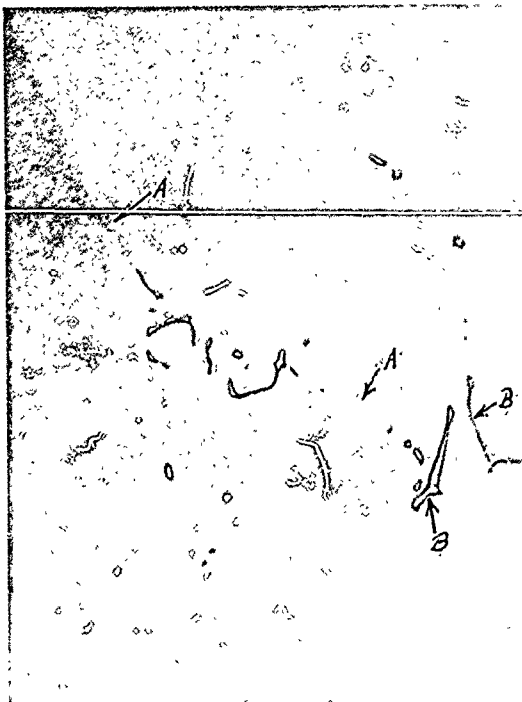
2150°F - 2 hrs.
  Air Cooled
1200°F - 16 hrs.
  Air Cooled

Etchant: HF-HNO$_3$,
          HCl-FeCl$_3$

Room Temp. Tensile Data

Y.S. (KSI)	T.S. (KSI)	El (%)	R.A. (%)
123	138	9	14

Chemical Analysis

Heat No.	C%	Cr%	Mo%	Cb+Ta%	Ti%	Al%	B%	Zr%	Ni%
65-456	0.06	12.50	4.32	2.30	0.83	6.06	0.0074	0.094	Bal.

MC-type carbide particles (B) show script morph-
ology. The particles in the boundary (A) are
thought to be gamma-prime. The general gamma-
prime precipitate is virtually unresolved.

CAST INCO 713 LC

Photomicrograph
No. AL 46501
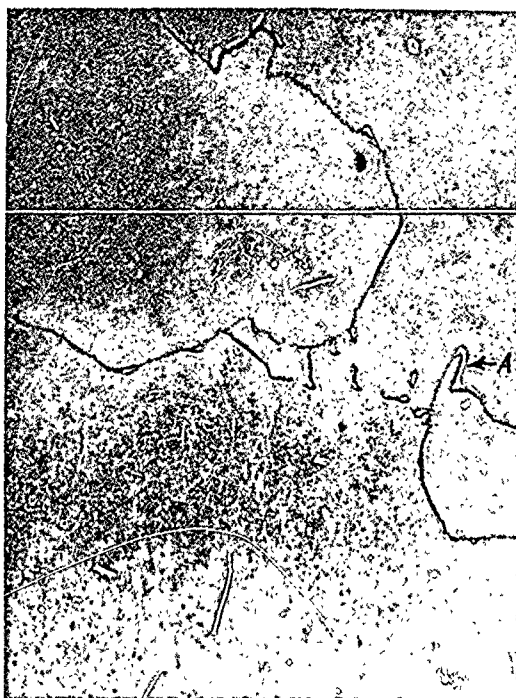
Figure 31
500X

2150°F - 2 hrs.
  Air Cooled
1550°F - 16 hrs.
  Air Cooled

Etchant: HF-HNO$_3$,
          HCl-FeCl$_3$

Room Temp. Tensile Data

Y.S. (KSI)	T.S. (KSI)	El (%)	R.A. (%)
121	137	5	8

Chemical Analysis

Heat No.	C%	Cr%	Mo%	Cb+Ta%	Ti%	Al%	B%	Zr%	Ni%
65-456	0.06	12.50	4.32	2.30	0.83	6.06	0.0074	0.094	Bal.

Arrow A indicates a MC carbide partly transformed
to $M_{23}C_6$ and gamma-prime. The general precipitate
is gamma-prime. Boundaries show MC, $M_{23}C_6$ and
gamma-prime.

CAST INCO 713 LC

Photomicrograph
No. AL 46101

Figure 32
500X

2150°F – 2 hrs.
Air Cooled
1700°F – 2 hrs.
Air Cooled

Etchant: $HF-HNO_3$,
$HCl-FeCl_3$

Room Temp. Tensile Data			
Y.S.	T.S.	El	R.A.
(KSI)	(KSI)	(%)	(%)
$\frac{119}{121}$	$\frac{129}{133}$	$\frac{6}{7}$	12

Chemical Analysis

Heat No.	C%	Cr%	Mo%	Cb+Ta%	Ti%	Al%	B%	Zr%	Ni%
65-456	0.06	12.50	4.32	2.30	0.83	6.06	0.0074	0.094	Bal.

Arrow A indicates partially transformed MC parti-
cles. The general gamma-prime precipitate shows
evidence of agglomeration.

CAST INCO 713 LC

Photomicrograph
No. AK 173003

Figure 33
200X

Tested at 1600°F-40KSI
longitudinal section
through fracture.

Etchant: $HF-HNO_3$,
$HCl-FeCl_3$

1600°F-40KSI SSR Data			
Life (Hrs)	MCR (%/Hr)	El (%)	R.A. (%)
161	0.016	6	5

Chemical Analysis

Heat No.	C%	Cr%	Mo%	Cb+Ta%	Ti%	Al%	B%	Zr%	Ni%
65-456	0.06	12.50	4.32	2.30	0.83	6.06	0.0074	0.094	Bal.

Arrow A indicates eutectic gamma-prime. The
circled area shows MC carbides. The original
cell structure due to dendritic segregation
is well defined.

-174-

CAST INCO 713 LC

Photomicrograph
No. AK 173004

Figure 34
500X

Tested at 1600°F-40KSI
Longitudinal Section
through fracture.

Etchant: HF-HNO$_3$,
HCl-FeCl$_3$

1600°F-40KSI SSR Data			
Life (Hrs)	MCR (%/Hr)	El (%)	R.A. (%)
161	0.016	6	5

Chemical Analysis

Heat No.	C%	Cr%	Mo%	Cb+Ta%	Ti%	Al%	B%	Zr%	Ni%
65-456	0.06	12.50	4.32	2.30	0.83	6.06	0.0074	0.094	Bal.

Arrow A indicates a group of MC type carbides
partially transformed to $M_{23}C_6$ and gamma-prime.
The general gamma-prime precipitate is relatively
coarse and almost resolvable. Matrix is gamma.

CAST INCO 713 LC

Photomicrograph
No. AK 172903
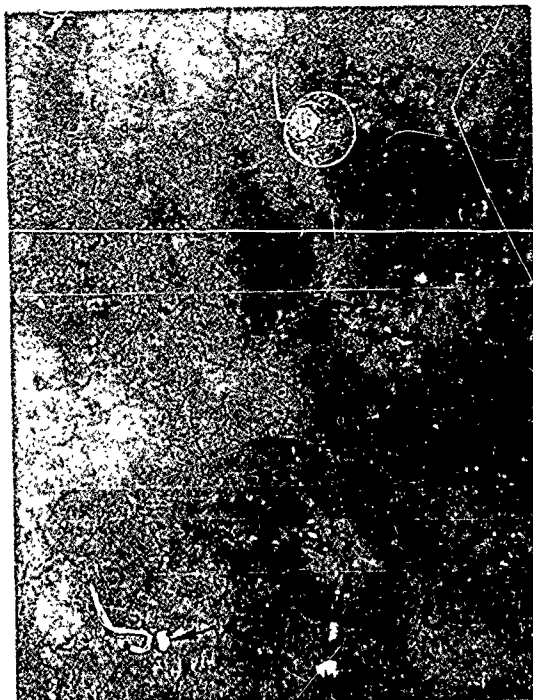
Solution Treated
2150°F - 2 hrs.
Air Cooled

Tested 1600°F-40KSI
Longitudinal section
through fracture.

1600°F-40KSI SSR Data

Life (Hrs)	MCR (%/Hr)	El (%)	R.A. (%)
244	0.005	6	5

Chemical Analysis

Heat No.	C%	Cr%	Mo%	Cb+Ta%	Ti%	Al%	B%	Zr%	Ni%
65-456	0.06	12.50	4.32	2.30	0.83	6.06	0.0074	0.094	Bal.

Arrows A indicate massive gamma-prime and arrows B
indicate MC-type carbides. The general gamma-prime
precipitate particles show some alignment and appear
as curved lines. This behavior is typical in solu-
tion-treated structures.

CAST INCO 713 LC

Photomicrograph
No. AK 172904

Solution-treated
2150°F - 2 hrs.
Air Cooled

Tested 1600°F - 40 KSI
Longitudinal section
through fracture.
—
Etchant: HF-HNO$_3$,
HCl-FeCl$_3$

1600°F-40KSI SSR Data			
Life (Hrs)	MCR (%/Hr)	El (%)	R.A. (%)
244	0.005	6	5

Chemical Analysis

Heat No.	C%	Cr%	Mo%	Cb+Ta%	Ti%	Al%	B%	Zr%	Ni%
65-456	0.06	12.50	4.32	2.30	0.83	6.06	0.0074	0.094	Bal.

Arrows A indicate MC-type carbides. Boundaries B consist of M$_{23}$C$_6$ particles enveloped by gamma-prime. Arrows C indicate massive gamma-prime, thought to have resulted from complete transformation MC carbides.

-177-

CAST INCO 713 LC

Photomicrograph
No. AK 172803
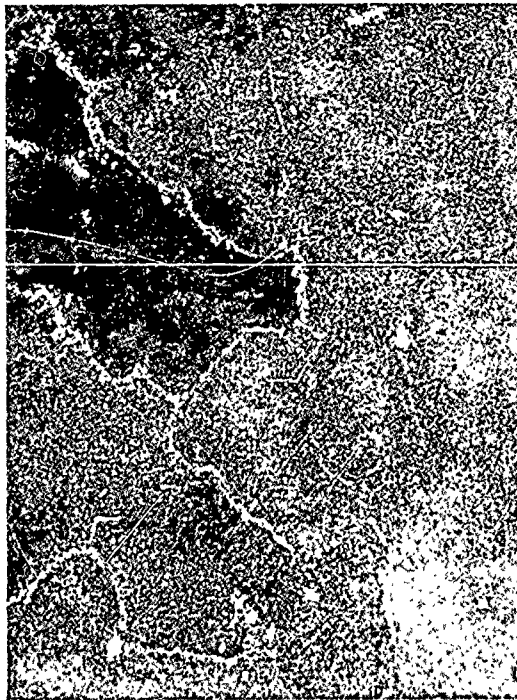
Figure 37
200X

Tested at 1800°F-22 KSI
Longitudinal Section
through fracture.
–

Etchant: HF-HNO$_3$,
HCl-FeCl$_3$

1800°F-22KSI SSR Data			
Life	MCR	El	R.A.
(Hrs)	(%/Hr)	(%)	(%)
64	0.038	7	7

Chemical Analysis

Heat No.	C%	Cr%	Mo%	Cb+Ta%	Ti%	Al%	B%	Zr%	Ni%
65-456	0.06	12.50	4.32	2.30	0.83	6.06	0.0074	0.094	Bal.

The general gamma-prime precipitate is relatively
coarse, indicating agglomeration. Extensive gamma-
prime (white) precipitation at grain boundaries.

CAST INCO 713 LC

Photomicrograph
No. AK 172804

Tested at 1800°F-22KSI
Longitudinal section
through fracture.

Etchant: HF-HNO$_3$,
HCl-FeCl$_3$

1800°F-22KSI SSR Data			
Life (Hrs)	MCR (%/Hr)	El (%)	R.A. (%)
64	0.038	7	7

Chemical Analysis

Heat No.	C%	Cr%	Mo%	Cb+Ta%	Ti%	Al%	B%	Zr%	Ni%
65-456	0.06	12.50	4.32	2.30	0.83	6.06	0.0074	0.094	Bal.

The general precipitate is relatively coarse gamma-
prime. Most of the MC carbides have reacted with
the gamma matrix to produce gamma-prime and $M_{23}C_6$
which can be seen readily at the boundaries. Ar-
rows A indicate partially reacted MC carbides.

CAST INCO 713 LC

Photomicrograph
No. AK 172703

Figure 39
200X

2150°F - 2 hrs.
Air Cooled
Tested at 1800°F-22KSI
Longitudinal section
through fracture.
−
Etchant: HF-HNO$_3$,
HCl-FeCl$_3$

1800°F-22KSI SSR Data

Life (Hrs)	MCR (%/Hr)	El (%)	R.A. (%)
63	0.037	11	7

Chemical Analysis

Heat No.	C%	Cr%	Mo%	Cb+Ta%	Ti%	Al%	B%	Zr%	Ni%
65-456	0.06	12.50	4.32	2.30	0.83	6.06	0.0074	0.094	Bal.

The general gamma-prime precipitate is relatively
coarse, indicating agglomeration. Extensive gamma-
prime (white) precipitation at grain boundaries.

CAST INCO 713 LC

Photomicrograph
No. AK 172704

2150°F – 2 hrs.
Air Cooled
Tested at 1800°F–22KSI
Longitudinal Section
through fracture.
—
Etchant: $HF-HNO_3$,
$HCl-FeCl_3$

1800°F–22KSI SSR Data			
Life (Hrs)	MCR (%/Hr)	El (%)	R.A. (%)
63	0.037	11	7

Chemical Analysis

Heat No.	C%	Cr%	Mo%	Cb+Ta%	Ti%	Al%	B%	Zr%	Ni%
65-456	0.06	12.50	4.32	2.30	0.83	6.06	0.0074	0.094	Bal.

The coarse general precipitate is agglomerated gamma-prime. The boundaries consist of $M_{23}C_6$ particles embedded in gamma-prime. Circled area indicates a MC carbide partly transformed to gamma-prime and $M_{23}C_6$.

CAST INCO 718

Photomicrograph
No. AK 188101

Figure 41
500X

As Cast

Etchant: 5% Aqueous
Cr$_2$O$_3$ Electrolytic
15V, 3.2A/in^2

Room Temp. Tensile Data

Y.S. (KSI)	T.S. (KSI)	El (%)	R.A. (%)
82	123	18	31

Chemical Analysis

Heat No.	C%	Cr%	Mo%	Cb+Ta%	Ti%	Al%	B%	Fe%	Co%	Ni%
65-506	0.05	17.85	3.04	5.06	0.95	0.57	0.0017	18.9	0.05	Bal.

The dark-etching constituent in interdendritic areas
is gamma-prime (Ni$_3$Cb). Arrow A indicates MC-type
columbium carbides. Arrow B indicates laves phase.
Matrix is gamma. This is a typical cast structure
of this alloy.

CAST INCO 718

Photomicrograph
No. AK 188201
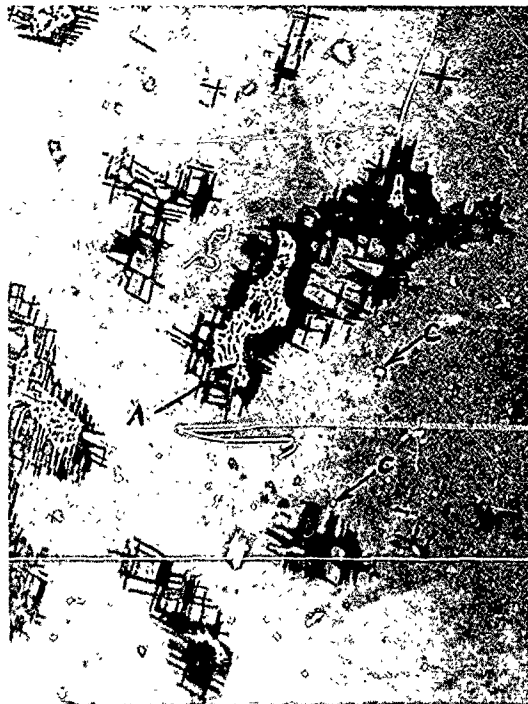
Figure 42.
200X

1800°F - 2 hrs.
Air Cooled
-
Etchant: 5% Aqueous
Cr_2O_3. Electrolytic
15V, 3.2 A/in^2

Room Temp. Tensile Data

Y.S. (KSI)	T.S. (KSI)	El (%)	R.A. (%)
41	92	29	30

Chemical Analysis

Heat No.	C%	Cr%	Mo%	Cb+Ta%	Ti%	Al%	B%	Fe%	Co%	Ni%
65-506	0.05	17.85	3.04	5.06	0.95	0.57	0.0017	18.9	0.05	Bal.

The acicular constituent is orthorhombic Ni_3Cb.
Arrow A indicates laves phase undissolved at 1800°F.
Arrows C indicate MC-type carbide particles. Matrix
is gamma.

-183-

CAST INCO 718

Photomicrograph
No. AK 188301

1800°F - 2 hrs.
Air Cooled
1325°F - 8 hrs.
Furnace Cooled to
1150°F - 8 hrs.
Air Cooled

Etchant: 5% Aqueous
Cr_2O_3, Electrolytic
15V, 3.2 A/in^2

Room Temp. Tensile Data

Y.S. (KSI)	T.S. (KSI)	El (%)	R.A. (%)
86	123	13	23

Chemical Analysis

Heat No.	C%	Cr%	Mo%	Cb+Ta%	Ti%	Al%	B%	Fe%	Co%	Ni%
65-506	0.05	17.85	3.04	5.06	0.95	0.57	0.0017	18.9	0.05	Bal.

The acicular constituent is orthorhombic Ni_3Cb.
Arrows A indicate laves phase. MC-type carbides
are indicated by arrows B. The matrix shows ev-
idence of gamma-prime (body centered tetragonal
Ni_3Cb) precipitation which is unresolvable. The
boundary precipitates are thought to be $M_{23}C_6$
and M_6C.

CAST RENE′ 41

Photomicrograph
No. AK 188501

Figure 44
200X

As Cast

Etchant: 92% HCl–
5% H_2SO_4–3% HNO_3

Room Temp. Tensile Data

Y.S. (KSI)	T.S. (KSI)	El (%)	R.A. (%)
$\frac{78}{80}$	$\frac{124}{128}$	16	$\frac{19}{23}$

Chemical Analysis

Heat No.	C%	Cr%	Mo%	Ti%	Al%	B%	Co%	Ni%
65-522	0.08	19.23	9.79	3.37	1.55	0.005	10.13	Bal.

Arrows A indicate MC-type titanium carbides.
The general precipitate is gamma-prime, $Ni_3(Ti, Al)$.

CAST RENE´ 41

Photomicrograph
No. AK 188502

Figure 45
500X

As Cast

Etchant:
92%HCl-5% H_2SO_4-3%HNO_3
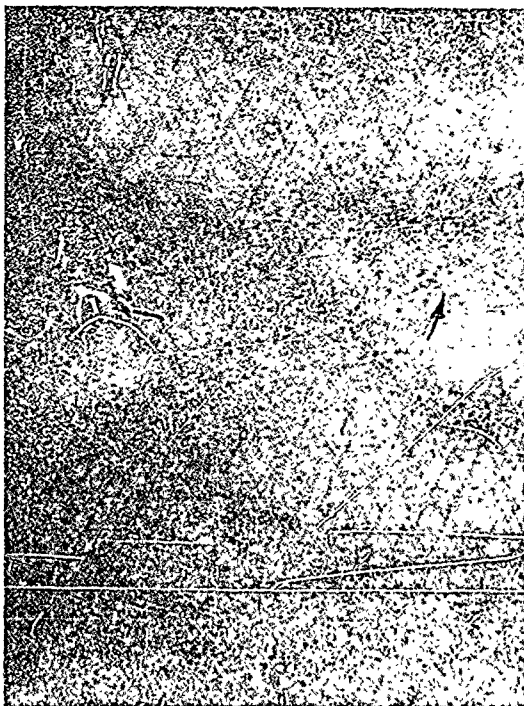
Room Temp. Tensile Data			
Y.S. (KSI)	T.S. (KSI)	El (%)	R.A. (%)
$\frac{79}{80}$	$\frac{124}{128}$	16	$\frac{19}{23}$

Chemical Analysis

Heat No.	C%	Cr%	Mo%	Ti%	Al%	B%	Co%	Ni%
65-522	0.08	19.23	9.79	3.37	1.55	0.005	10.13	Bal.

Arrows indicate carbide particles. The general
precipitate is gamma-prime. The geometric lines
are thought to be gamma-prime precipitated preferen-
tially in close-packed planes. Matrix is gamma.

CAST RENE' 41

Photomicrograph
No. AK 1 3602
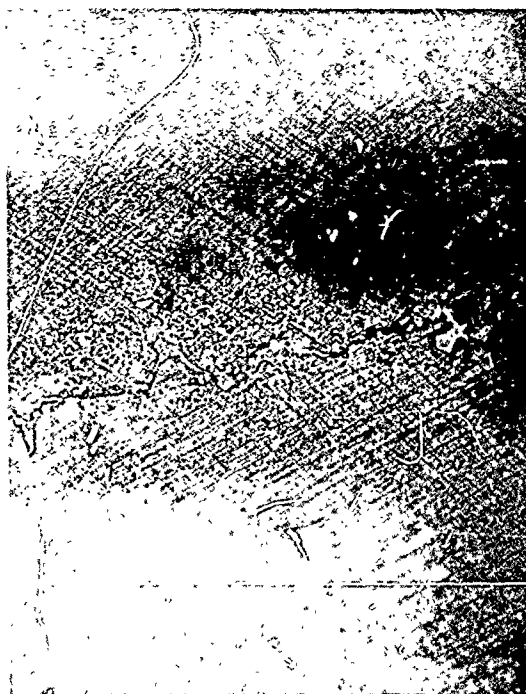
Figure 46
500X

1950°F - 4 hrs.
Air Cooled

Etchant:
92%HCl-5%H_2SO_4-3%HNO_3

Room Temp. Tensile Data

Y.S. (KSI)	T.S. (KSI)	El (%)	R.A. (%)
82	106	11	16
84	112	17	19

Chemical Analysis

Heat No.	C%	Cr%	Mo%	Ti%	Al%	B%	Co%	Ni%
65-522	0.08	19.23	9.79	3.37	1.55	0.005	10.13	Bal.

Boundary shows undissolved carbide particles.
Part of the general gamma-prime precipitate
is dissolved or reprecipitated due to the
1950°F treatment.

<u>CAST RENE 41</u>

Photomicrograph
No. AK 188702

2150°F - 2 hrs.
Air Cooled

Etchant:
92%HCl-5%H$_2$SO$_4$-3%HNO$_3$

<u>Room Temp. Tensile Data</u>

Y.S. (KSI)	T.S. (KSI)	El (%)	R.A. (%)
$\frac{81}{82}$	$\frac{126}{130}$	33	$\frac{30}{32}$

<u>Chemical Analysis</u>

Heat No.	C%	Cr%	Mo%	Ti%	Al%	B%	Co%	Ni%
65-552	0.08	19.23	9.79	3.37	1.55	0.005	10.13	Bal.

The general precipitate is gamma-prime precipi-
tated preferentially at close-packed planes.
The light boundary precipitate is thought to be
M$_6$C. The undissolved particles (white) are MC-
type titanium carbides. Matrix is gamma.

CAST RENÉ 41

Photomicrograph
No. AK 188802
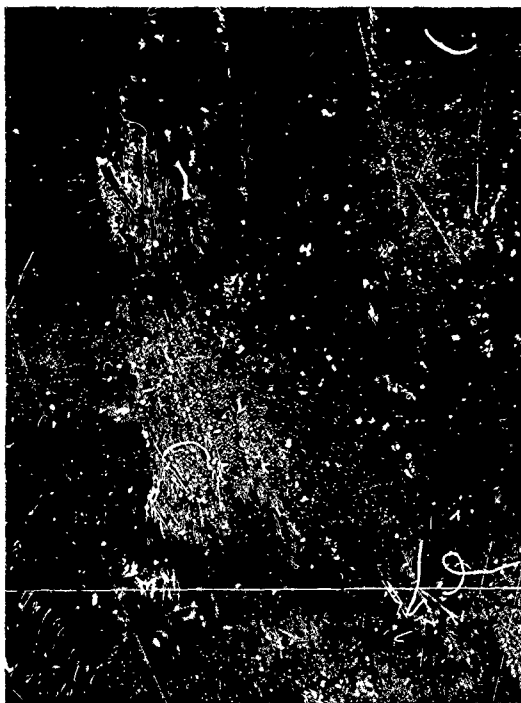
Figure 48
500X

1950°F – 2 hrs.
Air Cooled
1400°F – 16 hrs.
Air Cooled

Etchant:
92%HCl–5%H$_2$SO$_4$–3%HNO$_3$

Room Temp. Tensile Data			
Y.S. (KSI)	T.S. (KSI)	El (%)	R.A. (%)
98	112	3	8

Chemical Analysis

Heat No.	C%	Cr%	Mo%	Ti%	Al%	B%	Co%	Ni%
65-552	0.08	19.23	9.79	3.37	1.55	0.005	10.13	Bal.

The general precipitate is gamma-prime. Arrow A
indicates M$_{23}$C$_6$ and M$_6$C carbides and arrow B
indicates MC-type carbides. Boundary C is thought
to contain a continuous film of sigma. The rod-
like particles in the circled area are also be-
lieved to be sigma.
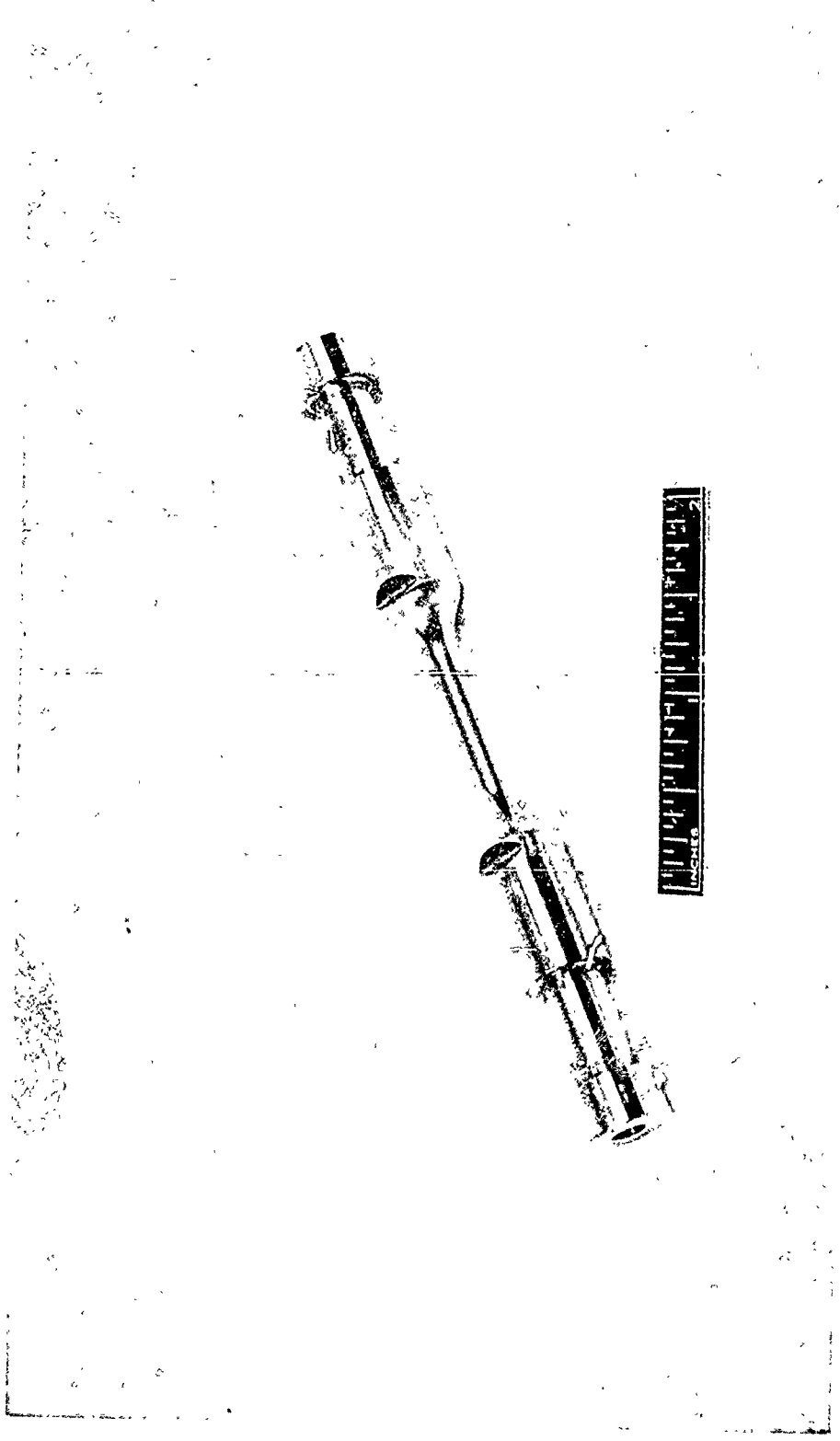
Figure 49

LOW CYCLE FATIGUE SPECIMEN

Nominal Gauge Length: 0.75 in.
Effective Gauge Length: 1.22 in.
Bar Diameter: 0.200 in.
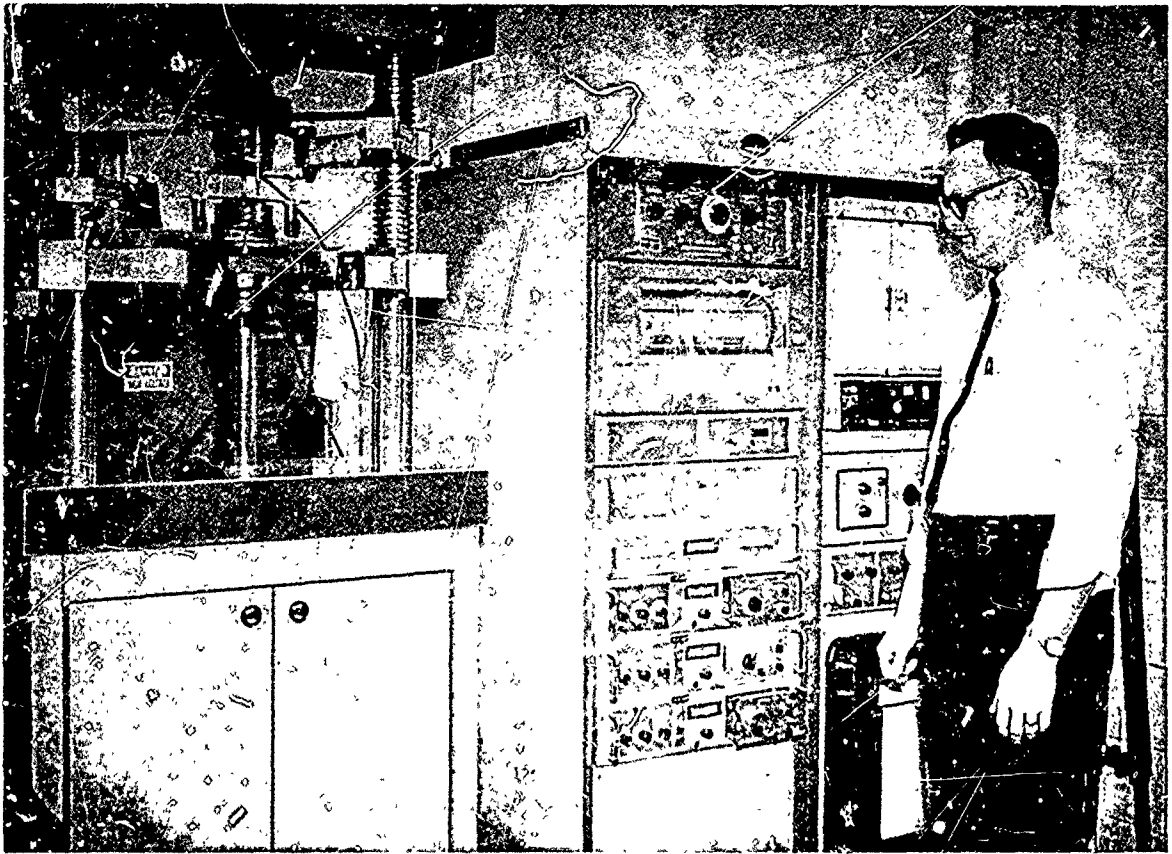
Figure 50

LOW CYCLE FATIGUE TEST SYSTEM
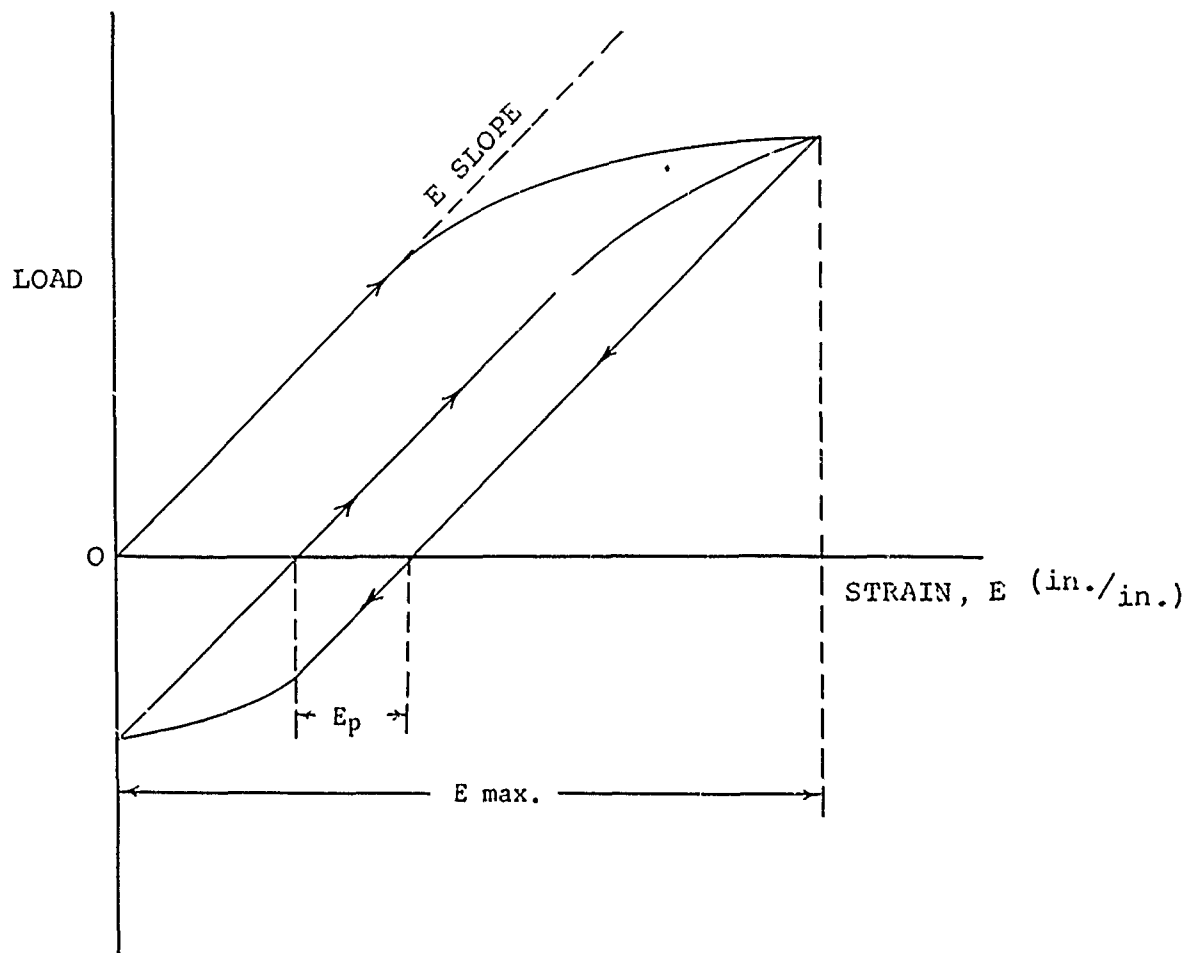
$$E \text{ max.} = E_e + E_p$$

$$E \text{ alt.} = \frac{E \text{ max.} - E \text{ min.}}{2}$$

$$E \text{ mean} = \frac{E \text{ max.} + E \text{ min.}}{2}$$

$$A \text{ Ratio} = \frac{E \text{ alt.}}{E \text{ mean}}$$

$$E = \frac{P}{AE_e}$$

Figure 51

TYPICAL FIRST CYCLE HYSTERESIS LOOP
OF INCONEL 713 LC

-192-
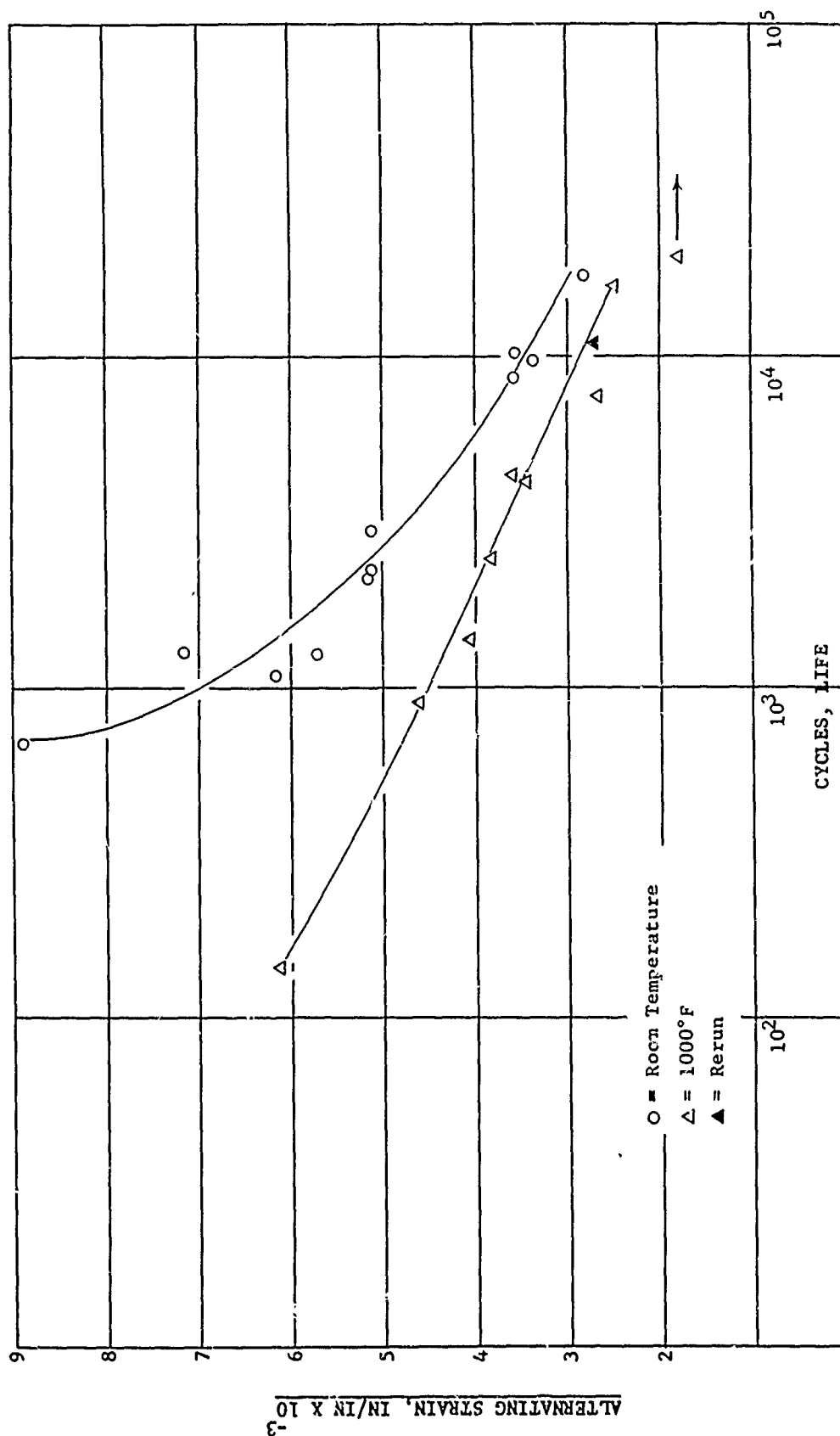
Figure 52

LOW CYCLE FATIGUE CURVES
CAST FOR INCONEL 713 LC
R.T. AND 1000°F
A = 1.0
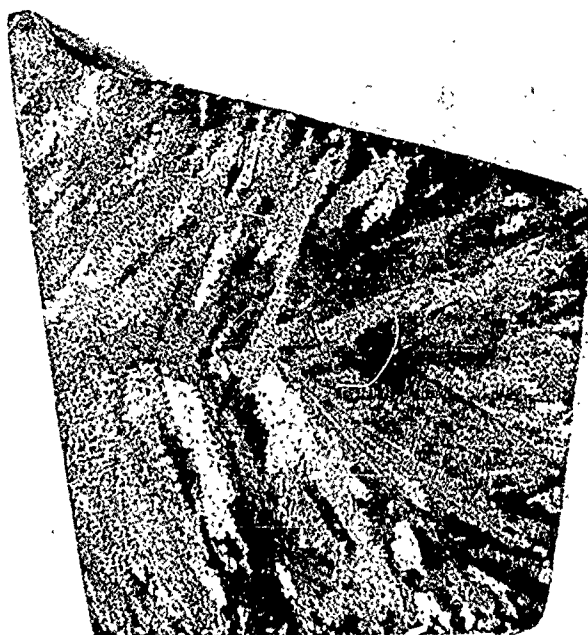
Figure 53 -   Cross-section of cast bar of Inconel 713
              low carbon illustrating grain orientation and
              morphology (rotated 90° counter clockwise
              from as cast orientation).
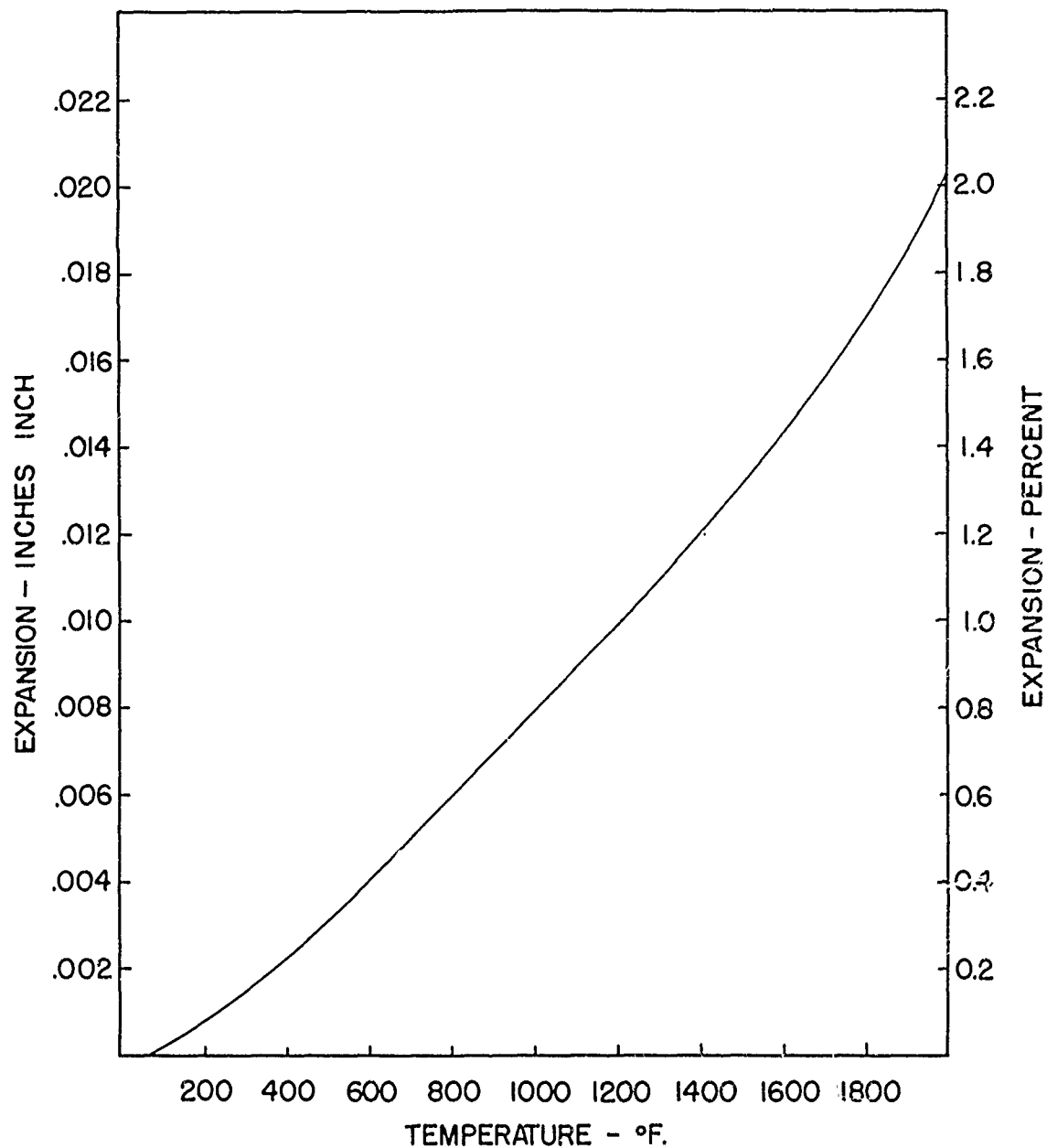
Figure 54

THERMAL EXPANSION OF ALLOY INCO 713LC IN THE
SOLUTION TREATED CONDITION

-195-
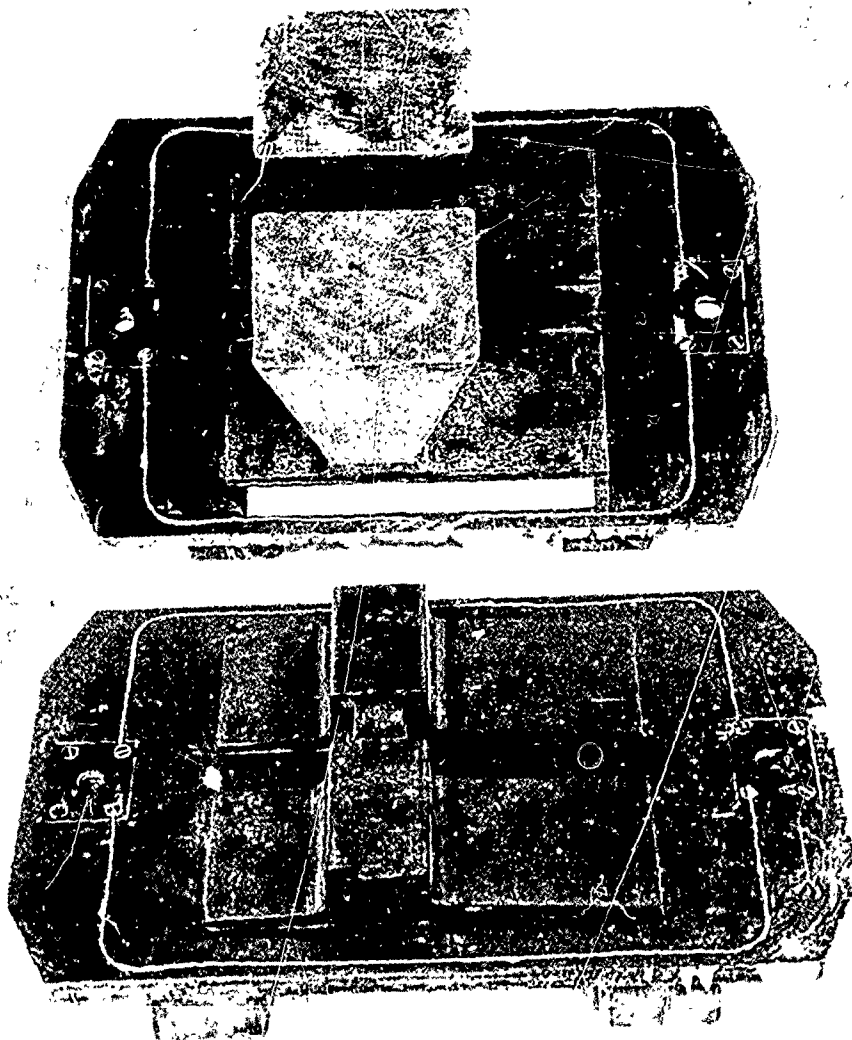
Figure 55

Cope (Top) and Drag Patterns
for
Feeding Distance Plate Castings
(2 Castings per Mold)

5"

5"

$\frac{1}{2}$"

6"

6"

$6\frac{1}{4}$"

3"

2"

3"

$\frac{1}{2}$"

₵

Approximately $\frac{1}{2}$" R.
fillets, blended

Plates tapered 6°, thickest
at riser, $\frac{1}{2}$" at ends

-197-
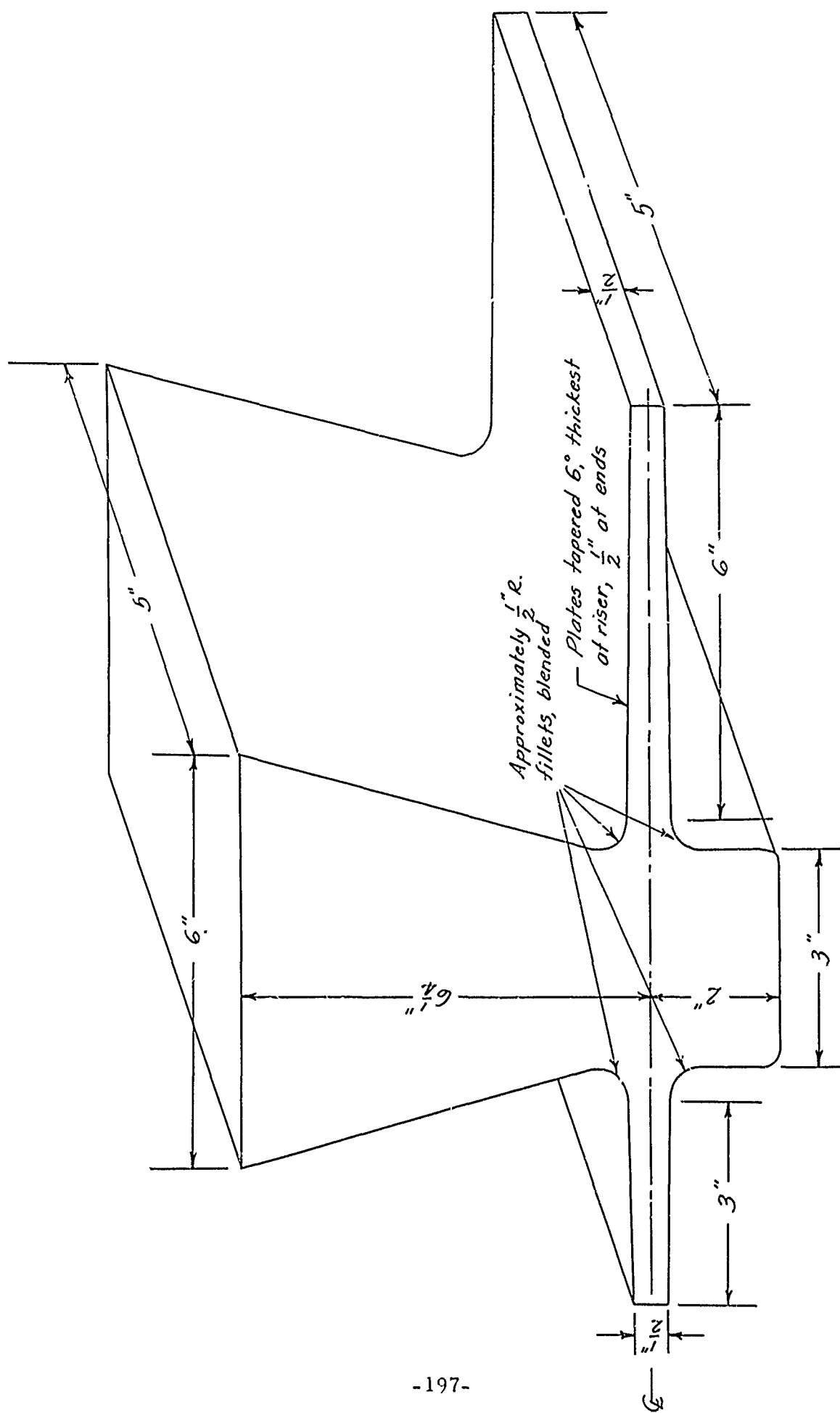
Figure 56   FEEDING DISTANCE PLATE CASTING
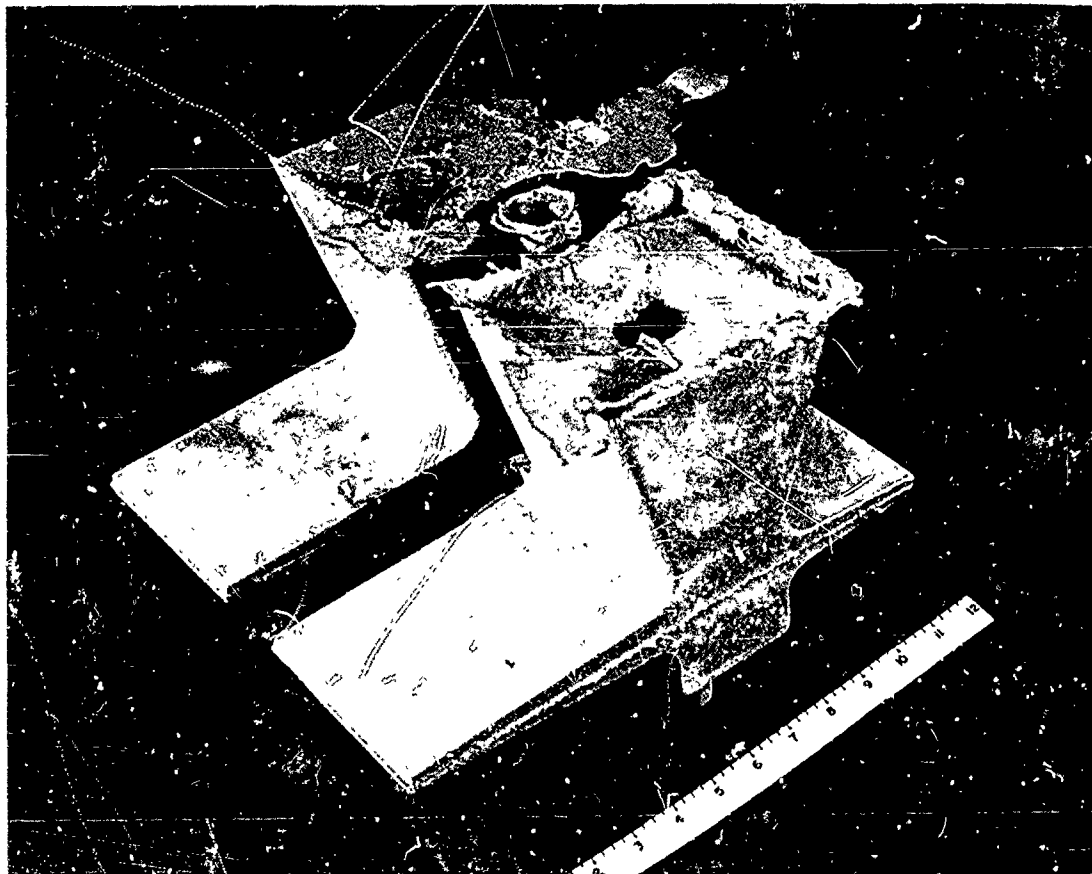
FIGURE 57

PLATE CASTING USED IN FOUNDRY VARIABLE STUDY

The two plate castings illustrated are the pro-
duct of a single mold. Both plate casting cavities and
risers are poured through the central downsprue located
between the risers. In practice, one full cavity (riser,
6" plate and 3" plate) was coated with a cobalt oxide
slurry to determine the effect of grain refining on feed-
ing distance and plate properties.

-198-
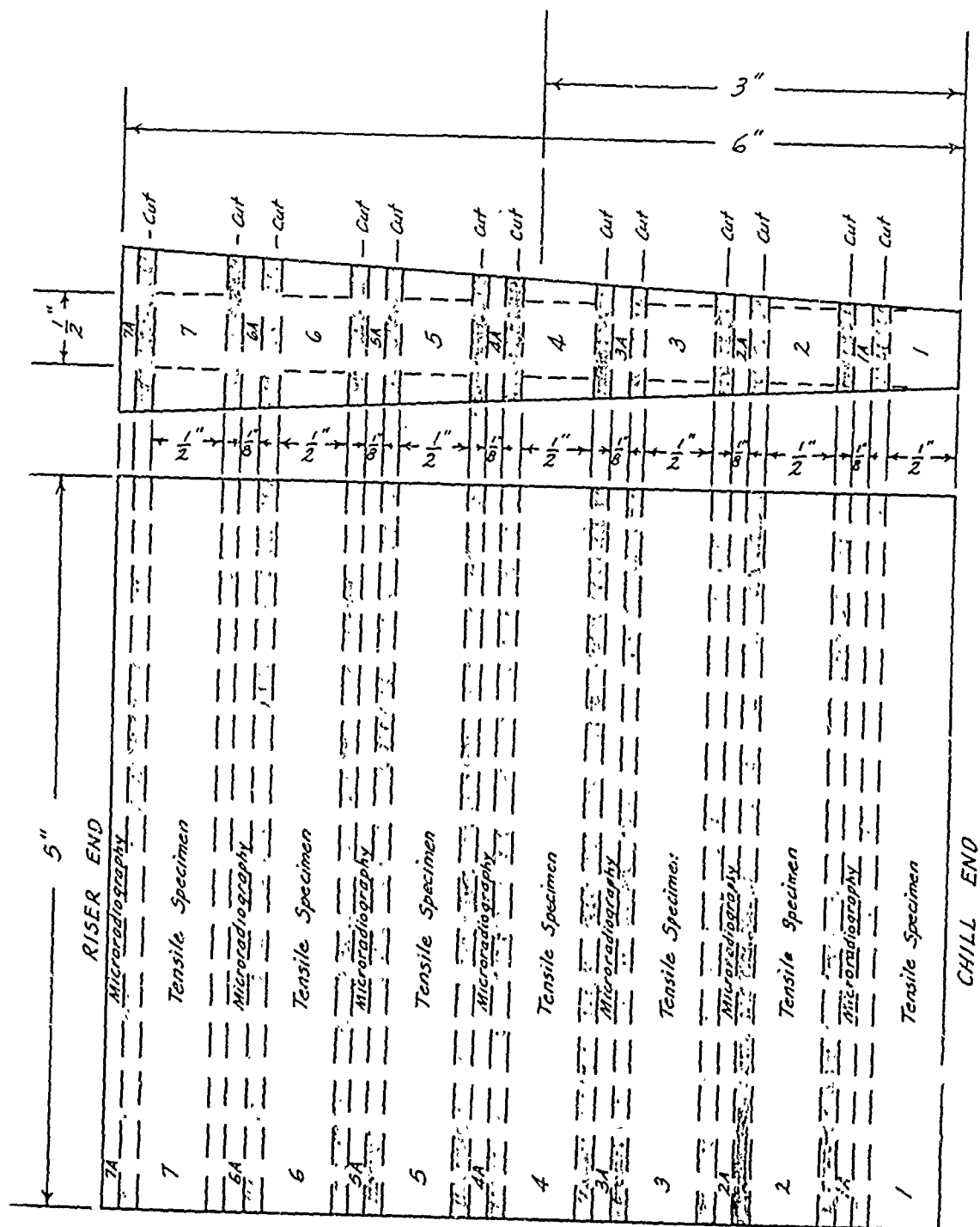
Figure 58

DIAGRAM OF SPECIMEN LOCATION

IN 6" AND 3" PLATES

-194-
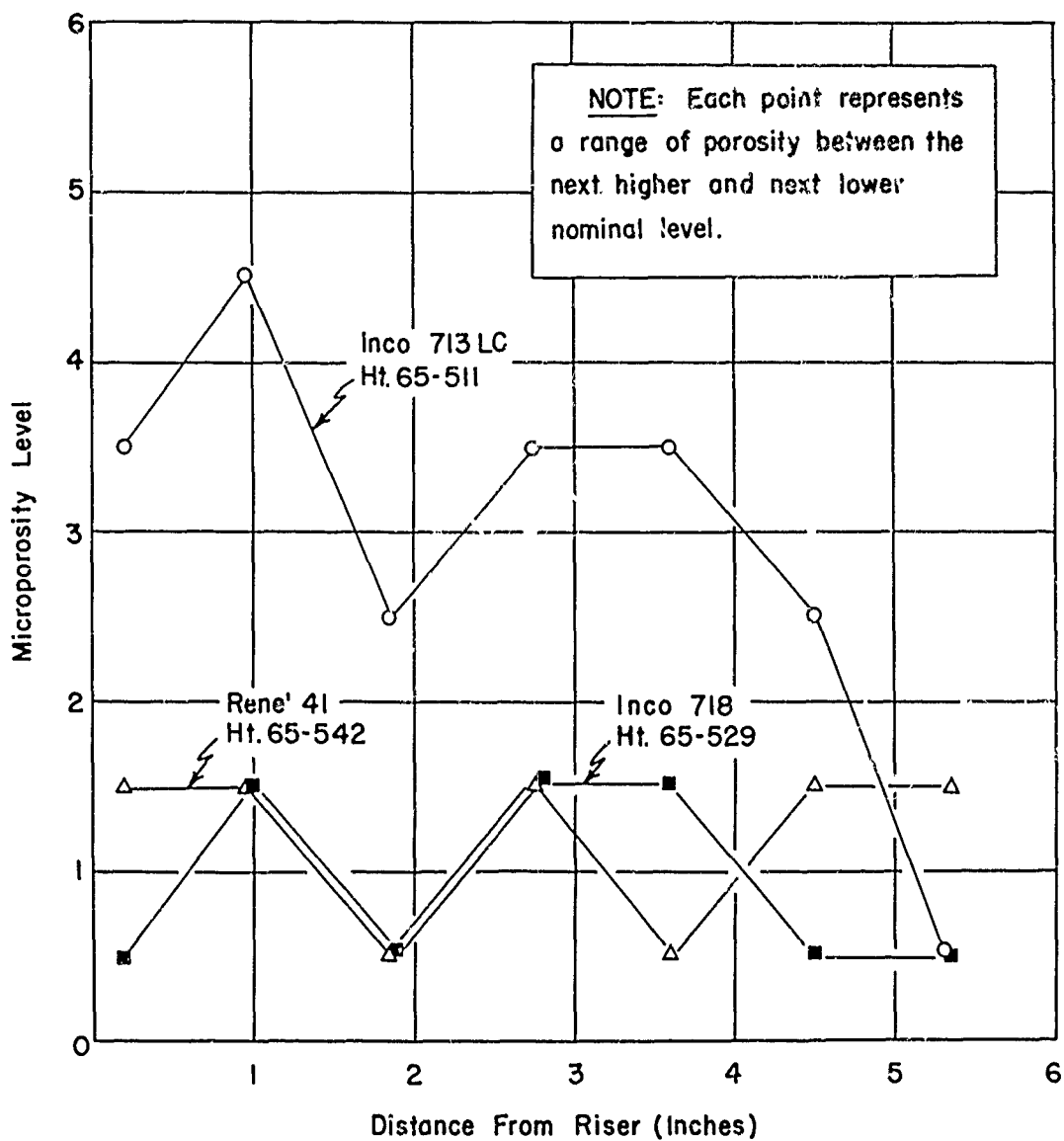
Figure 59

MICROPOROSITY LEVEL IN 6-INCH SUPERALLOY PLATES
CAST IN PLAIN, COLD CERAMIC MOLDS AT 100°F SUPERHEAT

-200-
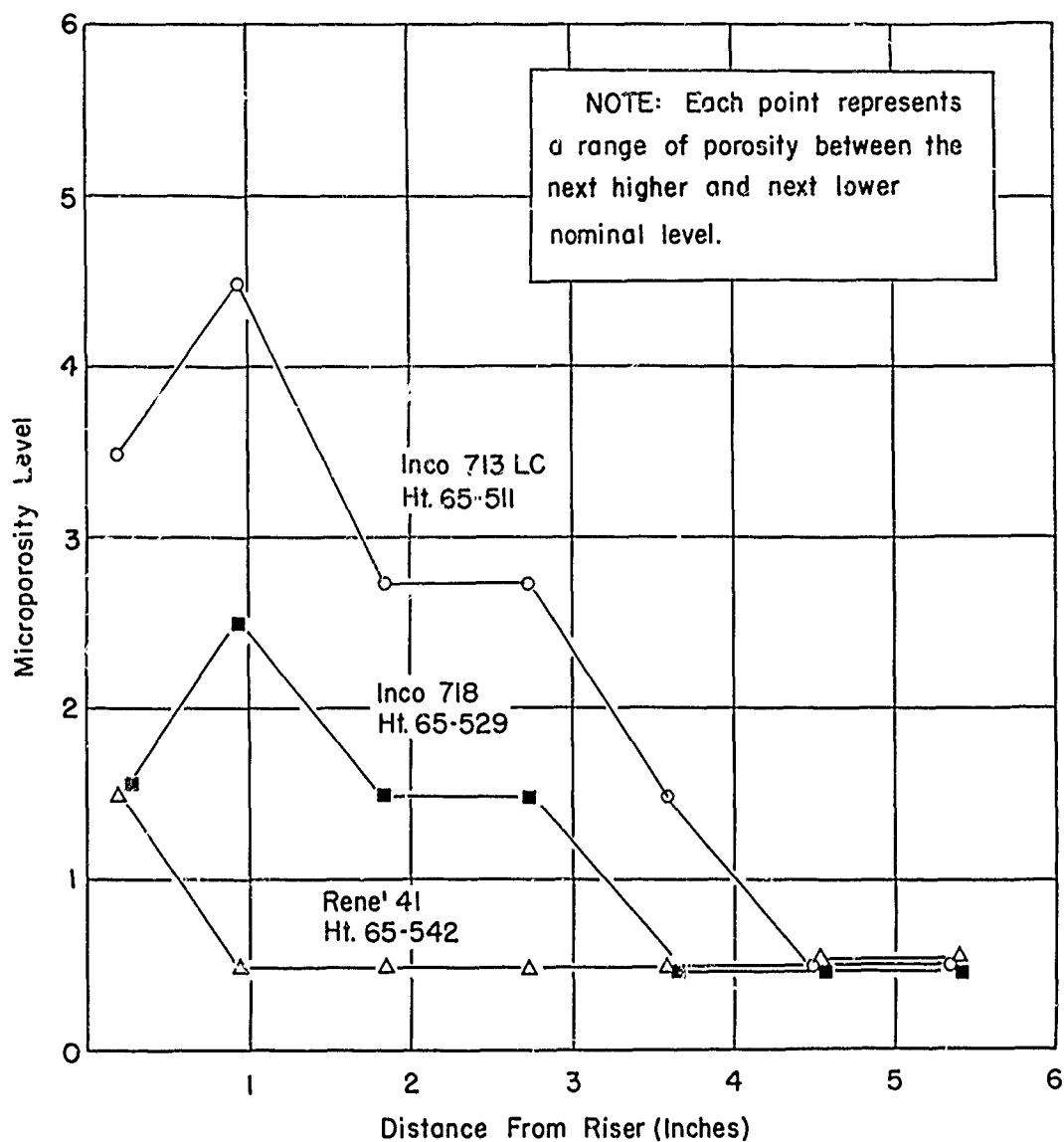
Figure   60

MICROPOROSITY LEVEL IN 6·INCH SUPERALLOY PLATES
CAST IN COLD, NUCLEATED, CERAMIC MOLDS AT 100°F. SUPERHEAT

-201-
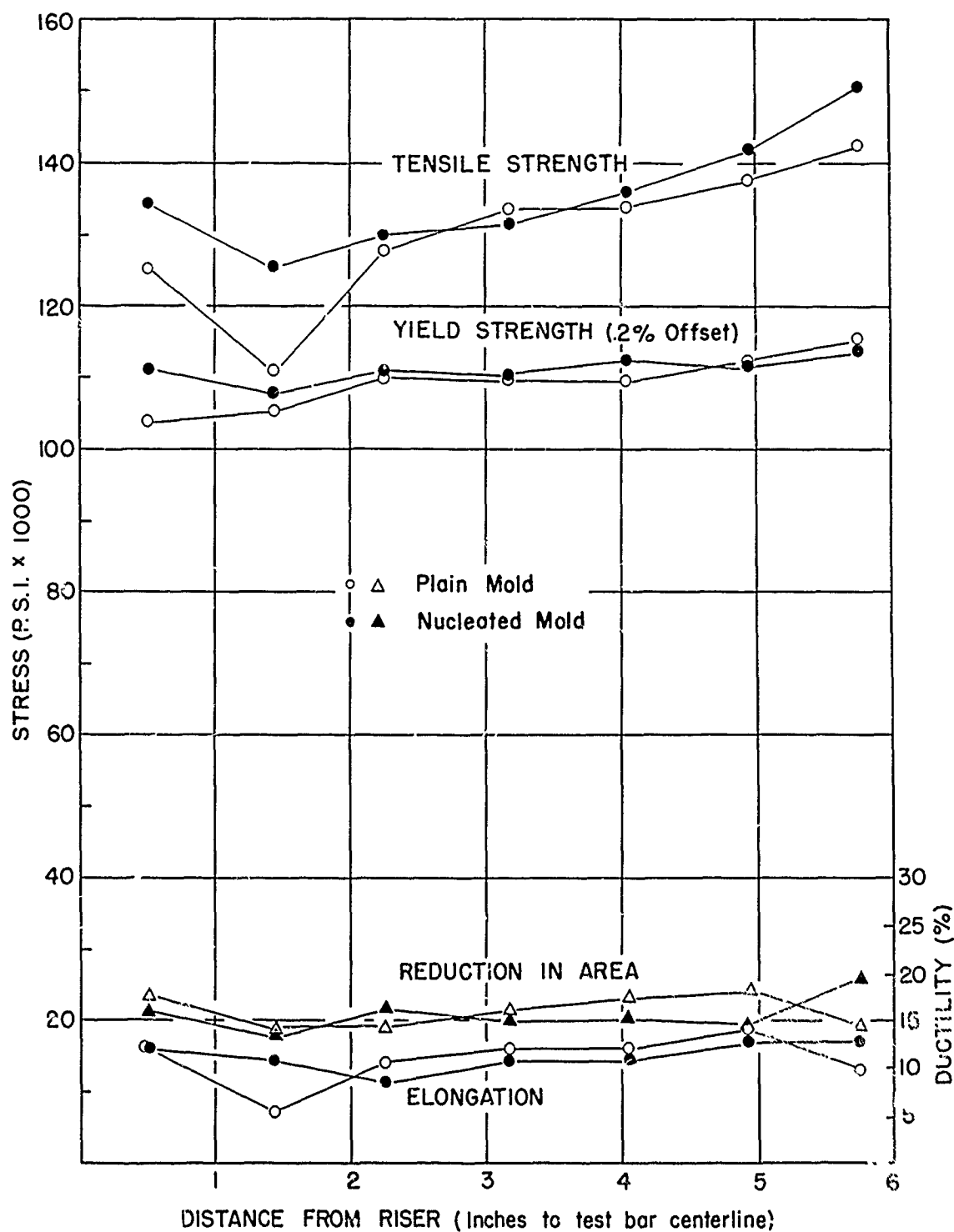
Figure 61

Room Temperature Tensile Properties of Solution
Treated Inco 713 LC Test Bars Cut From 6 Inch Long
Tapered Plates
Casting Number 65-511-1
PARAMETER LEVELS ILLUSTRATED

Pouring Temperature: Liquidus + 100°F
Mold Temperature: Cold Risers
      Mold Surface: -202-   Plain and Nucleated
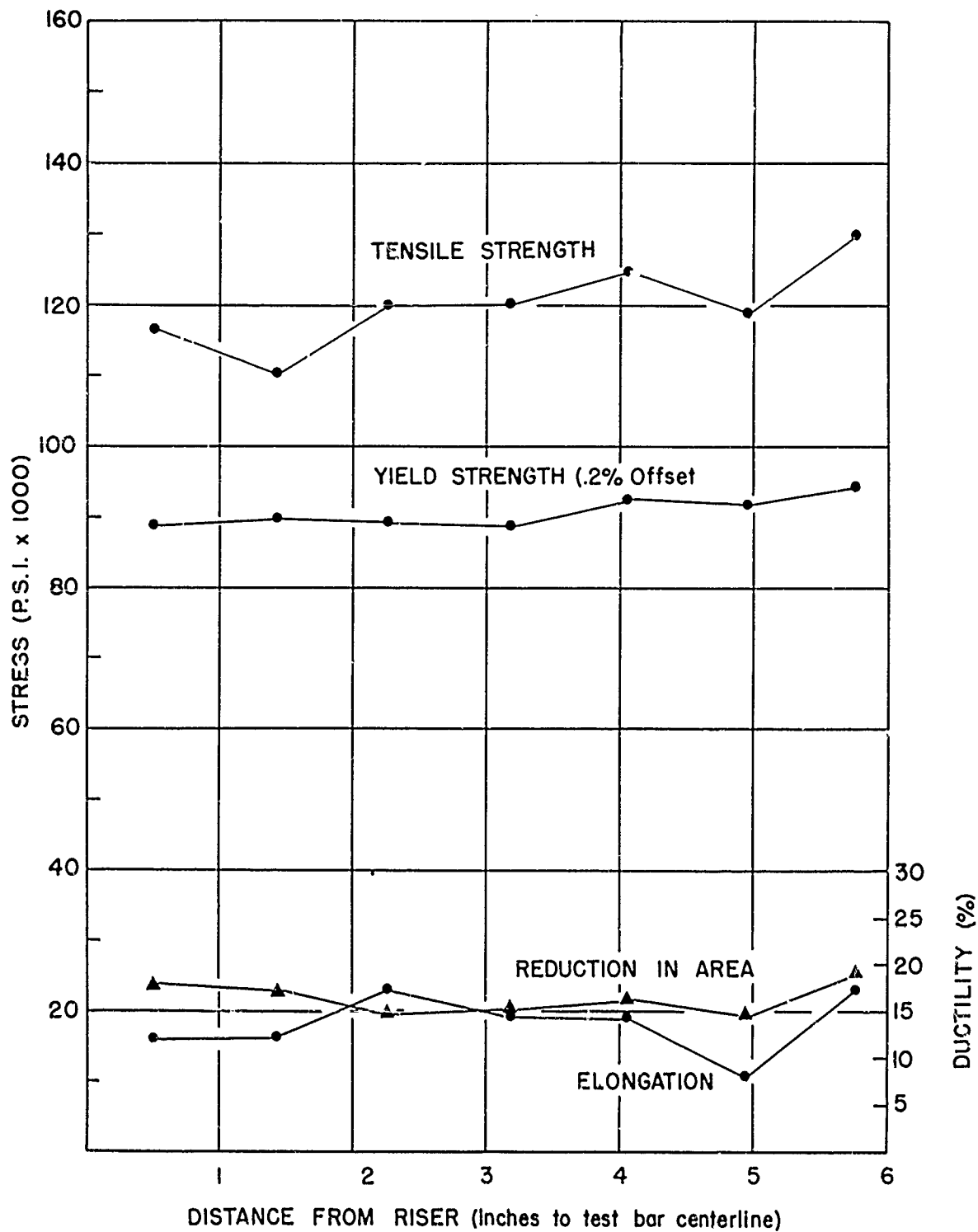
Figure 62

Room Temperature Tensile Properties of Solution
Treated Inco 718 Test Bars cut from 6-inch long
Tapered Plates
Casting Number 65-529-1
PARAMETER LEVELS ILLUSTRATED

Pouring Temperature: Liquidus + 100°F
Mold Temperature: -203-   Cold Risers
Mold Surface: Nucleated
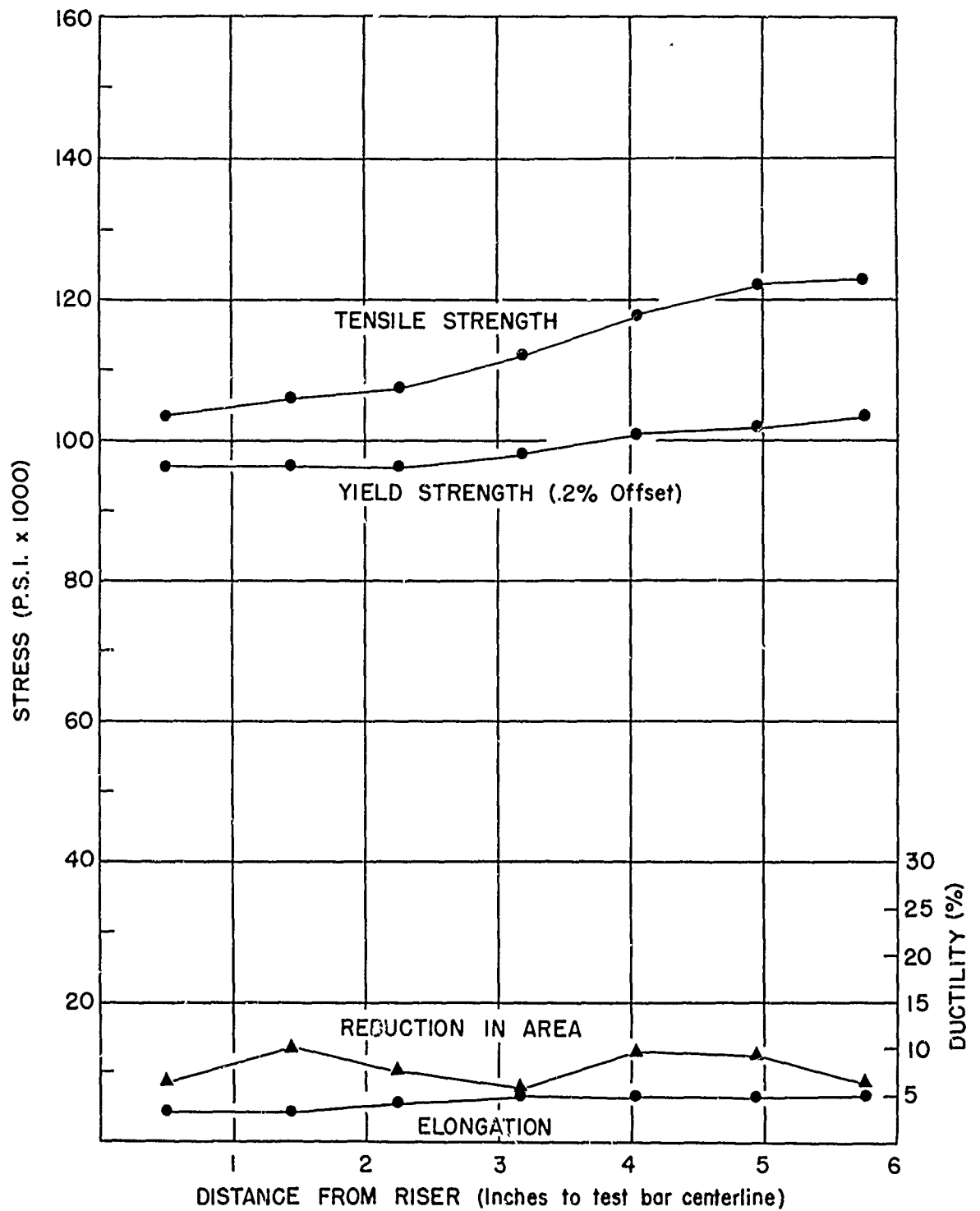
Figure 63

Room Temperature Tensile Properties of Solution Treated
Rene 41 Test Bars Cut From 6-Inch Long Tapered Plates
Casting Number 65-542-1
PARAMETER LEVELS ILLUSTRATED

Pouring Temperature:	Liquidus + 100°F
Mold Temperature:	Cold Risers
Mold Surface:	Nucleated

-204-
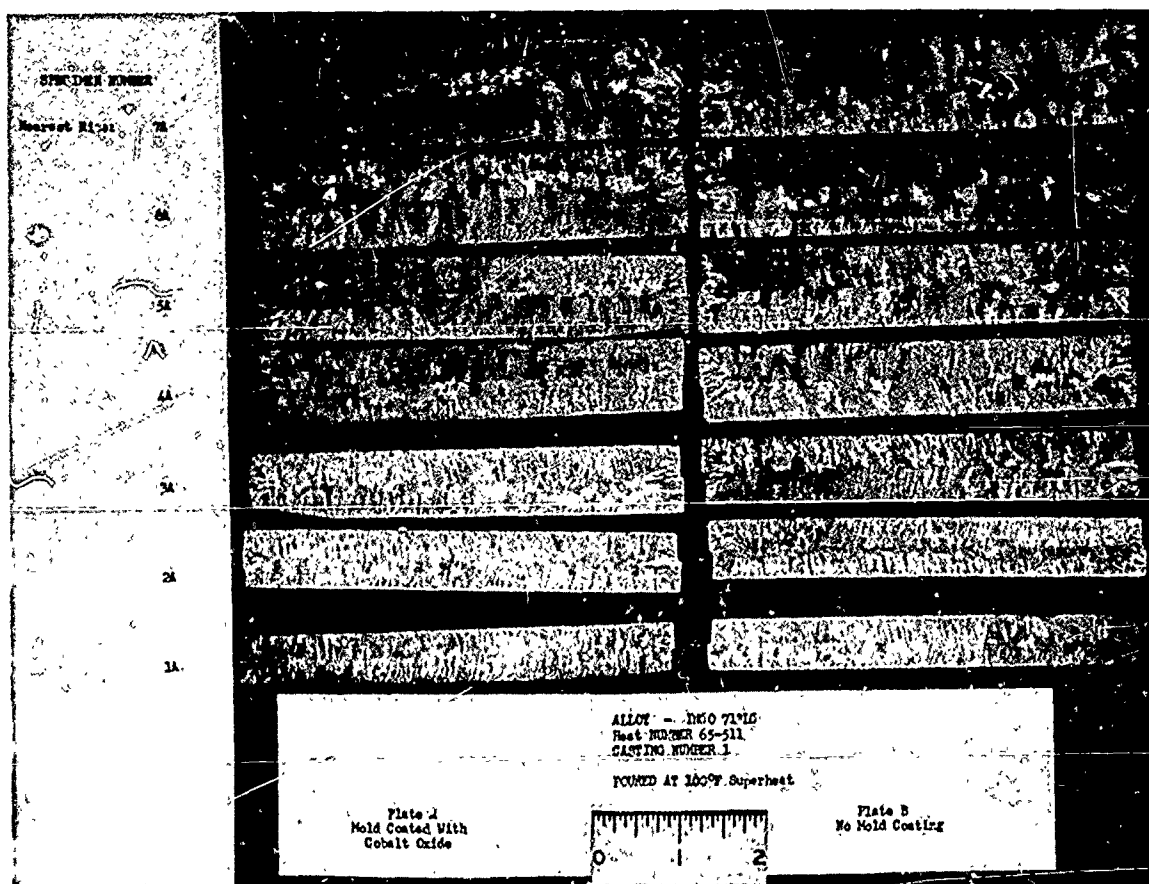
FIGURE 64

MACROETCHED RADIOGRAPHIC SPECIMENS
FROM 6" INCO 713LC PLATES
CAST AT 100°F. SUPERHEAT
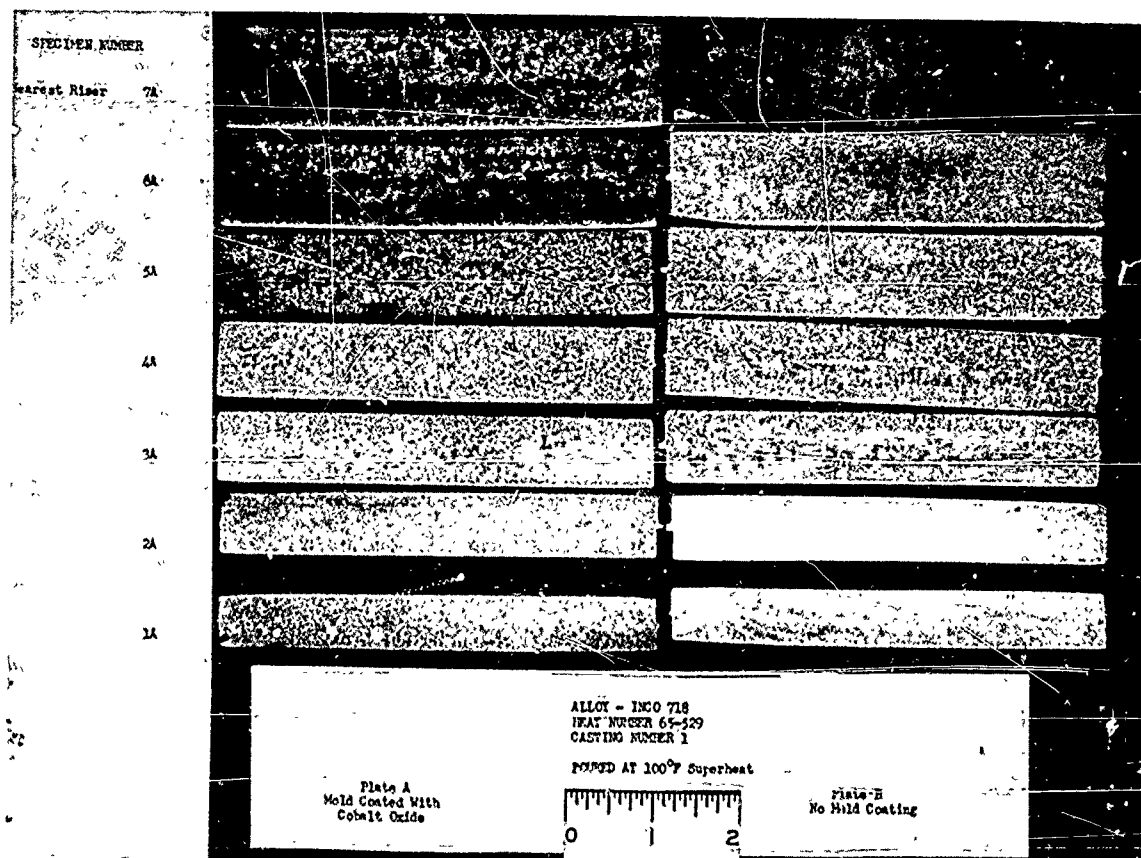
FIGURE 65

MACROETCHED RADIOGRAPHIC SPECIMEN
FROM 6" INCO 718 PLATES
CAST AT 200°F. SUPERHEAT
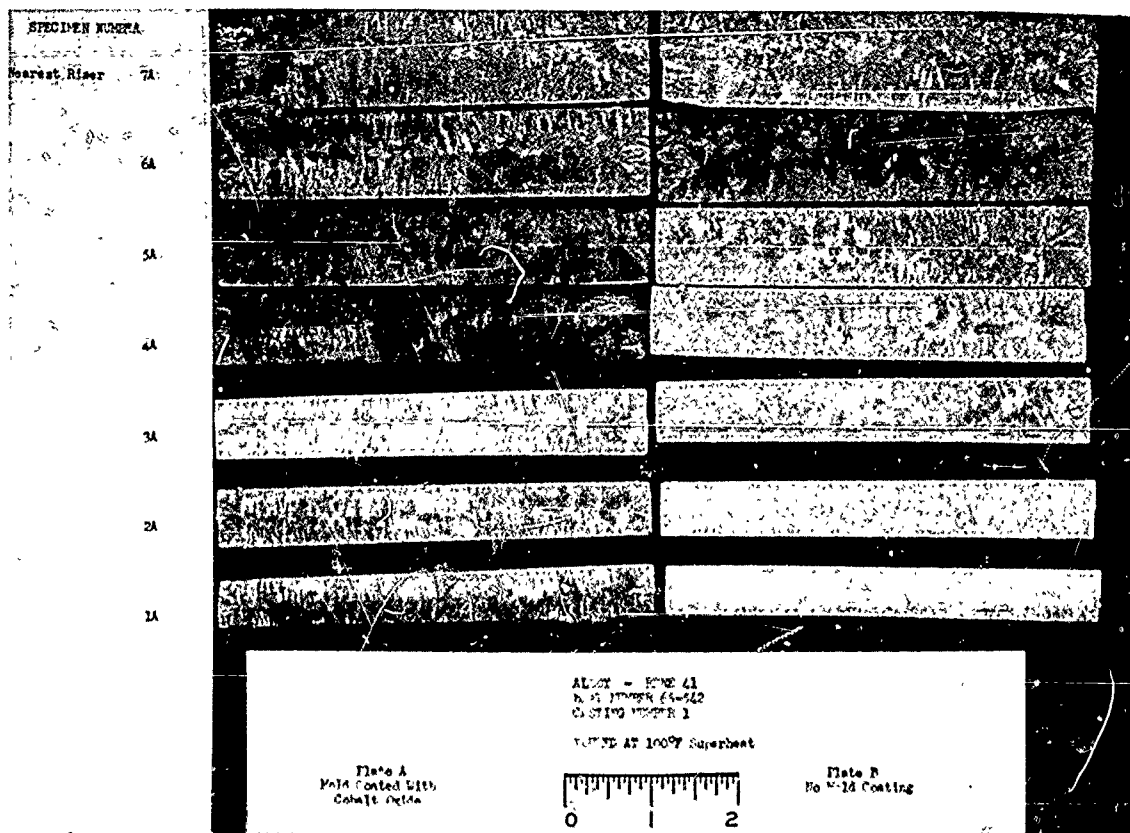
FIGURE 66

MACROETCHED RADIOGRAPHIC SPECIMENS
FROM 6" RENE 41 PLATES
CAST AT 100°F. SUPERHEAT
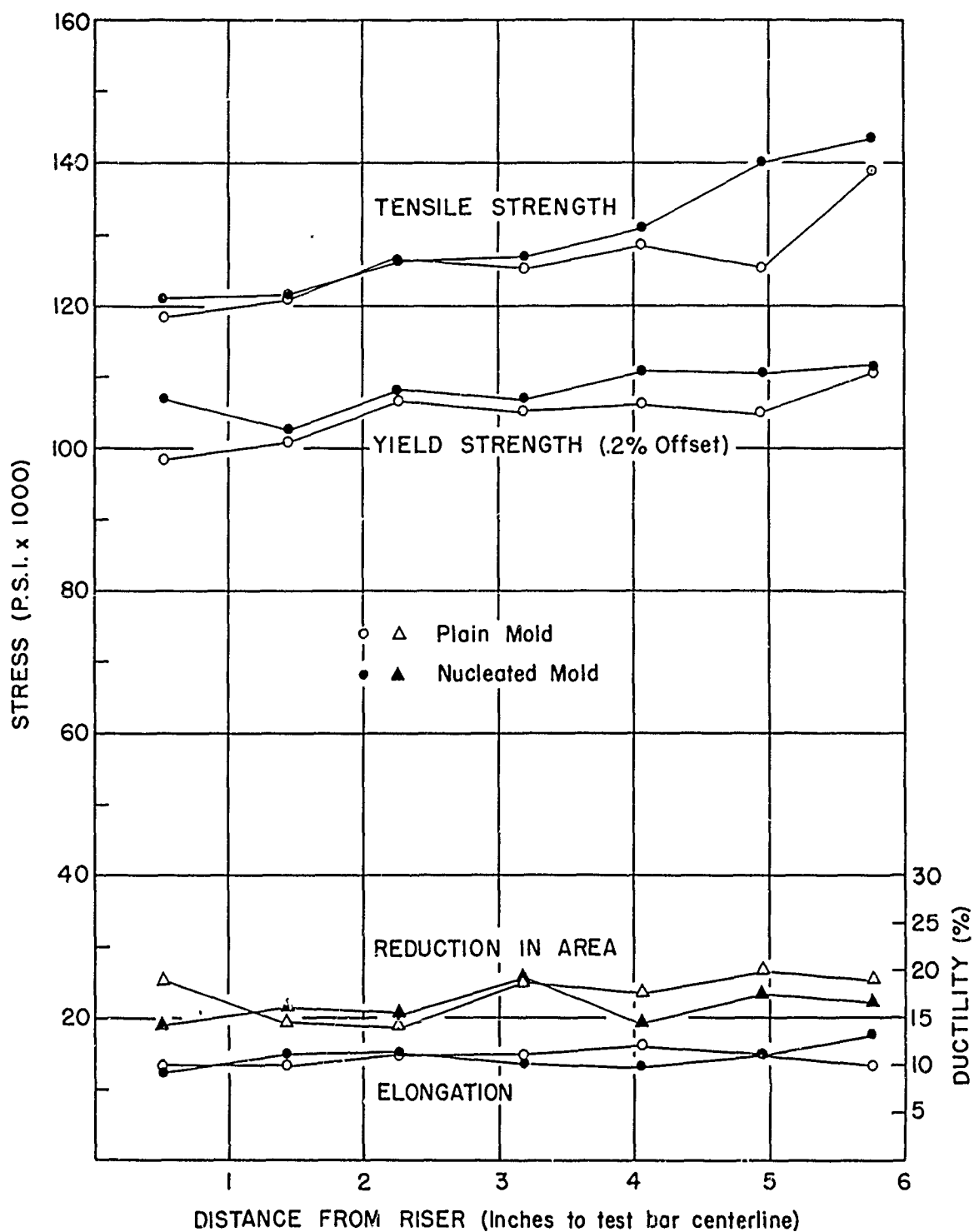
Figure 67

Room Temperature Tensile Properties of Solution Treated
Inco 713 LC Test Bars Cut From 6-Inch Long Tapered Plates
Casting Number 65-511-2

PARAMETER LEVELS ILLUSTRATED

Pouring Temperature:	Liquidus + 200°F
Mold Temperature:	Cold Risers
Mold Surface: -208-	Plain and Nucleated
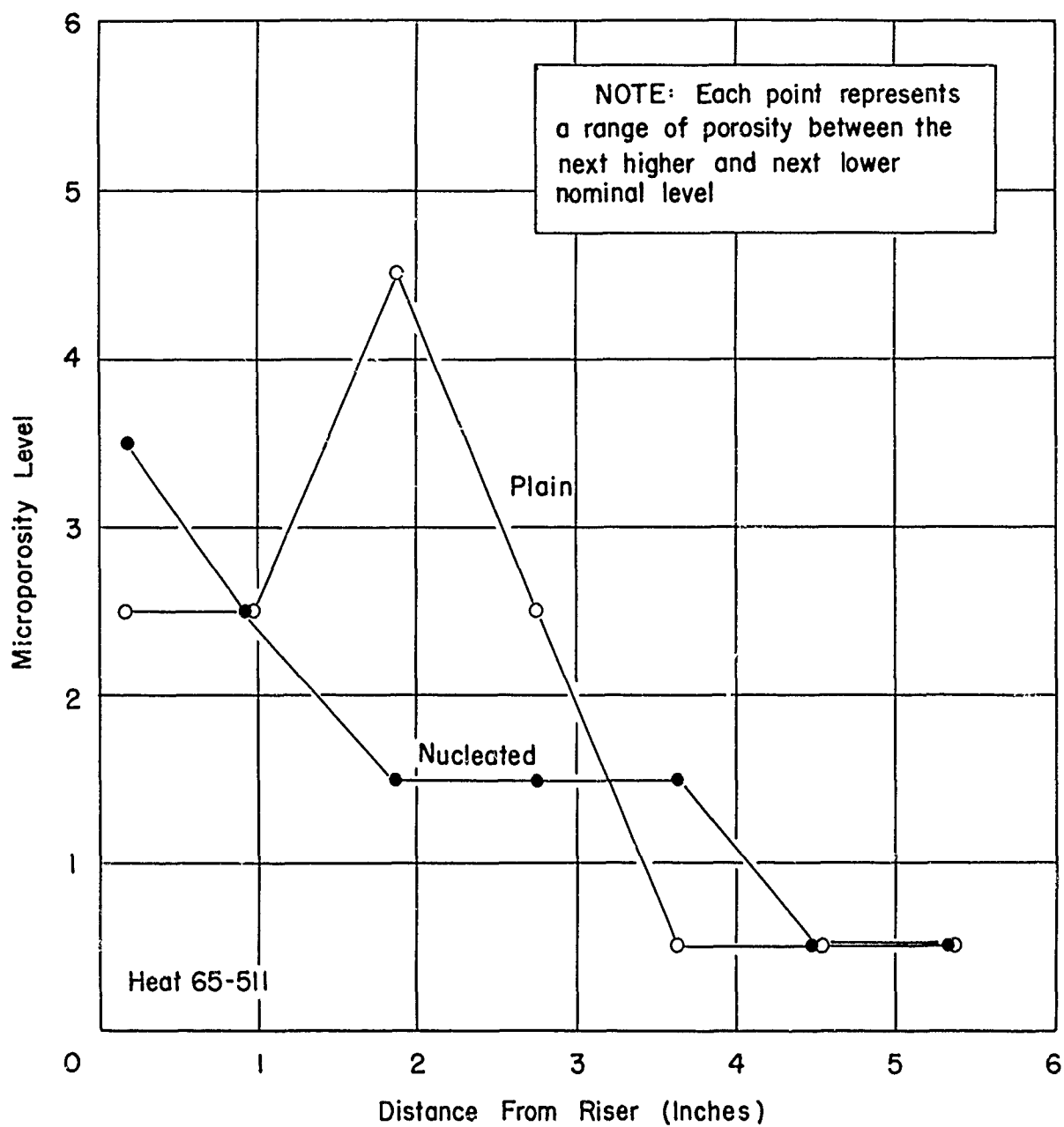
Figure 68

MICROPOROSITY LEVEL IN 6-INCH INCO 713 LC PLATES
CAST IN PLAIN AND NUCLEATED COLD CERAMIC MOLDS
AT 200°F. SUPERHEAT

-209-
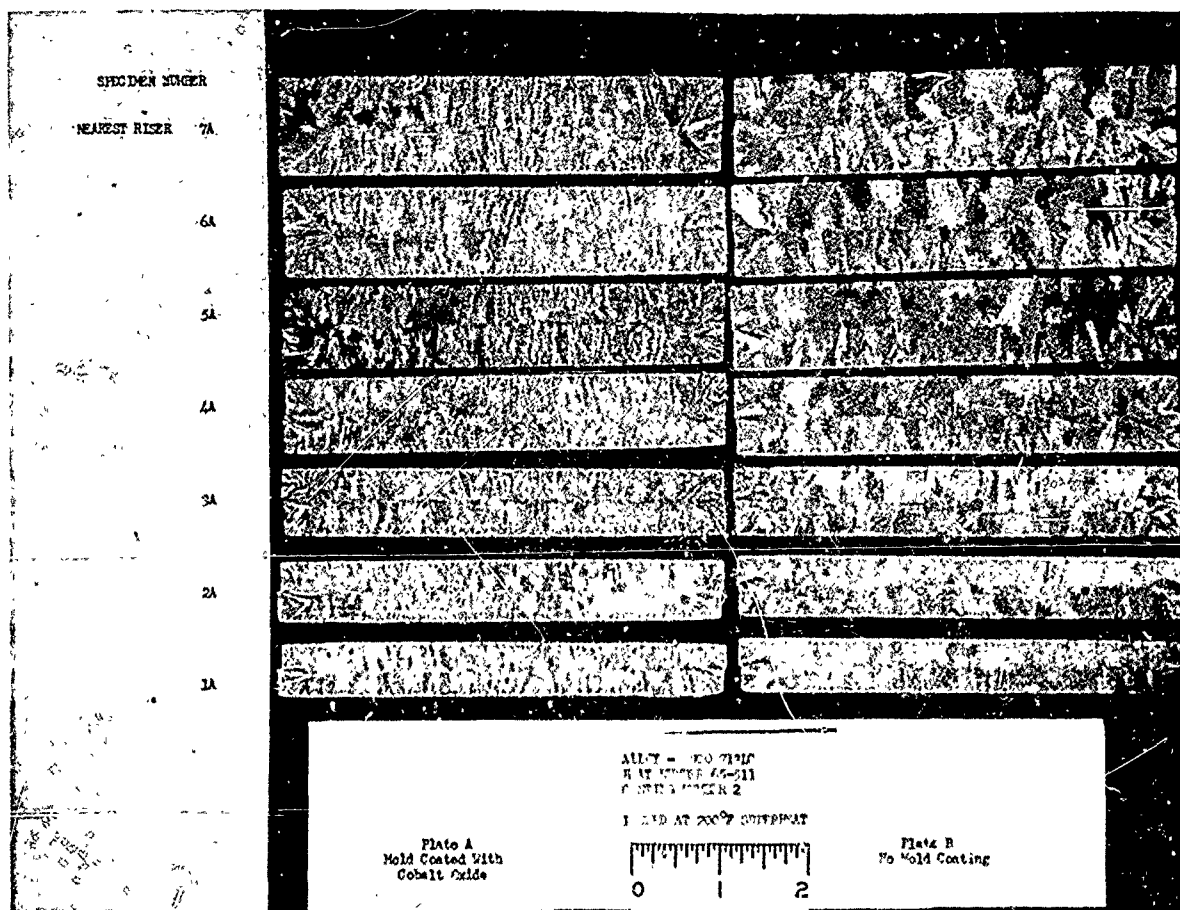
Figure 69

Macroetched Radiographic Specimens from Six
Inch Long Inco 713LC Plates Cast at 200°F.
Superheat.
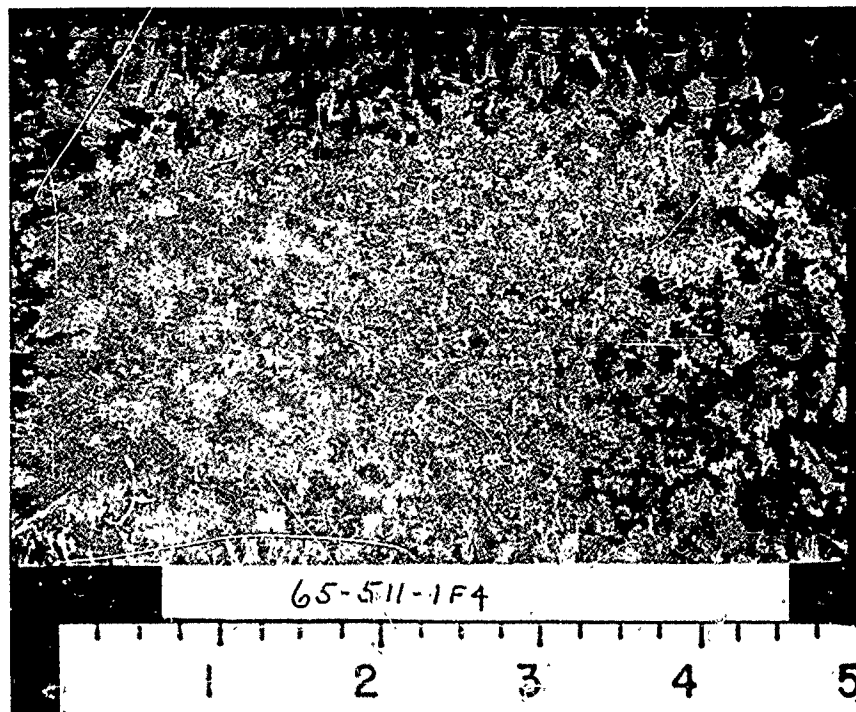
FIGURE 70

Keel Section from Plate Casting 65-511-1, INCO 713 LC, Plain Mold
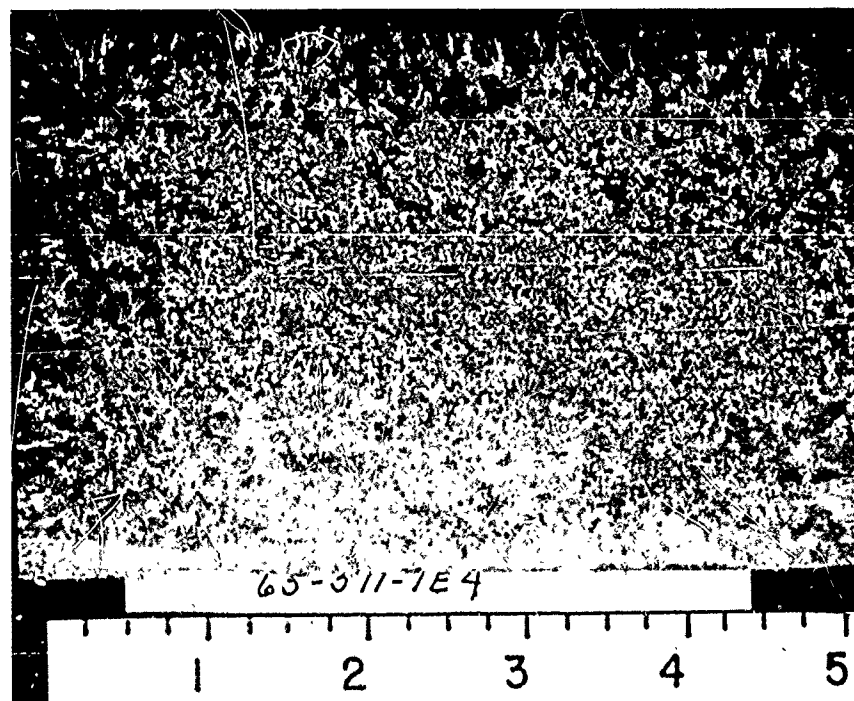
FIGURE 71

Keel Section from Plate Casting 65-511-1, INCO 713 LC, Nucleated Mold
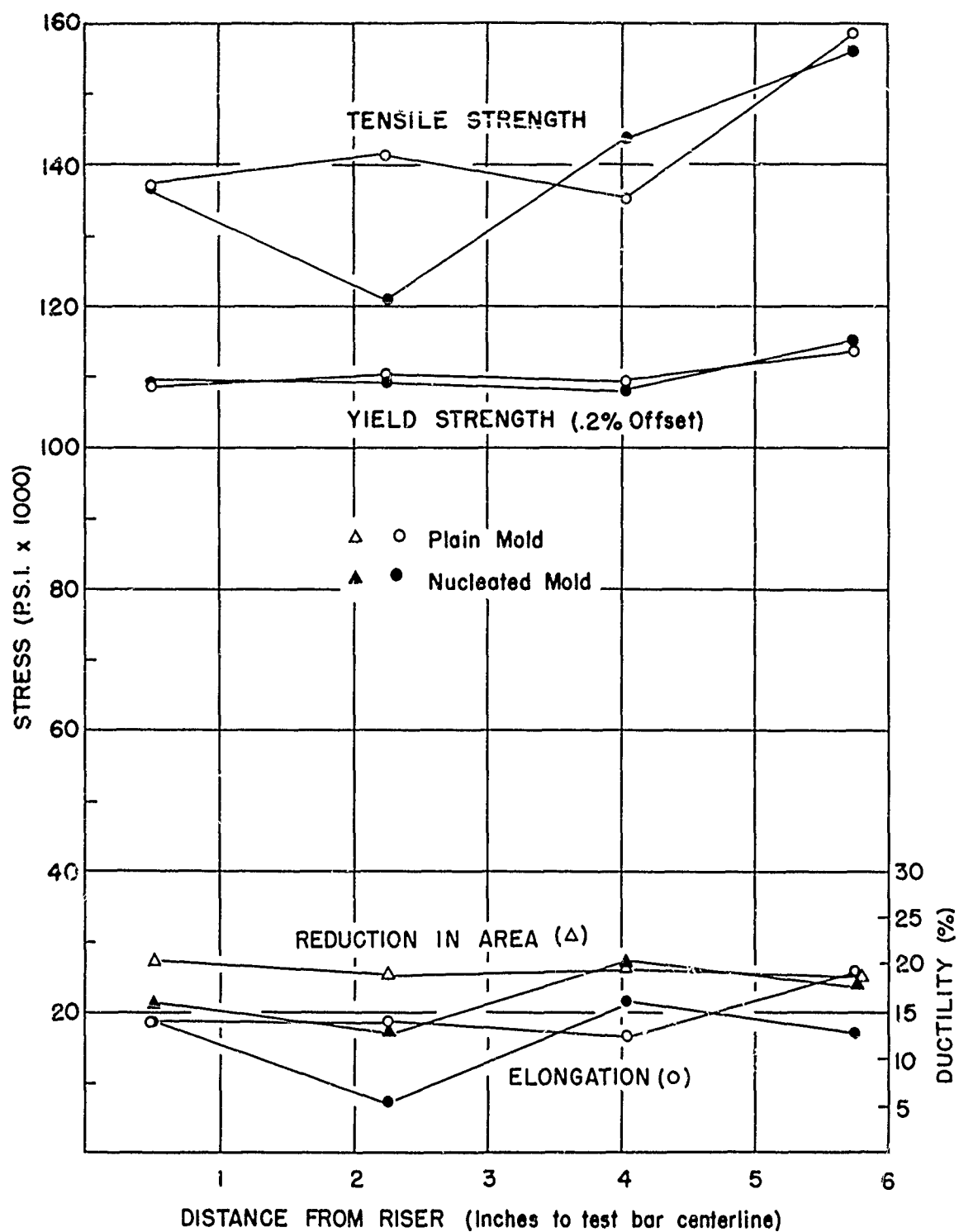
Figure 72

ROOM TEMPERATURE TENSILE PROPERTIES OF SOLUTION TREATED
INCO 713LC TEST BARS CUT FROM SIX-INCH LONG TAPERED PLATES

CASTING NUMBER 66-216-1

PARAMETER LEVELS ILLUSTRATED
POURING TEMPERATURE: LIQUIDUS PLUS 100°F
MOLD TEMPERATURE: RISERS PREHEATED
MOLD SURFACE: PLAIN AND NUCLEATED

-212-
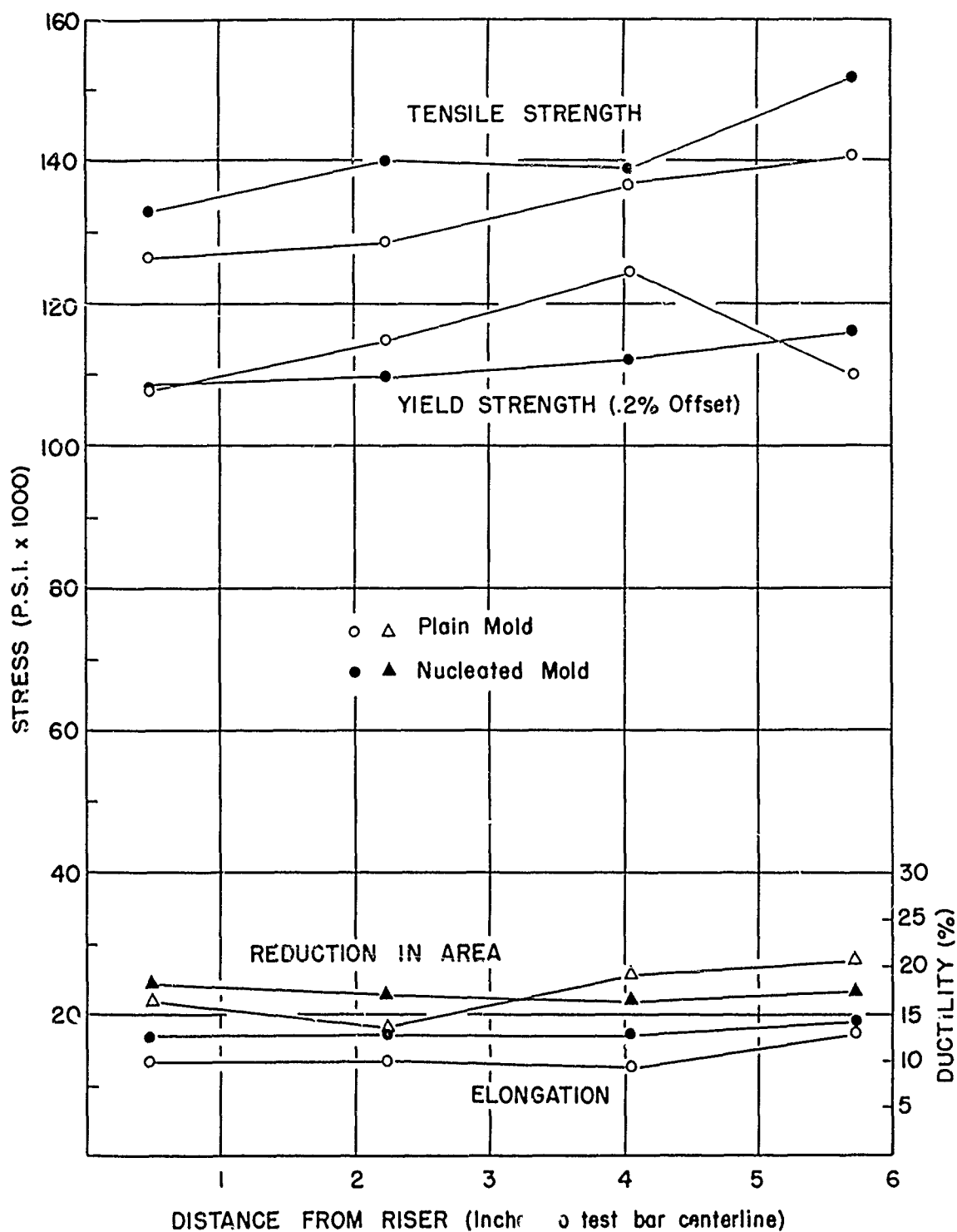
Figure 73

ROOM TEMPERATURE TENSILE PROPERTIES OF SOLUTION TREATED
INCO 713LC TEST BARS CUT FROM SIX-INCH LONG TAPERED PLATES

CASTING NUMBER 66-216-2

PARAMETER LEVELS ILLUSTRATED
POURING TEMPERATURE: LIQUIDUS PLUS 200°F
MOLD TEMPERATURE: RISERS PREHEATED
MOLD SURFACE: NUCLEATED AND PLAIN

-213-
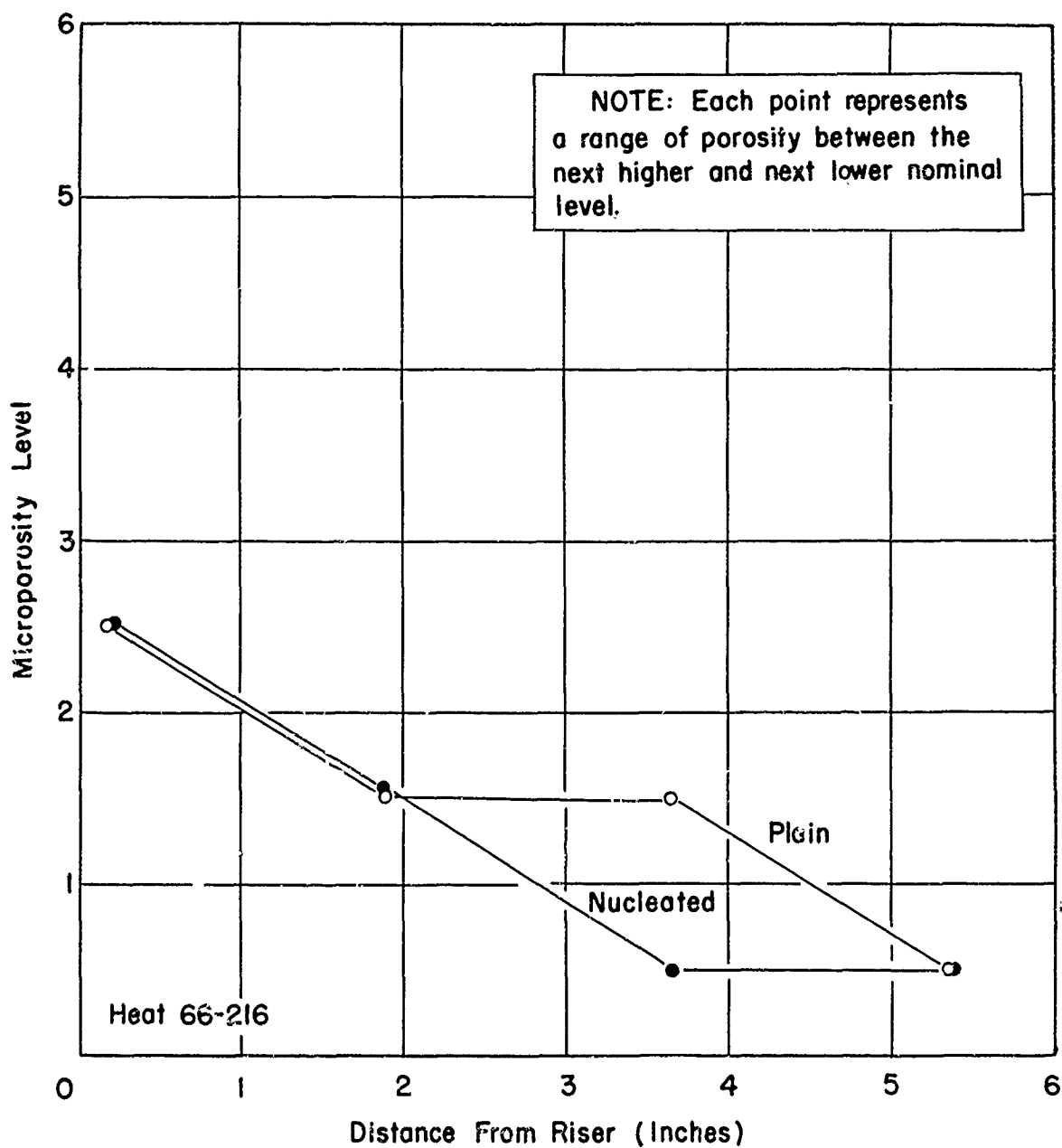
Figure 74

MICROPOROSITY LEVEL IN 6-INCH LONG INCO 713LC PLATES
CAST IN PLAIN AND NUCLEATED, PREHEATED CERAMIC
MOLDS AT 100°F SUPERHEAT

-214-

NOTE: Each point represents a range of porosity between the next higher and next lower nominal level.

Plain

Nucleated

Heat 66-216

Distance From Riser (Inches)
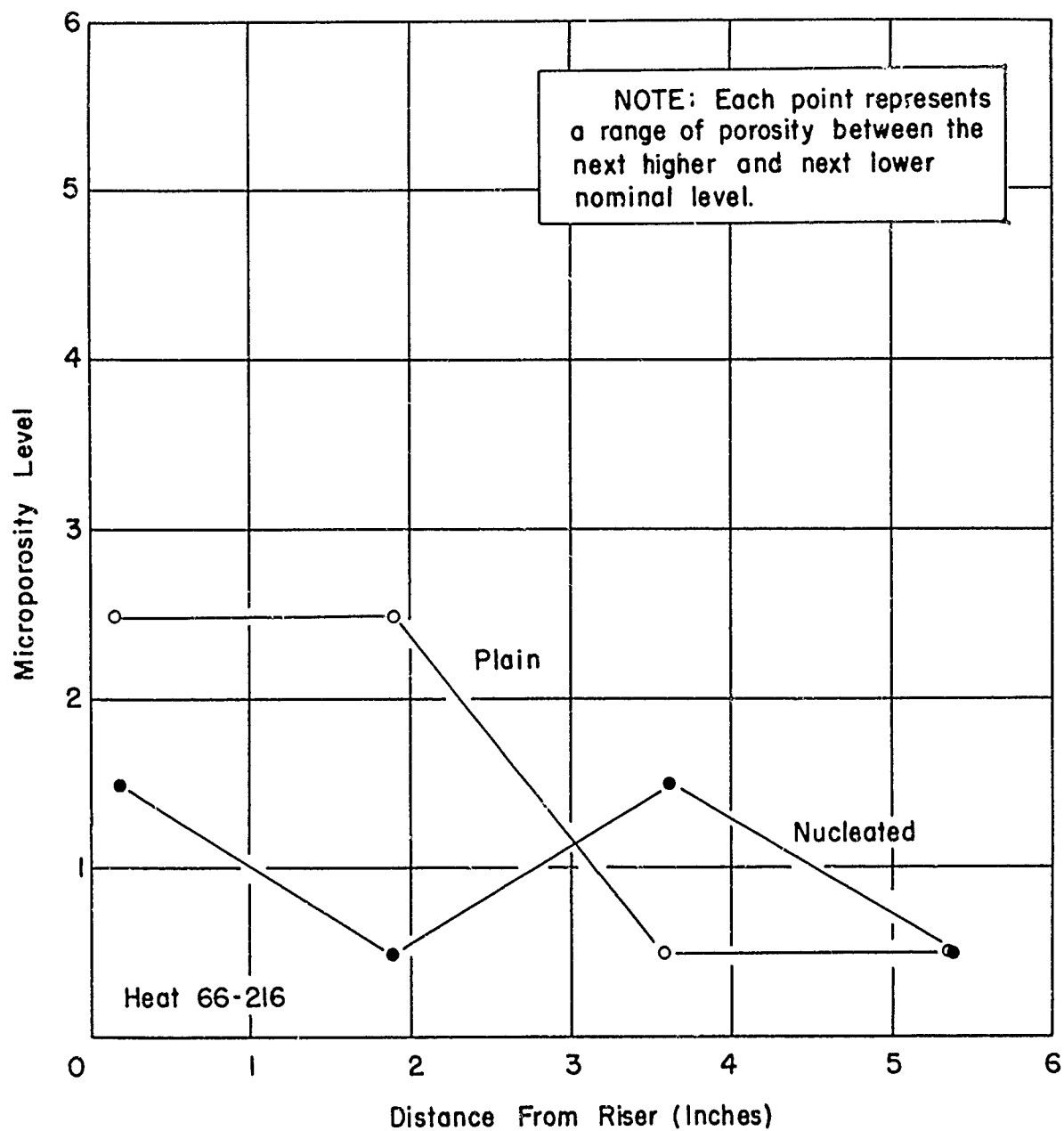
Figure 75

MICROPOROSITY LEVEL IN 6-INCH LONG INCO 713LC PLATES
CAST IN PLAIN AND NUCLEATED, PREHEATED CERAMIC
MOLDS AT 200°F SUPERHEAT
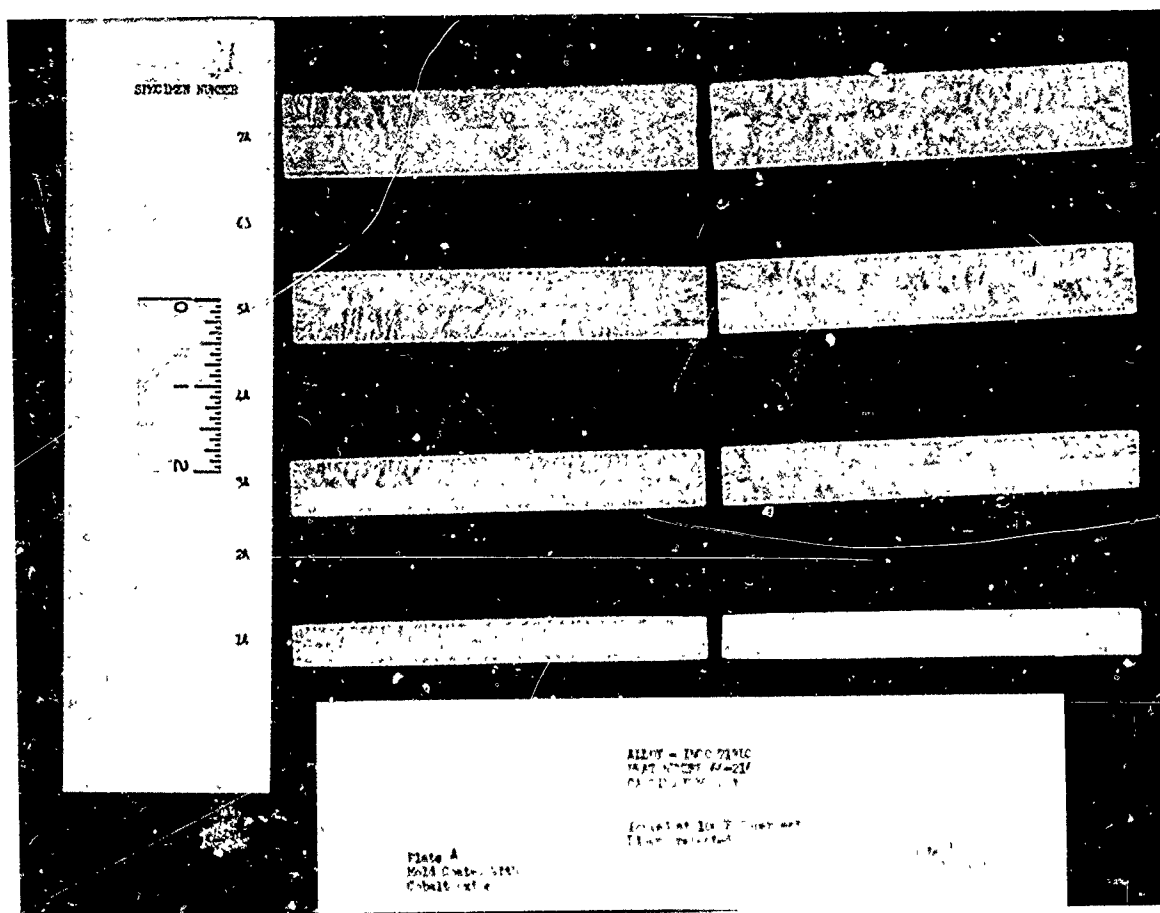
FIGURE 76

MACROETCHED RADIOGRAPHIC SPECIMENS
FROM 6-INCH LONG INCO 713LC
PLATES
CAST AT 100°F SUPERHEAT WITH
RISER CAVITIES PREHEATED

FIGURE 77

MACROETCHED RADIOGRAPHIC SPECIMENS
FROM 3-INCH LONG INCO 713LC
PLATES
CAST AT 100°F SUPERHEAT WITH
RISER CAVITIES PREHEATED
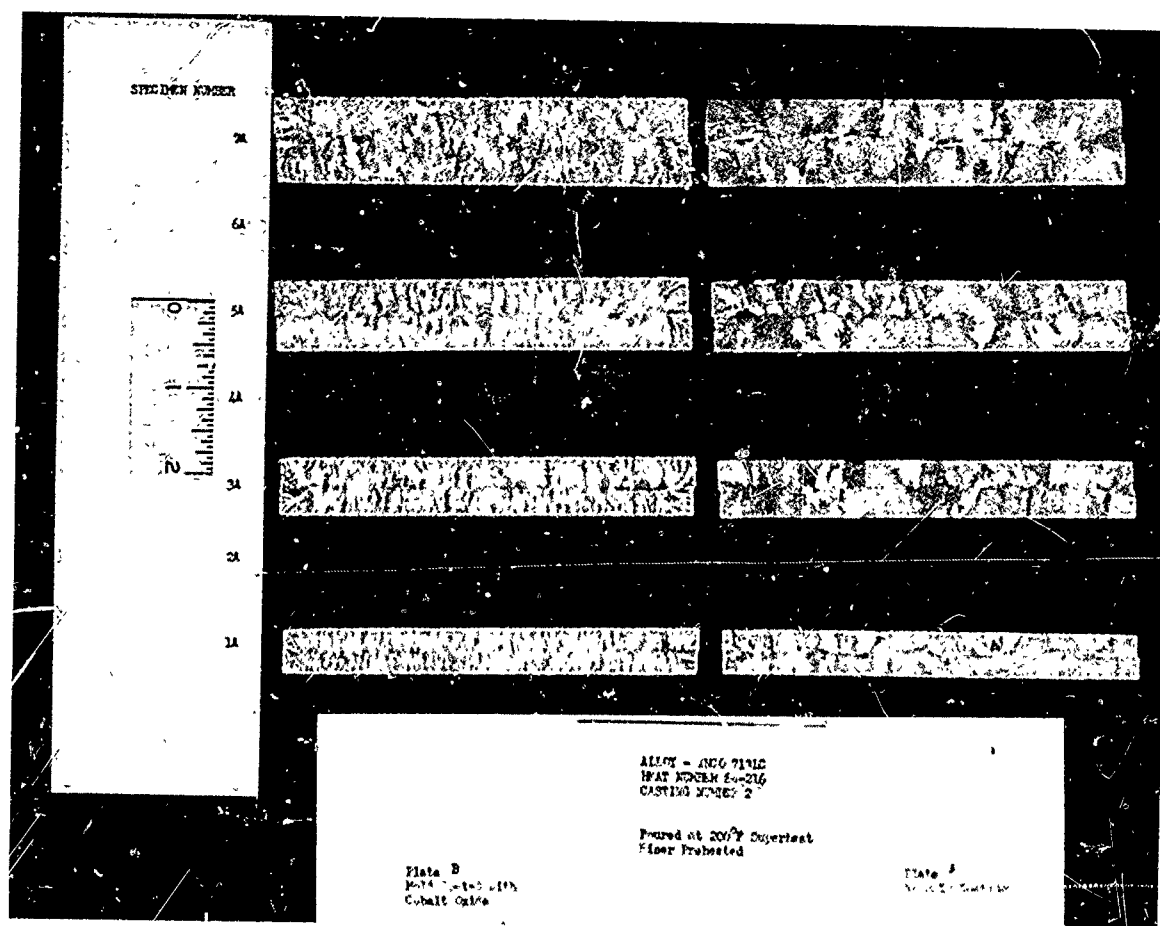
FIGURE 78

MACROETCHED RADIOGRAPHIC SPECIMENS
FROM 6-INCH LONG INCO 713LC
PLATES
CAST AT 200°F SUPERHEAT WITH
RISER CAVITIES PREHEATED

-218-
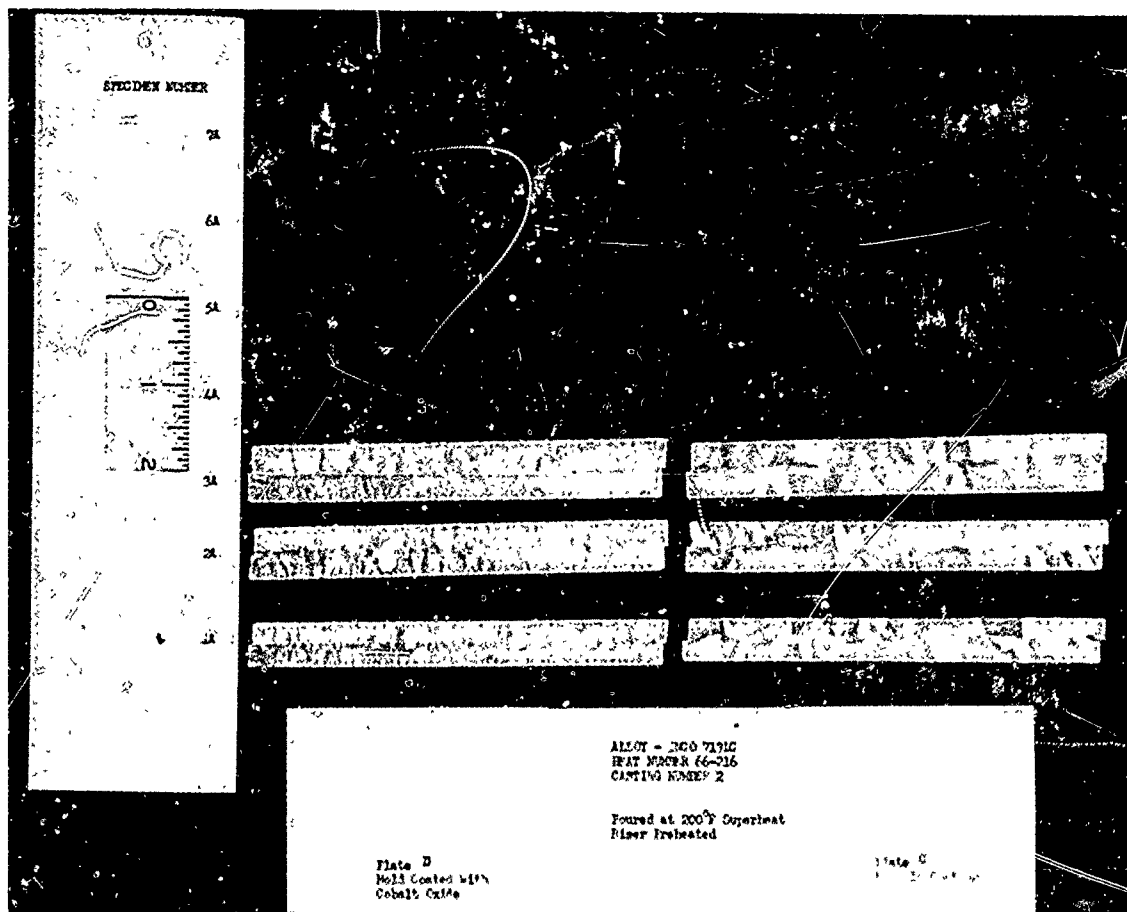
FIGURE 79

MACROETCHED RADIOGRAPHIC SPECIMENS
FROM 3-INCH LONG INCO 713LC
PLATES
CAST AT 200°F SUPERHEAT WITH
RISER CAVITIES PREHEATED
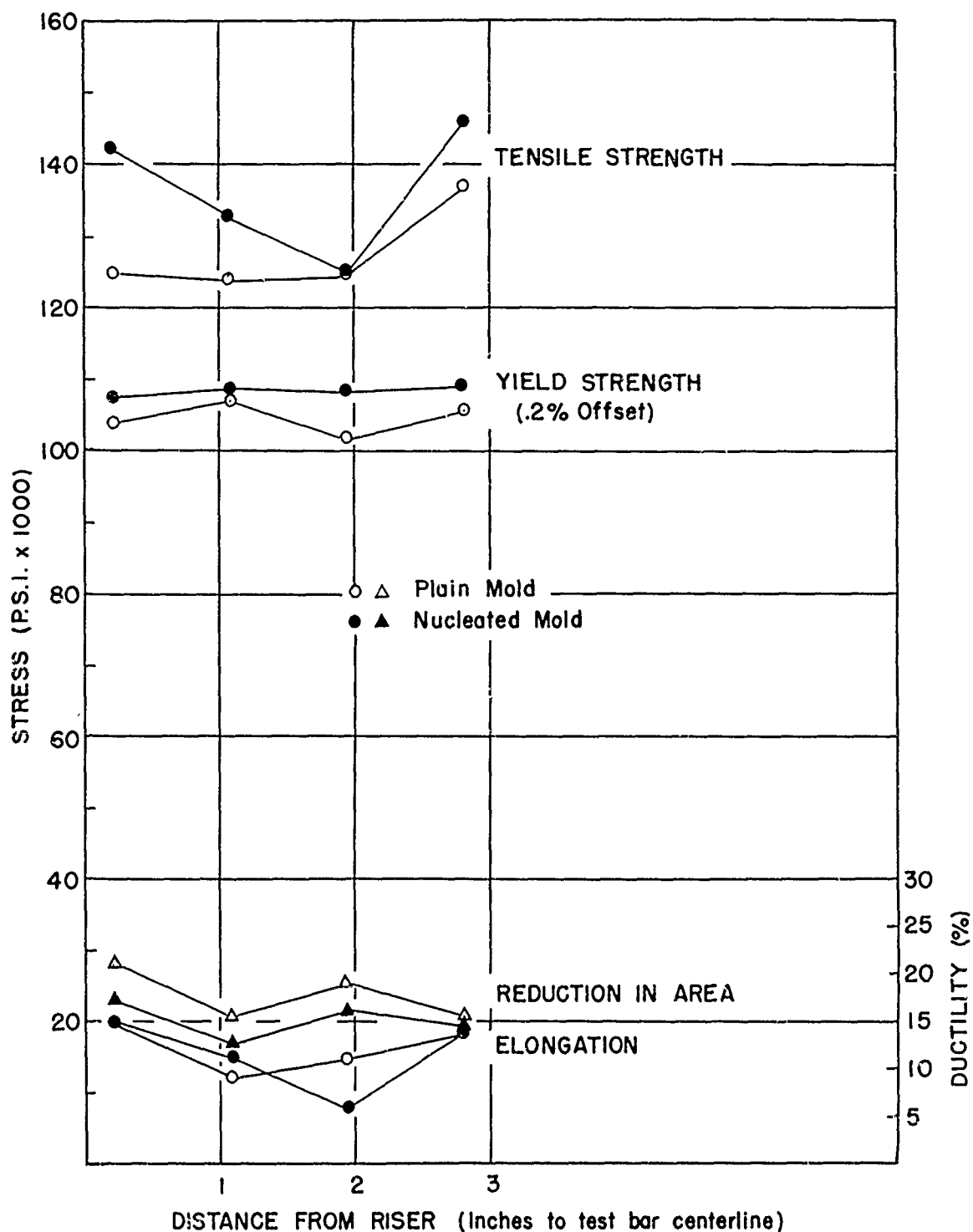
Figure 80

ROOM TEMPERATURE TENSILE PROPERTIES OF SOLUTION TREATED
INCO 713LC TEST BARS CUT FROM 3-INCH LONG TAPERED PLATES

CASTING NUMBER 66-267-1

PARAMETER LEVELS ILLUSTRATED
POURING TEMPERATURE: LIQUIDUS PLUS 100°F
MOLD TEMPERATURE: UNIFORMLY AT AMBIENT TEMP.
MOLD SURFACE: NUCLEATED AND PLAIN   -220-
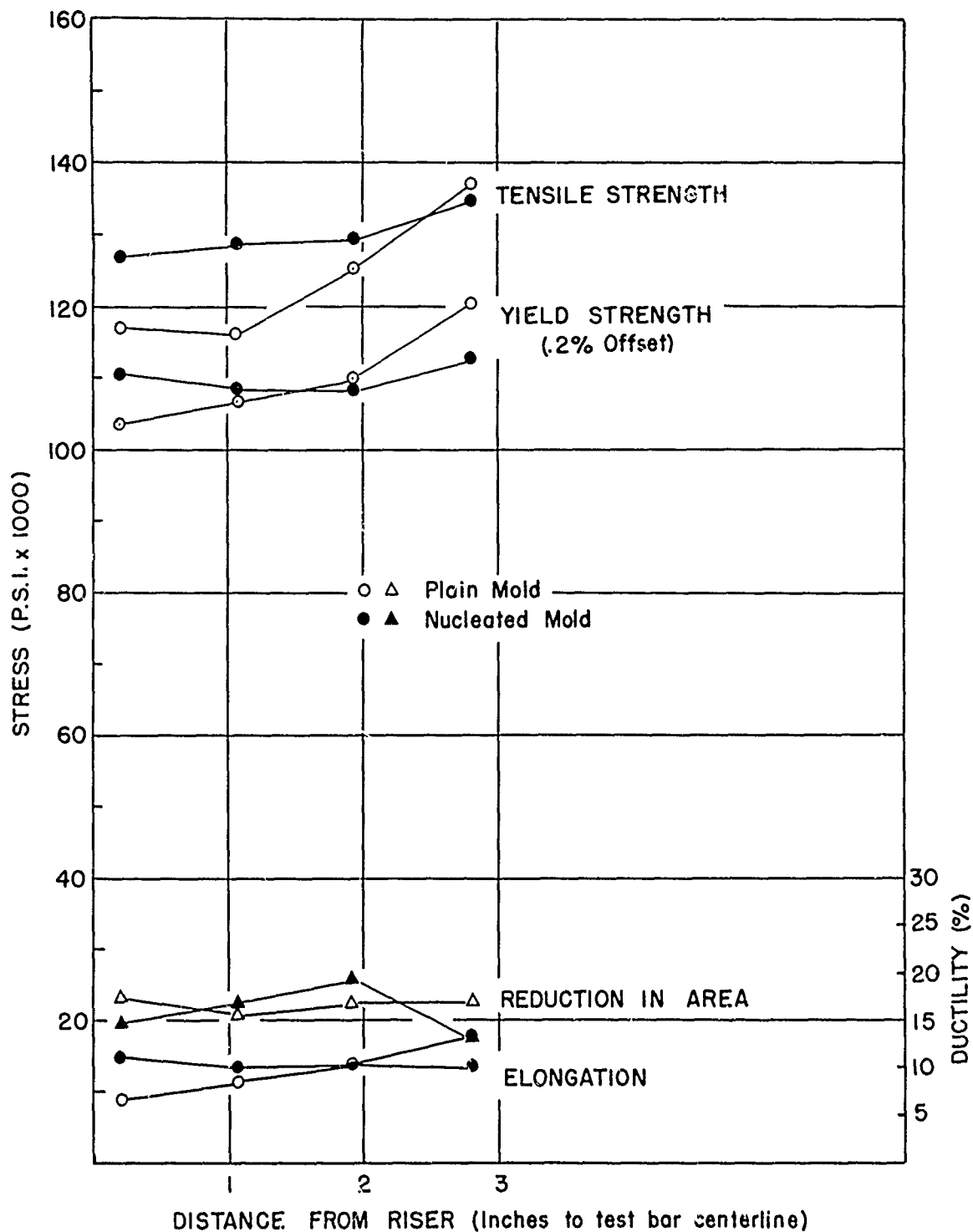
Figure 81

ROOM TEMPERATURE TENSILE PROPERTIES OF SOLUTION TREATED
INCO 713LC TEST BARS CUT FROM 3-INCH LONG TAPERED PLATES

CASTING NUMBER 66-267-2

PARAMETER LEVELS ILLUSTRATED
POURING TEMPERATURE: LIQUIDUS PLUS 200°F
MOLD TEMPERATURE: UNIFORMLY AT AMBIENT TEMP.
MOLD SURFACE: NUCLEATED AND PLAIN
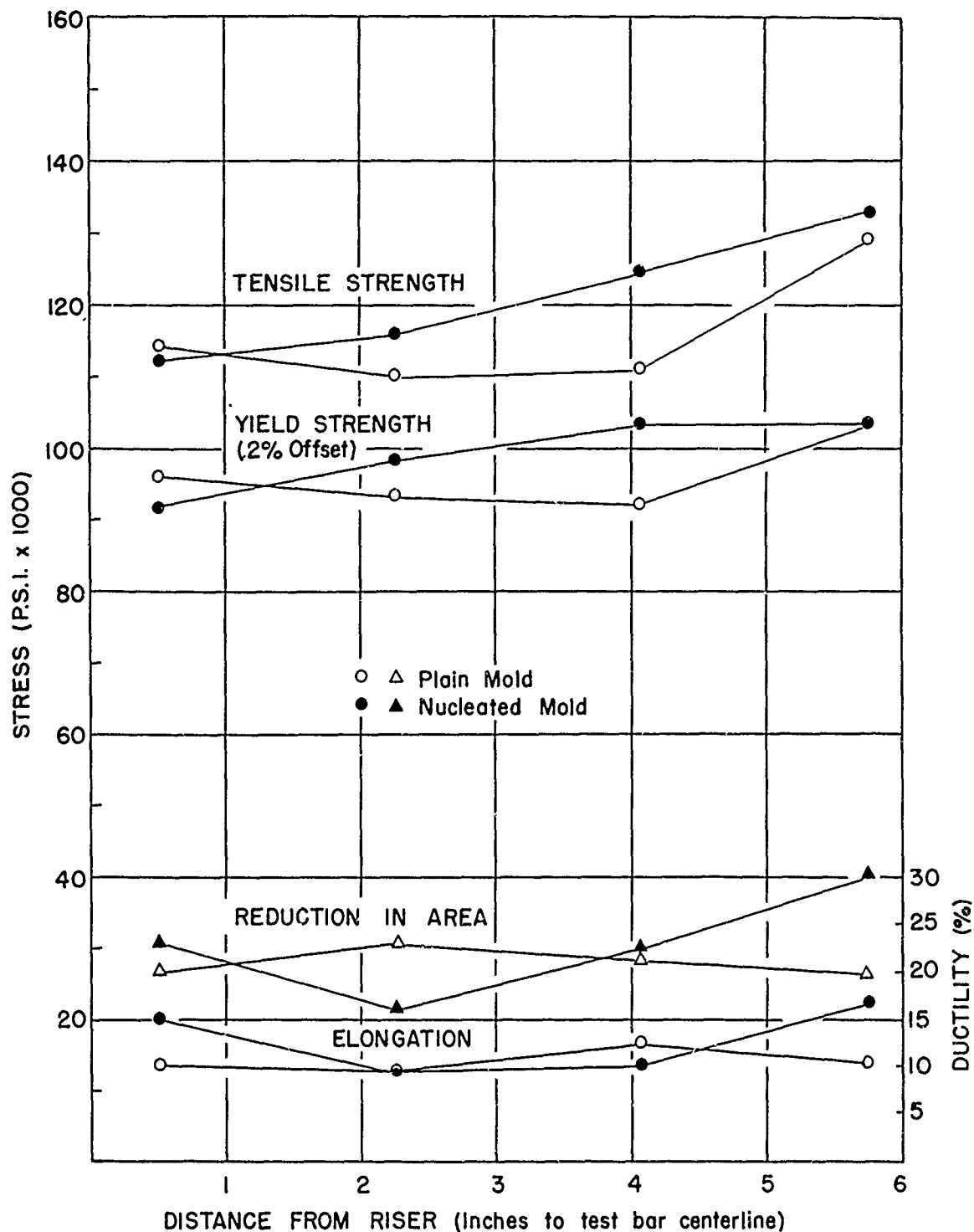
Figure 82

1200°F TENSILE PROPERTIES OF INCO 713LC TEST BARS
CUT FROM 6-INCH LONG TAPERED PLATES

CASTING NUMBER 66-267-1

PARAMETER LEVELS ILLUSTRATED
POURING TEMPERATURE: LIQUIDUS PLUS 100°F
MOLD TEMPERATURE: UNIFORMLY AT AMBIENT TEMP.
MOLD SURFACE: NUCLEATED AND PLAIN
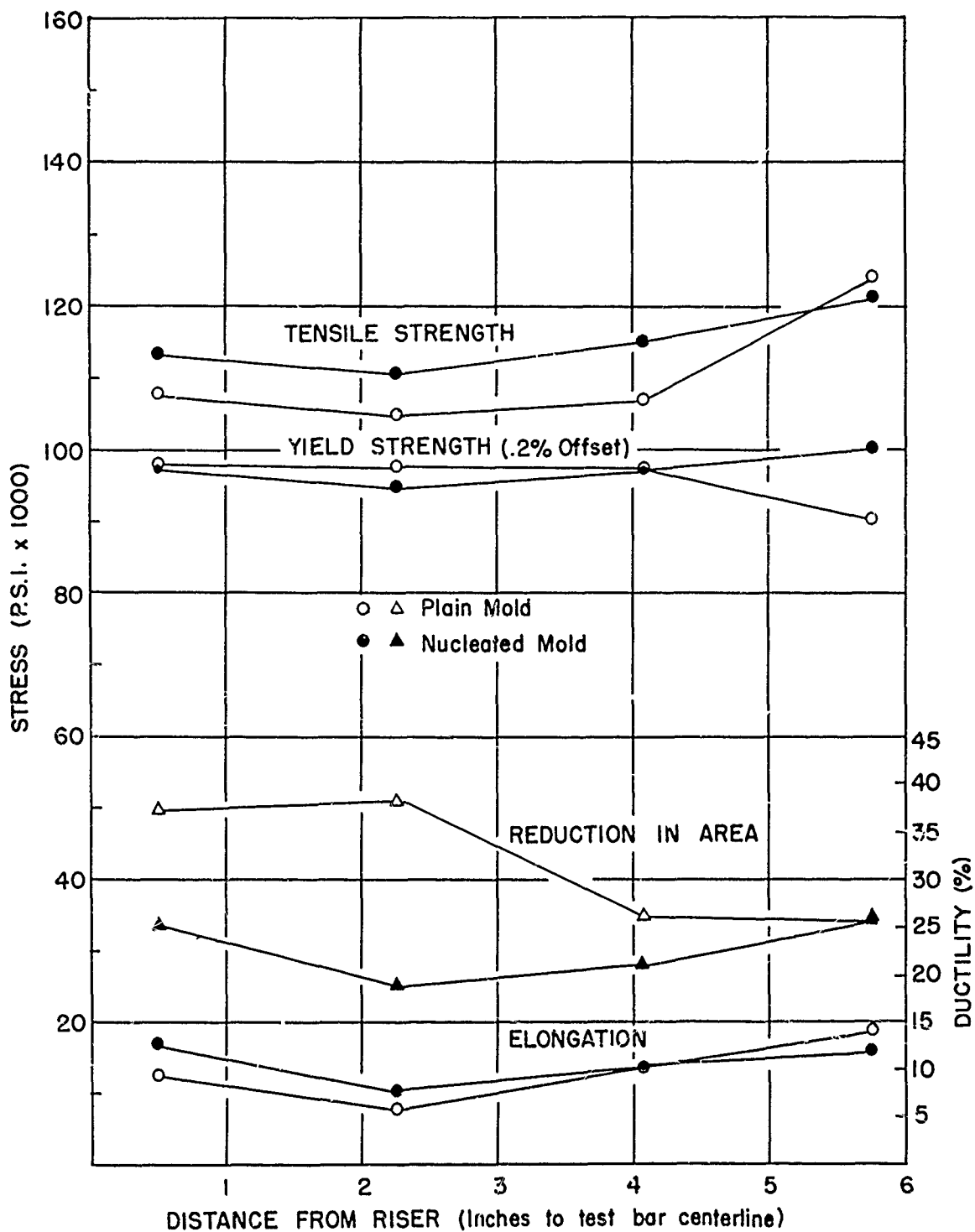
Figure 83

1200°F TENSILE PROPERTIES OF INCO 713LC TEST BARS
CUT FROM 6-INCH LONG TAPERED PLATES

CASTING NUMBER 66-267-2

PARAMETER LEVELS ILLUSTRATED
POURING TEMPERATURE: LIQUIDUS PLUS 200°F
MOLD TEMPERATURE: UNIFORMLY AT AMBIENT TEMP.
MOLD SURFACE: PLAIN AND NUCLEATED

-223-
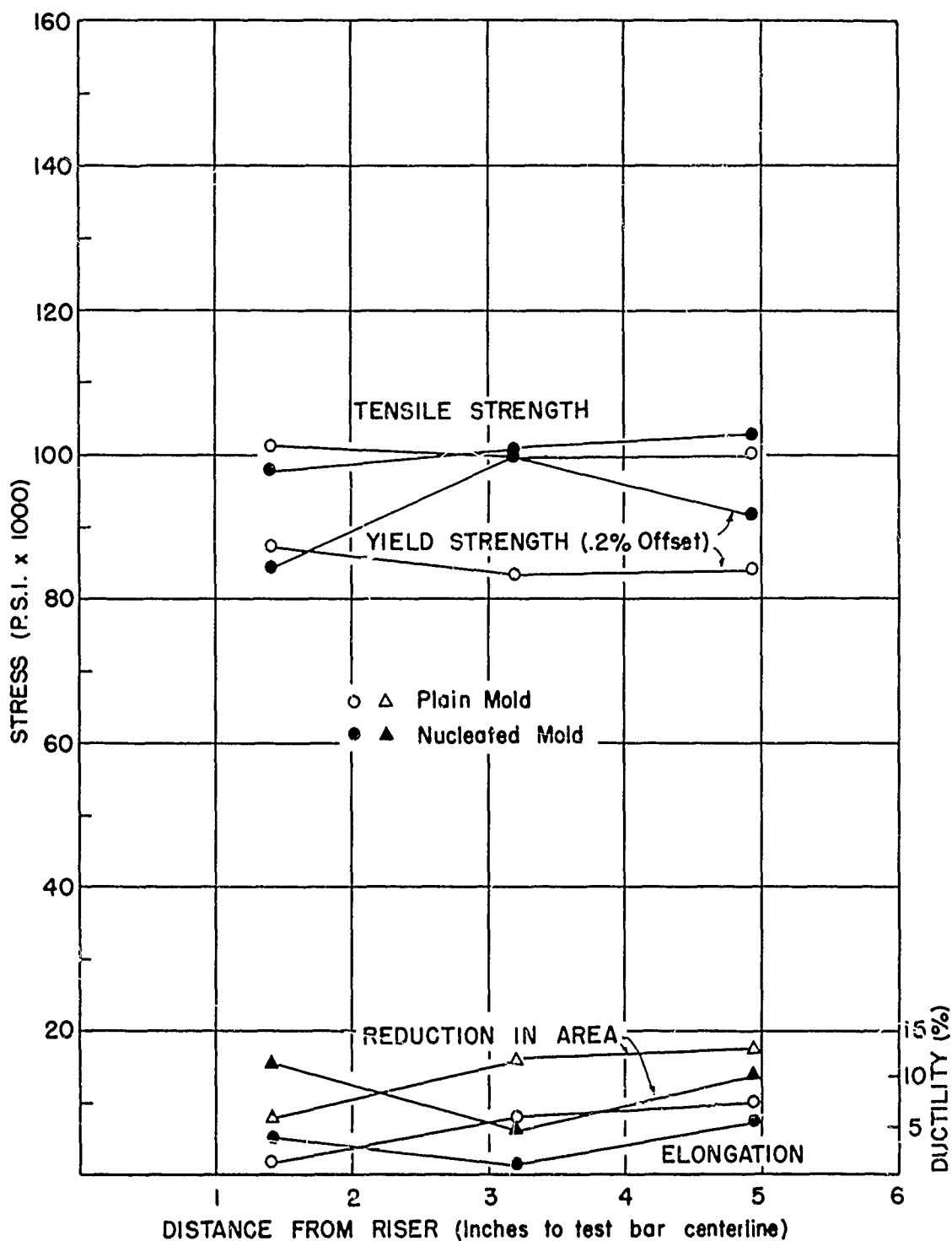
Figure 84

1600°F TENSILE PROPERTIES OF INCO 713LC TEST BARS
CUT FROM 6-INCH LONG TAPERED PLATES

CASTING NUMBER 66-267-1

PARAMETER LEVELS ILLUSTRATED
POURING TEMPERATURE: LIQUIDUS PLUS 100°F
MOLD TEMPERATURE: UNIFORMLY AT AMBIENT TEMP.
MOLD SURFACE: PLAIN AND NUCLEATED   -224-
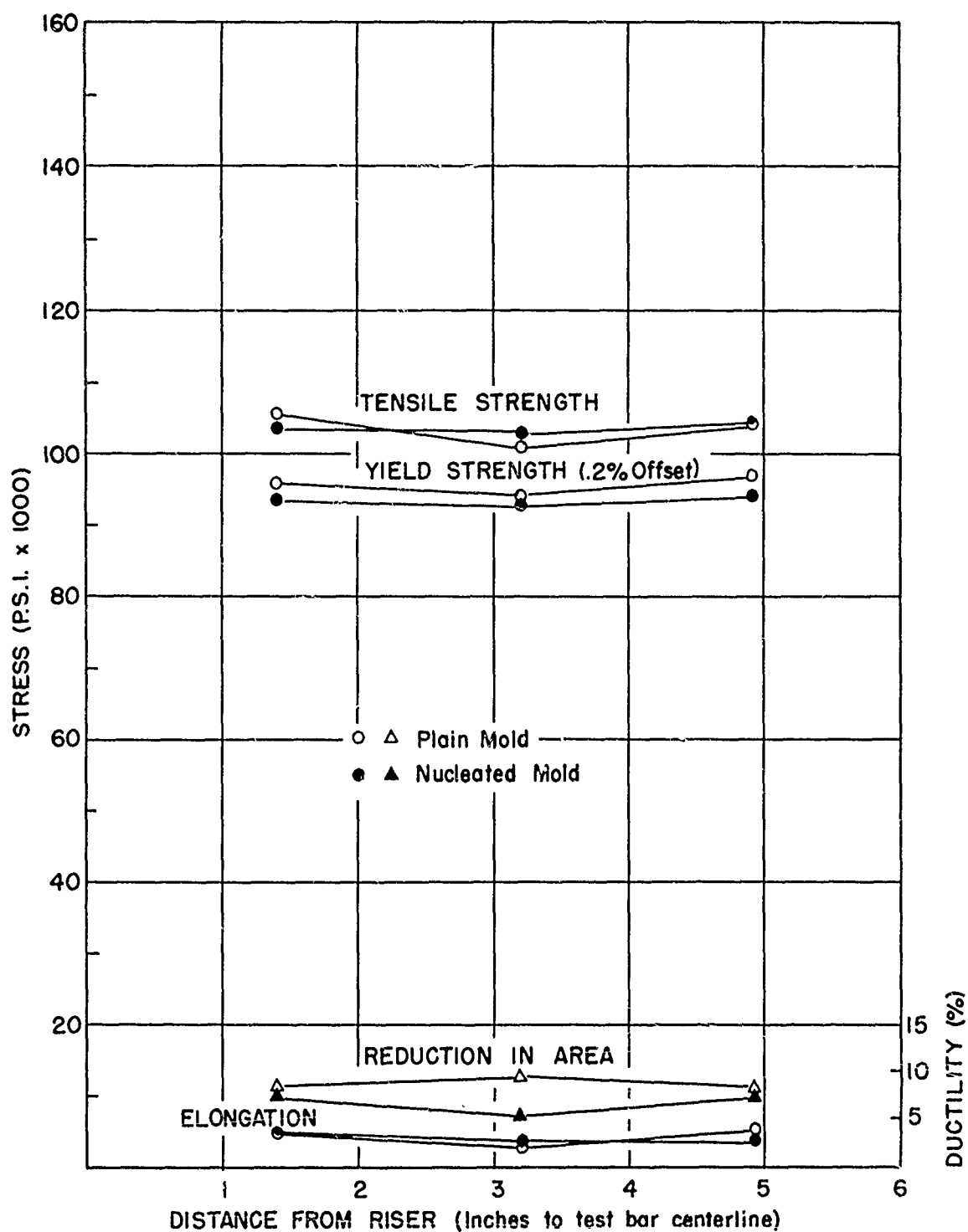
Figure 85

1600°F TENSILE PROPERTIES OF INCO 713LC TEST BARS
CUT FROM 6-INCH LONG TAPERED PLATES

CASTING NUMBER 66-267-2

PARAMETER LEVELS ILLUSTRATED
POURING TEMPERATURE: LIQUIDUS PLUS 200°F
MOLD TEMPERATURE: UNIFORMLY AT AMBIENT TEMP.
MOLD SURFACE: PLAIN AND NUCLEATED

-225-
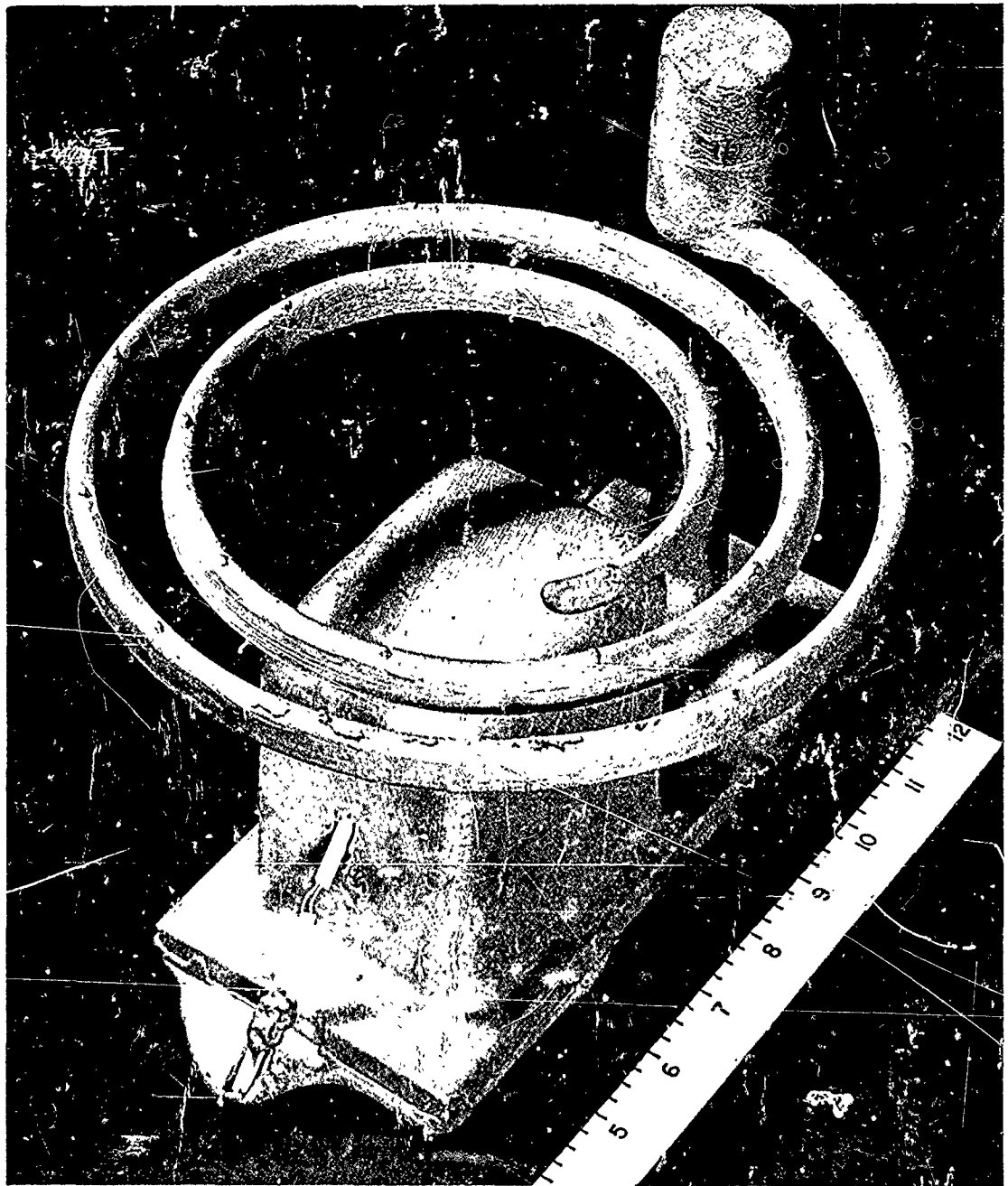
FIGURE 86

FLUIDITY SPIRAL CASTING

The thermocouple seen protruding from the pouring
basin is used to determine the pouring temperature and
freezing temperature of the spiral. Fluidity values are
determined by the length of the cast spiral.

Figure 87

Ceramic Octabar Mold
With Thermocouple in Position
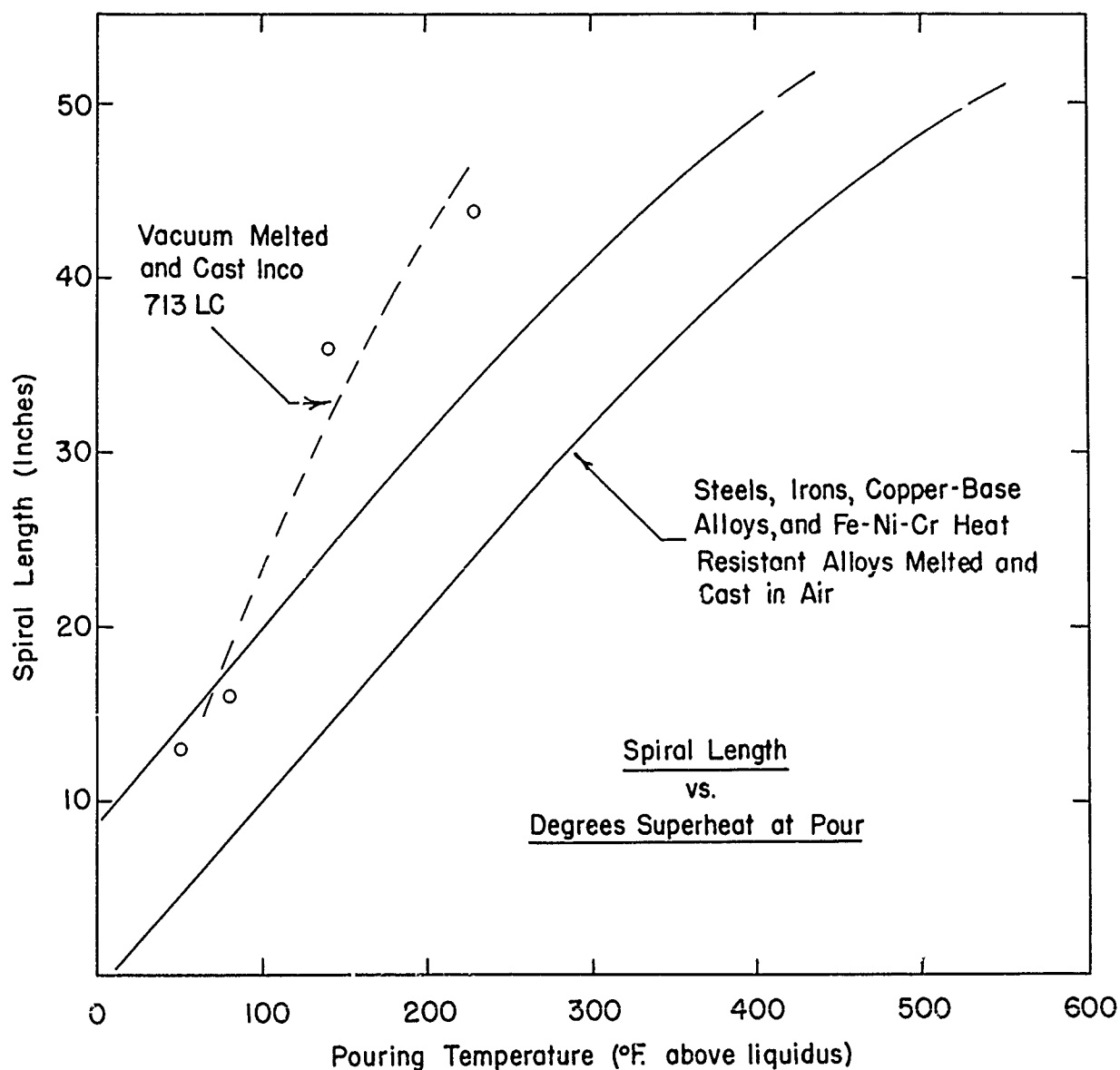
FIGURE 88

RELATIVE FLUIDITY OF VACUUM MELTED AND CAST
INCO 713LC
COMPARED   TO
SEVERAL AIR MELTED AND CAST ALLOYS

The band of data shown for the air-melted alloys is
based upon approximately 100 data points in the work of
Schaefer and Mott.(72)
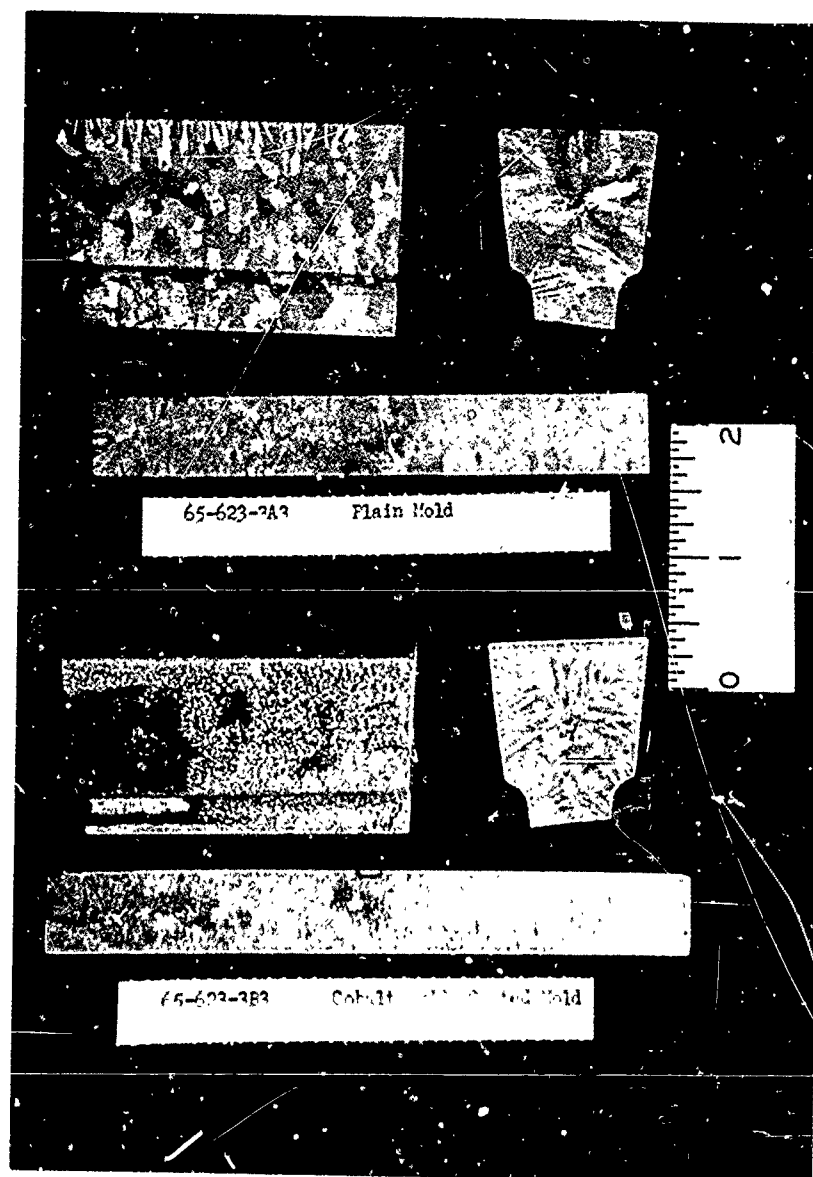
Figure 89

Surface and Cross Section Grain Size of
Nucleated and Non-Nucleated Inco 713LC.
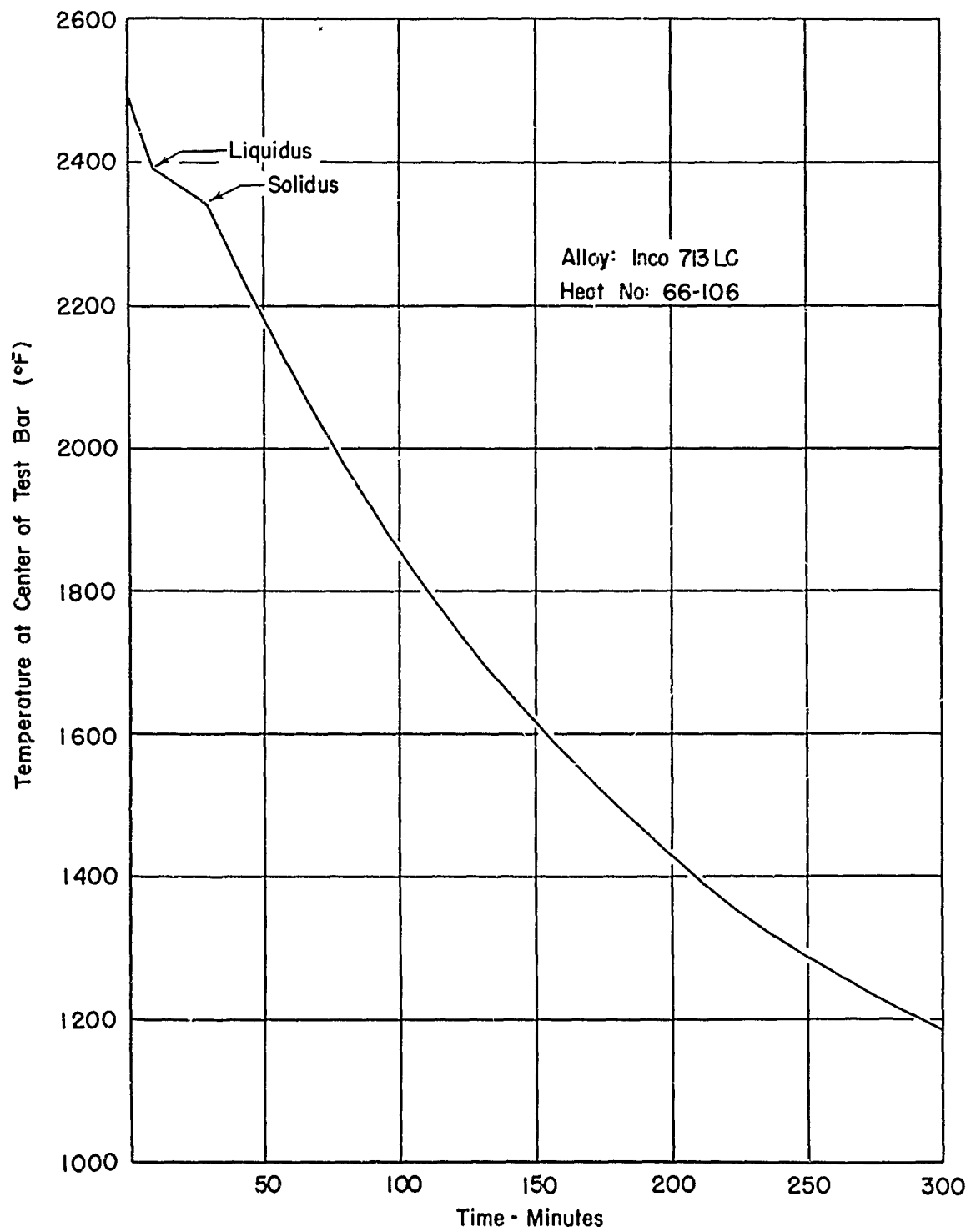
Figure 89a

COOLING CURVE FOR 1" SECTION
TEST BAR - OCTABAR CASTING

-230-

Figure 90

UNNUCLEATED OCTABAR   Specimen No. 66-106-2G

UNNUCLEATED BASIC TEST BAR SECTION   Specimen No. 65-623-2A3

NUCLEATED OCTABAR (1" SECTION)   Specimen No. 66-106-2A

NUCLEATED BASIC TEST BAR SECTION (½" SECTION)   Specimen No. 65-623-2B3

ALLOY INCO 713 LC

COMPARISON OF CAST GRAIN SIZE IN 1" and ½" SECTIONS
POURED AT 200°F SUPERHEAT
INTO COLD CERAMIC MOLDS WITH AND
WITHOUT NUCLEATION

Figure 91

-232-
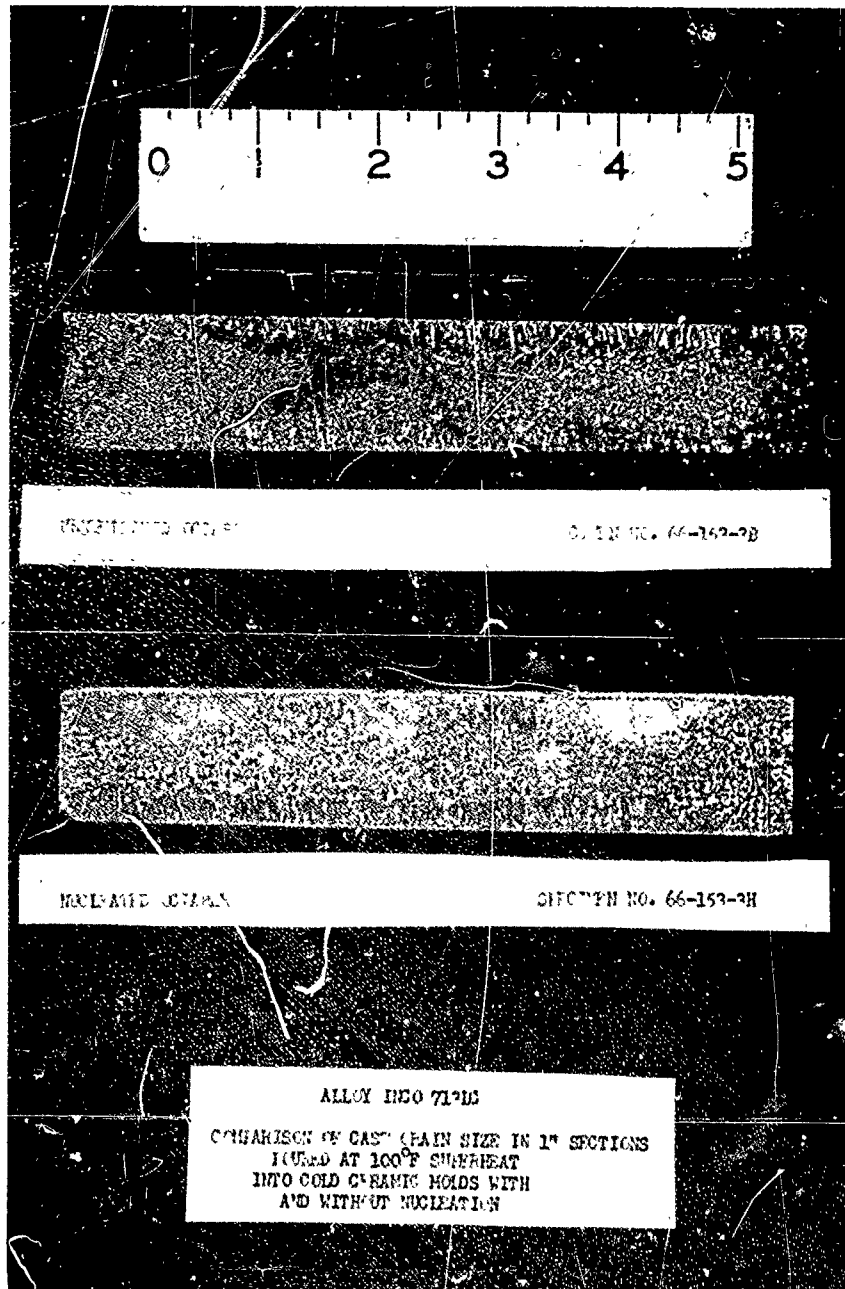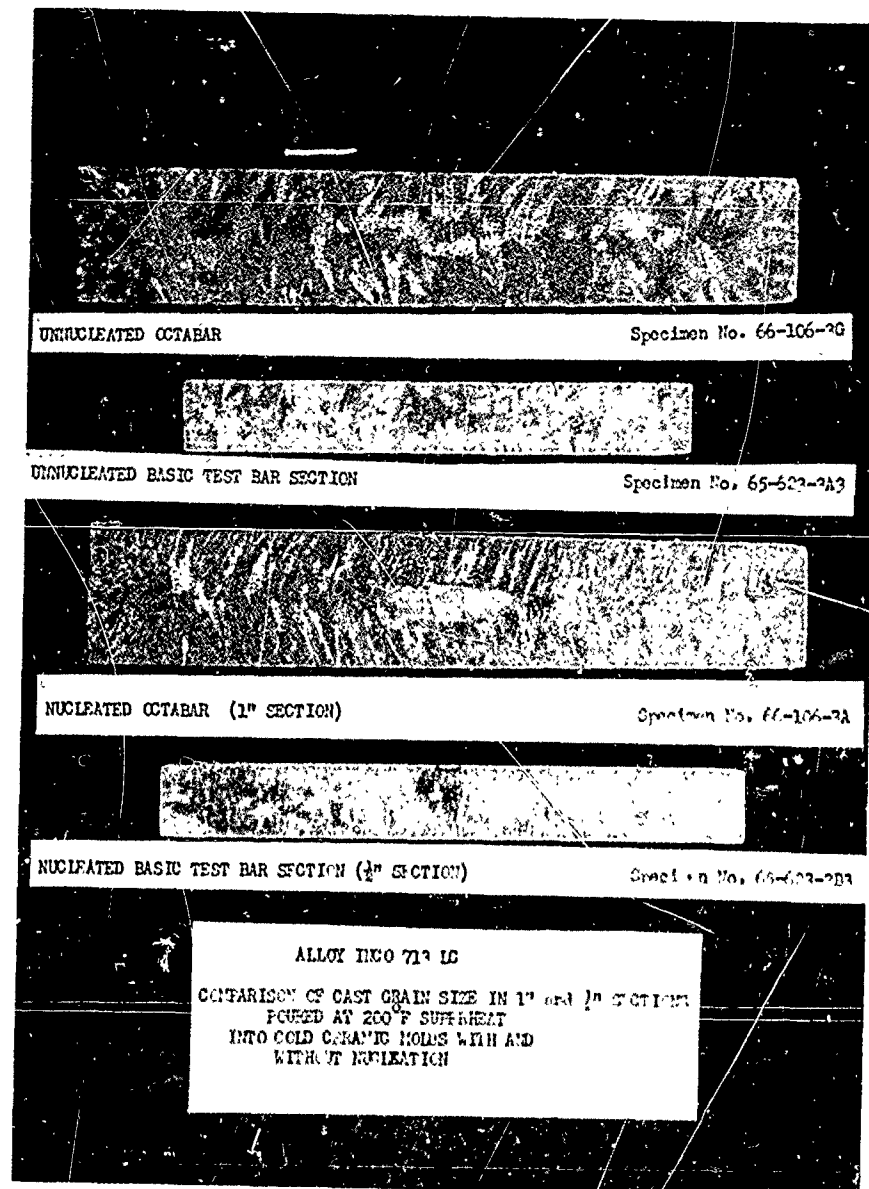
Figure 92

CONNECTOR YOKE CASTING
INCO 713 LC

Gross Weight: 500 lb.

End Product: One slotted connector yoke.

Figure 93

MACROETCHED CROSS SECTION OF 5 1/4-INCH THICK
CONNECTOR YOKE CAST IN INCO 713 LC

Note easily visible dendritic growth pattern within each "grain".
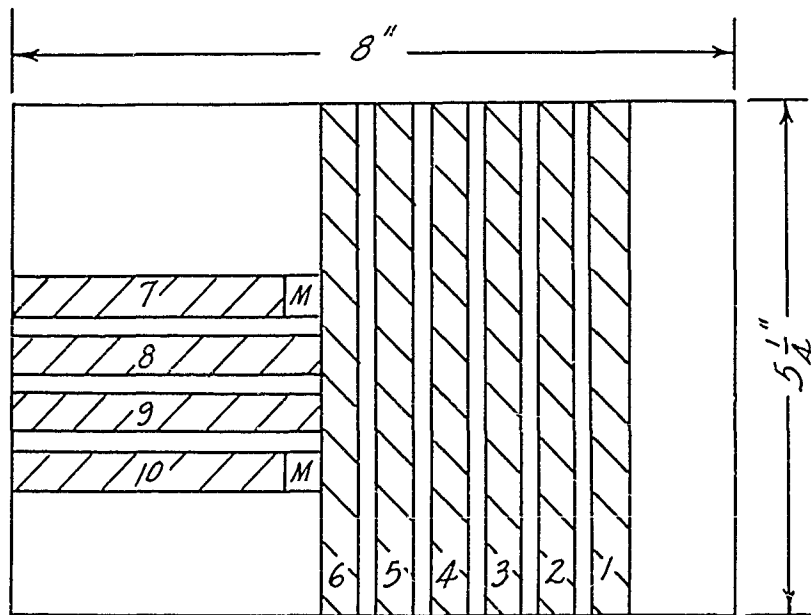
Figure 94

LOCATION OF TEST SPECIMENS
IN
HEAVY SECTION SLICE

Room temperature tensile tests	1, 3, 5, 8
Charpy impact tests, R.T.	7, 10
Creep-Rupture 1800°F - 22,000 psi	2, 4, 6, 9

Figure 95

MICROSTRUCTURE OF CAST INCO 713LC
AT CENTER OF 5 1/4-INCH SECTION-
UNETCHED.
ORIGINAL MAGNIFICATION: 100X, INCREASED
1.5 X DURING REPRODUCTION

Microporosity is shown selectively and is <u>not</u>
representative of the typical area at 100X.

Figure 96

GRAIN REFINEMENT OF INCO 713 LC BY
LESS COSTLY GRADES OF COBALT OXIDE POWDERS

Mix 1 – 100 grams ethyl silicate + 100 grams alcohol + 40 grams
"technical grade" CoO
Mix 2 – same, but with African Metals "gray" CoO
Mix 3 – same, but with African Metals "black" CoO
Mix 4 – same, but with African Metals "Metallurgical Grade" CoO

Test bar mold cavities brushed with above mixes prior
to final firing. Each cross section is shown beside "control"
section cast in uncoated mold cavity.
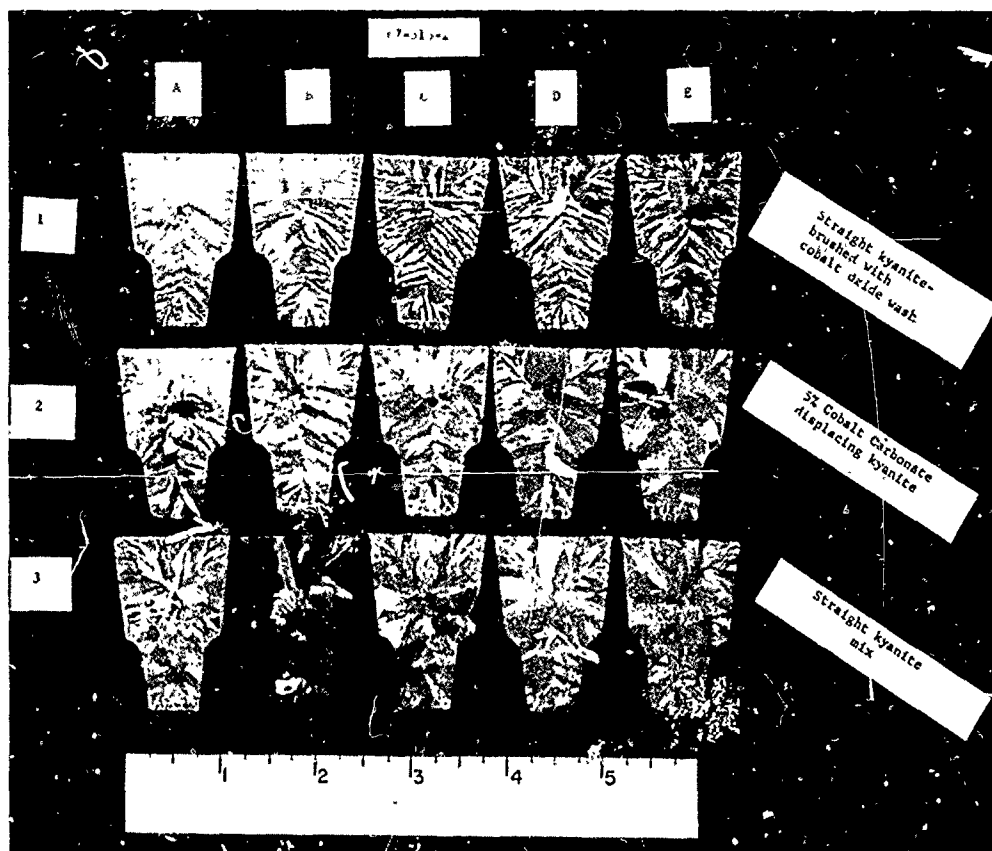
Figure 97

LACK OF GRAIN REFINEMENT OF INCO 713 LC
BY OXIDIZED COBALT CARBONATE
MACROETCHED TEST BAR CROSS SECTIONS

Top row: Mold brushed with ethyl silicate-alcohol-cobalt carbonate slurry before firing (control).

Center row: 5% cobalt carbonate blended into slurry.

Bottom row: No grain refining additives (control).
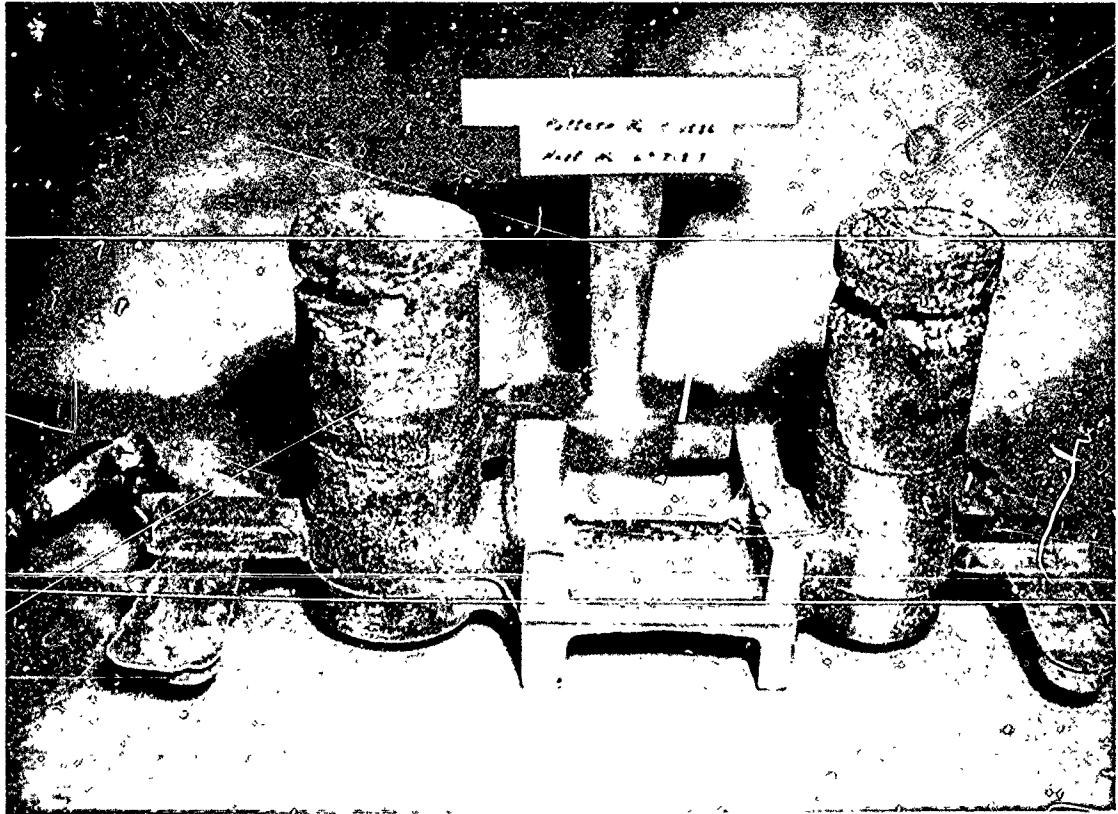
Figure 98

SMALL SECTION OF FIN BEAM CAST IN
AIR MELTED HEAT RESISTANT ALLOY

Note: Tapered sprue
        Sprue well
        Runners in drag, gates in cope
        Runner extensions

    The casting shown was poured at insufficient super-
heat, resulting in surface "folds" or cold shuts. The unusual
riser shrinkage is due to the exothermic riser sl.)ve.
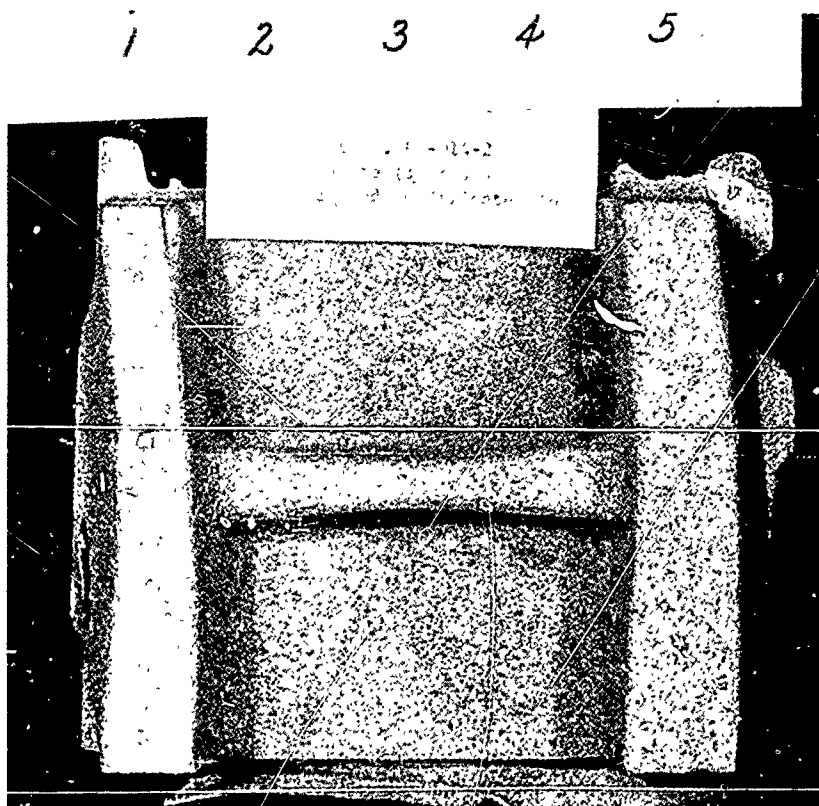
Figure 99

SURFACE FINISH OF
CASTING 68-014-2
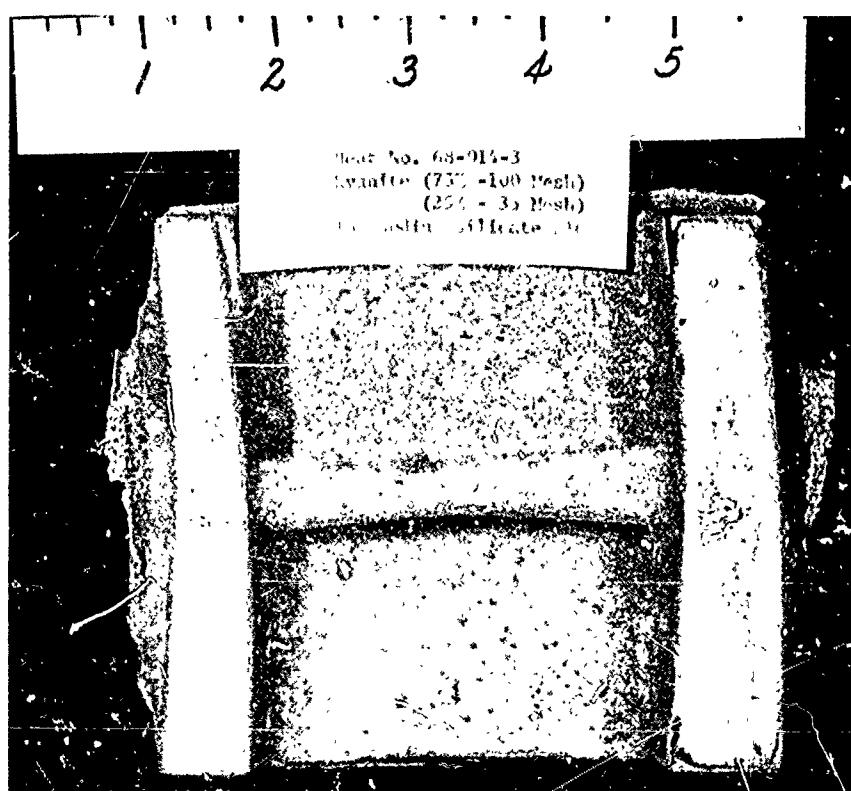
Figure 100

SURFACE FINISH OF
CASTING 68-014-3
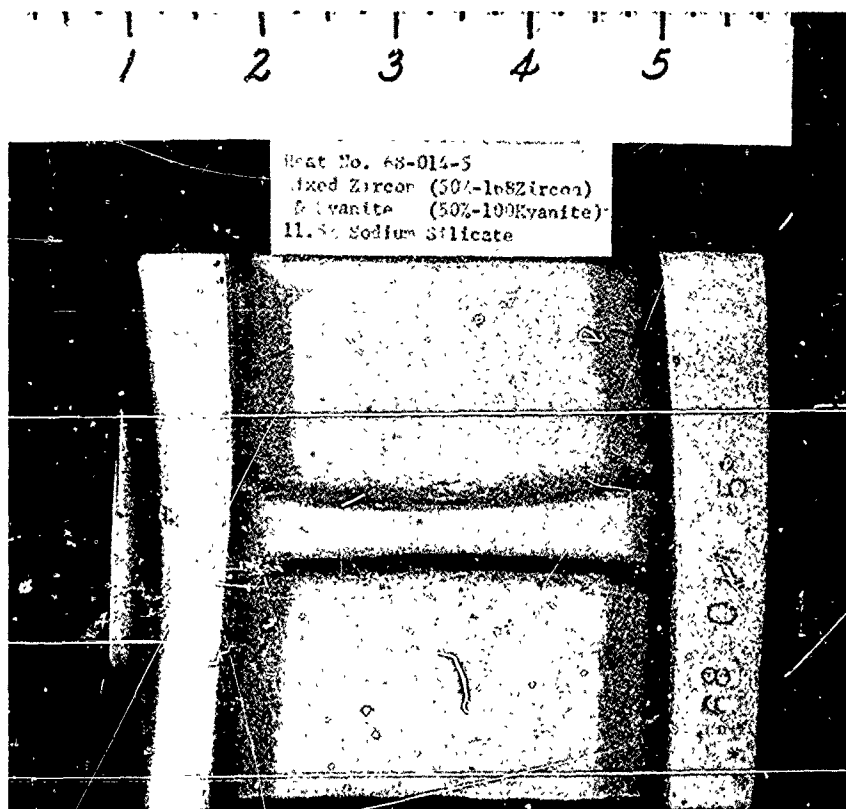
Figure 101

SURFACE FINISH OF
CASTING 68-014-5
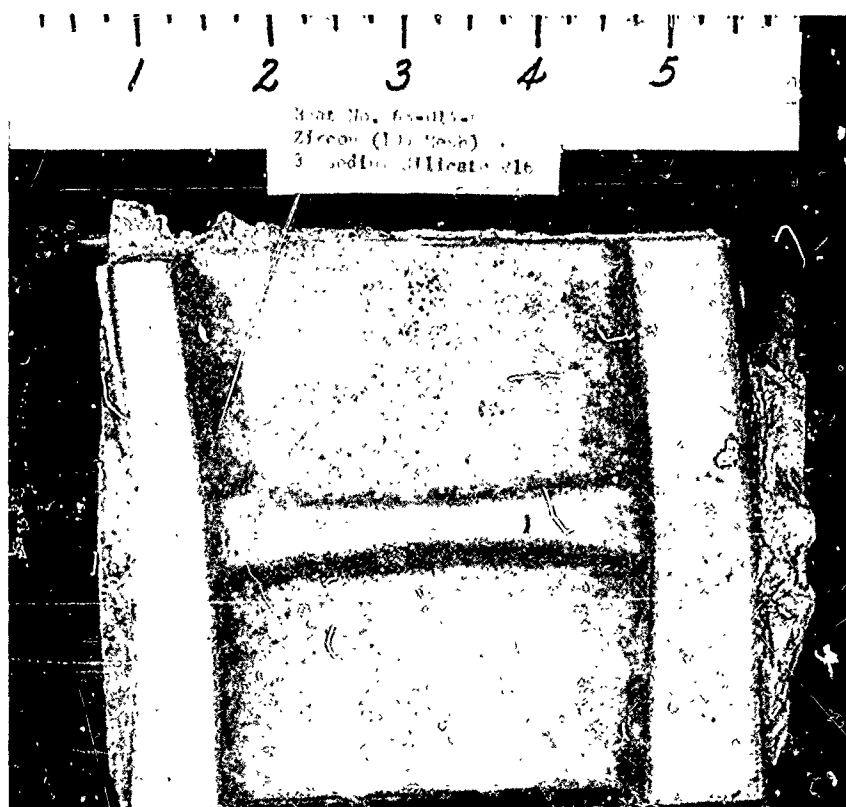
Figure 102

SURFACE FINISH OF
CASTING 68-014-6

-241-
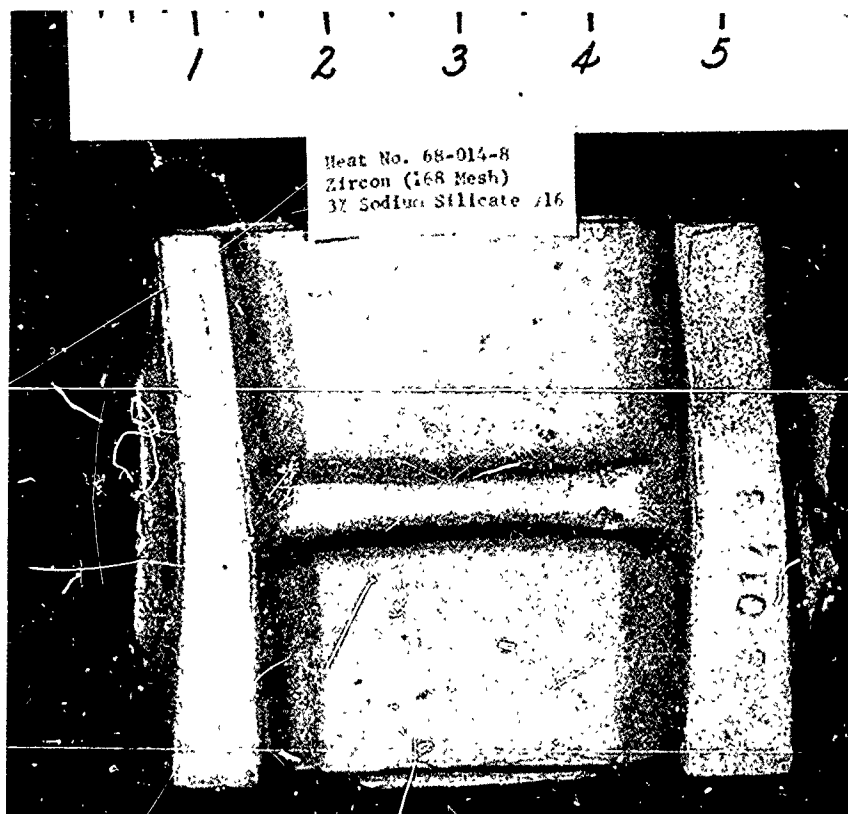
Figure 103

SURFACE FINISH OF
CASTING 68-014-8
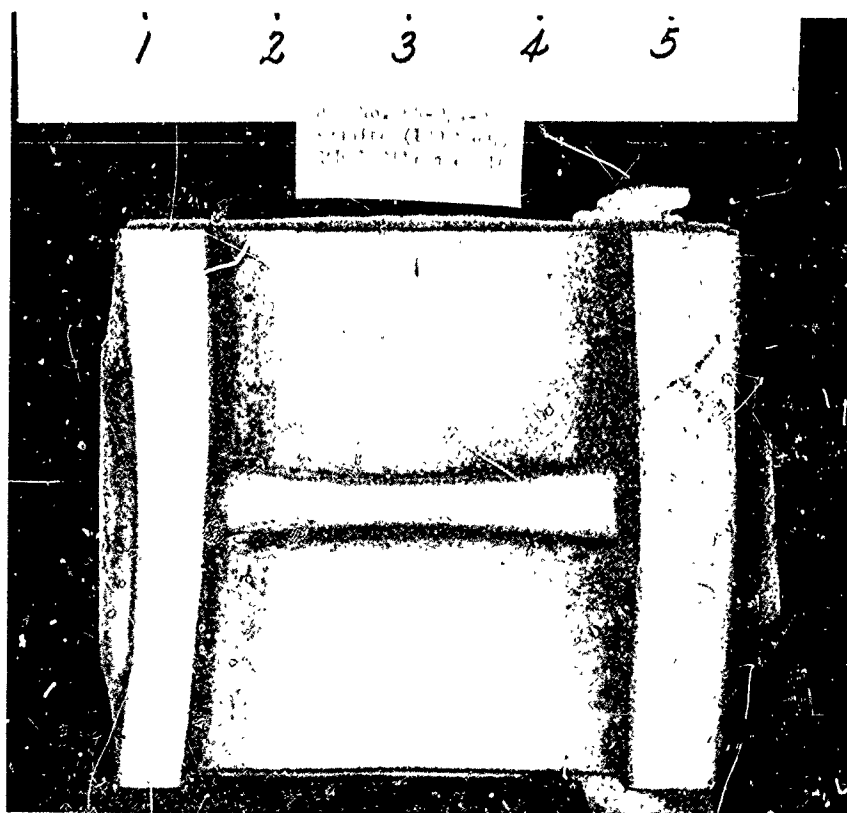
Figure 104

SURFACE FINISH OF
CASTING 68-014-9
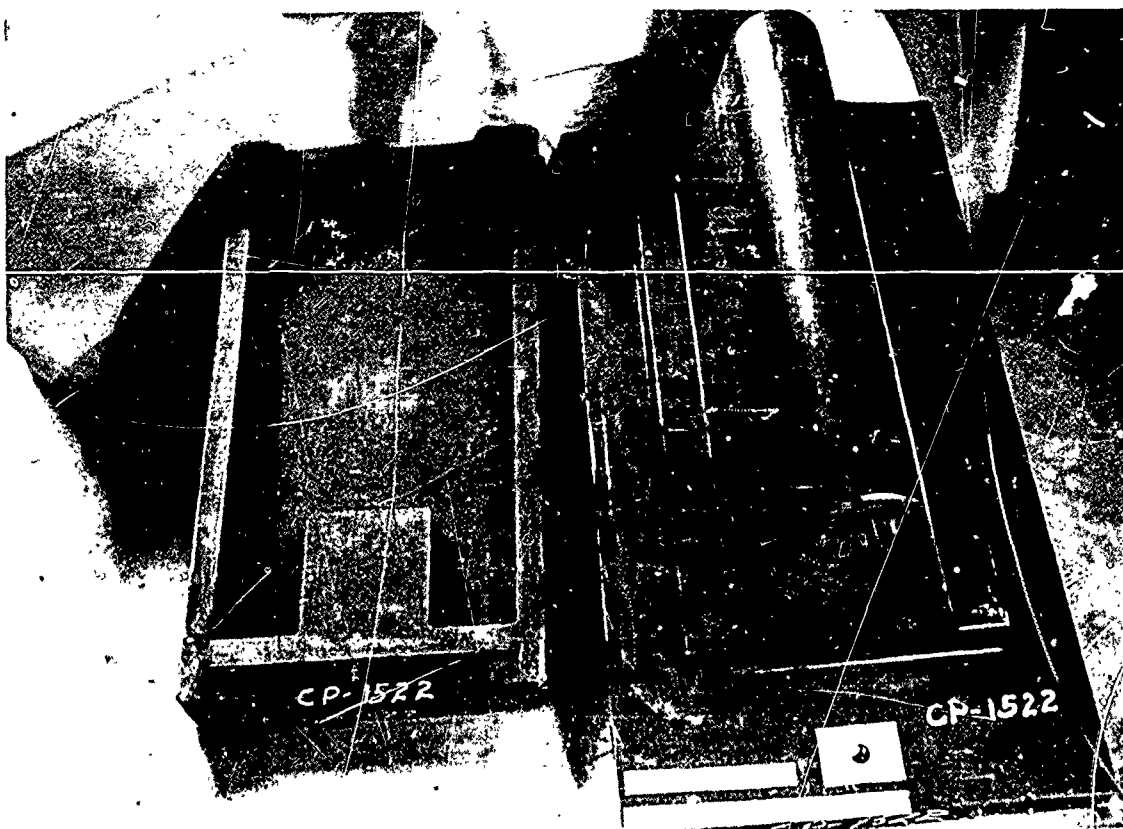
Figure 105

PATTERN EQUIPMENT - WEDGE BAR C-1522

Left: Core box for exothermic cover ccre.

Right: Pattern with recess for cover core.
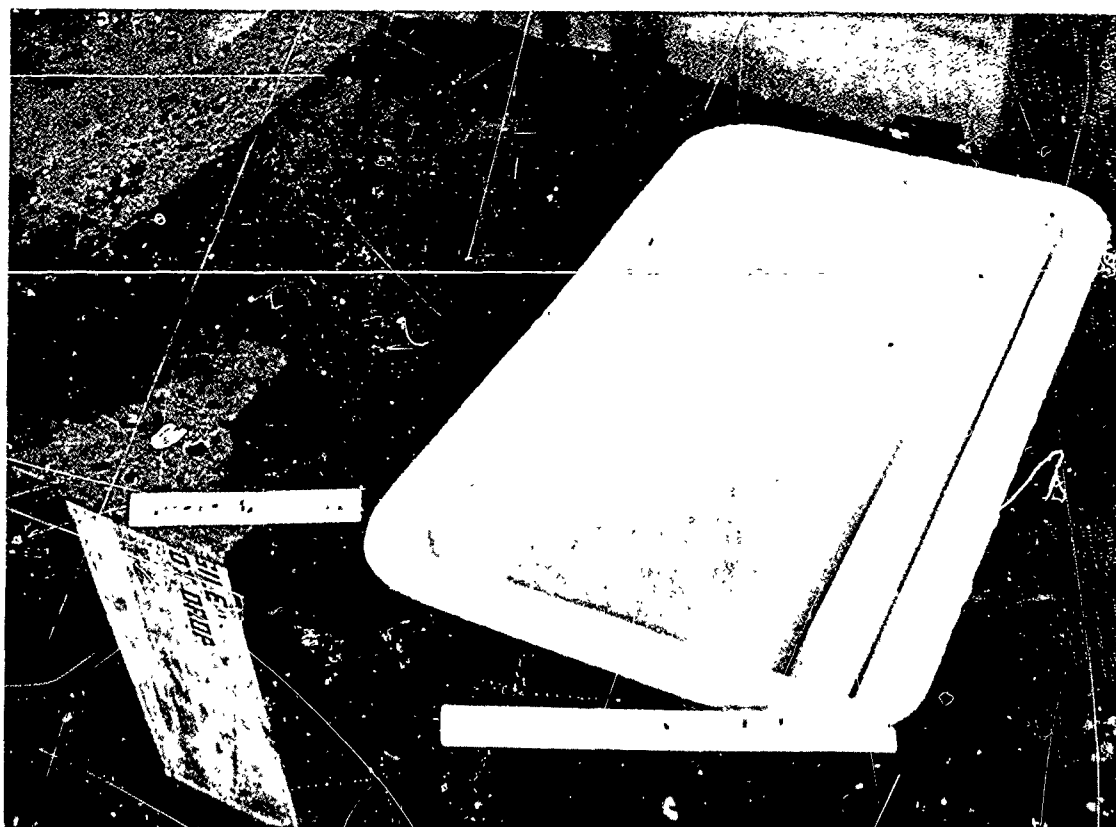
Figure 106

MOLD - WEDGE BAR

Left: Exothermic cover core - note opening for pour.

Right: Mold cavity.
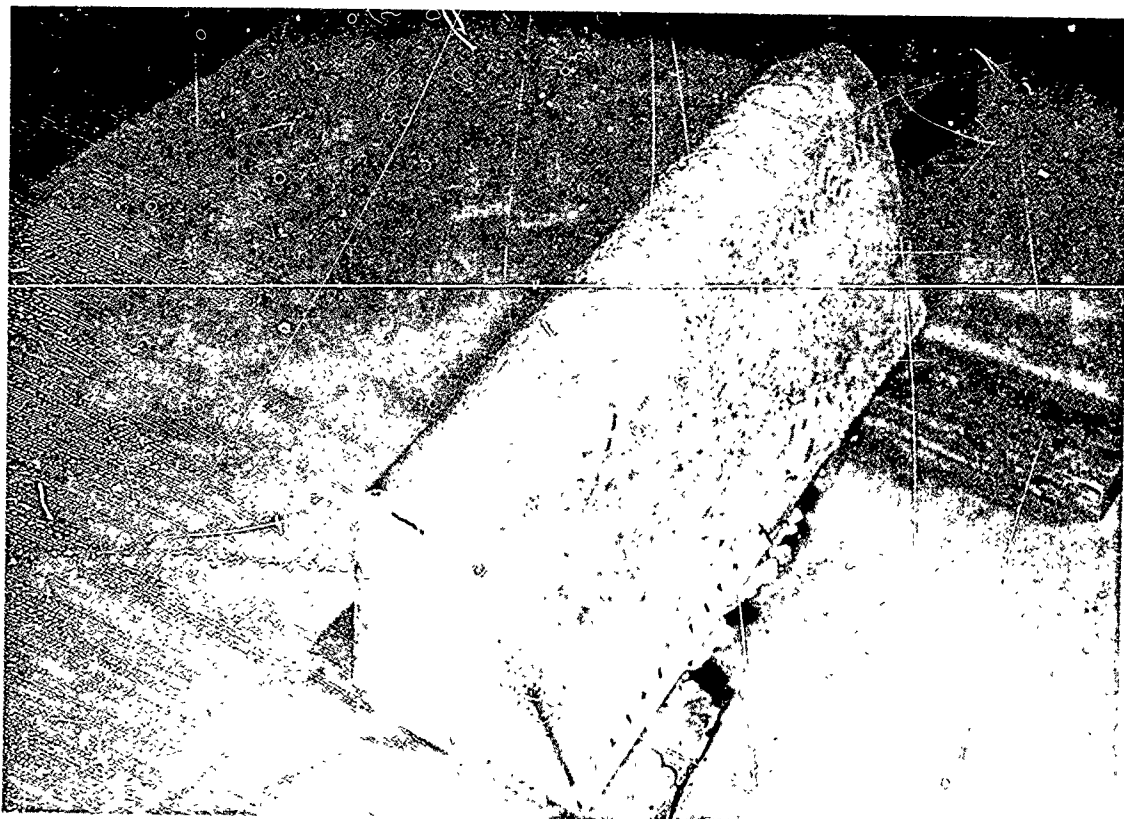
Figure 107

WEDGE BAR CASTING
INCO 713 LC

Gross Weight: 500 lb.

End Product: One 4" diameter x 25" long pull-bar.
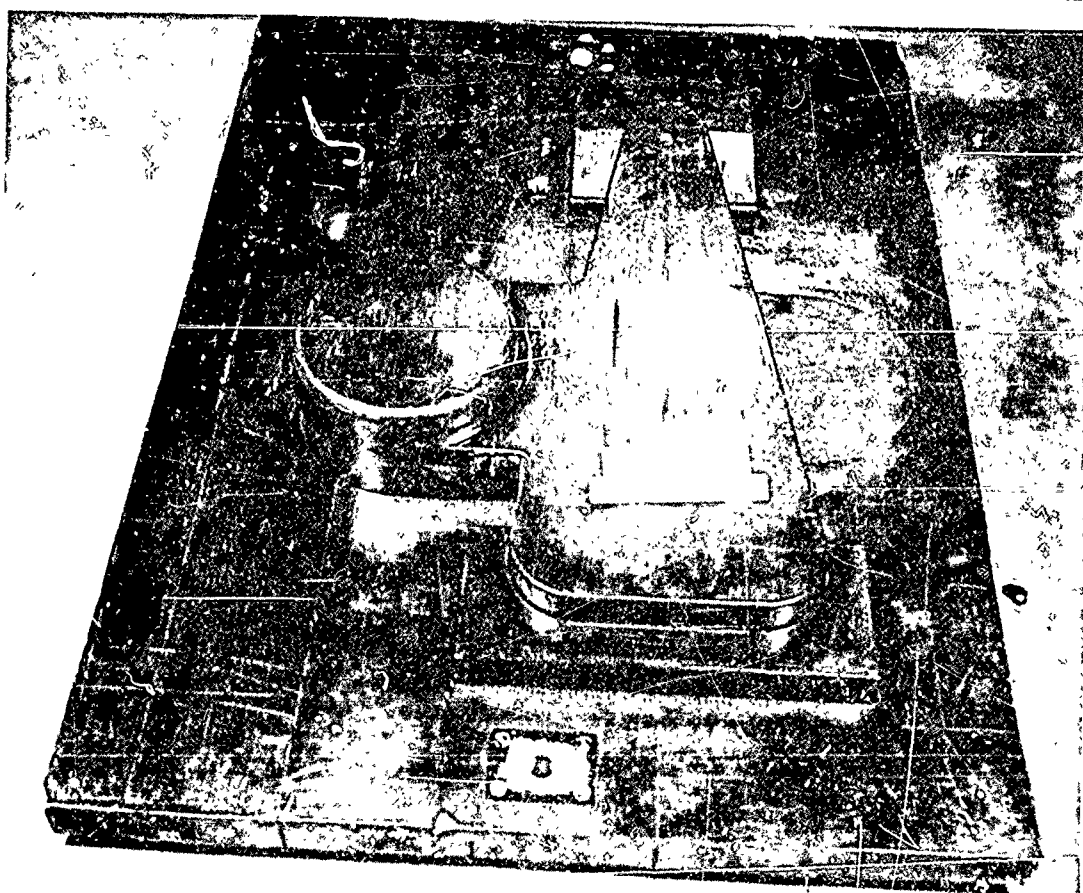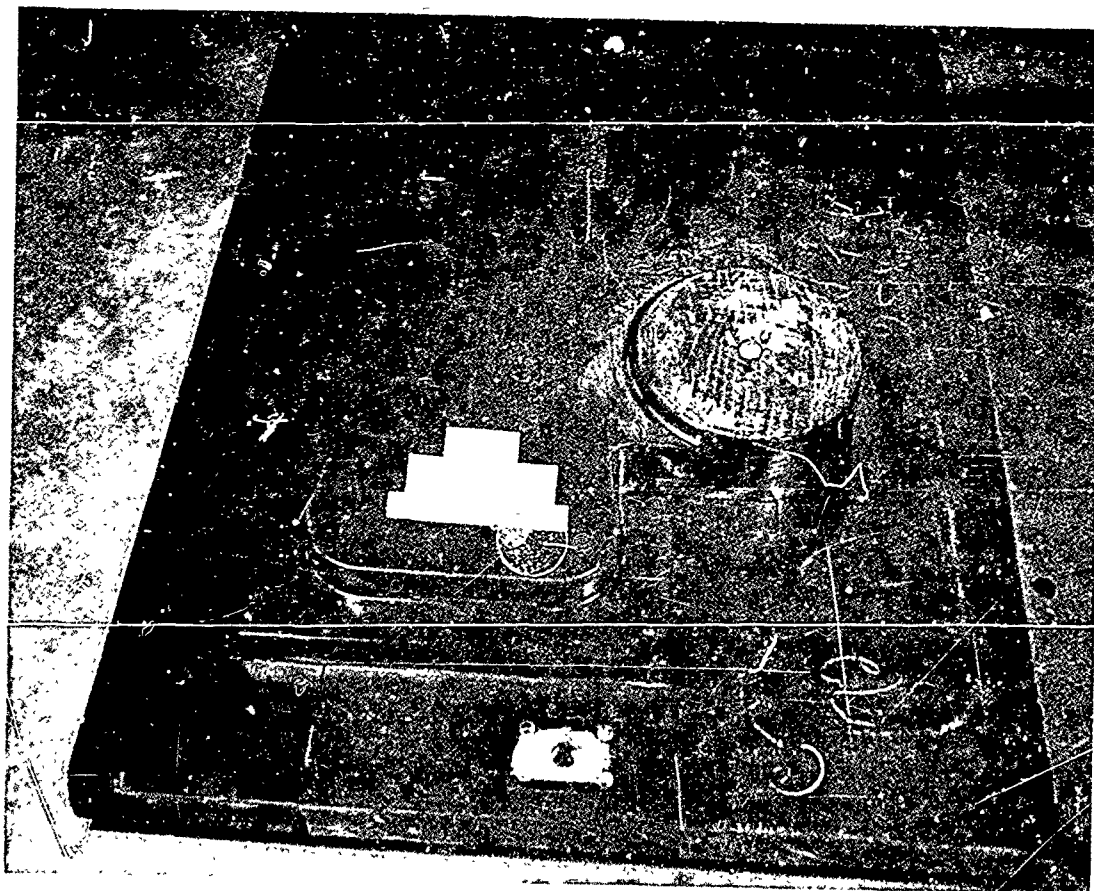
Figure 108

PATTERN EQUIPMENT - CONNECTOR YOKE C-1521

Top: Cope
Bottom: Drag
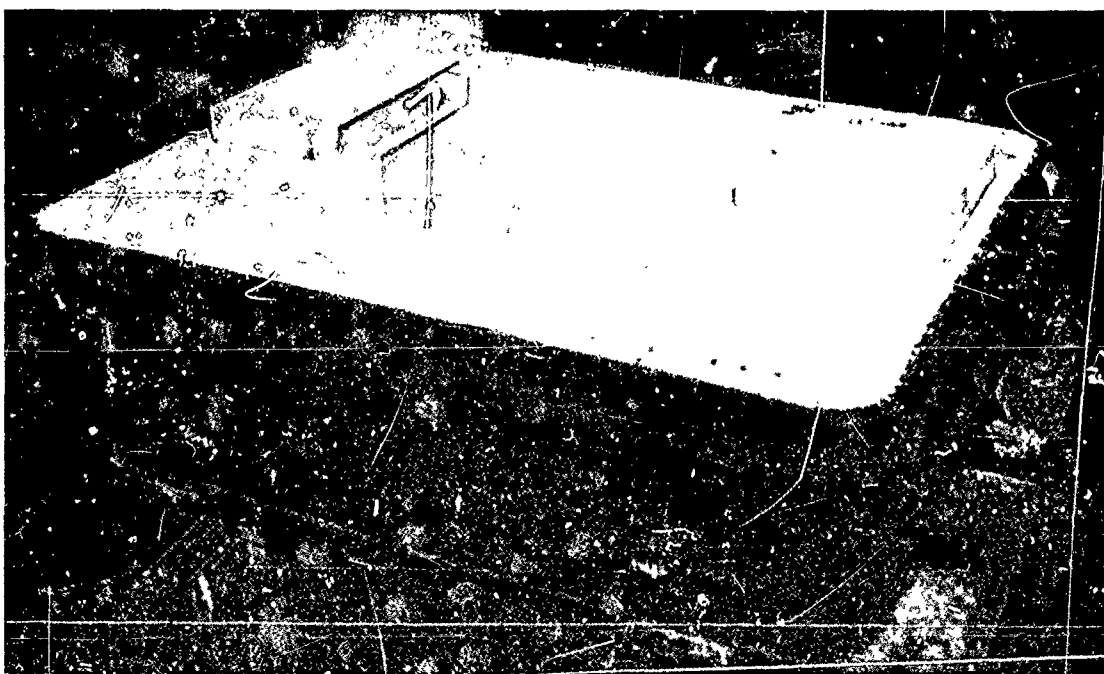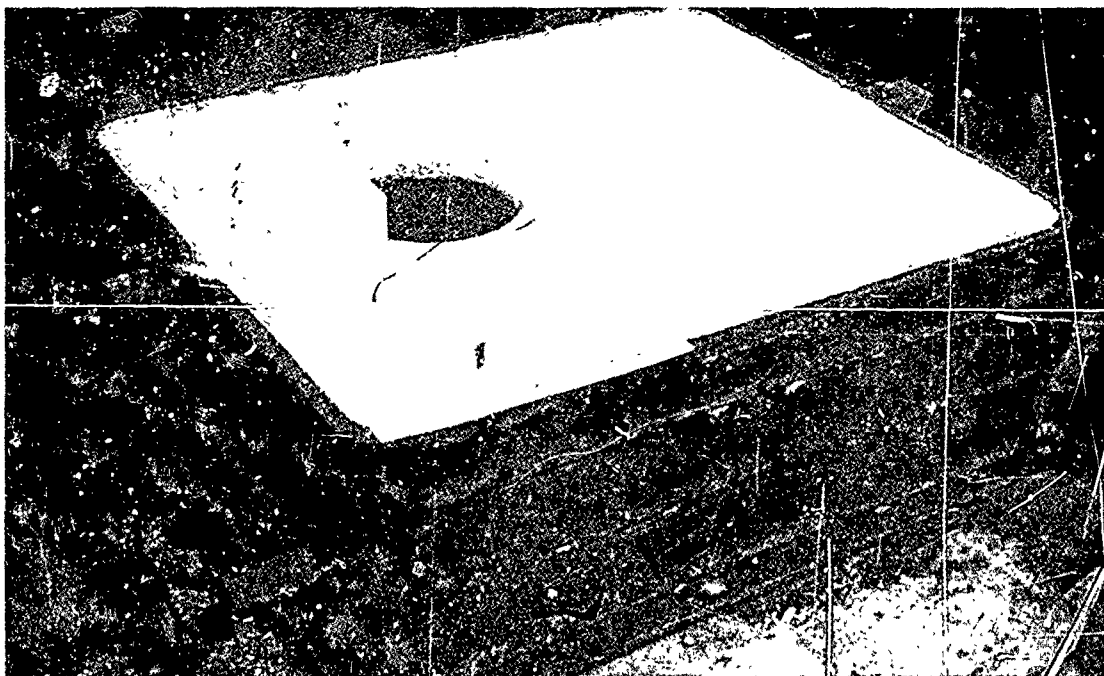
Figure 109

MOLD AND CORES - CONNECTOR YOKE

Top: Cope; note exothermic riser sleeve rammed in place.

Bottom: Drag; note thin slot cores at left.

-247-
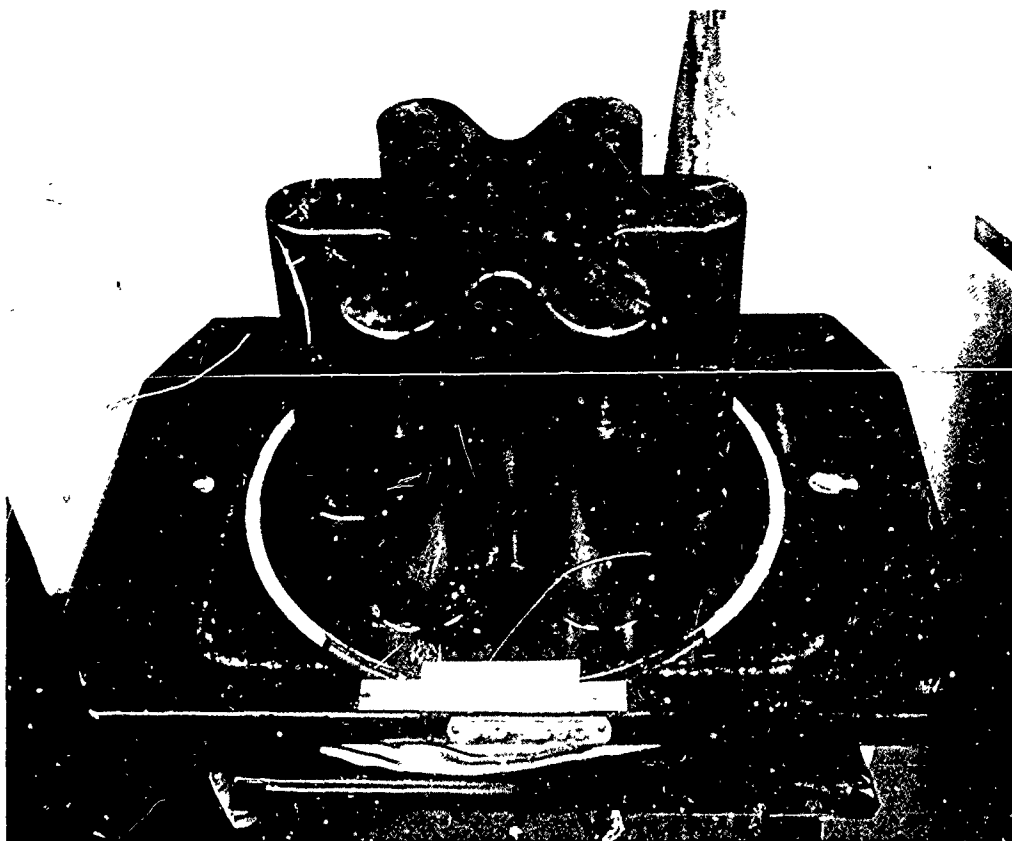
Figure 110

PATTERN EQUIPMENT - HEXABAR CASTING C-1523

End Product: Six 2" diameter x 7" long connector bars.
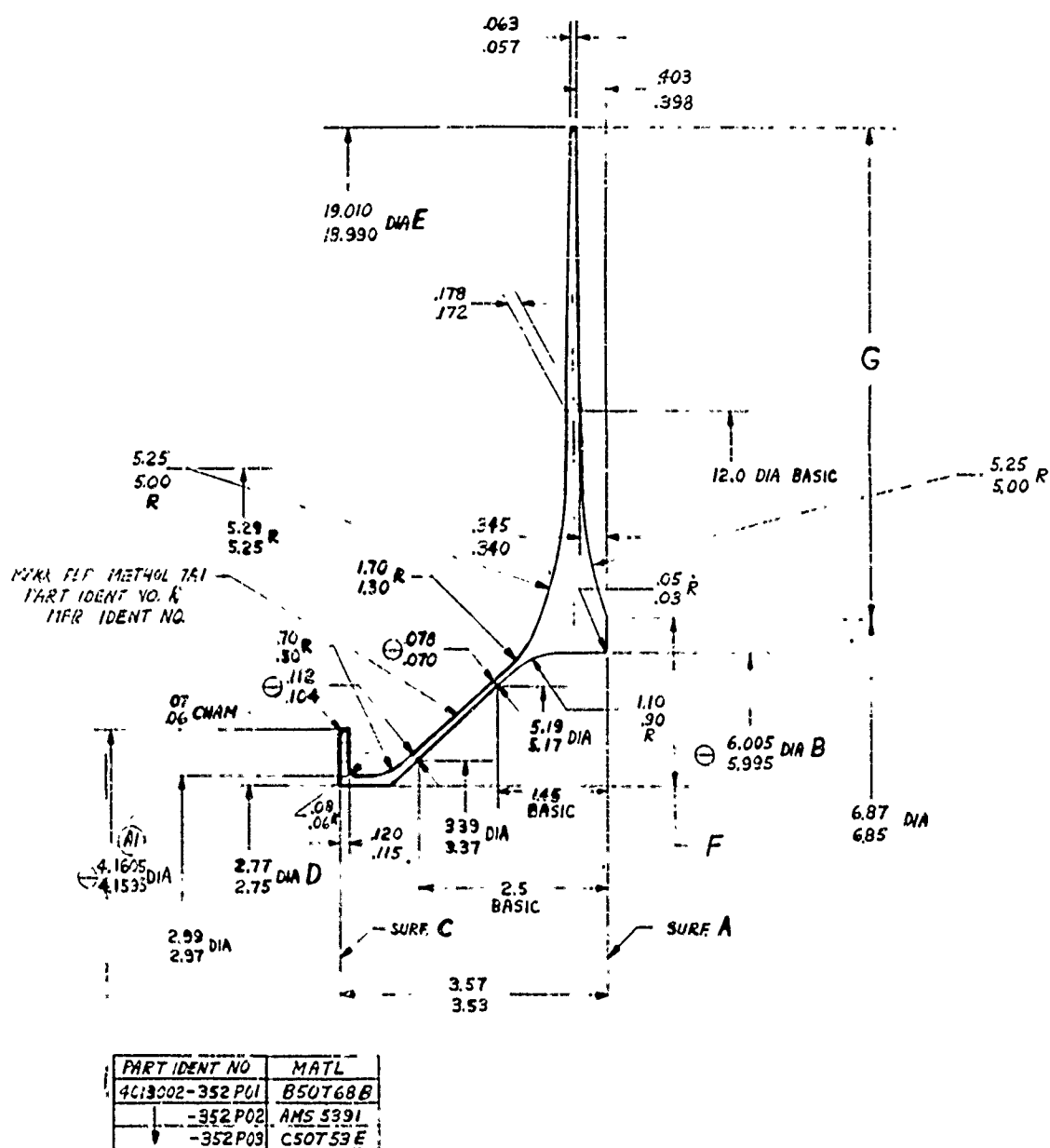
Figure 111
Burst Test Disc
Machine Drawing

-249-
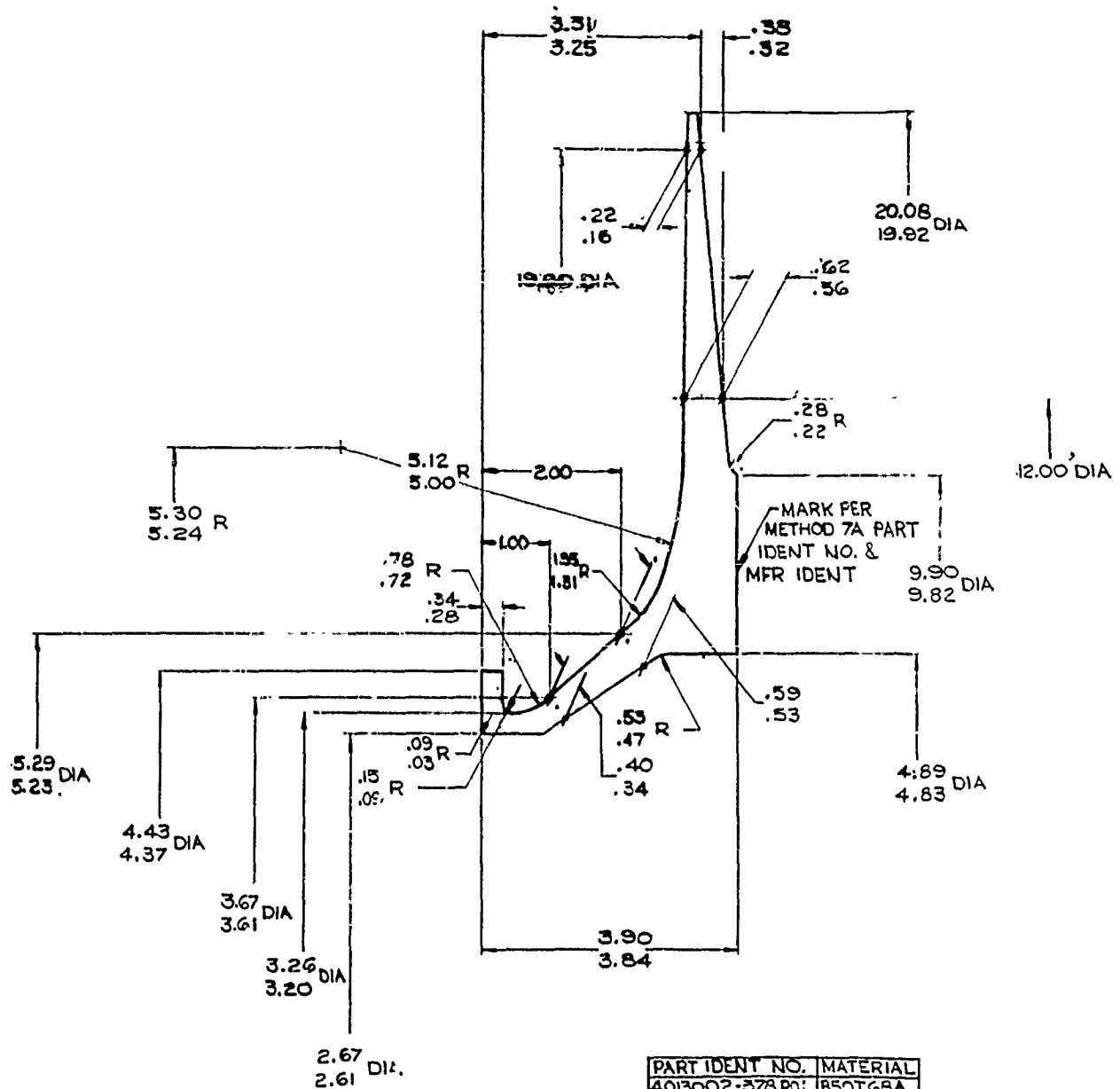
Figure 112
Burst Test Disc
Casting Drawing

-250-
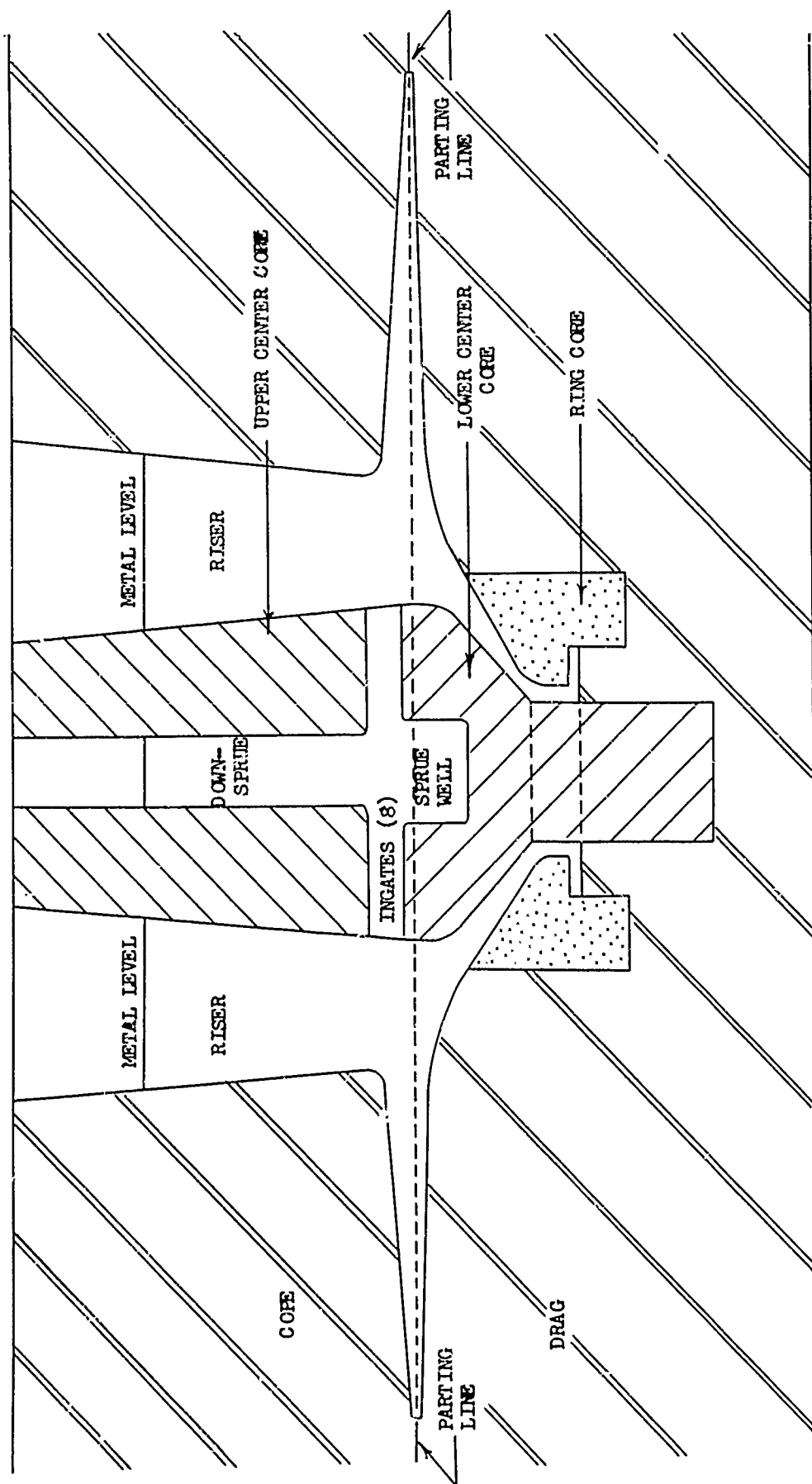
FIGURE 113
BURST TEST DISC RIGGING SKETCH

-251-
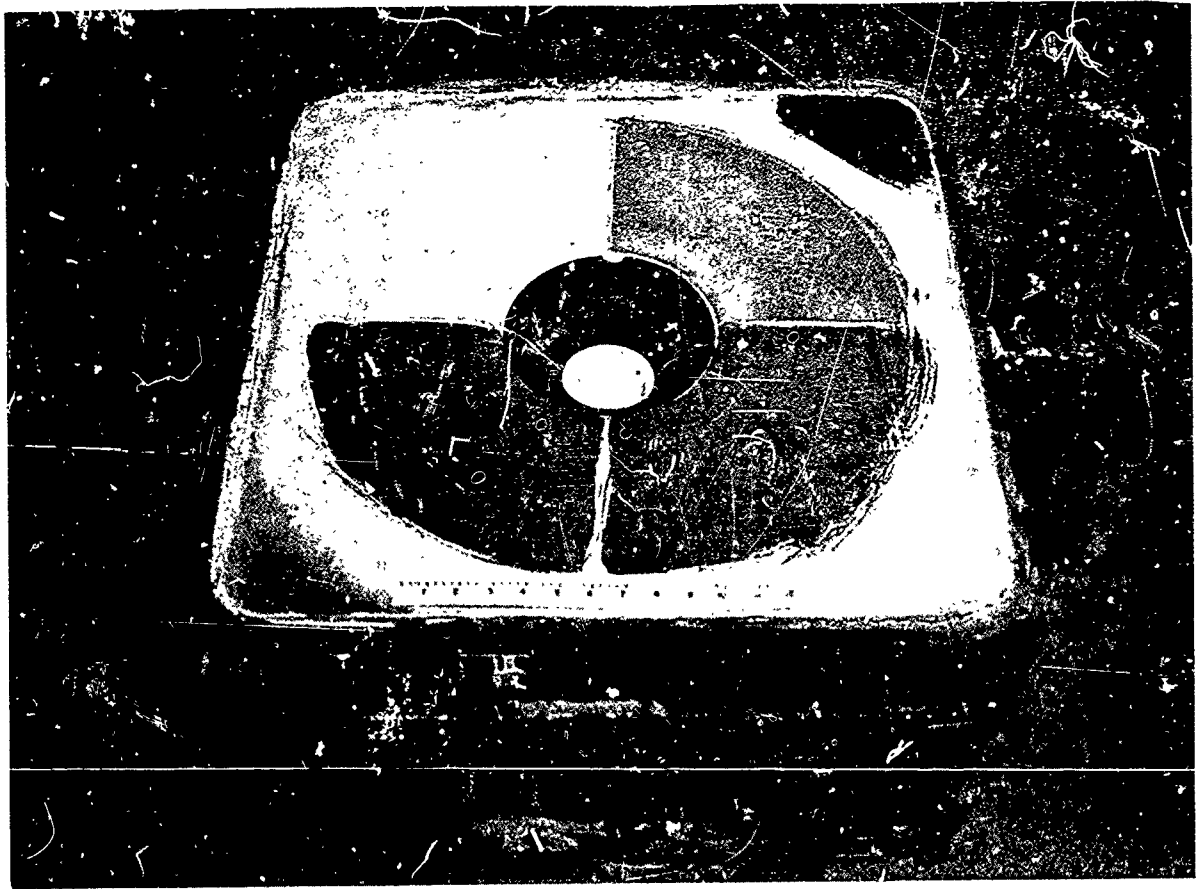
Figure 114

Drag Section of Disc Mold
With Ring-Core in Position
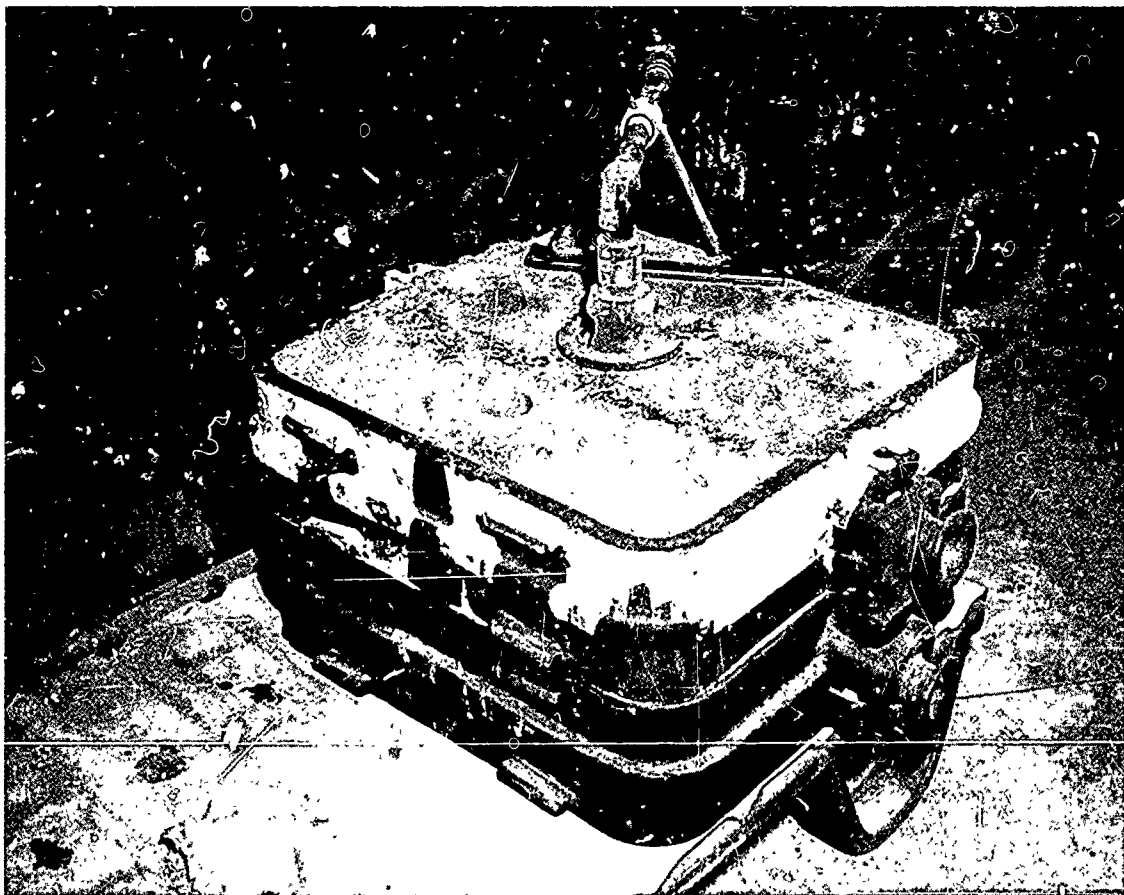
Figure 115

Firing Roof in Position on
Disc Mold Drag
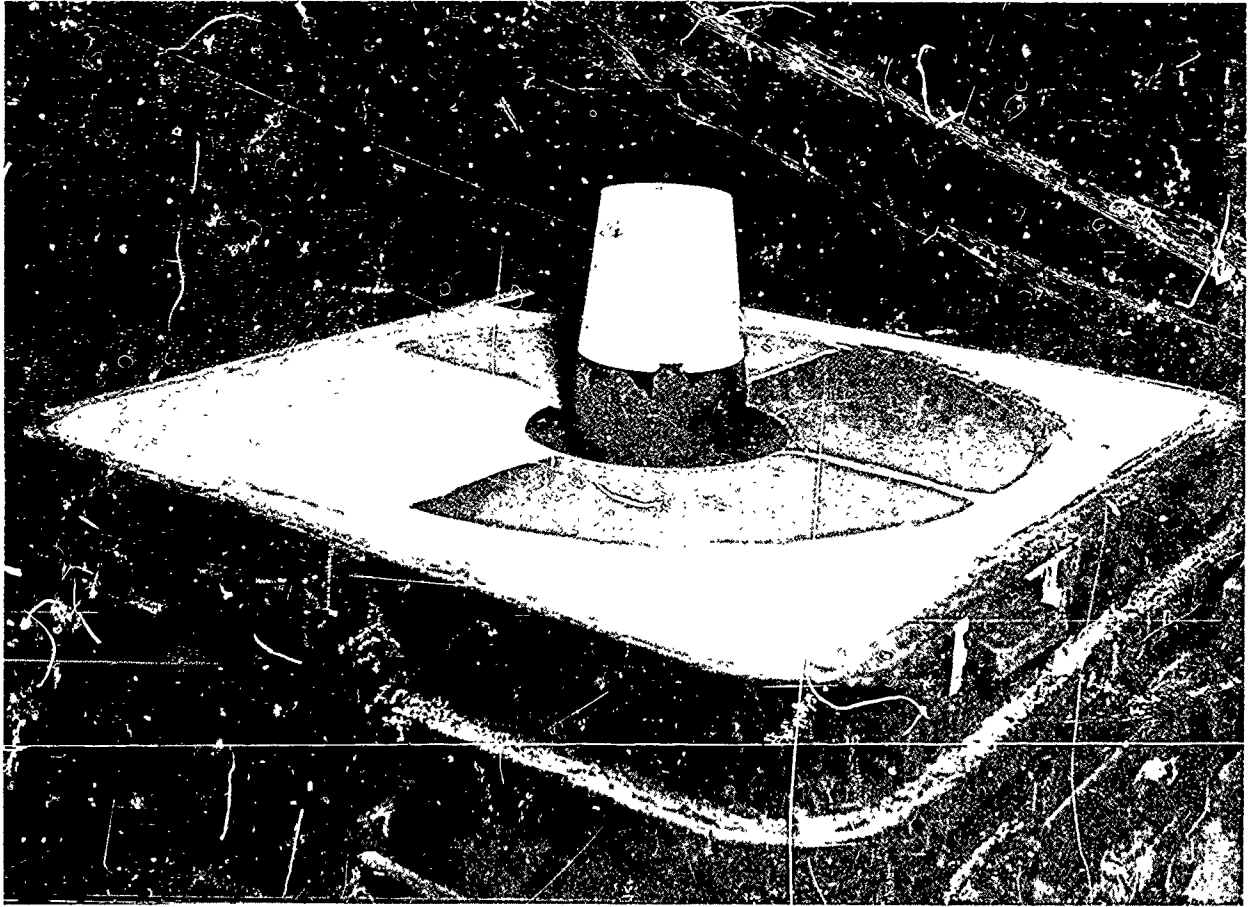
Figure 116

Drag Section of Disc Mold
with All Cores in Position
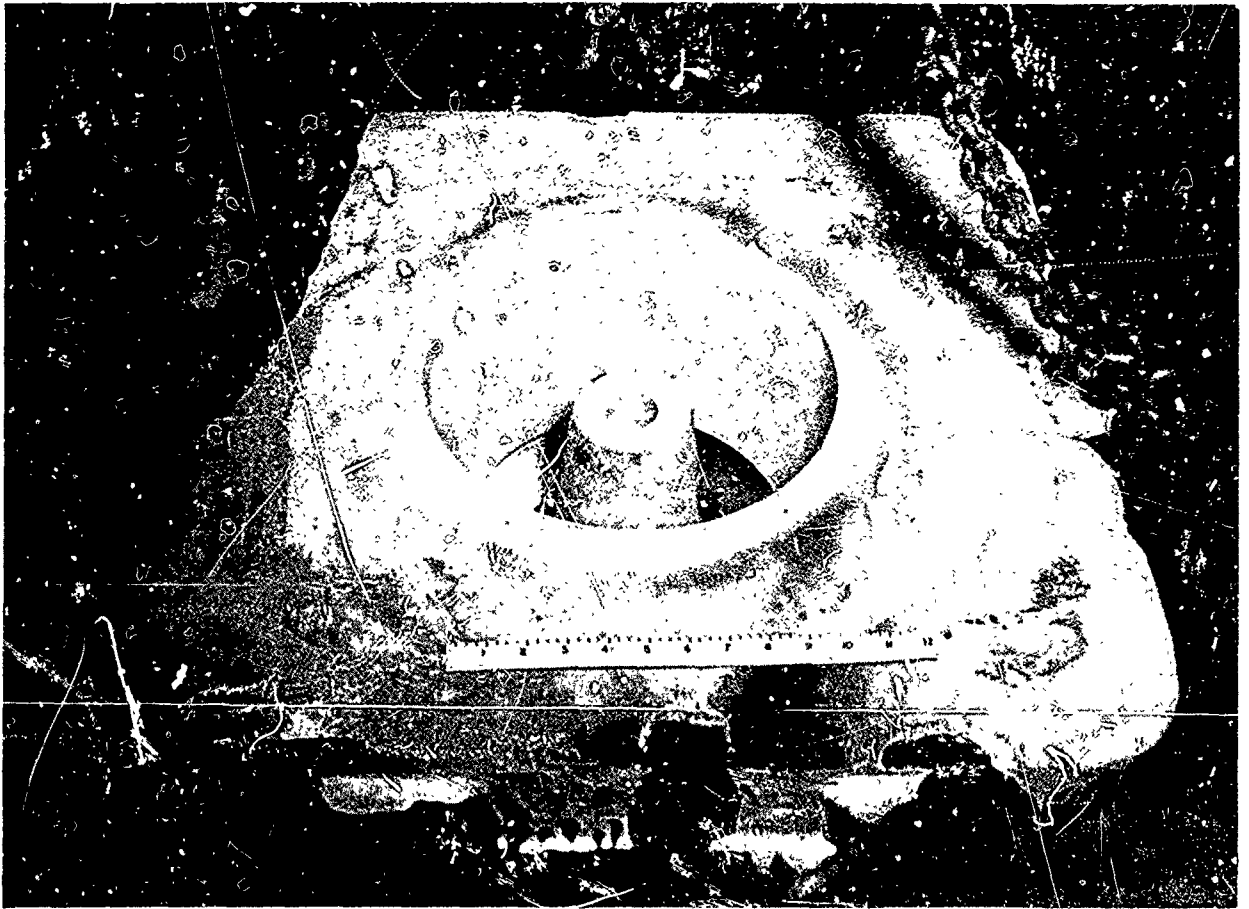
Figure 117

Closed Burst Test Disc Mold
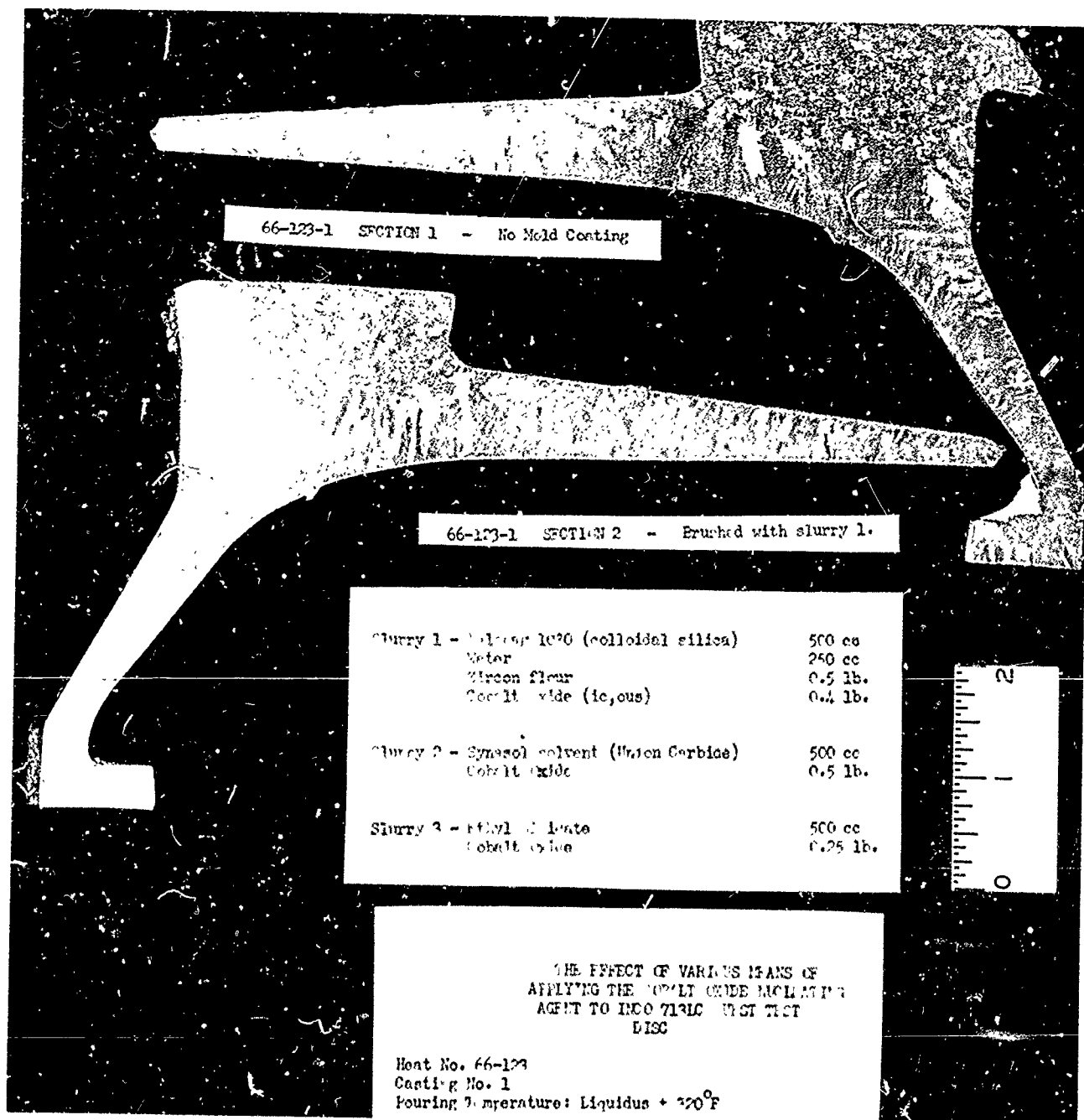
Figure 118

Macroetched Cross Sections of Inco 713 LC
Burst Test Disc

66-173-1 SECTION 3 - Brushed with slurry 2.

66-173-1 SECTION 4 - Brushed with slurry 3.

Slurry 1 - silicon 1050 (colloidal silica)   500 cc
          Water   250 cc
          Zircon flour   0.5 lb.
          Cobalt oxide (ic,ous)   0.4 lb.

Slurry 2 - synthetic solvent ("Union Carbide")   500 cc
          Cobalt oxide   0.5 lb.

Slurry 3 - ethyl silicate   500 cc
          cobalt oxide   0.4 lb.
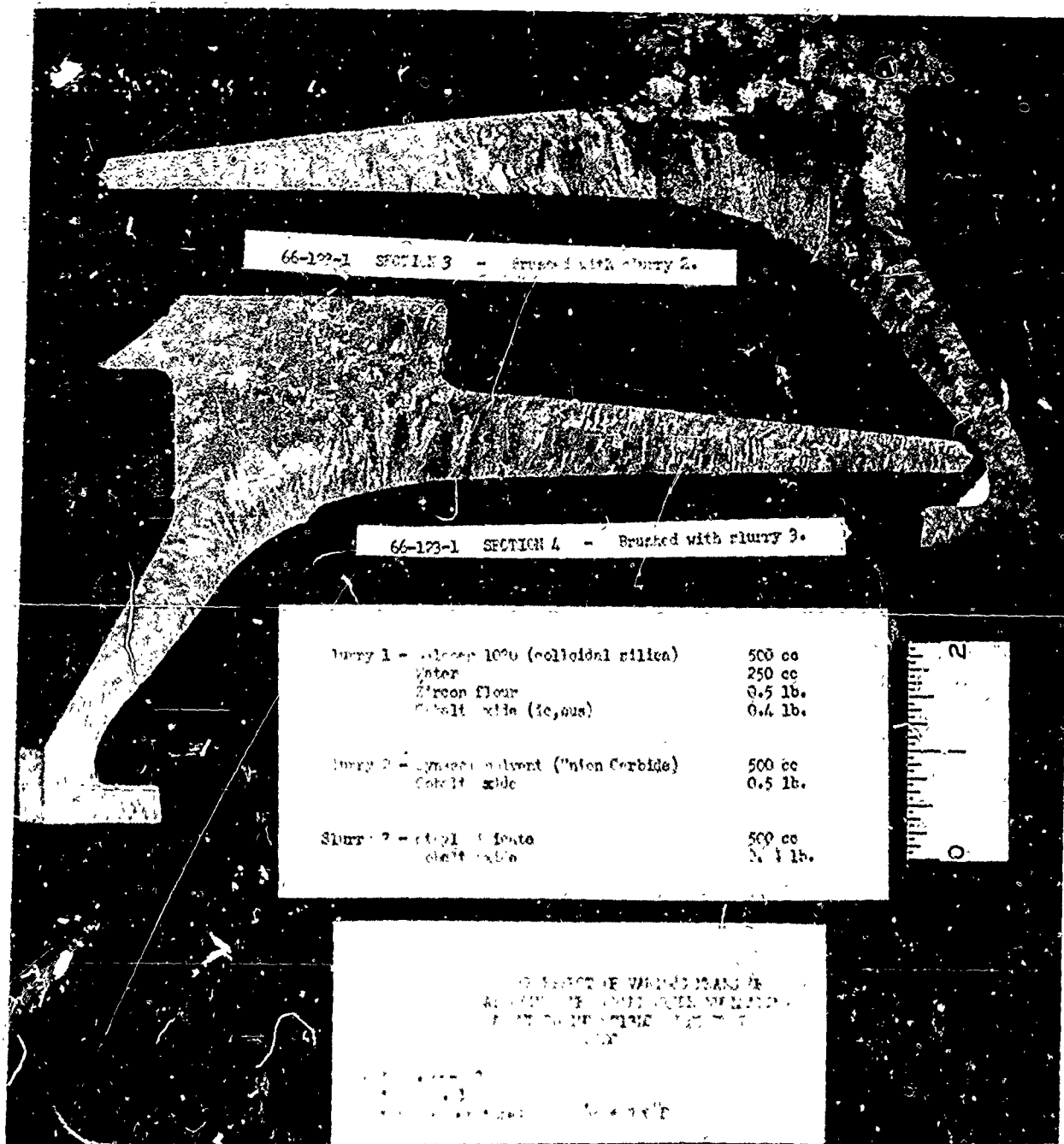
Figure 119

Macroetched Cross Sections of Inco 713 LC
Burst Test Disc

257-
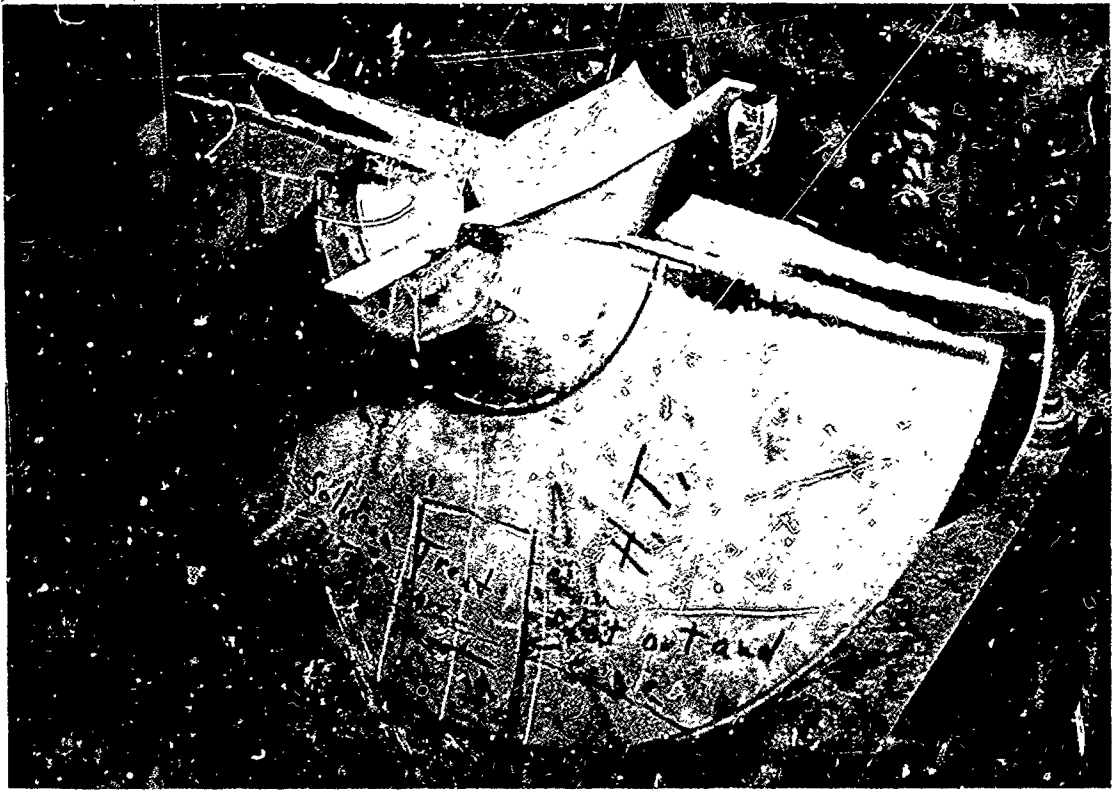
Figure 120

Spin Test Disc Fractured by Residual Stress
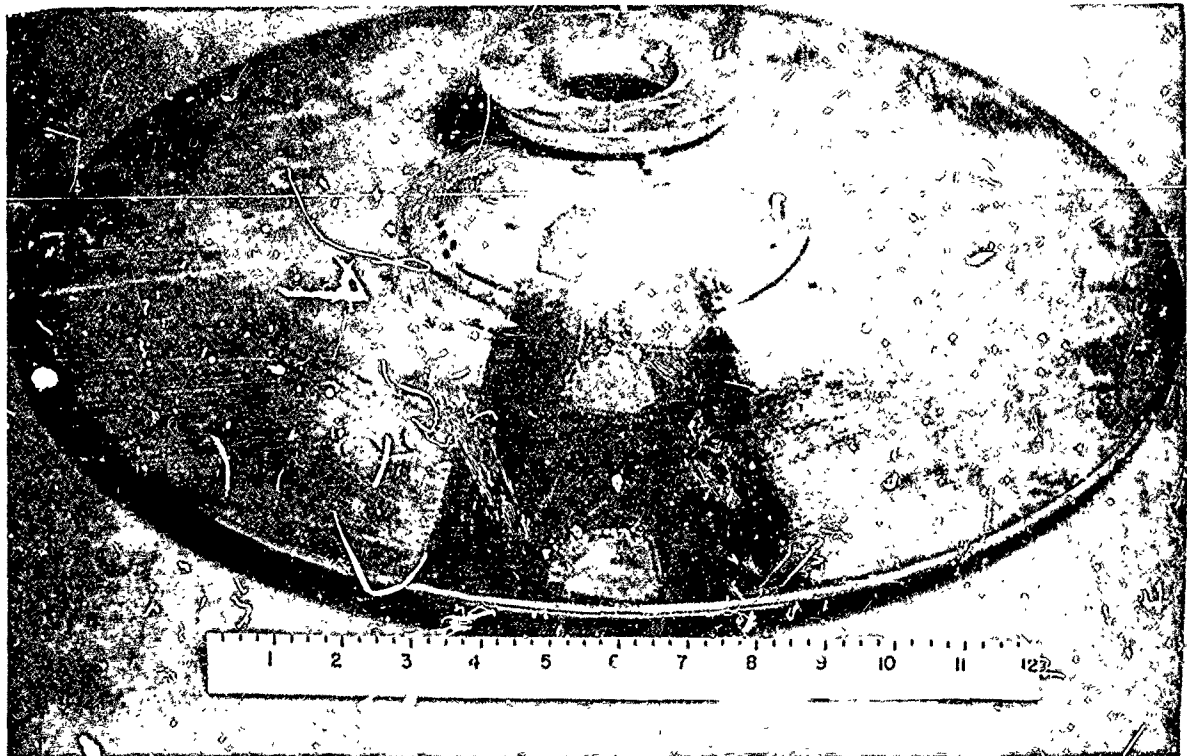
Figure 121
Rosette-Type SR-4 Strain Gauges in
Position on Spin Test Disc

Stress	Side	As Cast	Sol'n Tr't'd
Radial	A	4,480	-6,080
	B	22,580	-5,330
Hoop	A	20,820	-3,640
	B	61,220	7,270

Stress	Side	As Cast	Sol'n Tr't'd
Radial	A	34,350	-4,370
	B	38,550	8,410
Hoop	A	47,250	7,470
	B	50,400	5,950

Stress	Side	As Cast	Sol'n Tr't'd
Radial	A	46,400	19,740
	B	52,000	24,550
Hoop	A	12,200	4,060
	B	20,200	- 450

Stress	Side	As Cast	Sol'n Tr't'd
Radial	A	1,500	-12,350
	B	21,700	- 7,100
Hoop	A	-81,700	-15,650
	B	-66,500	-80,900

Scale 1:1

① ② ③ ④ - Rosette Gauges, SR-4 Type

+Tension
-Compress'n

FIGURE 122

RESIDUAL STRESS LEVELS
IN "AS CAST" AND SOLUTION TREATED
INCO 713LC SPIN TEST DISCS

Casting No. 66-123-1: "As cast", poured at 300°F superheat.
Casting No. 66-110-1: Solution heat treated, 2150°F-2hr-rapid air
cool, moving air symmetrical to rotational
centerline.
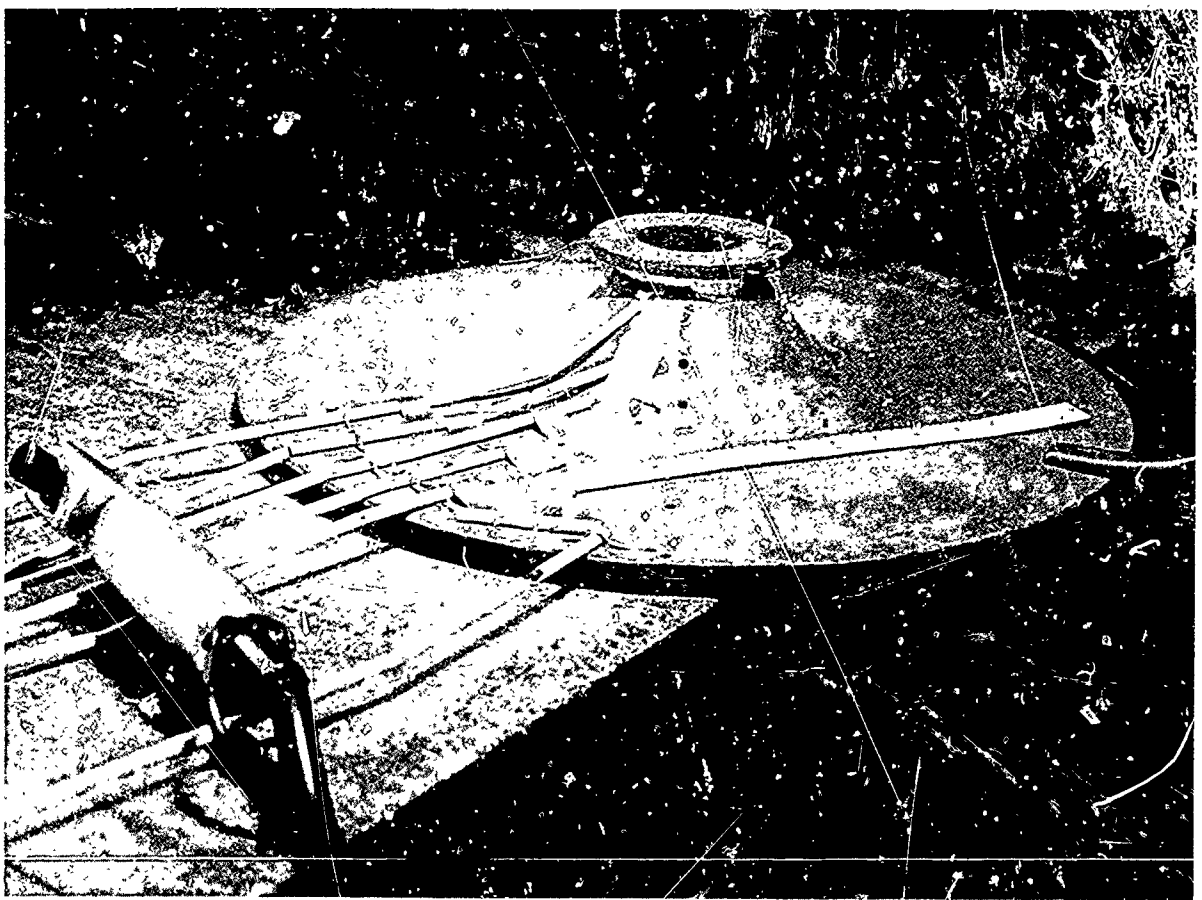
FIGURE 123

THERMOCOUPLE ARRANGEMENT FOR OBTAINING
THERMAL PROFILE OF BURST TEST DISC

The beads of six chromel-alumel thermocouples have
been flattened and spot welded in six locations from
O.D. to I.D. The couples are supported by heat re-
sistant alloy wire arches, also spot welded to the
disc surface. The portable spot-welding gun may be
seen in the left foreground.

The ceramic insulated wires were later replaced by
glass cloth insulated couples for ease of handling
during heat treatment and subsequent cooling.
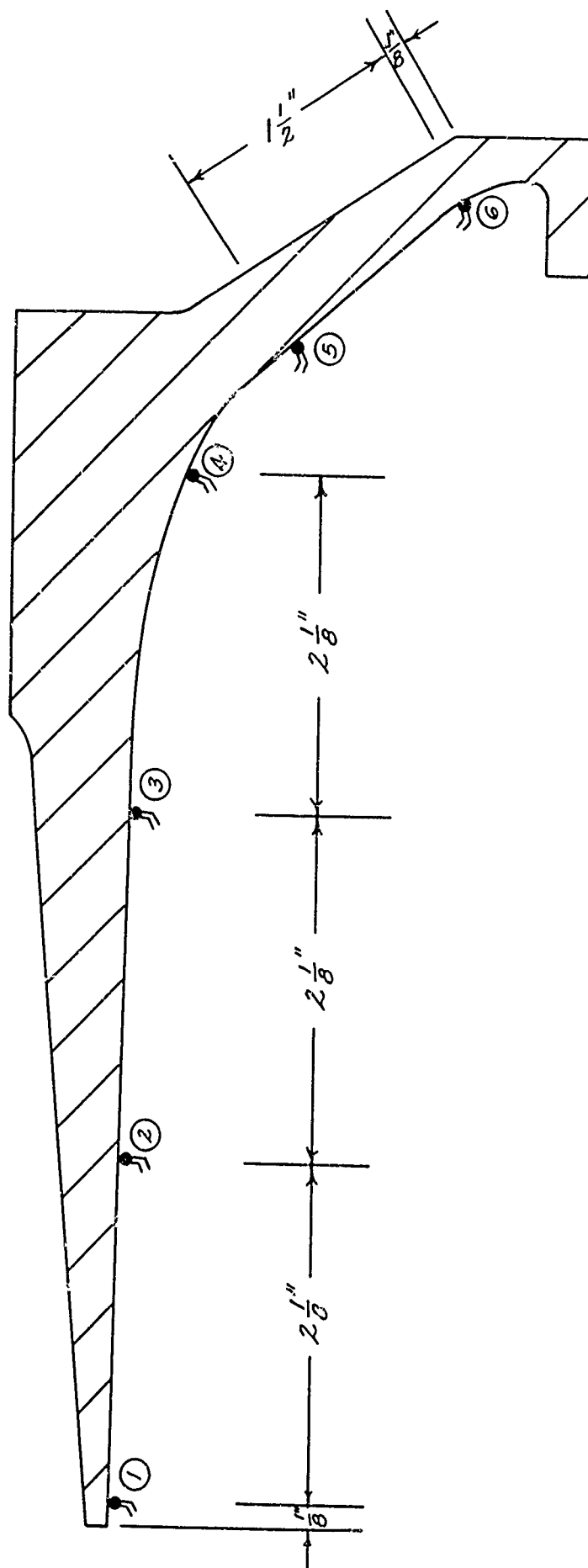
Figure 124

LOCATION OF THERMOCOUPLES FOR THERMAL PROFILE DETERMINATIONS

IN BURST TEST DISC 66-198-1
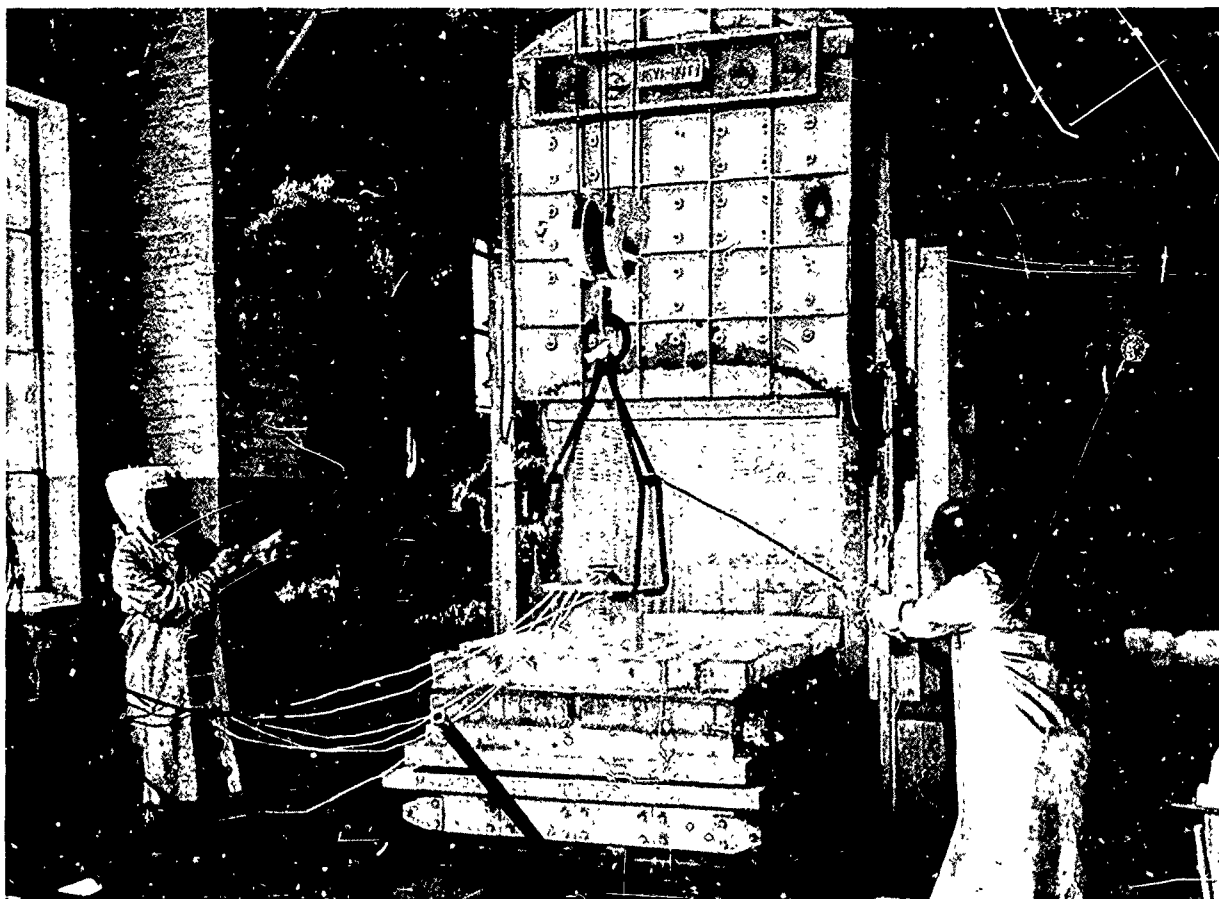
FIGURE 125

LOADING OF THE INSTRUMENTED BURST TEST DISC
INTO CAR-BOTTOM FURNACE FOR SOLUTION TREATMENT

An overhead crane manipulates the disc onto previously
arranged firebricks, after which the car is rolled into
the furnace and the door closed. Thermocouple wires
are guided into notches in the door firebrick.

For determining the thermal gradient during cooling, the
car is rolled out and the crane lifts the disc off the
bricks. The car is returned to the furnace and the disc
is left to cool while hanging freely on the crane hooks.
A six-point recorder (out of picture at left) records the
temperature throughout the treatment.

-262-
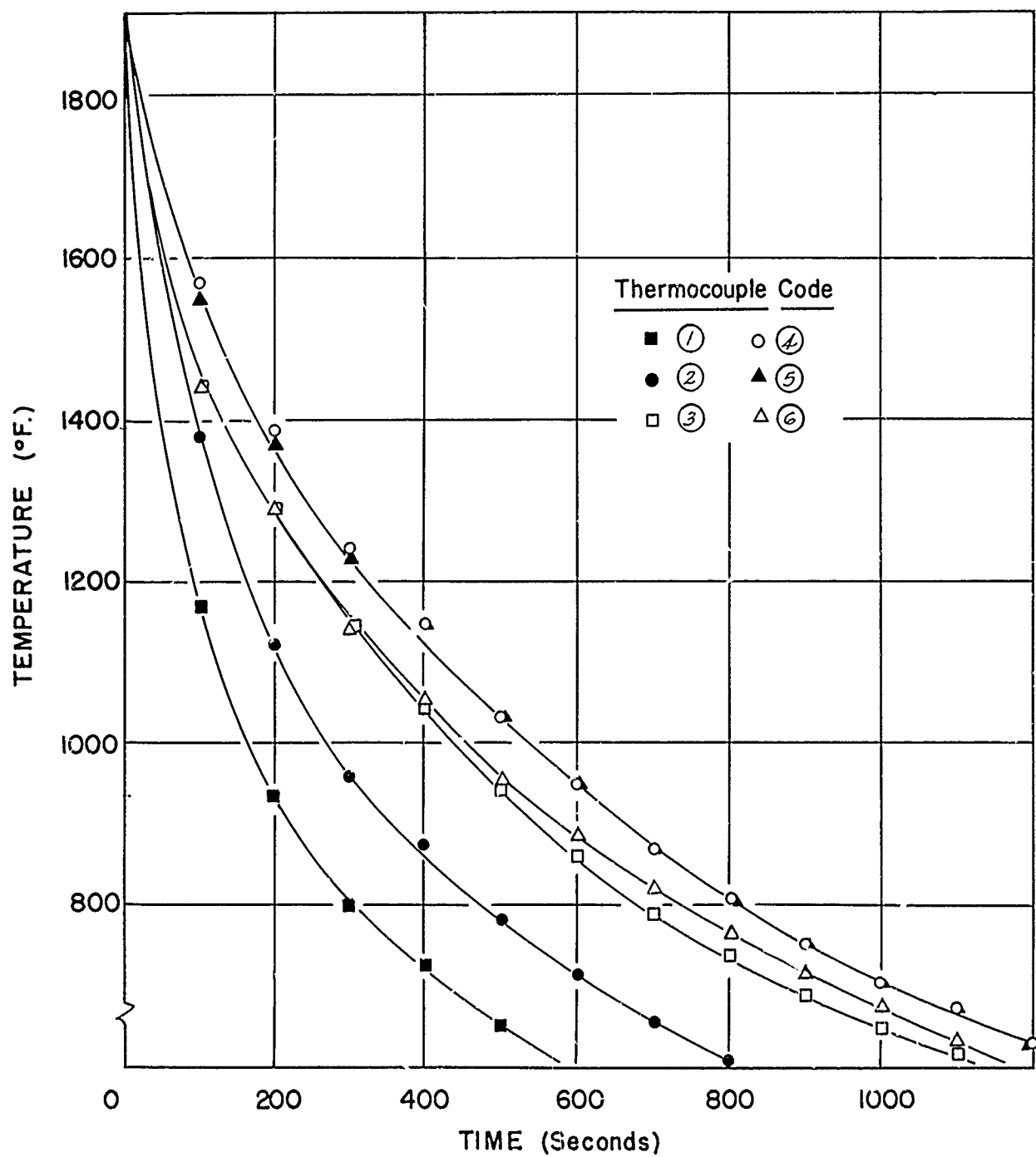
FIGURE .126

COOLING RATES OF BURST TEST DISC AT SIX THERMOCOUPLE LOCATIONS
SHOWN IN FIGURE 20

CONDITION: NO INSULATION
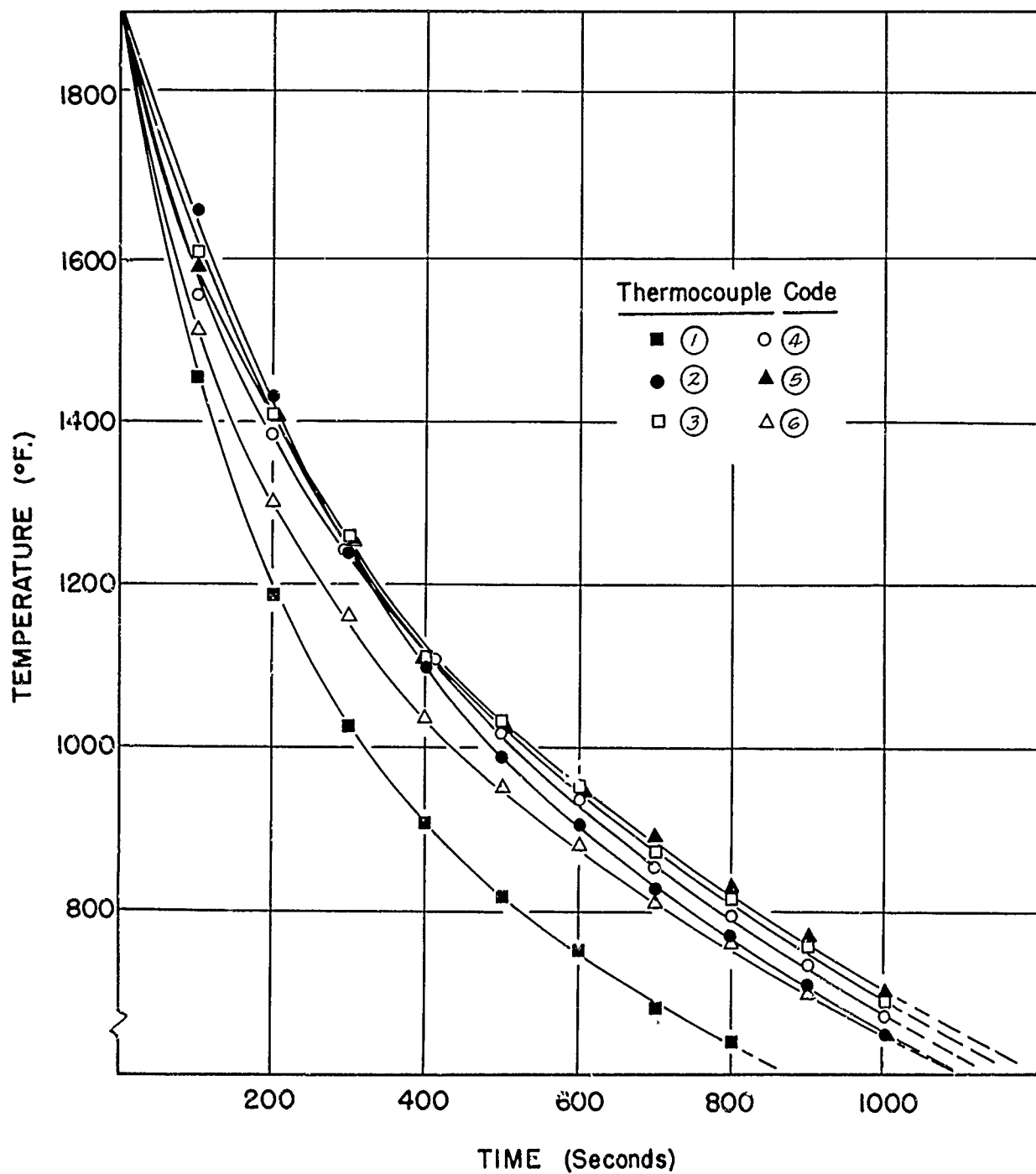
FIGURE 127

COOLING RATES OF BURST TEST DISC AT SIX THERMOCOUPLE LOCATIONS
SHOWN IN FIGURE 20

CONDITION: THIN CERAMIC COATING UP
TO AND INCLUDING THERMOCOUPLE (2)

-264-
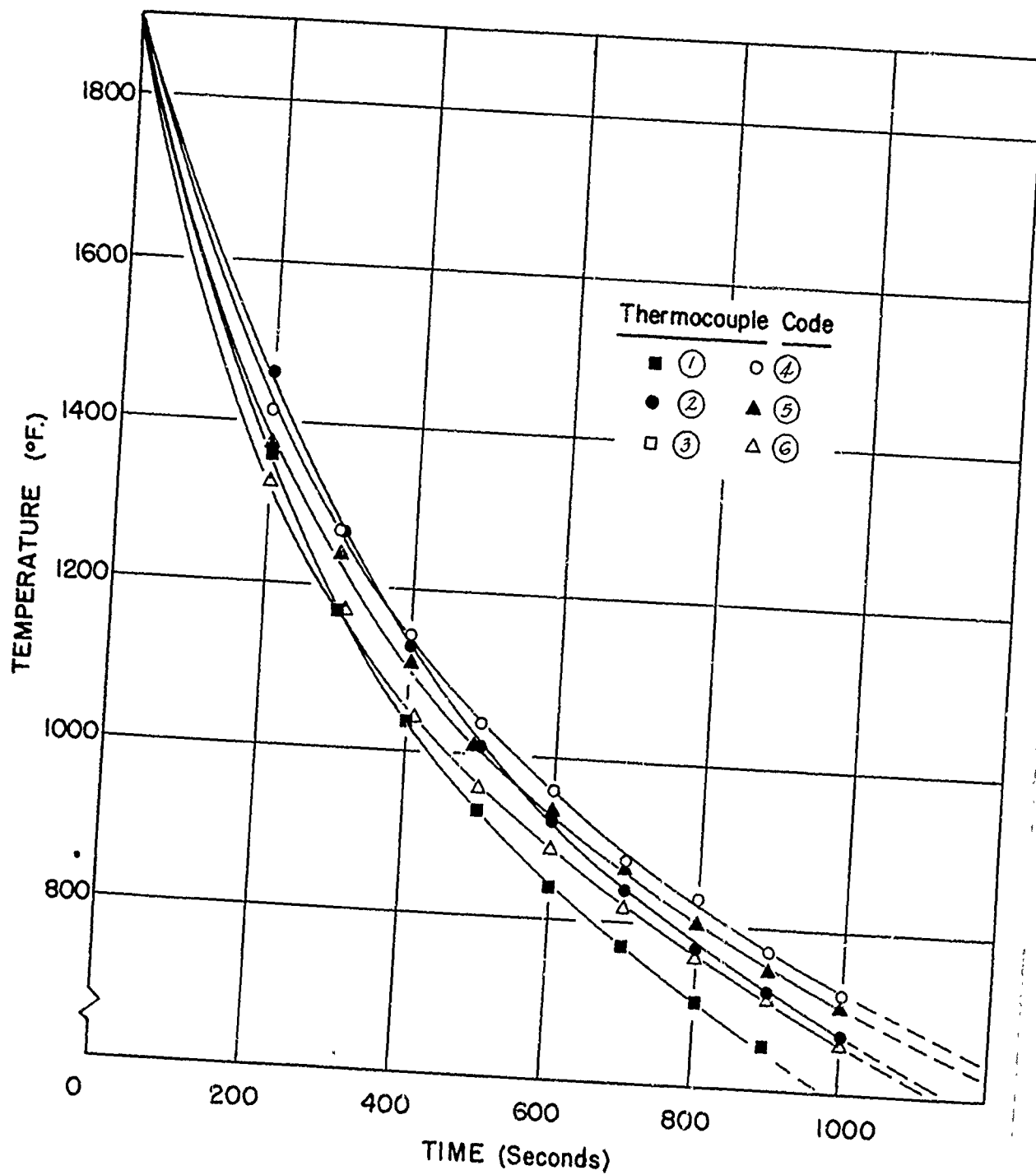
FIGURE 128

COOLING RATES OF BURST TEST DISC AT SIX THERMOCOUPLE LOCATIONS
SHOWN IN FIGURE 20

CONDITION: HEAVY CERAMIC INSULATOR
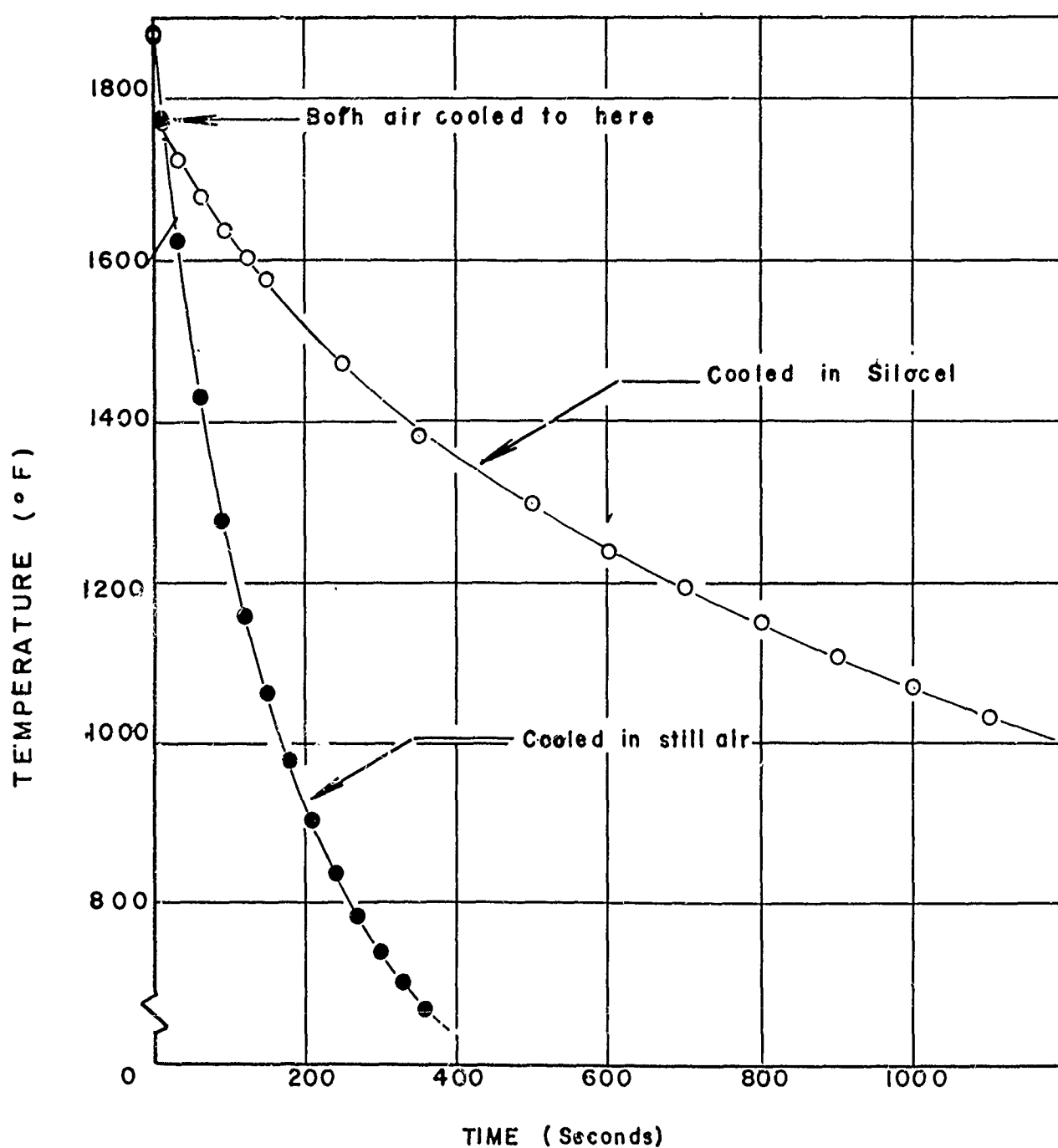
FIGURE 129

COOLING RATES OF STANDARD INCO 713LC TEST BAR SECTIONS COOLED
IN STILL AIR AND IN AN INSULATING MEDIUM
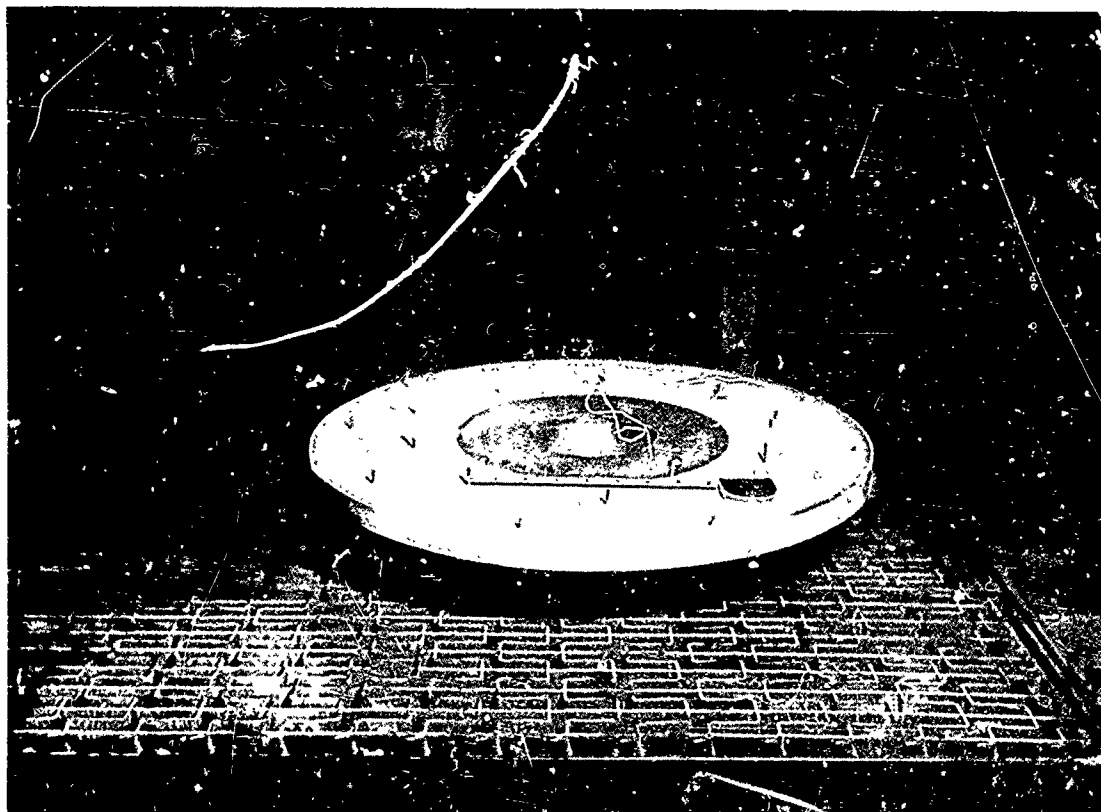
FIGURE 130

SPIN TEST DISC PREPARED FOR SOLUTION
HEAT TREATMENT AND CONTROLLED AIR COOL

After tack welding heavy heat resistant wires (as seen
protruding from ceramic) and providing a thin chromel
wire reinforcing grid, the ceramic insulator is poured
into place and hardened by normal methods.
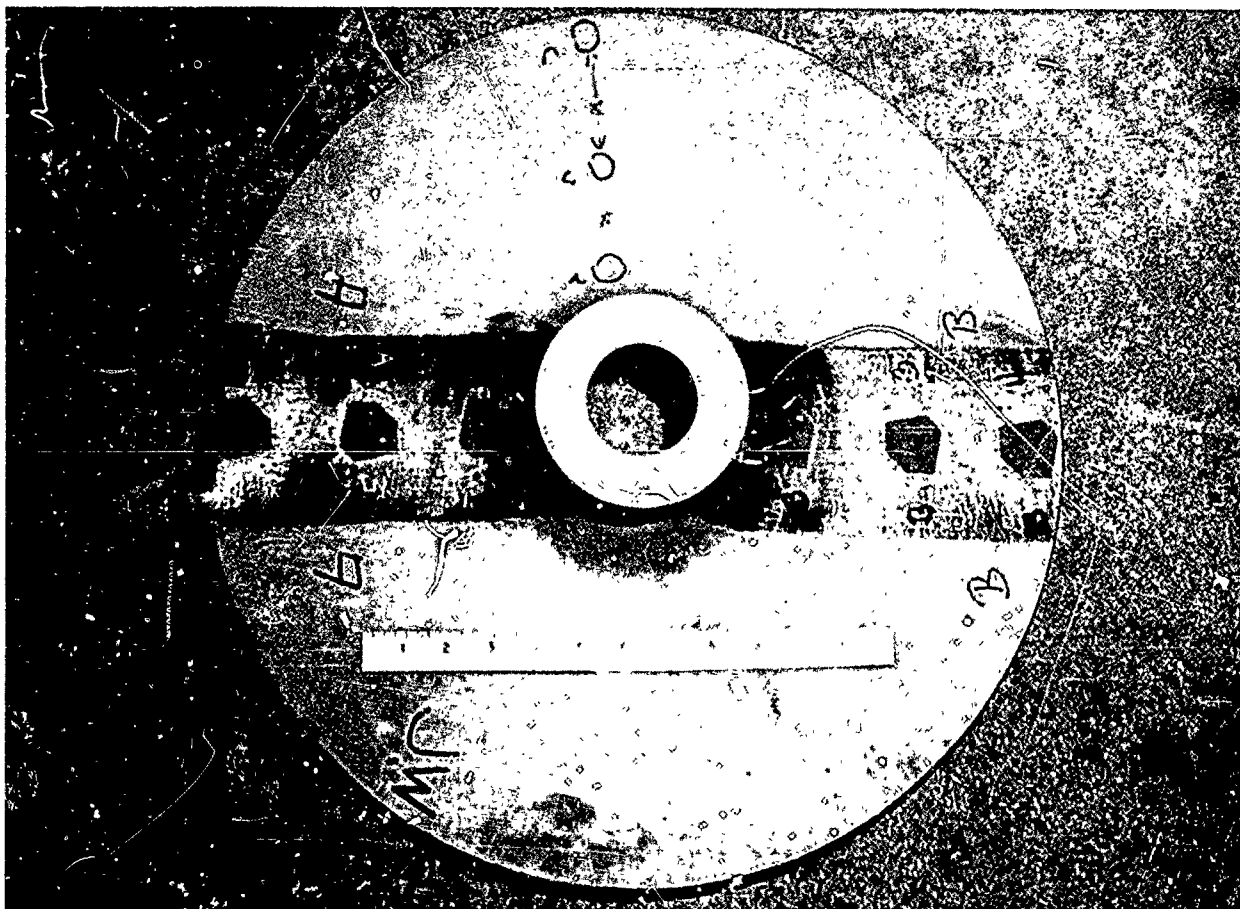
Figure 131

LOCATION OF ROSETTE SR-4 GAUGES ON
HEAT TREATED SPIN TEST DISCS

RADIAL DIRECTION
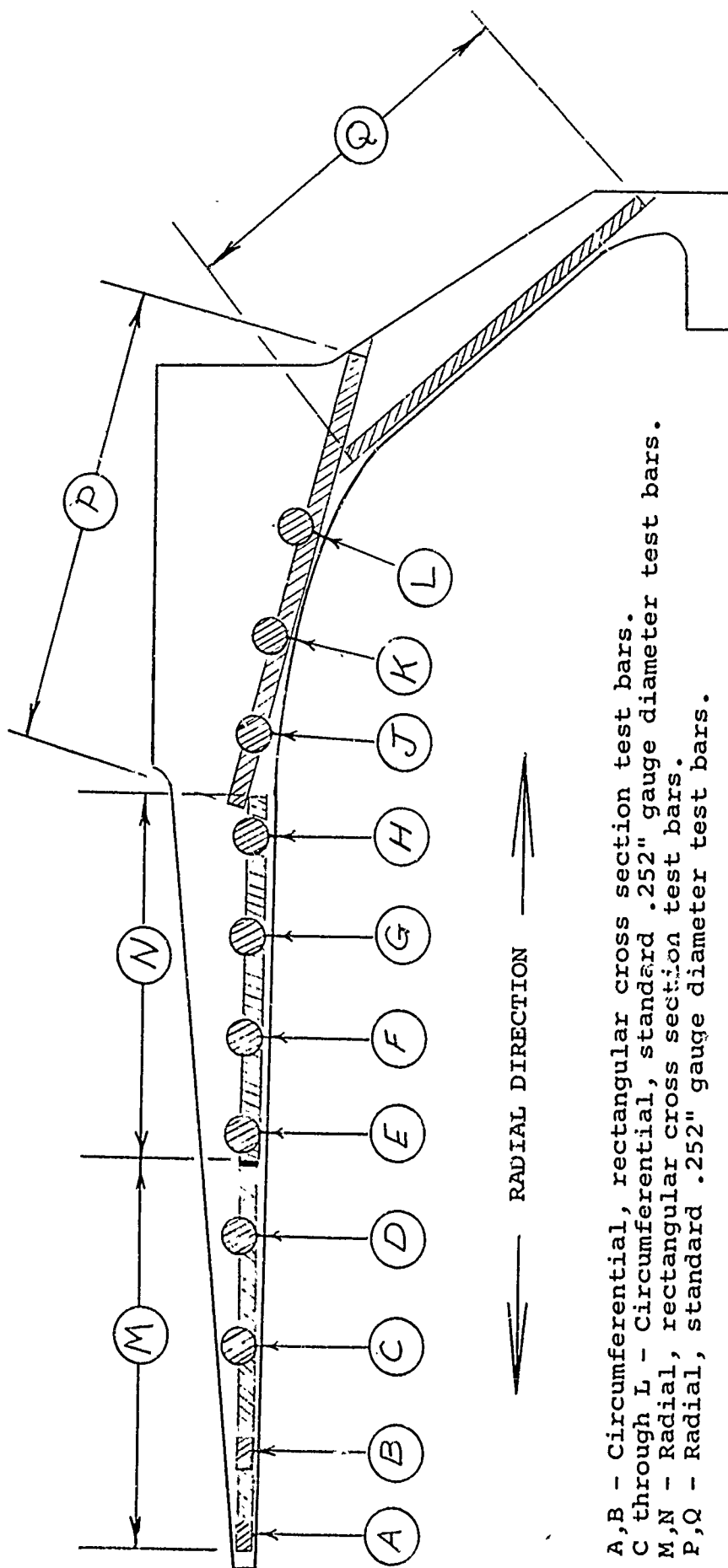
A,B – Circumferential, rectangular cross section test bars.
C through L – Circumferential, standard .252" gauge diameter test bars.
M,N – Radial, rectangular cross section test bars.
P,Q – Radial, standard .252" gauge diameter test bars.

Figure 132

LOCATION OF TENSILE TEST BARS
CUT FROM SPIN TEST DISCS

66-485-1
66-456-1
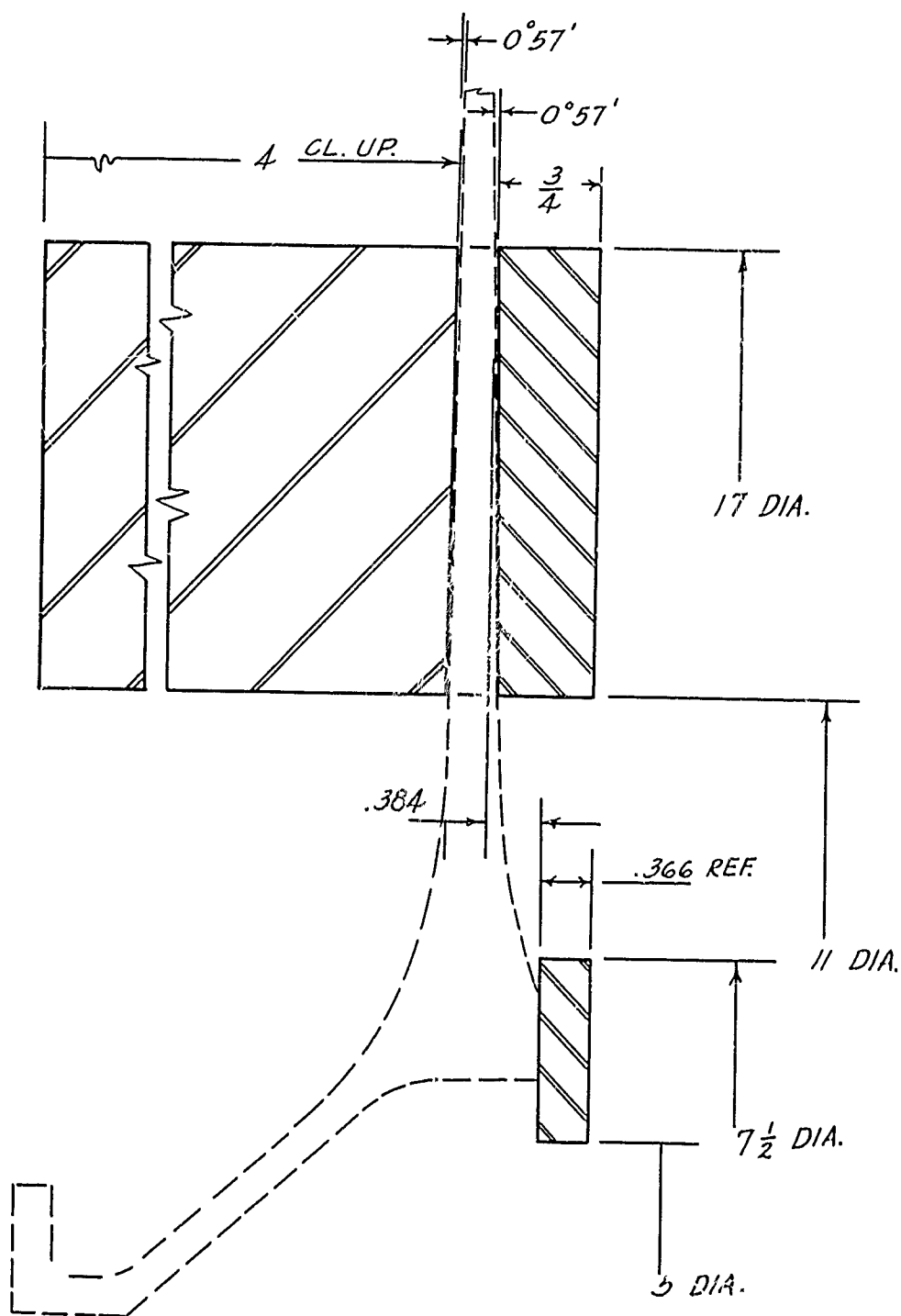
Figure 133

SKETCH OF HEAT TREATING FIXTURE USED IN
1200°F STRESS RELIEF OF SPIN-TEST DISCS AFTER MACHINING

Figure 134

CRACK IN MACHINED SPIN-TEST DISC
FOUND AFTER STRESS RELIEF AT 1200°F

Crack has been darkened with marker to more clearly
show location and shape. Rectangular mark was location of
radiographic gauge used in analysis of crack.

Note the rough machined surface.
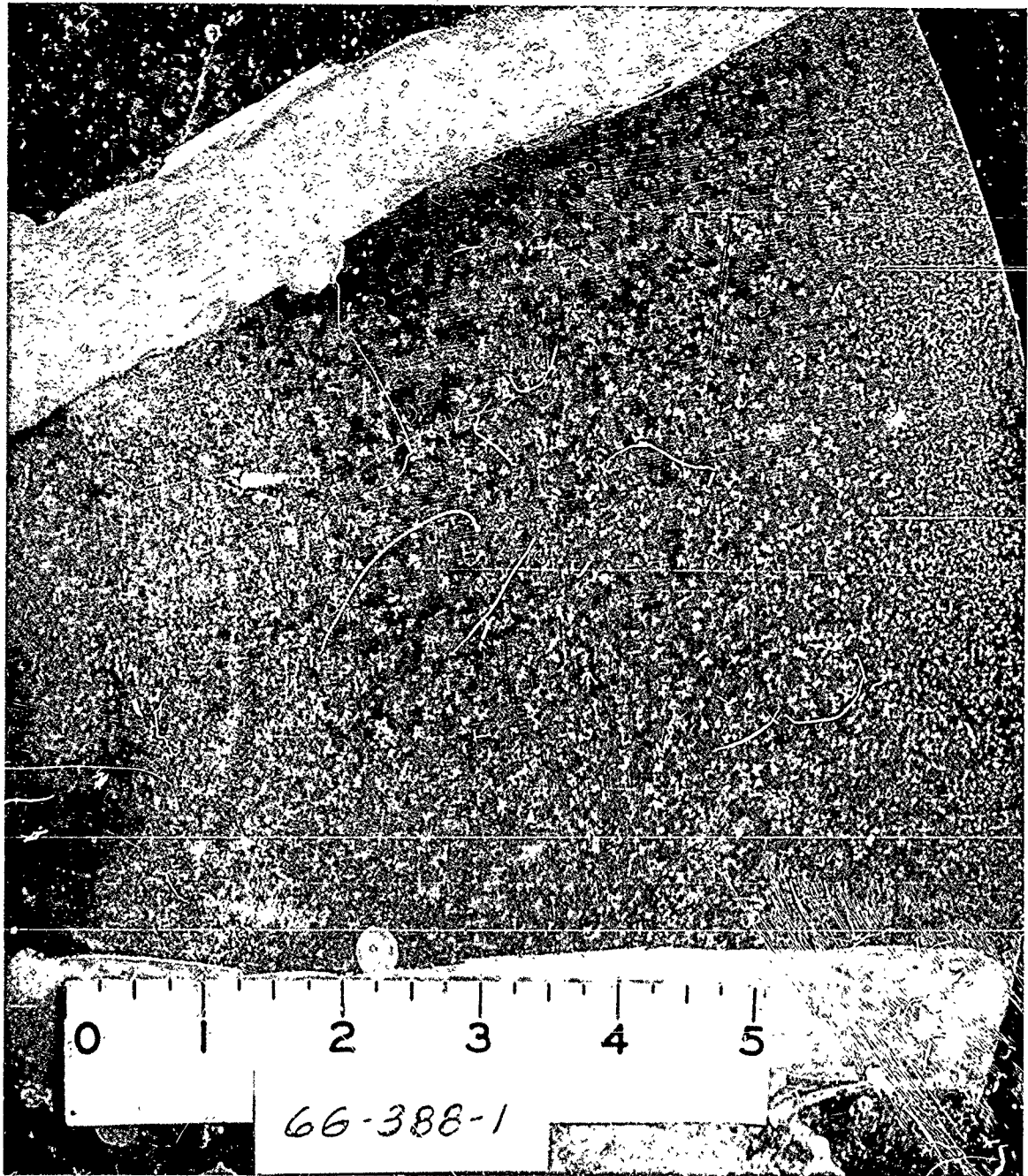
Figure 135

MACROETCHED SPIN-TEST DISC SURFACE
AFTER MACHINING AND STRESS RELIEF

No defects other than the crack shown in
Figure 49 were found. Note decreasing grain size
from I.D. to O.D.
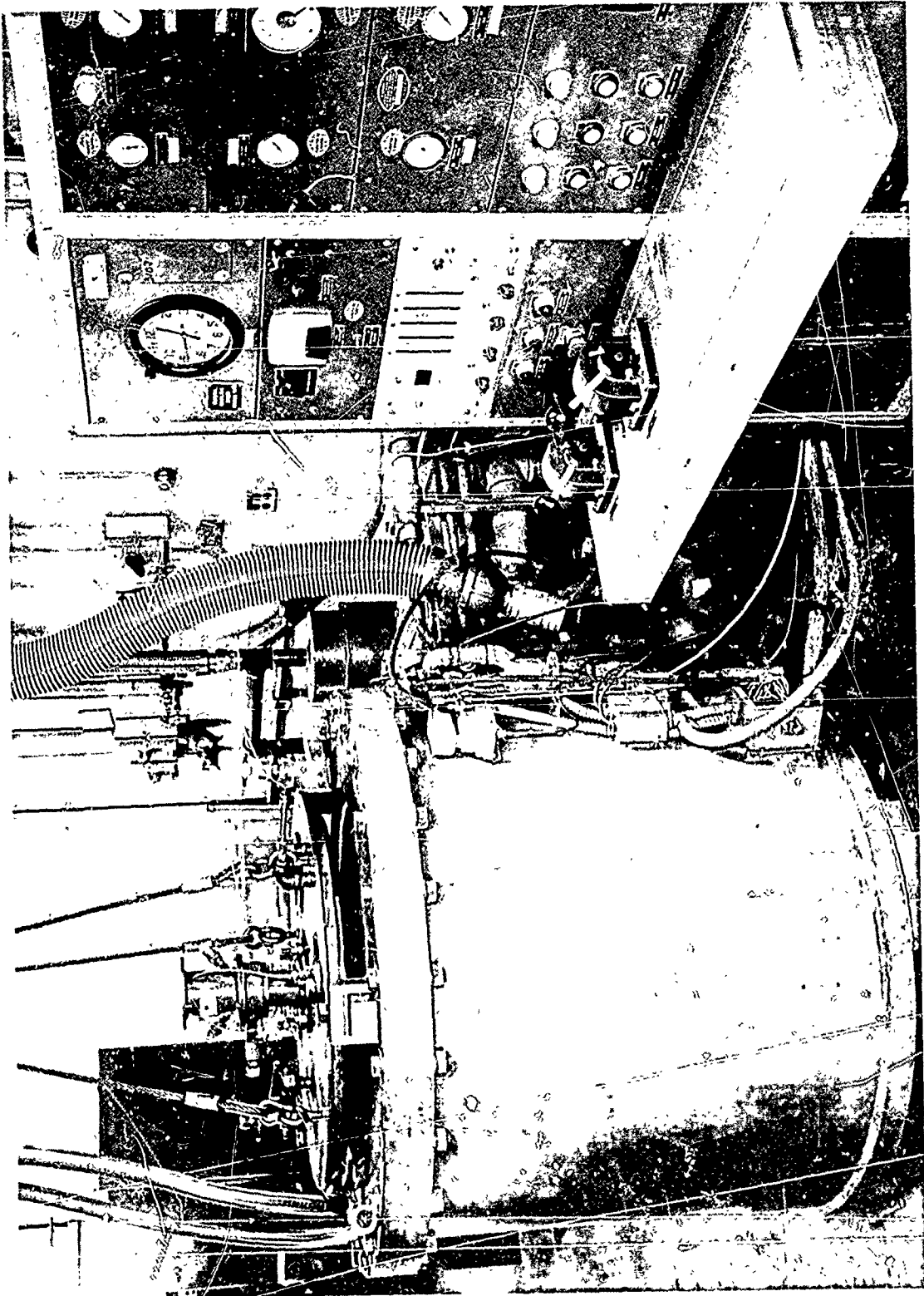
Figure 136

GENERAL ELECTRIC SPIN-TEST PIT FACILITY
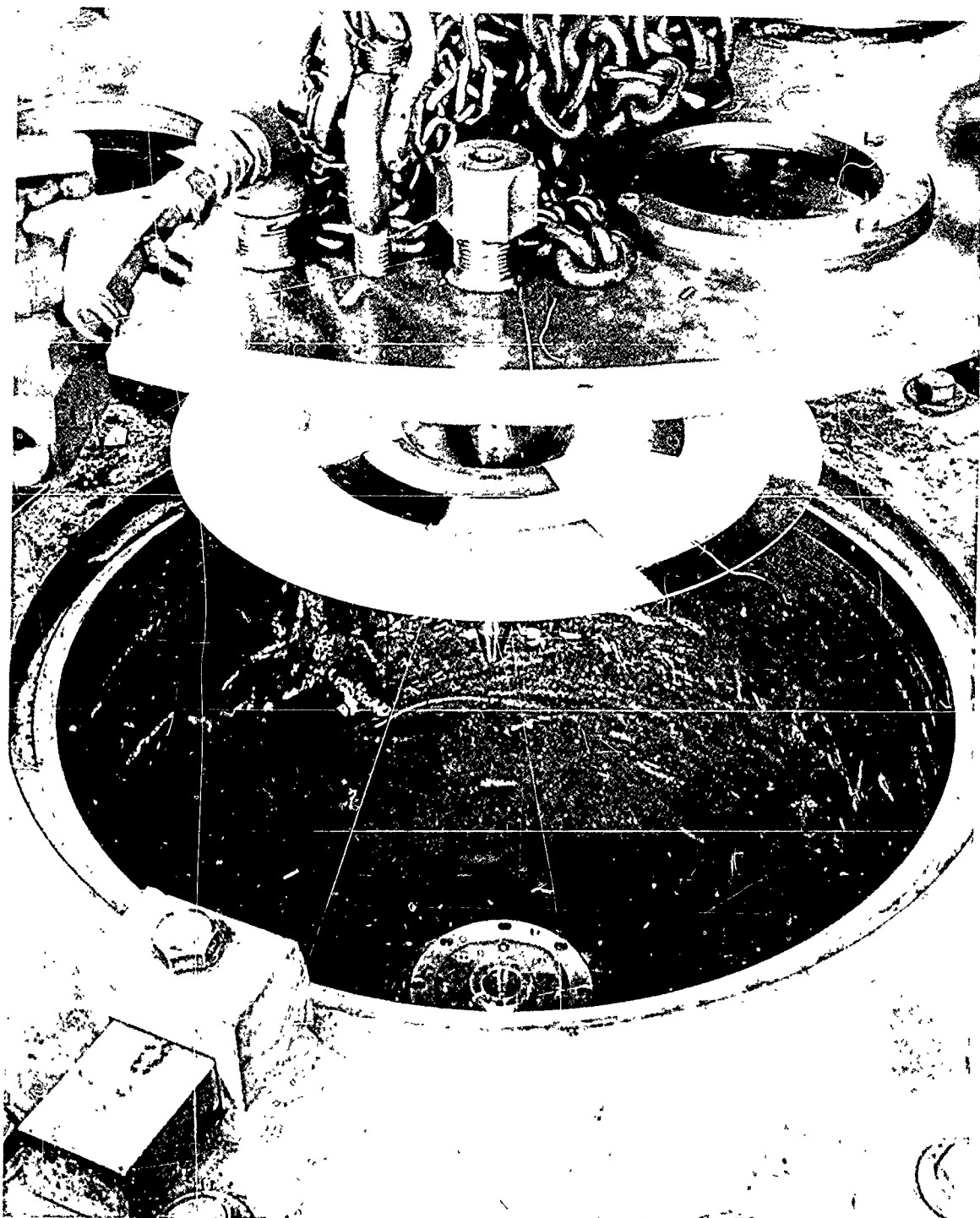
Figure 137

LOADING SPIN-TEST DISC 66-400-1
INTO SPIN-TEST PIT
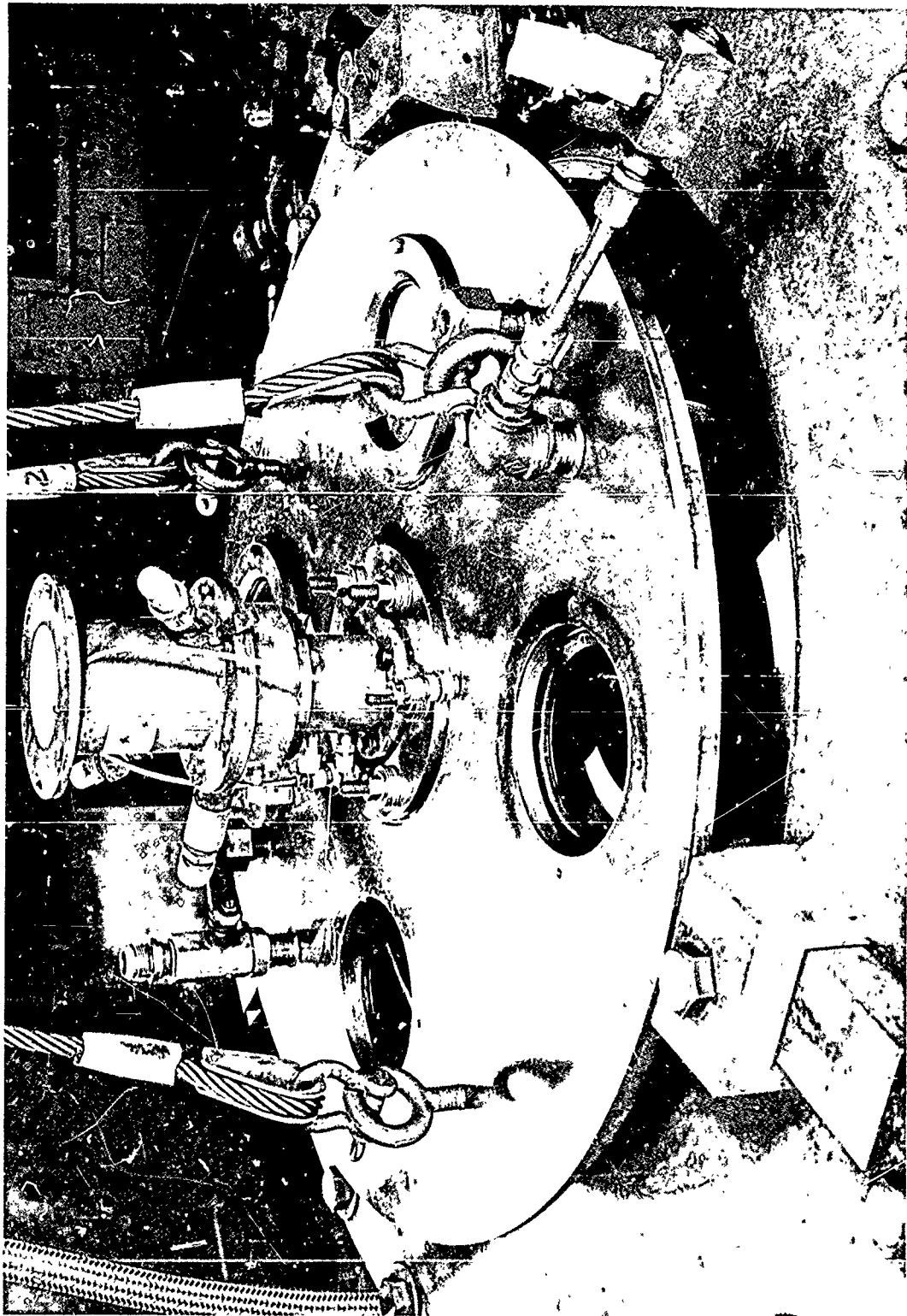
Figure 138

SPIN-TEST PIT JUST BEFORE FINAL CLOSING

Figure 139

INCO 713LC SPIN-TEST DISC NUMBER 66-400-1: COLOR CODED

Disc has been color coded over its surface to provide
identification of parts for re-assembly after bursting.
Note arbor mounted in bore.
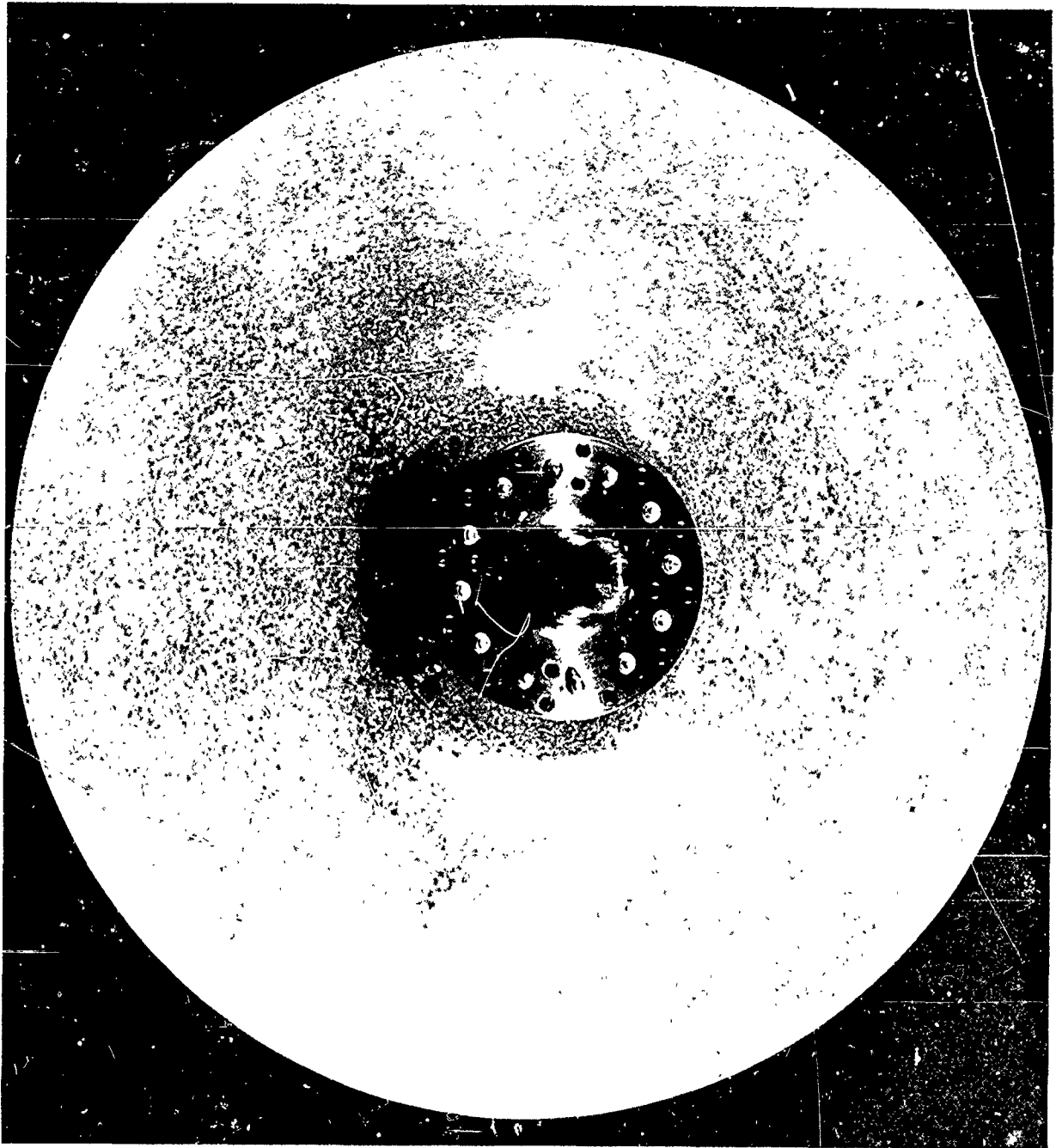
Figure 140

INCO 713 LC SPIN TEST DISC NUMBER 66-400-1:MACROETCHED
Disc has been fully machined and polished, then etched with a
mixture of HCl and H_2O_2 and fluorescent penetrant inspected.
The disc is ready for final testing preparation. The testing
arbor has been bolted in position on the disc hub.
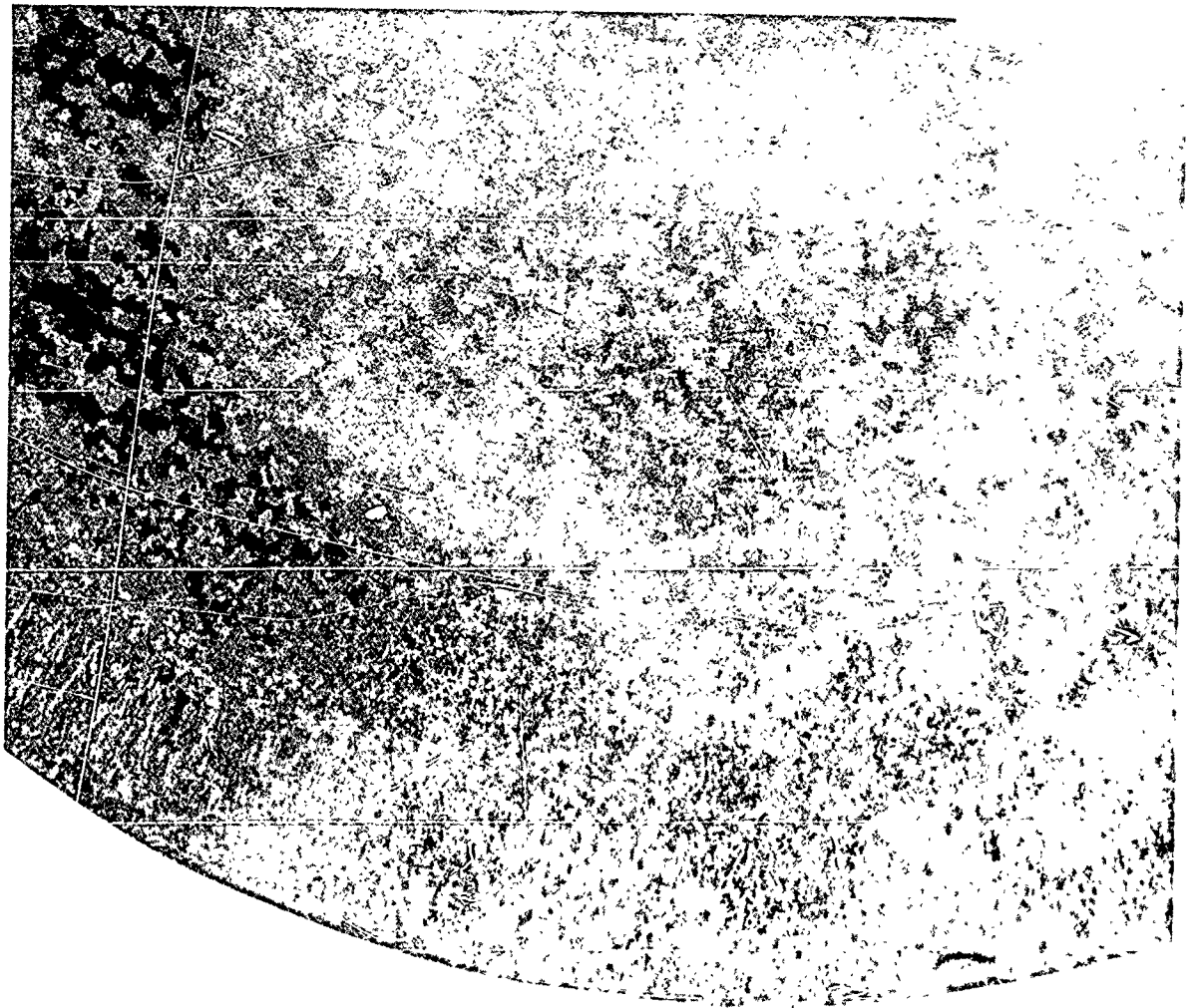
Figure 141

PARTIALLY COLUMNAR STRUCTURE NEAR O.D.
OF SPIN-TEST DISC NUMBER 66-400-1

This structure is typical of steep thermal
gradients during solidification and would
not, except under certain very unusual
circumstances, be considered detrimental.
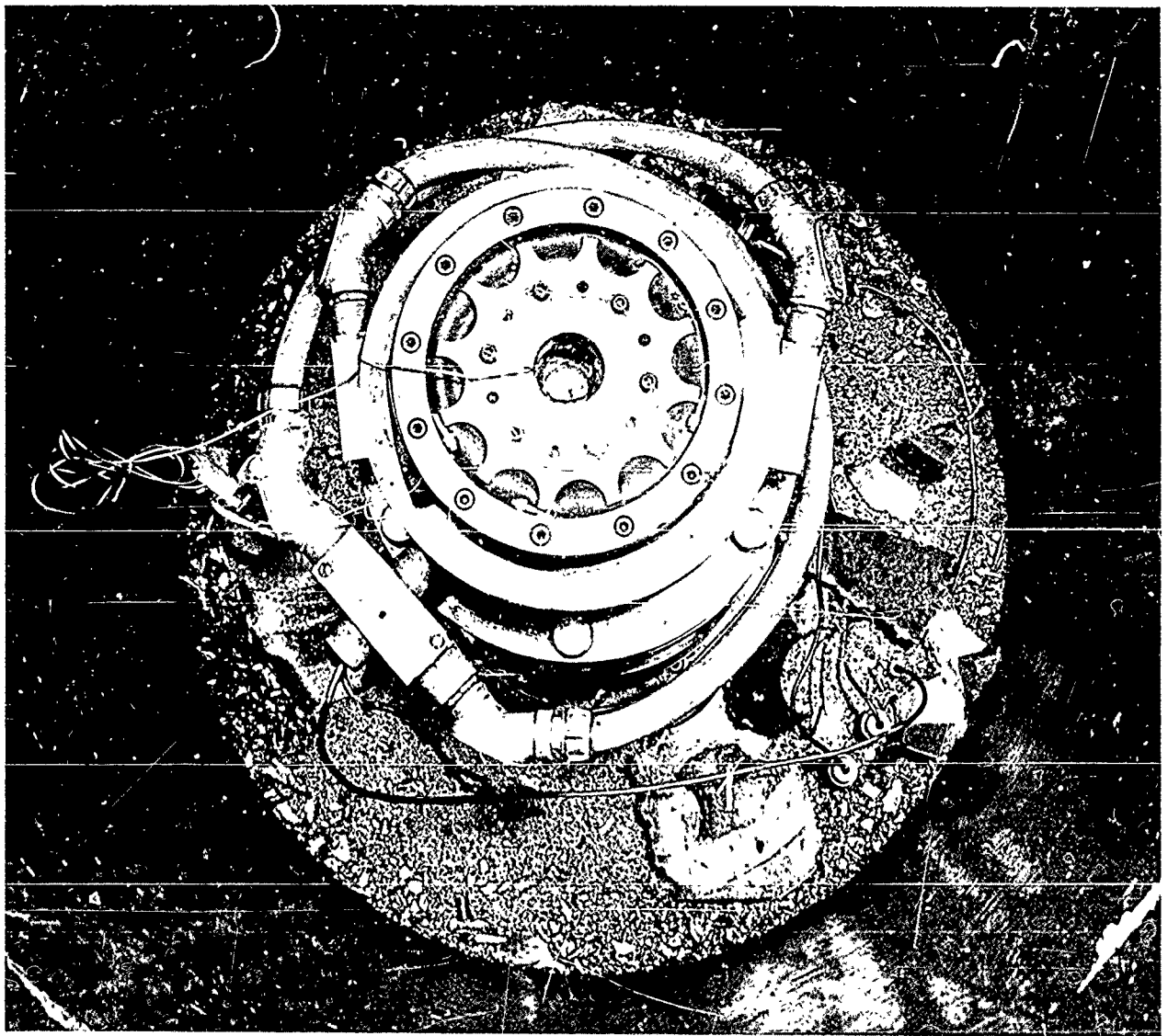
Figure 142

REMAINS OF SPIN-TEST DISC 66-400-1
AFTER BURSTING AT 23,800 RPM

This view into the test pit shows both
large and small pieces of the burst
disc laying on the pit floor after testing .

-279-
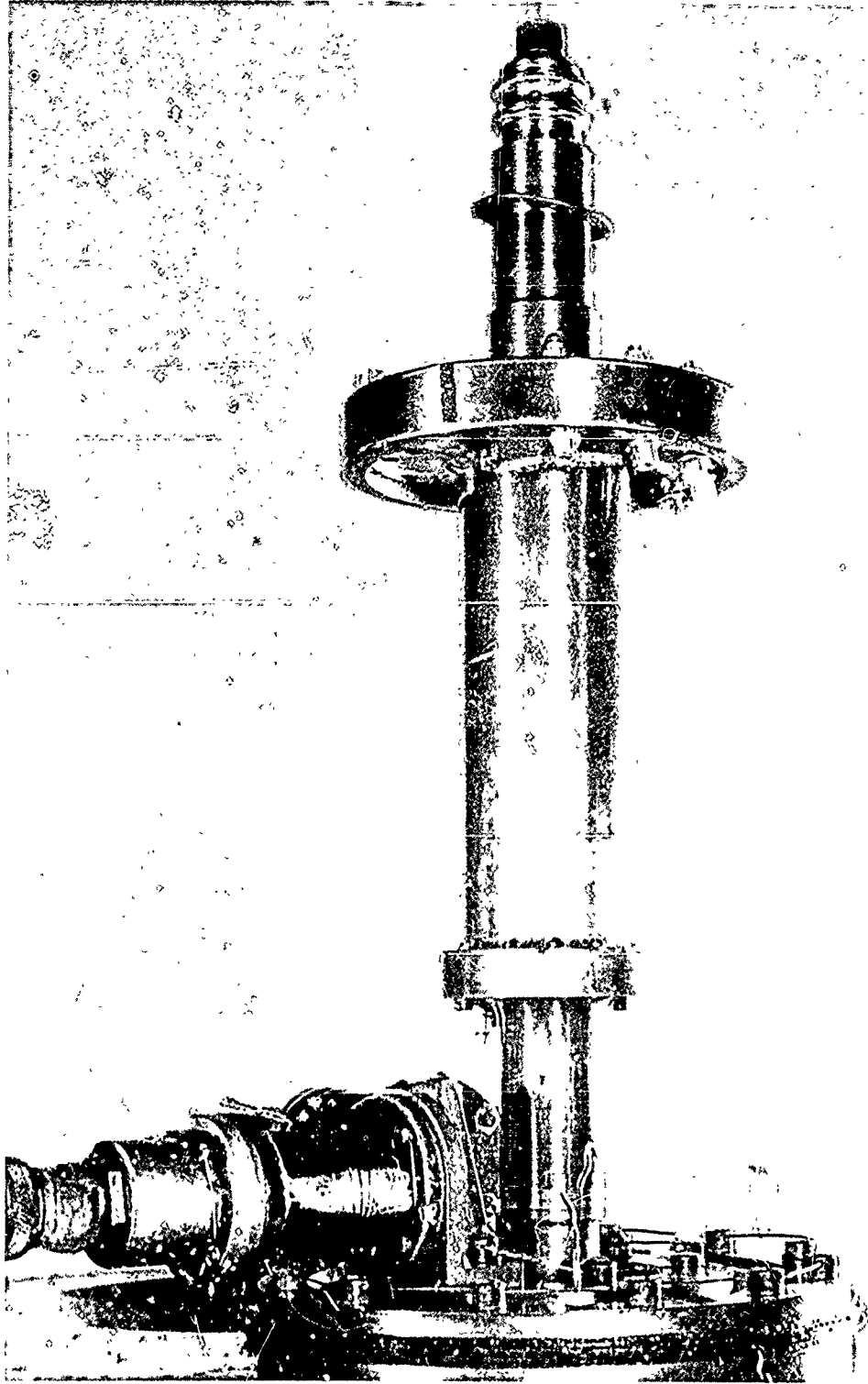
Figure 143

SPIN TEST ARBOR WITH SECTION
OF BURST DISC 66-400-1 ATTACHED
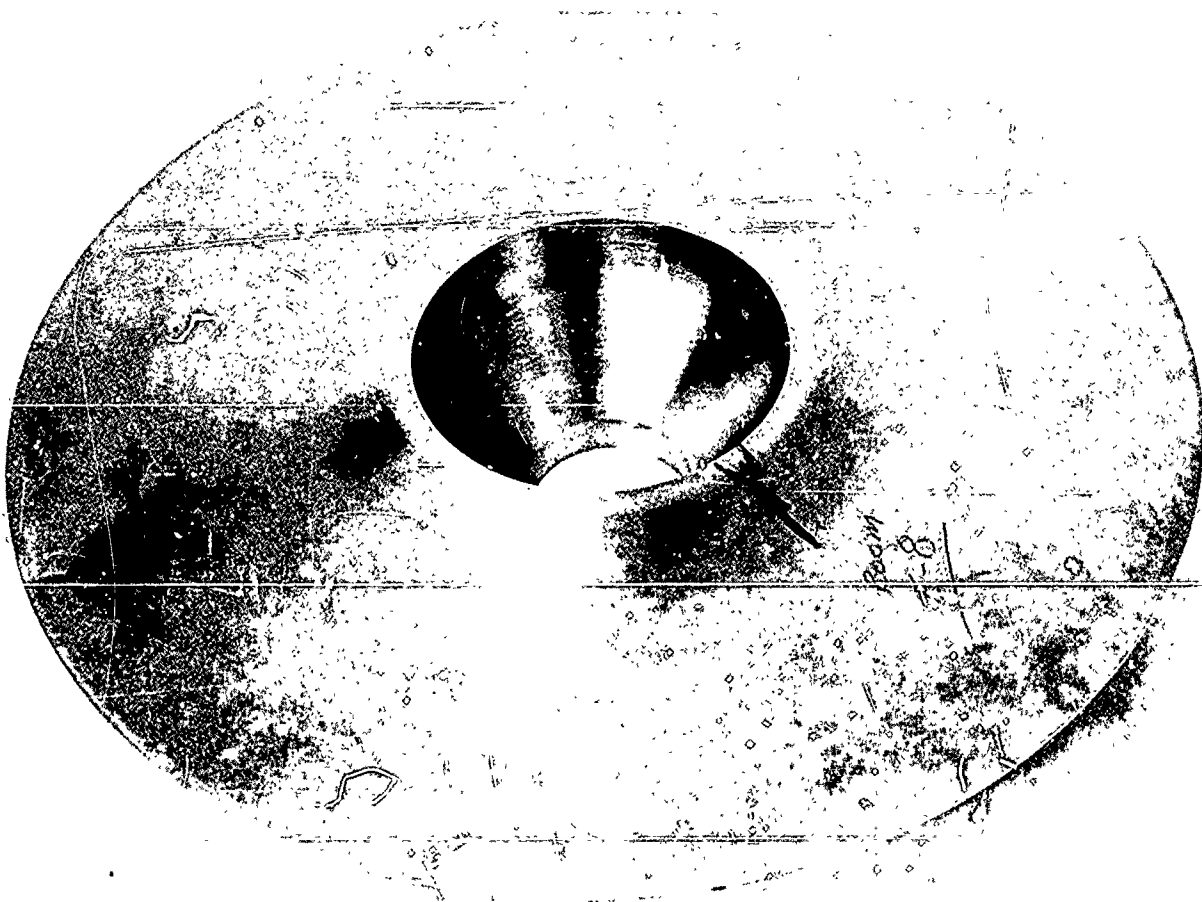
Roughly 1/3 Normal Size

Figure 144

SPIN-TEST DISC 66-433-1 SHOWING BORE
CRACK FOUND AFTER SPIN-TEST TO 91.7%
OF ULTIMATE TANGENTIAL STRENGTH

Roughly 2X size

Figure 145

BORE CRACK IN TESTED DISC 66-433-1
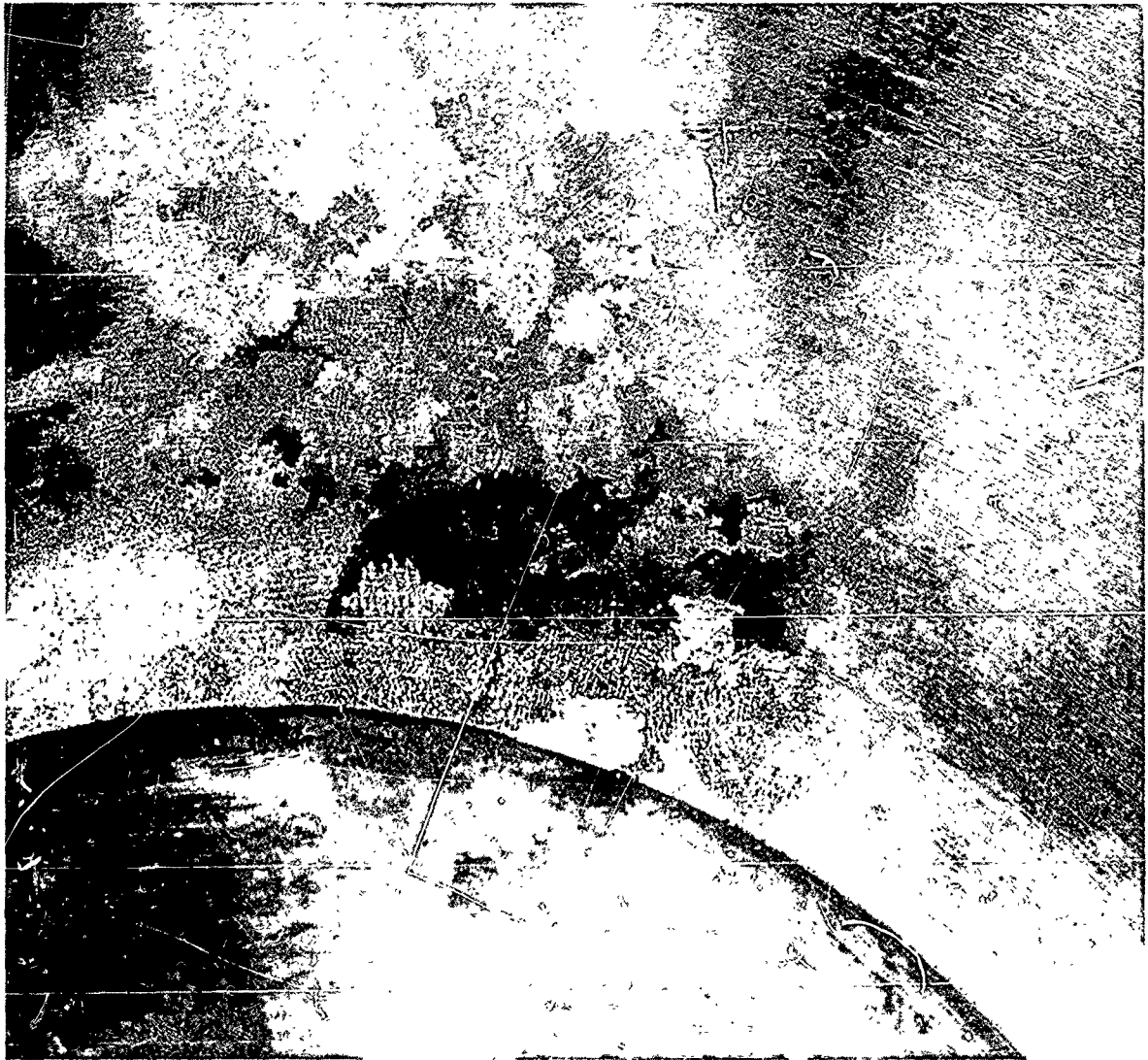
Figure 146

MACROSTRUCTURE ASSOCIATED WITH
BORE CRACK IN TESTED DISC 66-433-1

TABLE I

STATISTICAL DERIVED RUPTURE STRESS AND CREEP STRESS VALUES
FOR INCONEL 713C ALLOY
(Original Data Obtained From (54))

Temperature F	Stress, KSI for Rupture In Times Indicated					Stress, KSI for Designated Creep Rate			
	10 Hrs	100 Hrs	1,000 Hrs	10,000 Hrs	100,000 Hrs	0.000001%/Hr	0.00001%/Hr	0.0001%/Hr	0.001%/Hr
1400	107.9	79.9	59.2	43.8	32.4	24.5	32.3	42.6	56.3
1472	83.4	61.1	44.7	32.7	23.9	18.2	24.2	32.3	43.0
1500	75.5	55.0	40.1	29.2	21.3	16.2	21.6	29.0	38.8
1562	60.5	43.6	31.5	22.7	16.4	12.5	16.9	22.8	30.8
1600	52.8	37.8	27.1	19.4	13.9	10.6	14.5	19.7	26.7
1652	43.8	31.2	22.1	15.7	11.2	8.6	11.7	16.1	22.0
1700	36.9	26.0	18.4	13.0	9.1	7.0	9.7	13.3	18.4
1742	31.8	22.3	15.6	10.9	7.7	5.9	8.2	11.3	15.8
1800	25.8	17.9	12.4	8.6	6.0	4.6	6.5	9.1	12.7
1900	18.1	12.3	8.4	5.8	3.9	3.0	4.3	6.2	8.7

TABLE II

ORDERING SPECIFICATIONS FOR VACUUM REMELT INGOT

	Alloy 713LC		Alloy 41		Alloy 718	
Specification	AMS 5391A*		AMS 5545		AMS 5596A	
Analysis	min.	max.	min.	max.	min.	max.
C	0.03	0.07(55)	–	0.12	0.03	0.10
Cr	12.00	14.00	18.00	20.00	17.00	21.00
Co	–	1.00	10.00	12.00	–	1.00
S	–	0.015	–	0.015	–	0.015
Mn	–	0.25	–	0.10	–	0.35
Si	–	0.50	–	0.50	–	0.35
Ni	Bal		Bal		50.00	55.00
Zr	0.05	0.15	–	–	–	–
Mo	3.80	5.20	9.00	10.00	2.80	3.30
Fe	–	0.50	–	5.00	Bal	
Cu	–	0.50	–	–	–	0.10
A l	5.50	6.50	1.40	1.60	0.40	0.80
Ti	0.50	1.00	3.00	3.30	0.65	1.15
B	0.005	0.015	0.003	0.010	0.002	0.006
Cb/Ta	1.80	2.80	–	–	5.00	5.50

* Note exception. AMS 5391A is the current spec. for alloy 713C. LC grade carbon and iron levels taken from International Nickel Company Bulletin. (55)

TABLE III

TYPICAL

CHEMICAL ANALYSIS OF VACUUM MELTED
SUPERALLOY INGOT MELT STOCK

Element	Lot 6-3900 Inco 713LC		Lot 6-4220 Inco 718		Lot 6-4224 Rene 41	
	Vendor	Check	Vendor	Check	Vendor	Check
C	.05	.06	.05	.07	.08	.05
Mn	.10	.02	.10	.02	.10	.02
Cr	12.6	12.50	18.20	17.85	19.20	19.33
Si	.10	.04	.10	.03	.10	0.03
S	.003	.001	.003	.007	.004	.006
Mo	4.40	4.28	3.05	3.10	10.0	0.79
Ni	Bal	73.48	53.00	54.13	Bal	55.15
Cb&Ta	2.10	2.22	5.22	5.25	-	-
Ti	.73	.83	1.10	0.97	3.18	3.34*
Al	5.90	6.04	0.57	0.56	1.55	1.60
B	.008	.011	.004	.0047	.0043	.0049
Zr	.08	.092	-	-	-	-
Fe	.16	.16	Bal	Bal	.12	.53
Cu	.10	.02	.01	.02	-	-
Co	.10	-	0.53	0.55	11.1	10.13
P	-	-	.01	.003	-	-
H	-	1.1 ppm	-	5 ppm	-	9 ppm
N	-	12.4 ppm	-	32 ppm	-	27 ppm
O	-	13.1 ppm	-	22 ppm	-	28 ppm

Note: Purchasing Specifications: Inco 713LC - AMS 5391A
(Modified to low carbon grade) (For chemical analysis only)

Inco 718 - GE B50T68 S 3
AMS 5596A

Rene 41 - GE C50T53 S 7
AMS 5545

* Accepted at 0.04 above 3.30 max. required in GE C50T53 S 7 and AMS 5545

TABLE IV

MELTING AND CASTING DATA FOR SUPERALLOY HEATS

Casting Data

Heat Number	Alloy	Charge			Molds			Melting Pressure (microns)	Cold Leakup Rate (Microns per min.)	Liquidus Temp.* (°F)	Pouring Temp.*		Pouring Temp.* Recorded by Thermocouple in Mold
		Type	Lot or Heat No.	Wt. lbs.	Pattern No.	Type	No.				Mold No.	Super heat (°F)	
66-456	713LC	Ingot	6-3900	280	C-1489	Test Bars	2	19	-	2475	1	200	-
											2	200	-
65-506	718	Ingot	6.4220	281	C-1489	Test Bars	2	16	23	2440	1	200	-
											2	200	-
65-511	713LC	Ingot	6-3900	255	C-1490	Plates	2	16	-	2500	1	100	-
											2	200	-
65-522	R-41	Ingot	6-4224	292	C-1489	Test Bars	2	19	24	2525	1	100	-
											2	200	-
65-529	718	Ingot	6-4220	251	C-1490	Plates	2	20	-	2445	2	100	-
												200	-
65-542	R-41	Ingot	6-4224	252	C-1490	Plates	2	23	25	2445	2	100	-
												200	-
65-623	713LC	Revert	65-456	175.2	C-21	Spirals	2	5*	23	2450	1	200	-
			65-511	24.8	C-1489	Test Bars	1				2	200	-
											3	200	-
65-552	718	Revert	65-506	150	C-21	Spirals	2	8	24	2440	1	100	2435
					C-1489	Test Bars	1				2	100	2510***
											3	200	-
65-666	R-41	Revert	65-522	150	C-21	Spirals	2	8	28	2450	1	100	2435
					C-1489	Test Bars	1				2	100	2465
											3	200	-

*   Measured with Bi-Color pyrometer

**   Pirani gauges re-calibrated beginning with this heat.

*** Thermocouple break: reading is doubtful.

TABLE V

CHEMICAL ANALYSIS OF PHASE I VACUUM REMELT HEATS

Heat No.	Charge	Alloy	C%	Cr%	Mn%	Si%	S%	Mo%	Ni%	Cb&Ta%	Ti%	Al%	B%	Zr%	Fe%	Cu%	Co%
65-456	Ingot	713LC	.06	12.50	*.02	.03	.003	4.32	Bal.	2.30	.083	6.06	.0074	.094	.19	*.02	*.05
65-506	Ingot	718	.05	17.85	*.02	.06	.004	3.04	52.10	5.06	0.95	0.57	.0017	-	18.9	*.02	0.54
65-511	Ingot	713LC	.05	12.68	*.02	.05	.003	4.31	Bal.	2.22	.85	6.02	.009	.09	.20	*.02	*.05
65-522	Ingot	Rene 41	.08	19.23	*.02	.07	.006	9.79	55,15	-	3.37	1.55	.0054	-	.61	-	10.13
65-529	Ingot	718	.05	17.85	*.02	.06	.006	3.10*	54.13	5.23	0.99	0.44	.0038	-	18.04	*.02	0.64
65-542	Ingot	Rene 41	.07	19.62	*.02	.06	.004	9.54	55.15	-	3.21	1.44	.0054	-	.61	-	10.13
65-623	Revert	713LC	.05	12.30	*.02	.07	.003	4.39	Bal.	1.99	0.82	5.87	.0073	.09	.17	*.02	*.05
65-652	Revert	718	.05	17.97	*.02	.07	.012	3.10	Bal.	5.10	0.95	0.57	.0035	-	19.55	*.02	-
65-666	Revert	Rene 41	.07	19.00	*.02	.07	.005	9.57	Bal.	-	3.33	1.56	.0033	-	0.63	-	10.59
66-216	Ingot	713LC	.05	13.15	*.02	.06	.008	4.56	Bal.	2.25	0.83	6.05	.015	.087	0.10	*.02	*.05
66-267	50%Re-vert	713LC	.05	12.17	*.02	.05	.005	4.40	Bal.	2.24	0.66	6.10	.013	.105	0.18	*.02	*.05
66-296	100% Revert					No analysis required											
66-314	100% Revert					No analysis required											
66-377	Ingot	713LC	.04	12.60	*.02	.10	.007	4.53	Bal.	2.13	0.74	5.90	.013	.095	0.15	*.02	*.05
66-388	Ingot	713LC	.04	12.60	*.02	.10	.006	4.40	Bal.	1.94	0.71	5.90	.012	.070	0.14	*.02	*.05
66-400	Ingot	713LC	.04	12.41	*.02	.05	.008	4.59	Bal.	2.07	0.72	6.16	.013	.08	0.15	*.02	*.05
66-407	100% Revert					No analysis required											
66-416	66-407	713LC	.04	12.41	*.02	.07	.012	4.50	Bal.	2.05	0.72	6.18	.011	.076	0.15	*.02	*.05
66-433	Ingot	713LC	.06	13.48	*.02	.09	.006	4.43	Bal.	2.10	0.77	6.08	.011	.068	0.18	*.02	*.05
66-456	Ingot	713LC	.07	13.24	*.02	.07	.011	4.32	Bal.	2.10	0.88	5.85	.011	.050	0.12	*.02	*.05
66-485	Ingot	713LC	.06	13.82	*.02	.08	.007	4.48	Bal.	2.08	0.79	6.00	.012	.074	0.20	*.02	*.05
67-202	Ingot	718	.06	17.53	*.05	.02	.003	3.08	53.28	4.79	1.06	0.60	-	-	Bal.	.04	.68
67-268	Ingot	713LC	.06	13.30	.12	.06	.003	4.57	Bal.	2.18	0.69	6.00	.012	.105	0.19	*.02	*.05
67-284	Ingot	713LC	.05	13.90	*.02	.07	.012	4.48	Bal.	2.13	0.75	6.08	.011	.076	0.18	*.02	*.05

*Less than

Note: Where it is noted that no analysis was required, the heat was either a pilot heat for which no tests other than non-destructive tests were performed on the castings, or, as in the case of 66-407, the heat was made into ingots which were entirely remelted on the next heat.

TABLE V

CHEMICAL ANALYSIS OF PHASE I VACUUM REMELT HEATS

	Gas Analysis (ppm)		
	H	N	O
65-456	1.1	18.6	19.7
65-506	5.4	50.0	17.0
65-511	0.1	33.2	17.7
65-522	0.9	27.0	28.0
65-529	1.1	12.9	27.1
65-542	0.4	14.3	15.1
65-623	0.3	13.3	17.3
65-652	5.9	17.1	32.8
65-666	1.5	7.5	13.4

(Continued)

TABLE VI

BASE LINE MECHANICAL PROPERTIES
OF VACUUM MELTED AND CAST
INCO 713 LC

Heat Number 65-456

A.   Tensile Properties

Specimen Number	Thermal History	Test Temp. °F	Yield Strength .2% Offset PSI	Tensile Strength PSI	Elongation %	Reduction Area %
65-456-1A1	As Cast	R. T.	113, 040	132, 000	7. 0	11. 6
-1A2	"	R. T.	110, 400	131, 400	10. 0	15. 3
-1A3	"	R. T.	108, 000	123, 600	7. 0	14. 5
-1A5	"	R. T.	108, 240	130, 400	8. 0	9. 3
-1A6	"	R. T.	109, 680	128, 000	8. 0	14. 5
-1A7	ST.	R. T.	109, 440	131, 200	10. 0	17. 5
-1A8	"	R. T.	108, 000	131, 600	10. 0	14. 5
-1A9	"	R. T.	108, 000	133, 200	10. 0	19. 0
-1A10	"	R. T.	110, 160	137, 200	11. 0	13. 8
-1A11	"	R. T.	112, 800	137, 200	11. 0	18. 2
-2A4	As Cast	1000	101, 600	131, 600	8	24. 5
-2A5	"	1000	108, 000	129, 000	9	25, 9
-2A8	ST.	1000	107, 600	124, 800	12	30; 6
-2A9	"	1000	102, 400	127, 600	8	16. 7
-2A11	As Cast	1200	98, 000	135, 200	8	22. 4
-2A12	"	1200	100, 000	135, 800	7. 5	18. 2
-2B3	ST.	1200	103, 800	126, 000	10	23. 2
-2B5	"	1200	103, 200	125, 000	12	25. 3
-2B8	As Cast	1400	104, 000	130, 400	10	19. 6
-2B12	"	1400	96, 200	128, 400	5	9. 3
-1B9	ST.	1400	103, 600	125, 200	7	20. 3
-1C2	"	1400	108, 400	120, 000	4	18. 2
-2B14	As Cast	1600	68, 000	97, 000	7	13. 8
-2B15	"	1600	64, 000	98, 400	8	15. 3
-2B9	ST.	1600	93, 600	104, 000	6	8. 6
-2B10	"	1600	94, 000	104, 400	5	7. 8
-2A10	As Cast	1800	37, 040	58, 800	11	17. 5
-2B16	ST.	1800	51, 200	62. 600	10	18. 9

Test Speed - . 05 in. /min.
ST. = 2150°F - 2 hrs. - Air Cool
R. T. = Room Temperature

TABLE VI
(continued)

B. CREEP RUPTURE PROPERTIES

Specimen Number	Thermal History	Test Temp. °F	Stress PSI	Life Hrs.	Minimum Creep Rate %/Hr.	Elongation %	Reduction Area %
65-456-2B2	As Cast	1400	80,000	78.8	0.046	4.0	2.3
65-456-2B6	"	1600	40,000	161.0	0.016	6.0	5.5
65-456-2B4	St.	1600	40,000	243.7	0.005	6.0	5.5
65-456-2A16	As Cast	1800	22,000	64.4	0.038	7.0	7.0
65-456-2A14	ST.	1800	22,000	63.3	0.037	11.0	7.0

ST. = 2150°F - 2 hrs. - Air Cool

C. COMPRESSION PROPERTIES

Specimen Number	Thermal History	.2% Offset Compression Yield- PSI	Compression* Ultimate - PSI	E (psi)
65-456-1A12A	As Cast	106,000	300,000	7.8×10^6
B	"	109,500	361,000	7.1×10^6
C	"	104,900	335,000	7.2×10^6
65-456-1A13A	ST.	113,500	290,000	8.3×10^6
B	"	112,000	Not Detected	8.8×10^6
C	"	110,500	370,000	7.8×10^6

ST. = 2150°F - 2 hrs. Air Cool

*Based upon load at fracture and original cross sectional area. All fractures were shear with high ductility.

D. IMPACT PROPERTIES

Charpy Impact Test Data

Specimen Number	Thermal History	Test Temp. -°F	Impact-Strength Ft.-lbs.
65-456-1C10A	As Cast	-40	8.8
B	"	-40	6.8
65-456-1C11A	ST.	-40	12.2
B	"	-40	15.1
65-456-1C8A	As Cast	R.T.	8
65-456-1C9A	ST.	R.T.	13.9
B	"	R.T.	13.8
65-456-1C12A	As Cast	1200	9.9
B	"	1200	9.7
65-456-1C13A	ST.	1200	11.6
B	"	1200	13.5

TABLE VI
(continued)

E. FRACTURE TOUGHNESS TEST DATA*

Specimen Number	Thermal History	Test Temp. -°F	Energy to Fracture Ft. - lbs.	$G = \dfrac{\text{in-lbs.}}{\text{in}^2}$
65-456-1C16A	As Cast	-40	4.6	540
B	"	-40	5.5	642
65-456-2A1A	ST.	-40	8.8	988
B	"	-40	7.2	732
65-456-1C14A	As Cast	R.T.	5.5	712
B	"	R.T.	4.8	682
65-456-1C15A	ST.	R.T.	7.7	935
B	"	R.T.	8	8⌢⌢
65-456-2A2A	As Cast	1200	4.3	5⌢⌢
B	"	1200	5.9	689
65-456-2A3A	ST.	1200	6.6	756
B	"	1200	8.8	922

*All Tests Performed on Charpy Impact Test Specimens
Precracked in bending fatigue to an average depth of 0.2 inches at the root of the notch.

R.T. = Room Temperature
ST. = 2150°F - 2 hrs. - Air Cool

F. THERMAL FATIGUE

Specimen Number	Thermal History	Temp. Cycle-°F	Time Cycle-min..	Cycles To Failure	Heating Compressive Stress (psi)	Cooling Tensile Stress (psi)
65-456-2C5	As Cast	300-1600	5 heat-2.5 cool	196	132,000	57,700
-2C6	"	"	"	111	126,000	89,300
-2C7	ST.	"	"	430	105,000	86,600
-2C8	"	"	"	472	103,800	105,000
-2C9	"	"	"	187	92,000	123,000
-2C10	As Cast	300-1200	"	**	118,000	21,000
-2C11	"	"	"	**	107,500	38,000
-2C13	ST.	"	"	**	114,000	11,800
-2C14	"	"	"	**		

** Test discontinued after 1000 cycles without failure
AT. - 2150°F - 2 hrs. - Air Cool

TABLE VII

BASE LINE MECHANICAL PROPERTIES
OF VACUUM MELTED AND CAST
INCO 718

Heat Number 65-506

A. Tensile Properties

Specimen Number	Thermal History	Test Temp. °F.	Yield Strength .2% Offset PSI	Tensile Strength PSI	Elongation %	Reduction Area %
65-506-1A1	As Cast	R.T.	73,200	115,200	17	25.9
-1A2	"	R.T.	82,560	122,800	18	30.6
-1A3	"	R.T.	85,680	120,400	10	31.2
-1A4	ST_2	R.T.	40,800	91,200	35	35.9
-1A5	"	R.T.	40,800	91,600	29	29.7
-1A6	"	R.T.	41,280	92,000	33	34.3
-1A7	ST_2+A	R.T.	82,080	115,200	20	23
-1A8	"	R.T.	86,400	122,200	13	22.3
-1A9	"	R.T.	86,640	117,200	12	18.9
-1A10	"	1000	76,000	104,400	21	30.6
-1A11	"	1000	75,600	104,200	20	34.5
-1A12	"	1000	78,800	106,000	21	33.2
-1A13	"	1200	74,600	99,600	17.5	33.2
-1A14	"	1200	77,400	103,000	17.0	31.9
-1A15	"	1200	80,600	104,800	13.0	31.9
-1A16	"	1400	68,000	84,400	10.0	16.7
-1B1	"	1400	57,600	77,600	12.5	33.8
-1B2	"	1400	61,600	75,200	10	24.5

Test Speed = .05 in./min.
ST_2 - 1800°F-2 hrs-Air Cool
A = Aged: 1325°F-8 hrs-furnace cool to 1150°F-hold for 8 hrs-Air Cool
R.T. - Room Temperature

TABLE VII
(continued)

B. Creep-Rupture Properties

Specimen Number	Thermal History	Test Temp. °F.	Stress PSI	Life Hrs.	Minimum Creep Rate %/Hr.	Elongation %	Reduction Area %
65-506-1C8	ST$_2$+A	1200	100,000	– *	– *	17.0	26.5
-1C10	"	1300	72,500	9.3	0.105	4.0	3.2
-1C13	ST$_3$+A	1300	72,500	9.8	0.054	1.0	3.2
-1C14	ST$_2$+A	1300	60,000	109.6	0.010	7.0	6.3
-1C9	ST$_3$+A	1300	40,000	500D	0.0009	0	0
-1C16	ST$_2$+A	1200	68,000	67.6	0.0018	4.0	4.0

ST$_2$ = 1800°F-2 hrs-Air Cool
ST$_3$ = 1900°F-2 hrs-Air Cool
A = Aged: 1325°F-8 hrs-Furnace cool to 1150°F-hold 8 hrs-Air Cool
* = Failure on Loading
D = Test discontinued

C. Compression Properties

Specimen Number	Thermal History	.2% Offset Compression Yield-PSI	Compression* Ultimate-PSI	E (psi)
65-506-1B3A	ST$_2$	35,000	Not detected	6.3x10^6
B	"	41,300	380,000	5.8x10^6
-1B4A	ST$_2$+A	84,000	366,000	6.4x10^6
B	"	87,100	321,000	6.8x10^6

ST$_2$ = 1800°F-2 hrs-Air Cool
A = Aged: 1325°F-8 hrs-Furnace Cool to 1150°F-hold 8 hrs-
          Air Cool
*Based upon load at failure and original cross sectional area.
 All failures were ductile shear type.

D. Impact Properties

Charpy Impact Test Data			
Specimen Number	Thermal History	Test Temp.-°F.	Impact-Strength Ft.-lbs.
65-506-1B8A	ST$_2$+A	-40	10.0
B		-40	13.2
-1B9A		-40	12.6
B		-40	11.2
-1B6A		R.T.	12.7
B		R.T.	13.7
-1B7A		R.T.	15.7
B		R.T.	13.6
-1B10A		1200	18.6
B		1200	16.8
-1B11A		1200	19.8
B		1200	18.5

TABLE VII
(continued)

E. Fracture Toughness Test Data*

Specimen Number	Thermal History	Test Temp.-°F.	Energy to Fracture Ft.-lbs.	$G = \dfrac{\text{in-lbs.}}{\text{in}^2}$
65-506-1B14A	ST_2+A	-40	6.6	733
B		-40	6.5	666
-1B15A		-40	6.8	752
B		-40	6.5	709
-1B12A		R.T.	8.0	840
B		R.T.	7.8	828
-1B13A		R.T.	5.7	640
B		R.T.	5.8	595
-1B16A		1200	10.7	1182
B		1200	12.7	1268
-1C1A		1200	9.3	1046
B		1200	10.6	1173

ST_2 = 1800°F-2 hrs.-Air Cool
A = Aged: 1325°F-8hrs-Furnace Cool to 1150°F-hold for
        8 hrs.-Air Cool
R.T.= Room Temperature
*All tests performed on Charpy Impact Test Specimens pre-
 cracked in bending fatigue to an average depth of 0.2
 inch   at the root of the notch.

F. Thermal Fatigue

Specimen Number	Thermal History	Temp. Cycle-°F	Time Cycle-Min.	Cycles to Failure	Heating Compressive Stress	Cooling Tensile Stress
65-506-1C2	ST_2+A	300-1400	.5 Heat-2.5 Cool	*	92,000	76,200
-1C3	"	"	"	771	78,800	92,000
-1C4	"	"	"	387	86,600	89,300
-1C6	"	300-1200	"	*	59,900	82,700
-1C7	"	"	"	*	110,000	36,800

*Test discontinued after 1000 cycles without failure.

ST_2 = 1800°F-2 hrs-Air Cool
A = Aged: 1325°F-8 hrs.-Furnace Cool to 1150°F-hold for 8 hrs.-
        Air Cool.

TABLE VIII

BASE LINE MECHANICAL PROPERTIES
OF VACUUM MELTED AND CAST
RENE 41

Heat Number 65-522

A. Tensile Properties

Specimen Number	Thermal History	Test Temp. °F.	Yield Strength .2% Offset PSI	Tensile Strength PSI	Elongation %	Reduction Area %
65-522-1A1	As Cast	R.T.	79,680	128,000	16	23.1
-1A2	"	R.T.	78,480	124,400	16	18.9
-1A3	"	R.T.	77,520	126,400	19	19.7
-1A4	ST_4	R.T.	81,840	108,800	15	16.7
-1A5	"	R.T.	83,520	106,800	11	18.9
-1A6	"	R.T.	82,080	112,000	17	16
-1A7	ST_1	R.T.	81,600	126,000	33	32.6
-1A8	"	R.T.	81,600	129,600	33	29.9
-1A9	ST_4+A_1	R.T.	97,920	117,600	5	8.6
-1A10	"	R.T.	98,400	111,600	3	7.7
-1A11	"	R.T.	101,280	114,000	5	9.3
-1A12	ST_1+A_2	R.T.	89,280	112,000	8	7.8
-1A13	"	R.T.	88,320	110,400	7	9.3
-1A15	ST_4+A_1	1000	88,800	109,200	7	17.5
-1A16	"	1000	87,000	108,000	6.5	16.0
-1B2	"	1200	86,000	102,400	7	18.9
-1B3	"	1200	80,800	100,600	8	24.5
-1B5	ST_1+A_2	1200	80,200	101,800	11	20.3
-1B6	"	1200	78,000	99,400	11.5	24.5
-1B8	ST_4+A_1	1400	83,800	103,000	5	11.6
-1B7	"	1400	80,600	96,800	7	16.7
-1B10	"	1600	76,800	81,400	12	31.2
-1B11	"	1600	77,600	81,600	15	35.7
-1B13	"	1800	35,200	35,600	23	49.5
-1B14	"	1800	33,640	35,200	22.5	55.5

Test Speed = .05 in./min.
ST_1 = 2150°F-2 hrs-Air Cool
ST_4 = 1950°F-4 hrs- Air Cool
A_1 = Aged: 1400°F-16 hrs.-Air Cool
A_2 = Aged: 1650°F.-4 hrs.-Air Cool

TABLE VIII
(continued)

B. Creep-Rupture Properties

Specimen Number	Thermal History	Test Temp. °F.	Stress PSI	Life Hrs.	Minimum Creep Rate %/Hr.	Elongation %	Reduction Area %
65-522-2A15	ST_1+A_2	1650	25,000	72.8	0.145	6.0	7.8
-2A16	"	1600	40,000	31.7	0.028	6.0	7.0
-2B1	"	1400	60,000	101.7	0.007	1.0	0.8
-2A14	ST_4+A_1	1400	60,000	149.5	0.006	4.0	5.5

ST_1 = 2150°F-2 hrs-Air Cool.
ST_4 = 1950°F-4 hrs-Air Cool
A_1 = Aged: 1400°F-16 hrs-Air Cool
A_2 = " : 1650°F-4 hrs -Air Cool

C. Compression Properties

Specimen Number	Thermal History	.2% Offset Compression Yield-PSI	Compression* Ultimate-PSI	E (psi)
65-522-1C1A	ST_4	82,500	375,000	6.4×10^6
B	"	82,500	440,000	6.9×10^6
-1C2A	ST_4+A_1	97,100	348,000	7.8×10^6
B	"	97,500	336,000	7.0×10^6

ST_4 = 1950°F-4 hrs-Air Cool
A_1 = Aged: 1400°F-16 hrs-Air Cool
*Based upon load at failure and original cross section area. All failures ductile shear type.

D. Impact Properties

Charpy Impact Test Data

Specimen Number	Thermal History	Test Temp.-°F.	Impact-Strength Ft.-lbs.
65-522-1C3A	ST_4+A_1	-40	7.2
B	"	-40	7.9
-1C4A	"	-40	10.0
B	"	-40	7.9
-1C5A	"	R.T.	10.4
B	"	R.T.	6.9
-1C6A	"	R.T.	7.3
B	"	R.T.	8.1
-1C7A	ST_1+A_2	R.T.	7.0
B	"	R.T.	10.8
-1C8A	ST_4+A_1	1200	8.2
B	"	1200	8.1
-1C9A	"	1200	7.4
B	"	1200	6.1

TABLE VIII
(continued)

E. Fracture Toughness Test Data*

Specimen Number	Thermal History	Test Temp. -°F	Energy to Fracture Ft. -lbs.	$G = \dfrac{\text{in-lbs.}}{\text{in}^2}$
65-522-1C10A	ST_4+A_1	-40	9.2	928
B	''	-40	6.0	660
-1C11A	''	-40	6.3	619
B	''	-40	4.7	664
-1C12A	''	R.T.	12.1	1262
B	''	R.T.	6.5	634
-1C13A	''	R.T.	7.5	738
- B	''	R.T.	9.8	1188
-1C14A	''	1200	5.3	575
- B	''	1200	10.1	1056
-1C15A	''	1200	8.3	845
- B	''	1200	5.9	717

*All test performed on Charpy Impact Test Specimens precracked in
blending fatigue to an average depth of 0.2 inch   at the root of the
notch.

R.T. = Room Temperature
ST_1 = 2150°F-2 hrs. -Air Cool
ST_4 = 1950°F-4 hrs. -Air Cool
A_1 = Aged: 1400°F-16 hrs. -Air Cool
A_2 = Aged: 1650°F-4 hrs. -Air Cool

F. Thermal Fatigue

Specimen Number	Thermal History	Temp. (a) Cycle-°F	Cycles to Failure	Compressive Stress (psi) (Heating)	Tensile Stress (psi) (Cooling)
65-522-2A4	ST_1+A_2	300-1600	243	107,000	79,400
2A2	ST_1+A_2	''	297	101,000	76,520
2A3	ST_4+A_1	''	57	114,800	95,000
2A7	ST_4+A_1	''	129	106,300	95,500
2A5	ST_1+A_2	300-1200	(b)	101,100	36,900
2A8	ST_4+A_1	''	(b)	105,900	28,600

(a) Time cycle, 30 seconds heating, 150 seconds cooling
(b) Test discontinued after 1000 cycles without failure

-298-

TABLE IX

THE EFFECT OF SPECIAL HEAT TREATMENTS
ON THE TENSILE PROPERTIES
OF INCO 713LC, INCO 718, AND RENE 41

Alloy and Specimen Number	Thermal History	Test Temp. °F	Yield Strength .2% Off-set (PSI)	Tensile Strength (PSI)	Elong. (%)	Reduction in Area (%)
RENE 41						
65-522-2B5	(1)	1200	86,400	98,800	7.0	15.3
65-522-2B6	(1)	1200	85,600	101,600	6.0	18.9
INCO 718						
65-506-1C9	(2)	RT	120,480	148,000	8.0	19.6
INCO 713LC						
65-456-1B6	(3)	RT	109,200	122,800	5.0	10.8
65-456-1C3	(4)	RT	120,720	136,800	5.0	7.8
65-456-1A15	(5)	RT	119,280	129,600	7.0	11.6
65-456-1A16	(5)	RT	120,480	133,200	6.0	12.3
65-456-1B7	(6)	RT	105,840	119,200	8.0	16.1
65-456-1B11	(6)	RT	108,240	116,800	6.0	15.3
65-456-1B5	(7)	RT	122,880	137,600	9.0	14.5
65-456-1C7	(8)	RT	115,680	135,200	8.0	10.8

Thermal Histories:
- (1) 1975°F-3hrs-water quench, repeated three times, followed by 1400°F-16hrs-air cool.
- (2) 1900°F-2hrs-air cool, plus 1325°F-8hrs-furnace cool to 1150°F-hold 8hrs-air cool, then held in creep test at 40,000 psi-1300°F for 500 hrs. Creep test terminated and tensile strength determined.
- (3) 1550°F-16hrs-air cool.
- (4) 2150°F-2hrs-air cool + 1550°F-16hrs-air cool.
- (5) " + 1700°F-16hrs-air cool.
- (6) 1700°F-16hrs-air cool.
- (7) 2150°F-2hrs-air cool + 1200°F-16hrs-air cool.
- (8) 1200°F-16hrs-air cool

TABLE X

THE EFFECT OF HIGH TEMPERATURE HEAT TREATMENT
ON THE TENSILE PROPERTIES OF INCO 718 TEST BARS

Heat and Specimen Number	Heat Treatment AC = Air cool OQ = Oil Quench	Yield Strength (psi at .2% offset)	Ultimate Strength (psi)	Elongation (%)	Reduction in Area (%)	Hardness Rc
65-506-1A7*	1850°F - 2 hr - AC + Age**	82,080	115,200	20	23.0	
1A8*	1850°F - 2 hr - AC + Age	86,400	122,200	13	22.3	
1A4*	1850°F - 2 hr - AC	40,800	91,200	35	35.9	
67-202-1B5	1850°F - 2 hr - AC + Age	109,440	142,400	17	22.4	35
1B6	1850°F - 2 hr - AC + Age	110,400	145,600	18	23.7	35
1A12	2150°F - 2 hr - AC	39,840	86,000	51	50.0	Rb 82
1A13	2150°F - 2 hr - AC	40,560	82,800	46	51.7	Rb 81
1A14	2150°F - 2 hr - OQ	32,880	80,000	53	51.2	Rb 81
1A15	2150°F - 2 hr - OQ	32,160	84,700	65	54.0	Rb 82
1B7	2150°F - 2 hr - AC + Age	128,400	148,000	22	35.1	38
1B9	2150°F - 2 hr - AC + Age	129,840	151,200	27	34.5	38
1B10	2150°F - 2 hr - OQ + Age	135,600	148,000	13	38.3	39
1B11	2150°F - 2 hr - OQ + Age	136,080	147,600	9	29.2	38
1B1	2150°F - 2 hr - AC +	79,680	130,000	28	28.5	29
1B2	1850°F - 2 hr - AC + Age	92,400	129,600	12	25.9	33
1B3	2150°F - 2 hr - OQ +	122,880	144,000	17	26.5	34
1B4	1850°F - 2 hr - AC + Age	124,800	141,600	16	30.5	36

* Note: These data included for comparison and represent the original Inco 718 heat described in IR 8-297(II)

** Note: Ageing treatment in all cases as follows: 1325°F - 8 hrs - furnace cool to 1150°F - hold for 8 hrs - air cool to room temperature.

TABLE XI

ROOM TEMPERATURE TENSILE PROPERTIES OF INCO 713LC
HELD AT 1200°F FOR 50 AND 100 HOURS

Heat and Specimen No.	Prior Heat Treatment	Time at 1200°F	Yield Strength (psi) at .2% Offset	Ultimate Strength (psi)	Elongation (%)	Red. in Area (%)	Hardness Rc
65-456-1A1*	None	None(control)	113,040	132,000	7	11.6	35
66-173-2B4	None	100 hrs.	120,480	147,200	9	18.2	35
2B5	None	100 hrs.	124,320	154,000	9	13.8	34
2B7	None	100 hrs.	123,160	149,200	9	13.8	35
65-456-1A7*	2150°F-2 hr-AC	None	109,440	131,200	10	17.5	
66-173-2A7	2150°F-2 hr-AC	50 hrs.	125,280	151,200	9	13.8	39
2A8	"	50 hrs.	129,840	154,000	10	13.1	39
2A9	"	50 hrs.	132,480	158,400	10	10.1	38
2A3	"	100 hrs.	132,480	160,000	9	16.7	36
2A4	"	100 hrs.	131,280	151,600	9	16.7	40
2A5	"	100 hrs.	128,160	153,600	9	18.9	38
2A10	"	100 hrs.	132,240	152,000	7	12.3	38
2B1	"	100 hrs.	135,600	156,800	9	15.3	39

* Note: These data taken from TABLE VI, and are included for easy comparison.

TABLE XII

CHEMICAL ANALYSIS OF CERAMIC SHELL-MOLD HEATS OF CAST-TO-SIZE TEST BARS

Element	Alloy 713LC H(No. AK-1683	Alloy 718 H(AL-8	Alloy Rene 41 H(No. AL-9)
	(%)	(%)	(%)
C	0.06		
Mu	< .02		
Cr	12.38		
Si	0.04	Incomplete	Incomplete
S	0.003		
Mo	4.36		
Ni	Balance		
Cb&Ta	2.29		
Ti	0.86		
Al	6.02		
B	0.009		
Zr	0.13	–	
Fe	0.15		
Cu	< .02		
Co	< .05		
P	–		
H	6.0 ppm	5.0 ppm	1.4 ppm
N	18.2 ppm	32.0 ppm	14.7 ppm
O	38.2 ppm	22.0 ppm	22.5 ppm

TABLE XIII

ROOM TEMPERATURE
TENSILE PROPERTIES OF CAST-TO-SIZE
TEST BARS

Alloy & Heat Number	Specimen Number	Thermal History	Yield Strength at .2% Offset (PSI)	Ultimate Strength (PSI)	Elongation (%)	Red. in Area (%)
713LC	A-1	A.C.	94,000	101,000	20	-
AK-1683	1	S.T.$_1$	102,480	136,000	16	24.5
	2	S.T.$_1$	133,440	154,400	9	16.0
	3	S.T.$_1$	111,840	140,000	20	23.8
	4	S.T.$_1$	113,520	128,000	15	22.4
	5	S.T.$_1$	108,240	125,600	11	23.1
	6	S.T.$_1$	116,400	121,600	11	20.3
	7	S.T.$_1$	115,440	119,200	11	24.5
	8	S.T.$_1$	114,720	124,400	11	21.7
	9	S.T.$_1$	118,080	128,800	17	28.6
	10	S.T.$_1$	123,600	156,000	12	23.1
Inco 718	A-1	A.C.	94,000	138,000	20	-
AL-8	1	S.T2+A	112,800	138,400	5	18.2
	2	"	112,800	141,200	5	16.0
	3	"	115,200	140,800	5	15.3
	4	"	117,600	146,000	8	17.5
	5	"	120,880	139,200	5	16.7
	6	"	115,200	139,600	5	16.7
	7	"	110,160	141,200	9	16.7
	8	"	109,920	144,400	10	18.2
	9	"	112,800	138,400	6	14.5
	10	"	110,400	144,000	7	19.6
Rene' 41	A-1	A.C.	93,000	140,000	12.0	-
AL-9	1*	ST3+A2	112,560	113,200	0	0
	2	"	115,440	136,800	4	8.6
	3	"	118,560	143,200	4	7.8
	4	"	114,720	134,800	4	7.8
	5	"	109,440	136,000	5	10.8
	6	"	117,360	135,200	3	6.3
	7	"	118,080	142,800	3	7.8
	8*	"	122,400	136,000	0	0
	9	"	113,280	135,200	4	10.1

-303-

Notes:

        Test Speed   0.05 in./min.

ST_1 = 2150°F - 2hrs - air cool
ST_2 = 1800°F - 2hrs - air cool
ST_3 = 1950°F - 4hrs - air cool
A_1 = 1325°F - 8hrs furnace cool to 1150°F - 8hrs- air cool to room temp.
A_2 = 1400°F - 16hrs - air cool
AC = As Cast, no heat treatment.

*Porosity visible in fracture.

TABLE XIV

LOW CYCLE FATIGUE DATA

Inconel 713 Low Carbon – R.T. and 1000°F – A Ratio = 1.0

Spec. No.	Test Temp.	%ϵ_T *	%ϵ_{Alt} *	%ϵ_e *	%ϵ_p *	Modulus ** psi $\times 10^{-6}$ E	Cycles to Failure	Failure Location and/or Comments
66-456-2G	R.T.	1.78	.89	1.00	.78	28.1	694	Test Section
66-400-2F	R.T.	1.23	.615	.87	.36	31.0	1,111	Test Section
66-433-2D	R.T.	1.14	.57	.81	.33	27.8	1,286	Test Section
66-433-2J	R.T.	1.43	.715	.93	.50	28.6	1,306	Test Section
66-456-2J	R.T.	1.03	.515	.74	.29	28.6	2,162	Test Section
66-388-2K	R.T.	1.02	.51	.79	.23	29.8	2,298	Test Section
66-456-2D	R.T.	1.02	.51	.80	.22	26.9	2,988	Test Section
66-400-2K	R.T.	.71	.355	.66	.05	30.2	8,632	Test Section
66-388-2D	R.T.	.67	.335	.66	.01	28.0	9,928	Test Section
66-388-2J	R.T.	.71	.355	.69	.02	28.4	10,321	Test Section
66-433-2K	R.T.	.56	.28	.55	.01	29.8	17,710	Test Section
66-388-2E	1000°F	1.22	.61	.96	.26	25.4	145	Test Section
66-433-2F	1000°F	.922	.461	.882	.04	24.7	799	Test Section
66-456-2K	1000°F	.811	.405	.790	.02	24.6	1,417	Test Section
66-433-2E	1000°F	.76	.38	.75	.01	24.3	2,437	Test Section
66-400-2G	1000°F	.684	.342	.67	.01	24.5	4,199	Test Section
66-400-2J	1000°F	.715	.357	.71	.005	23.9	4,418	Test Section
66-433-2H	1000°F	.53	.265	.52	.01	24.8	7,665	Test Section
66-388-2G	1000°F	.50	.25	.49	.01	24.3	16,282	Test Section
66-388-2H	1000°F	.357	.18	.347	.01		20,000 ↑	No Failure
66-388-2H	1000°F	.54	.27	.53	.01	23.7	11,201	Test Section

* Values measured at 1/2 of cyclic life
** Moduli measured on 1st cycle

Symbols: T = Total
Alt = Alternating
e = Elastic
p = Plastic

-305-

TABLE XV

COEFFICIENT OF THERMAL EXPANSION
OF CAST INCO 713LC

Temperature Range $^{\circ}F$	Coefficient of Thermal Expansion on/in/$^{\circ}F$
RT- 200	5.60×10^{-6}
" 400	7.08×10^{-6}
" 600	7.62×10^{-6}
" 800	8.41×10^{-6}
" 1000	8.65×10^{-6}
" 1200	8.89×10^{-6}
" 1400	8.91×10^{-6}
" 1600	9.38×10^{-6}
" 1800	9.80×10^{-6}
" 2000	10.55×10^{-6}

Sample No. 65-456-1B2

Heat Treated:
$2150^{\circ}F$ - 2 hrs - Air Cool

TABLE XVI

NOTCHED TENSILE AND STRESS RUPTURE PROPERTIES
OF CAST INCO 713LC

Heat Treatment: 2150°F - 2 hrs - air cool

Heat and Specimen Number	Test Temp. (°F)	Stress Concentration Factor(K_t)	Root Radius	Yield Strength (psi .2% off.)	Tensile Strength (psi)	Elong. (%)	Stress (psi)	Life (hrs)	Elong. (%)
66-400-2C	Room	Smooth bar-no notch		110,880	148,000	16.0	-	-	-
66-400-2D	Room	2.0	.025"	177,800	193,300	1.0	-	-	-
66-400-2E	Room	3.0	.009"	182,700	192,400	0	-	-	-
66-400-2H	Room	3.7	.0055"	187,100	191,600	0	-	-	-
65-456-2B3*	1200	Smooth bar-no notch		103,800	126,000	10.0	-	-	-
66-173-2B3	1200	2.0	.025"	(no curve)	198,276	1	-	-	-
66-173-2B8	1200	3.0	.009"	194,250	200,300	1	-	-	-
66-173-2B10	1200	3.7	.0055"	196,700	199,900	1	-	-	-
65-456-2A14*	1800	Smooth bar-no notch		-	-	-	22,000	63.3	11
66-173-2A2	1800	Smooth bar-no notch		-	-	-	22,000	60.9	10
66-173-2B2	1800	2.0	.025"	-	-	-	22,000	445.0	6
66-173-2B6	1800	3.0	.009"	-	-	-	22,000	625.0	3
66-173-2B9	1800	3.7	.0055"	-	-	-	22,000	208.9	3

* Base line data heat, See Table VI

Average Notched-Unnotched Tensile Ratio: At 1200°F, 1.58
At Room Temp., 1.30

TABLE XVII

LOW TEMPERATURE CREEP TEST DATA - CAST INCO 713LC - FINAL SUMMARY TABLE

Form: Cast and heat treated 1/2" section keel block test bars.
Heat Treatment: Solution treated 2150°F, 2 hrs., air cooled.

Heat and Specimen Number	Test Temperature	Stress (psi)	Maximum Creep Prior to Rupture (%)	Time to Reach Max. Creep (hrs)	Rupture Data Life (hrs)	Elongation (%)	Red. in Area (%)
66-456-2F	1000°F	70,000	-0.012	526	Test terminated without failure		
66-456-2H	1000°F	80,000	-0.016	500	"	"	"
66-456-2E	1000°F	90,000	-0.018	503	"	"	"
67-506-2B	1000°F	105,000	+0.029	523	"	"	"
66-433-2G	1200°F	70,000	-0.034	526	Test terminated without failure		
66-485-2F	1200°F	80,000	-0.024	500	"	"	"
66-485-2G	1200°F	90,000	+0.021	503	"	"	"
67-496-2A	1200°F	95,000	+0.085	502	"	"	"
67-496-2B	1200°F	100,000	+0.072	475.5	495.3	0.4	2.6
67-506-2A	1200°F	105,000	+0.209	454.8	471.9	1.1	3.6
66-097-2J	1200°F	110,000	+0.182	26.7	33.6	0.2	2.4

TABLE XVIII

ROOM TEMPERATURE TENSILE PROPERTIES AND POROSITY LEVEL
OF INCO 713LC TEST BARS
CUT FROM SIMPLE PLATE CASTINGS

Heat Number 65-511

(All bars heat treated 2150°F, 2 hrs, air cool)

Specimen Number	Plate Length (inches)	Pouring Temperature (Liquidus+°F)	Mold Condition	Microporosity Level	Yield Strength .2% Offset (psi)	Tensile Strength (psi)	Elongation %	Reduction in Area %
1A1	6	100	Nucleated	0-1	113,280	150,800	13	19.6
1A2	5	100	"	0-1	111,360	142,000	13	14.5
1A3	6	100	"	1-2	112,800	136,000	11	15.3
1A4	6	100	"	2-3	110,400	131,200	11	14.5
1A5	6	100	"	2-3	110,880	130,000	9	16.0
1A6	6	100	"	4-5	108,000	125,600	11	13.1
1A7	6	100	"	3-4	111,360	134,800	12	16.0
1C1	3	100	Nucleated	0-1	111,360	150,800	12	18.2
1C2	3	100	"	0-1	107,760	143,600	15	18.9
1C3	3	100	"	0-1	108,000	136,000	13	14.5
1B1	6	100	Plain	0-1	115,680	142,400	10	14.5
1B2	6	100	"	2-3	112,320	137,600	14	18.2
1B3	6	100	"	3-4	109,920	134,000	12	17.5
2B4	6	100	"	3-4	109,680	133,600	12	16.0
1B5	6	100	"	2-3	109,680	128,000	11	14.5
1B6	6	100	"	4-5	105,360	116,000	6	14.5
1B7	6	100	"	3-4	104,160	125,200	12	17.5
1D1	3	100	Plain	0-1	112,080	144,400	10	15.3
1D2	3	100	"	0-1	112,360	140,000	10	16.7
1D3	3	100	"	0-1	109,920	131,200	10	16.7

TABLE XVIII. (Continued)

Specimen Number	Plate Length (inches)	Pouring Temperature (Liquidus+.°F)	Mold Condition	Microporosity Level	Yield Strength .2%Offset (psi)	Tensile Strength (psi)	Elongation %	Reduction in Area %
2A1	6	200	Nucleated	0-1	111,360	143,600	13	16.7
2A2	6	"	"	0-1	110,640	140,000	11	17.5
2A3	6	"	"	1-2	110,400	130,800	10	14.5
2A4	6	"	"	1-2	106,400	126,400	10	19.6
2A5	6	"	"	1-2	108,000	126,000	11	15.3
2A6	6	"	"	2-3	102,720	121,600	11	16.0
2A7	6	"	"	3-4	107,040	120,800	9	13.8
2C1	3	200	Nucleated	0-1	101,760	146,800	17	23.1
2C2	3	"	"	0-1	104,400	135,200	15	18.2
2C3	3	"	"	0-1	99,120	132,000	15	21.8
2C4	3	"	"	0-1	100,800	128,000	16	20.3
2B1	6	200	Plain	0-1	110,400	139,200	10	18.8
2B2	6	"	"	0-1	105,120	125,600	11	19.7
2B3	6	"	"	0-1	106,320	128,400	12	17.5
2B4	6	"	"	2-3	105,600	125,200	11	18.9
2B5	6	"	"	4-5	106,560	126,400	11	13.8
2B6	6	"	"	2-3	100,800	120,800	10	14.6
2B7	6	"	"	2-3	98,160	118,400	10	18.9
2D1	3	200	Plain	0-1	108,960	140,000	15	16.0
2D2	3	"	"	0-1	106,800	126,000	13	19.6
2D3	3	"	"	0-1	105,600	122,400	12	18.9
2D4	3	"	"	0-1	108,000	125,200	9	16.8

ROOM TEMPERATURE TENSILE PROPERTIES AND POROSITY LEVEL OF INCO 718 TEST BARS CUT FROM SIMPLE PLATE CASTINGS

Heat Number 65-529

(All bars heat treated 1800°F, 2 hrs, air cool plus 8 hours at 1325°F, cooled to 1150°F at 100°F/minute, held at 1150°F for 8 hours, air cooled.)

Specimen Number	Plate Length (inches)	Pouring Temperature (Liquidus+°F)	Mold Condition	Microporosity Level	Yield Strength .2% Offset (psi)	Tensile Strength (psi)	Elongation %	Reduction in Area %
1A1	6	100	Nucleated	0-1	94,320	130,000	17	18.9
1A2*	"	"	"	0-1	91,920	119,200	8	14.5
1A3	"	"	"	0-1	92,880	124,800	14	16.0
1A4	"	"	"	1-2	88,800	120,400	14	15.3
1A5	"	"	"	1-2	89,520	120,000	17	14.5
1A6	"	"	"	2-3	90,000	110,400	12	16.7
1A7	"	"	"	1-2	89,290	116,800	12	17.5
1C1	3	100	Nucleated		96,400	133,600	16	21.7
1C2	"	"	"		93,800	130,000	16	18.2
1C3	"	"	"		93,360	126,800	16	26.6
1B1	6	100	Plain	0-1				
1E2	"	"	"	0-1				
1B3	"	"	"	1-2				
1B4	"	"	"	1-2				
1B5	"	"	"	0-1				
1B6	"	"	"	1-2				
1B7	"	"	"	0-1				
1D1	3	100	Plain		103,920	143,600	16	19.6
1D2	"	"	"		97,200	134,400	18	18.9
1D3	"	"	"		95,760	126,800	16	19.0

*Defective test bar.

TABLE XX

ROOM TEMPERATURE TENSILE PROPERTIES AND POROSITY LEVEL OF RENE'41 TEST BARS CUT FROM SIMPLE PLATE CASTINGS

Heat Number 65-542

(All bars heat treated 1950°F, 4 hrs, air cool plus 1400°F, 16 hrs, air cool.)

Specimen Number	Plate Length (inches)	Pouring Temperature (Liquidus+°F)	Mold Condition	Microporosity Level	Yield Strength .2% Offset (psi)	Tensile Strength (psi)	Elongation %	Reduction in Area %
1A1	6	100	Nucleated	0-1	103,920	123,200	5	6.3
1A2	"	"	"	0-1	102,000	122,400	5	9.3
1A3	"	"	"	0-1	101,040	118,000	5	9.3
1A4	"	"	"	0-1	98,400	112,400	4	5.5
1A5	"	"	"	0-1	96,240	107,600	4	7.7
1A6	"	"	"	0-1	96,720	106,000	3	10.0
1A7	"	"	"	1-2	96,240	103,600	3	6.3
1C1	3	100	"		106,080	126,800	4	6.3
1C2	"	"	"		102,480	117,200	4	5.5
1C3	"	"	"		99,120	112,800	4	8.6
1B1	6	100	Plain	1-2				
1B2	"	"	"	1-2				
1B3	"	"	"	0-1				
1B4	"	"	"	1-2				
1B5	"	"	"	0-1				
1B6	"	"	"	1-2				
1B7	"	"	"	1-2				
1D1	3	100	Plain		102,720	123,600	4	9.3
1D2	"	"	"		100,080	111,200	3	6.3
1D3*	"	"	"		101,520	109,600	1	4.0

*Broke in shoulder.

TABLE XXI

ROOM TEMPERATURE TENSILE PROPERTIES AND POROSITY LEVEL
OF INCO 713LC TEST BARS
CUT FROM SIMPLE PLATE CASTINGS

Heat Number 66-216
(All bars heat treated 2150°F, 2 hrs, air cool)

Specimen Number	Plate Length (inches)	Pouring Temperature (Liquidus+°F)	Mold Condition	Microporosity Level	Yield Strength .2% Offset (psi)	Tensile Strength (psi)	Elongation %	Reduction in Area %
1A1*	6	100	Nucleated, Riser pre-heated.	0 - 1	115,200	156,000	13.0	17.5*
1A3	6	100	"	0 - 1	108,000	144,000	16.0	20.3
1A5	6	100	"	1 - 2	109,440	121,200	6.0	13.1
1A7	6	100	"	2 - 3	109,920	136,800	14.0	21.0
1C1	3	100	Nucleated, riser pre-heated	0 - 1	114,480	160,800	18.0	21.7
1C2	3	100	"	1 - 2	112,320	142,400	12.0	18.2
1C3	3	100	"	1 - 2	111,120	146,000	12.5	21.1
1C4	3	100	"	N.S.	110,640	142,800	12.0	18.2
1B1*	6	100	Plain, riser preheated	0 - 1	113,520	158,400	19.0	18.9*
1B3	6	100	"	1 - 2	109,680	135,600	13.0	19.6
1B5	6	100	"	1 - 2	110,640	140,400	14.0	18.9
1B7	6	100	"	2 - 3	109,200	137,200	14.0	20.3
1D1	3	100	Plain, riser preheated	0 - 1	117,600	156,400	13.0	16.8
1D2*	3	100	"	1 - 2	114,480	130,200	7.0	16.7*
1D3	3	100	"	1 - 2	115,200	140,400	10.0	17.5
1D4	3	100	"	N.S.	110,880	135,600	12.0	18.2

* Broke out of 1 inch gauge length.
N.S. = No Specimen

TABLE XXI (Continued)

ROOM TEMPERATURE TENSILE PROPERTIES AND POROSITY LEVEL OF INCO 713LC TEST BARS CUT FROM SIMPLE PLATE CASTINGS

Heat Number 66-216
(All bars heat treated 2150°F, 2 hrs, air cool)

Specimen Number	Plate Length (inches)	Pouring Temperature (Liquidus+°F)	Mold Condition	Microporosity Level	Yield Strength 0.2% Offset (psi)	Tensile Strength (psi)	Elongation %	Reduction in Area %
2A1	6	200	Plain	0 - 1	110,880	141,200	13.0	21.0
2A3	6	200	riser	0 - 1	124,560	136,800	9.0	18.9
2A5	6	200	preheated.	2 - 3	115,200	129,200	10.0	13.8
2A7	6	200	"	2 - 3	108,000	127,200	10.0	16.7
2C1	3	200	Plain	0 - 1	107,760	136,000	14.0	13.8
2C2	3	200	riser	0 - 1	103,680	136,800	14.0	14.5
2C3	3	200	preheated	1 - 2	104,880	130,000	13.0	17.5
2C4	3	200	"	N.S.	104,880	124,800	13.0	21.9
2B1	6	200	Nucleated	0 - 1	116,160	152,400	14.0	17.4
2B3	6	200	riser	1 - 2	112,560	139,200	13.0	16.7
2B5	6	200	preheated	0 - 1	110,160	140,400	13.0	17.5
2B7	6	200	"	1 - 2	108,960	133,200	13.0	18.1
2D1	3	200	Nucleated	0 - 1	112,800	147,600	15.0	19.5
2D2	3	200	riser	1 - 2	110,880	142,400	13.0	18.2
2D3	3	200	preheated	1 - 2	108,480	136,000	15.0	18.2
2D4	3	200	"	N.S.	109,920	134,000	12.0	20.3

N.S. = No specimen

TABLE XXII

ROOM TEMPERATURE TENSILE PROPERTIES OF INCO 713LC TEST BARS CUT FROM THREE INCH LONG PLATE CASTINGS

Heat Number 66-267

(All bars heat treated 2150°F, 2 hrs, air cool)

Specimen Number	Plate Length (inches)	Pouring Temperature (Liquidus+°F)	Mold Condition	Microporosity Level	Yield Strength 0.2% Offset (psi)	Tensile Strength (psi)	Elongation %	Reduction in Area %
1C1	3	100	Plain	Not determined	105,600	136,800	14	15.3
1C2	3	100	"		101,760	124,800	11	19.6
1C3	3	100	"		106,800	124,000	9	15.3
1C4	3	100	"		103,920	122,800	15	21.7
1D1	3	100	Nucleated		109,680	146,000	14	14.5
1D2*	3	100	"		108,240	125,200	6	16.0
1D3	3	100	"		108,960	133,200	11	12.3
1D4	3	100	"		107,520	142,400	15	17.5
2C1	3	200	Plain		120,160	137,200	13	16.7
2C2	3	200	"		109,920	125,200	10	16.0
2C3	3	200	"		106,560	116,000	8	15.3
2C4	3	200	"		103,440	116,800	7	17.5
2D1*	3	200	Nucleated		112,800	134,800	10	13.1
2D2	3	200	"		108,000	129,200	10	19.6
2D3	3	200	"		108,240	128,400	10	16.7
2D4	3	200	"		110,400	126,800	11	14.5

*Broke outside gauge marks.

TABLE XXIII

1200°F TENSILE PROPERTIES OF INCO 713LC TEST BARS CUT FROM SIMPLE PLATE CASTINGS

Heat Number 66-267

(All bars heat treated 2150°F, 2 hrs, air cool)

Specimen Number	Plate Length (inches)	Pouring Temperature (Liquidus+°F)	Mold Condition	Microporosity Level	Yield Strength 0.2% Offset (psi)	Tensile Strength (psi)	Elongation %	Reduction in Area %
1B1	6	100	Nucleated	Not determined	103,600	132,800	17	30.6
1B3	6	100	"		103,600	124,800	10	22.4
1B5	6	100	"	–	98,400	116,000	9	16.0
1B7	6	100	"		91,800	112,400	15	23.1
1A1	6	100	Plain		103,600	129,200	10	19.6
1A3	6	100	"	–	92,000	111,000	12	21.4
1A5	6	100	"		93,200	110,000	9	23.1
1A7	6	100	"		96,000	114,400	10	20.3
2B1	6	200	Nucleated		100,400	121,200	12	26.6
2B3	6	200	"		97,200	115,200	10	21.0
2B5	6	200	"	–	94,800	110,800	8	18.8
2B7	6	200	"		97,200	113,600	13	24.9
2A1	6	200	Plain		90,200	120,400	14	25.2
2A3	6	200	"	–	97,600	106,800	10	25.9
2A5	6	200	"		97,200	104,600	6	37.7
2A7	6	200	"		98,000	107,800	9	37.0

TABLE XXIV

1600°F TENSILE PROPERTIES OF INCO 713LC TEST BARS CUT FROM SIMPLE PLATE CASTINGS

Heat Number 66-267

(All bars heat treated 2150°F, 2 hrs, air cool)

Specimen Number	Plate Length (inches)	Pouring Temperature (Liquidus+°F)	Mold Condition	Microporosity Level	Yield Strength 0.2% Offset (psi)	Tensile Strength (psi)	Elongation %	Reduction in Area %
1B2	6	100	Nucleated	Not determined	92,000	102,800	6	10.1
1B4	6	100	"		100,000	100,600	1	4.7
1B6	6	100	"		82,400	98,600	4	11.6
1A2	6	100	Plain		84,000	100,000	7	13.1
1A4	6	100	"	—	83,000	100,000	6	11.6
1A6	6	100	"		87,000	101,000	1	6.3
2B2	6	200	Nucleated		94,000	104,000	3	7.0
2B4	6	200	"	—	92,400	102,400	3	5.5
2B6	6	200	"		93,460	103,600	4	7.0
2A2	6	200	Plain		96,800	104,000	4	8.6
2A4	6	200	"	—	94,000	100,400	2	9.3
2A6	6	200	"		95,800	105,200	4	8.6

TABLE XXV

FLUIDITY DATA FOR VACUUM MELTED AND CAST INCO 713LC

Heat & Casting No.	Casting Description	Liquidus Temperature (Bi-Color)	Liquidus Temperature (Thermocouple)	Casting Temperature (Bi-Color)	Casting Temperature (Thermocouple)	Spiral Length (Inches)
66-106-1	Spiral	2500°F	-	2600°F	2475°F	16
66-106-2	"	"	-	2700°F	2575°F	44
66-106-3	Octabar	"	2390°F	2700°F	-	-
66-153-1	Spiral	2450°F	-	2520°F	2440°F	13
66-153-2	"	"	-	2600°F	2530°F	36
66-153-3	Octabar	"	2390°F	2560°F	-	-

-318-

TABLE XXVI

PROPERTIES OF INCO 713LC TEST BARS CAST FROM A 100% REVERT CHARGE
(ALL GATES AND RISERS)

Heat and Specimen Number	Mold Condition	Thermal History	Test Temperature °F	Yield Strength at 0.2% Offset (PSI)	Tensile Strength (PSI)	Elongation (%)	Reduction in Area (%)
65-623-3A1	Plain	2150-2-AC	Room	115,440	140,000	14.0	15.3
65-623-3A2	Plain	"	Room	113,040	139,600	14.0	19.6
65-623-3B1	Nucleated	"	Room	119,280	144,000	13.0	16.7
65-623-3B2	Nucleated	"	Room	116,640	137,600	8.0*	16.0
65-623-3A4	Plain	"	1200	100,000	121,400	10.0	26.6
65-623-3A9	Plain	"	1200	92,800	123,400	10.0	29.2
65-623-3B4	Nucleated	"	1200	100,000	127,600	13.0	32.0
65-623-3B5	Nucleated	"	1200	103,200	125,600	11.0	28.6
65-623-3A6	Plain	"	1600	85,200	104,000	5.0	13.8
65-623-3A7	Plain	"	1600	69,400	105,000	5.0	12.3
65-623-3B6	Nucleated	"	1600	94,800	105,400	4.0	7.0
65-623-3B7	Nucleated	"	1600	92,200	105,600	5.0	9.3

*Test bar broke out of gauge length.

Heat and Specimen Number	Mold Condition	Thermal History	Test Temperature °F	Stress (PSI)	Minimum Creep Rt. (%)	Life (hrs)	El (%)	RA (%)
65-623-3B8	Nucleated	2150-2-AC	1800°F	22,000	0.045	60.8	3.0	3.2
65-623-3A8	Plain	"	1800	22,000	0.071	61.4	4.0	9.3

TABLE XXVII

TENSILE PROPERTIES OF 0.505" DIAMETER TEST BARS
FROM ONE-INCH SECTION OCTABAR CASTINGS

Heat and Specimen Number	Mold Condition	Thermal History	Test Temperature °F	Yield Strength at 0.2% Offset (PSI)	Tensile Strength (PSI)	Elongation (%)	Reduction in Area
66-106-3B	Nucleated	As Cast	Room	107,700	120,000	7.5	12.6
66-106-3F	Plain	As Cast	Room	105,900	119,500	7.5	13.8
66-106-3C	Nucleated	As Cast	1200	90,800	119,000	9.0	16.3
66-106-3E	Plain	As Cast	1200	88,900	117,000	10.0	18.1
66-153-3C	Plain	2150-2-AC	Room	120,300	140,500	8.0	13.7
66-153-3E	Nucleated	2150-2-AC	Room	122,400	137,000	6.5	11.9
66-153-3D	Plain	2150-2-AC	1200	108,000	116,250	4.0	12.7
66-153-3F	Nucleated	2150-2-AC	1200	105,200	129,000	6.0	13.4

Note: Casting 66-106-3 poured at liquidus +200°F.
      Casting 66-153-3 poured at liquidus +100°F.
      See Figures 90 and 91.

-320-

TABLE XXVIII

HEAVY SECTION PROPERTIES OF CAST INCO 713LC

Heat Treatment: 2150°F, two hours, cooled in retort to 1200°F, air cooled.

Section Size: 5 1/4 inches.

Specimen Number	Yield Strength at 0.2% offset (psi)	Ultimate Tensile Strength (psi)	Elongation (%)	Reduction in Area (%)	Hardness (Rockwell C)
67-334-2A1	88,800	96,800	8	22.5	32
3	96,000	105,200	4	16.8	33
5	98,640	114,000	9	16.8	34
8	98,830	110,000	9	10.1	34

Specimen Number	Rupture Life (hr) 1800°F, 22,000 psi	Minimum Creep Rate (%/hr.)	Elongation (%)	Reduction in Area (%)
67-334-2A2	29.2	0.07	8.0	12.3
4	42.9	0.09	14.0	29.2
6	28.3	0.14	12.0	21.0
9	19.6	Not Determined	20.0	13.1

Impact Strength (Ft-Lbs, Charpy "V" notched)

Specimen Number	
67-334-2A7	13.9
10	13.2

Table XXIX

SPECIFICATIONS FOR AFRICAN METALS CORPORATION
COBALT OXIDE

	Gray Co Oxide 75/76% Co	Black Co Oxide 71 and 73% Co	Met-Grade Co Oxide 76/77% Co
Composition:			
Co3O4	45%	88%	20%
CoO	55%	12%	80%
Top Density: (gr per cc)	2.6	1.6	2.7
Particle Size -200	99.85%	99.75%	99.90%
Standard Pkg:	100-kilo kegs	250-lb. kegs	250-lb. kegs
Price:	$1.36 per lb. delivered E. of Miss. R.	71%--$1.28 per lb. 73%--$1.32 per lb. del'd E. of Miss. R.	$1.85 per lb. Co element contained FOB Port of N. Y.

Note: These prices may be compared with $31.75/lb. for technical grade cobalt
oxide from a chemical supply company.

-322-

TABLE XXX

AGGREGATE MIXES EVALUATED FOR SURFACE FINISH

Binder: Sodium silicate
Alloy cast: AMS 5355A
Pouring Temperature: 3000°F (L+330°F)

Heat & Casting Number	Aggregate		Percent Binder
68-014-2	35 mesh kyanite*	100%	12
68-014-3	100 mesh kyanite 35 mesh kyanite	75% 25%	18
68-014-4	100 mesh kyanite	100%	20
68-014-5	168 mesh zircon 100 mesh kyanite	50% 50%	11.5
68-014-6	105 mesh zircon	100%	3
68-014-7	168 mesh zircon 105 mesh zircon	50% 50%	3
68-014-8	168 mesh zircon	100%	3
68-014-9	100 mesh kyanite, ethyl silicate binder (Control)		3

* calcined kyanite

TABLE XXXI

SUMMARY OF INITIAL EXPERIMENTS USING MOLDABLE EXOTHERMIC COMPOUNDS IN VACUUM CASTING
OF INCO 713LC

Heat and Casting Number	Riser 1	Riser 2	Pouring Temperature	Pressure at Pour	Results
66-601-1	Pre-formed vacuum exothermic, 4" I.D. with 1" wall.	–	200°F Superheat	16 microns	Extremely violent outgassing from sleeve as soon as metal made contact. Continued until solidification.
66-601-2	Pre-formed vacuum exothermic, 4" I.D. with 1" wall.	–	200°F Superheat	20 microns	Same as for 66-601-1. Difficult to evaluate riser effectiveness due to gas.
66-601-3	Plain riser, 4" I.D.	–	200°F Superheat	20 microns	Quiet, no reaction. Riser surface froze off flat. Large shrink cavity at base of riser extended into plate.
66-601-4	Plain riser, 4" I.D.	–	200°F Superheat	20 microns	Same as 66-601-3.
67-021-1	Pre-formed vacuum exothermic, 4" I.D. with 1" wall. Greatly increased venting.	Plain 4" I.D.	250°F Superheat	500 mm ARGON	No violent outgassing. Smoke generated by exothermic could be seen issuing from vent holes in sleeve. Metal was quiet. A clear feeding advantage for the exothermic riser was noted in cross sectioned casting.
67-021-2	Pre-formed vacuum exothermic, 4" I.D., 1" wall. Greatly increased venting.	Plain 4" I.D.	250°F Superheat	20 microns	Extremely violent outgassing as for 66-601-1 in the riser containing exothermic. Feeding advantage still detectable, however.
67-068-1	Rammed vacuum exothermic, 4" I.D. with 1" wall. Well vented.	Plain 4" I.D.	250°F Superheat	100 mm ARGON	No violent outgassing. Vents relieved pressure on metal. Smoke generated dictated re-pumping before casting second mold. Clear feeding advantage for exothermic riser.
67-068-2	Rammed steel type exothermic, 4" I.D. 1" wall - vented.	Plain 4" I.D.	250°F Superheat	100 mm ARGON	Same as 67-068-1 except a fine powder was released in large volume into the vacuum chamber atmosphere - could be detrimental to pumps. Feeding advantage similar to 068-1. Ignition later than for vacuum exothermic.

TABLE XXXII

CHEMICAL ANALYSES AND FOUNDRY DETAILS FOR INCO 713LC TEST FIXTURE CASTINGS

Heat and Casting Number	Pattern No. & Description	CHEMICAL ANALYSIS (%)															
		C	Cr.	Mn	Si	S	Mo	Ni	CB/TA	Ti	Al	B	Zr	Fe	Cu	Co
67-323-2	C-1522 Wdg Br	.06	12.28	<.05	0.20	.003	4.55	Bal	2.37	0.84	6.07	.013	0.104	0.26	<.01	0.24
67-331-2	C-1522 Wdge Br	.05	12.38	0.07	0.18	.005	4.90	Bal	2.34	0.85	6.32	.014	0.103	0.24	<.01	0.22
67-364	C-1522 Wdge Br	.07	12.38	0.05	0.20	N.D.	4.52	Bal	2.15	0.75	6.32	.014	0.104	0.23	<.02	0.09
67-354-2	C-1521 Yoke	.08	12.65	0.04	0.25	.005	4.40	Bal	2.02	0.73	6.35	.012	0.103	0.55	<.01	0.20
67-354-2	C-1521 Yoke	.08	12.92	<.05	0.24	.005	4.32	Bal	2.00	0.70	5.91	.012	0.101	0.30	<.01	0.03
67-340-2 &3	C-1523 Hexabars	.07	12.80	0.05	0.21	.005	4.47	Bal	2.15	0.74	6.30	.013	0.098	0.35	<.01	0.15

FOUNDRY DATA

Heat and Casting Number	Pouring Temperature	Pressure at Pour	Gross Weight of Casting
67-323-2	200°F Superheat	100mm Argon	510 pounds
67-331-2	200°F Superheat	100mm Argon	505 pounds
67-364-2	200°F Superheat	100mm Argon	500 pounds
67-334-2	300°F Superheat	100mm Argon	500 pounds
67-354-2	200°F Superheat	100mm Argon	500 pounds
67-340-2	300°F Superheat	100mm Argon	160 pounds
67-340-3	300°F Superheat	100mm Argon	160 pounds

-325-

TABLE XXXIII

SUMMARY OF OBJECTIVES AND DISPOSITION OF ALL SPIN-TEST DISC CASTINGS

Heat & Casting No.	Procedure/Purpose/Disposition
66-091-2	Casting scrapped - extremely severe cold shuts all over cope and drag surfaces. Pouring temperature too low at 270°F above the liquidus.
66-097-1	Pouring temperature increased to 300°F above the liquidus and and speed of pouring increased. The surface condition was much improved. X-Ray inspection revealed no internal defects. This casting was destroyed in connection with determination of tensile properties of test bars cut from the casting. The casting first revealed the existence of high residual stresses by bursting during sectioning.
66-110-1	Pouring temperature decreased to liquidus plus 250°F with very high pouring speed. Drag side shows about one and one half to two inches of tiny cold laps near O.D. No internal defects revealed by X-Ray inspection. This casting has been destroyed in connection with determination of residual stresses in the solution treated condition.
66-123-1	The mold for this casting was especially treated in order to study the effect of various methods of applying the cobalt oxide nucleating agent to the mold surface. The casting was poured at 330°F above the liquidus with a fast pour. The surface condition was excellent independent of the mold coating. No internal defects were found by X-Ray inspection. This casting was destroyed in connection with determination of the effect of the various mold coatings and

TABLE XXXIII
(continued)

in connection with the determination of residual stresses in the "as cast" condition.

66-173-1   Casting poured at 330° F above the liquidus. Surface condition is satisfactory, but short pour of riser resulted in questionable integrity of microstructure below riser. This casting is currently being held for possible future destructive testing.

66-198-1   The main intent of this casting was to evaluate a new pouring basin designed to permit better control over pouring rate under the unusual conditions encountered in the vacuum furnace. In addition, the value of a small ring runoff around the O.D. of the disc and connected to the disc by thin gates at 2-inch intervals was determined. The pouring basin was found to be satisfactory and the ring runoff adopted for future discs as it was found to minimize the occurrence of tiny cold shuts at the O.D. This casting was used for thermal studies in connection with residual stress analysis.

66-296-1   Objective: The two pilot discs cast just prior to this one both exhibited dispersed porosity under the riser and in the heavy I.D. of the disc. This and the following casting were made to determine the height of the riser necessary to promote soundness in these areas.

Procedure: Normal molding and casting techniques were used, except that the riser was intentionally limited to about four inches high. The riser cavity was preheated.

Disposition: The casting was quartered and the riser removed. Porosity was found in the same areas as in the two previous castings, both by radiography and after sectioning.

66-314-1   Objective: The same as for 66-296.

TABLE XXXIII
(continued)

Procedure: Except that the riser was filled to the capacity of the cope section, the procedures were the same as for 66-296-1.

Disposition: Radiography indicated that the sections in question were sound. However, hot tearing due to the ring run-off previously described was first found in this casting. Further examination of other castings revealed tearing in the same locations that had not previously been discovered. The casting, having served its purpose, was returned for remelting.

66-317-1

Objective: This casting was to have been shipped to G.E. for testing. however, the discovery of the hot tearing in 66-314 did not precede its molding and casting. Unfortunately, the ring run-off again promoted tearing at the O.D.

Disposition: The casting was returned for remelt.

66-388-1
66-400-1
66-433-1

Objective: To provide three test castings for the General Electric Company.

Procedure: Procedures for manufacture of these castings were based upon the descriptions provided in IR-8-297(III) and modified according to preceding discussions in this section of the current report.

Disposition: Heat treated and prepared for shipment to the General Electric Company for spin testing. Residual stresses controlled by procedures presented in the next section. 66-388-1 cracked during 1200°F stress relief.

66-456-1
66-485-1

Objective: (1) To investigate the source of dye penetrant indications and

(2) To provide (if defect free) a disc for final residual stress analysis.

-328-

TABLE XXXIII
(continued)

Procedure: Each mold was provided with an area in which the cobalt oxide coating contained excess oxide. Other procedures were normal.

Disposition: Both castings exhibited severe dye-penetrant indications in the subject areas, thus proving the relationship between excess CoO and surface defects.

Casting 66-456-1 heat treated per methods to be described in the next section and destroyed for determination of residual stresses.

Objective: To replace cracked disc 66-388-1 and to serve as a spare against contingencies.

Procedure: Procedures were identical to 66-388, 433, and 400 except, cobalt oxide grain refining coating was eliminated, and the molds were cast at a pressure of 100 mm of Argon gas.

Disposition: Both castings were shipped to the machining vendor after full heat treatment by the methods for the reduction of residual stress to acceptable levels. Casting 67-284-2 suffered core shift and was dimensionally off, although acceptable. 67-284-2 is still in storage unmachined.

67-268-2
67-284-2

TABLE XXXIV

ROOM AND ELEVATED TEMPERATURE PROPERTIES OF INCO 713LC
COOLED AT VARIOUS RATES FROM 2150°F SOLUTION TREATING TEMPERATURE

Test Bar No.	Cooling Medium	ROOM TEMPERATURE PROPERTIES				1200°F PROPERTIES					
		Yld. Str. at .2% Offset(psi)	Tensile Strength (psi)	Elong. (%)	Red. in Area(%)	Yld. Str. at .2% Offset(psi)	Tensile Strength (psi)	Elong. (%)	Red. in Area(%)	Rupture* Life (Hours)	Ductility (%El)
66-198-2A	Water	123,600	154,400	16	18.1	-	-	-	-	-	-
66-198-2B	Water	123,840	150,000	15	18.2	-	-	-	-	-	-
66-097-2C	Water	-	-	-	-	104,200	115,600	8	21.0	-	-
66-097-2B	Water	-	-	-	-	-	-	-	-	26.0	2.0
66-198-2C	Oil	121,480	155,200	16	20.3	-	-	-	-	-	-
66-198-2D	Oil	121,920	156,000	16	18.9	-	-	-	-	-	-
66-198-2E	Air	117,840	149,200	15	18.2	-	-	-	-	-	-
66-198-2F	Air	118,800	154,800	14	16.7	-	-	-	-	-	-
66-097-2D	Air	-	-	-	-	106,200	126,800	8	20.3	-	-
66-198-2J	Silocel	115,200	153,600	16	15.3	-	-	-	-	-	-
66-198-2K	Silocel	116,400	155,200	16	18.2	-	-	-	-	-	-
66-097-2H	Silocel	-	-	-	-	104,000	137,000	11	23.8	-	-
66-097-2E	Silocel	-	-	-	-	-	-	-	-	48.3	6.0
66-198-2G	Furnace	100,800	127,200	15	13.1	-	-	-	-	-	-
66-198-2H	Furnace	100,800	127,200	13	11.6	-	-	-	-	-	-

* Stress: 22,000 psi
Temperature: 1800°F

Notes: Bars cooled in Silocel were pulled from furnace and immersed in Silocel immediately.
Furnace cooled bars were air cooled after reaching 500°F in 15 hours.

TABLE XXXV

RESIDUAL STRESSES IN BURST TEST DISC
WITH REDUCED THERMAL GRADIENTS
DURING COOLING FROM 2150°F

Position	Direction	Side	Residual Stress (psi)*
1	Radial	A	-1,330
		B	-850
	Hoop	A	-6,050
		B	-13,150
2	Radial	A	-13,588
		B	+190
	Hoop	A	+9,812
		B	+14,190
3	Radial	A	+19,400
		B	+15,860
	Hoop	A	+44,600
		B	+24,140
4	Radial	A	+4,900
		B	+4,900
	Hoop	A	-63,500
		B	-54,100

\+ Tensile
− Compressive

Table XXXVI

SUMMARY OF RESIDUAL STRESSES IN G.E. SPIN TEST DISCS
(Negative stresses are Compressive)

Position	Direction	Side	66-123-1	66-110-1	66-485-1	66-456-1
1	Radial	A	4,430	-6,080	-1,330	-4,097
		B	22,580	-5,330	- 850	-6,390
	Circumferential	A	20,820	-3,640	-6,050	-2,903
		B	61,220	7,270	-13,150	-9,130
2	Radial	A	34,350	-4,370	-13,588	-4,290
		B	38,550	8,410	190	*
	Circumferential	A	47,250	7,470	9,812	-1,050
		B	50,400	5,950	14,190	*
3	Radial	A	46,400	19,740	19,400	5,090
		B	52,000	24,550	15,860	2,430
	Circumferential	A	12,200	4,060	44,600	350
		B	20,200	-450	24,140	6,110
4	Radial	A	1,500	-12,350	4,900	1,460
		B	21,700	-7,100	4,900	740
	Circumferential	A	-81,700	-15,650	-63,500	-12,340
		B	-66,500	-80,900	-54,100	-13,940

* Gauge broken during cutting

66-123-1   As Cast
66-110-1   2150°F (argon) - 2 hrs - air cooled
66-485-1   2150°F (argon) - 2 hrs - air cooled with ceramic insulator
66-456-1   2150°F (argon) - 2 hrs - cooled in retort (in furnace) to 1200°F - retort spray quenched to room temperature.

TABLE XXXVII

PROPERTIES OF CONTROL TEST BARS CAST WITH BURST TEST DISCS

Specimen and Heat No.	Thermal History	Test Temp. °F	Yield Str. .2% Offset PSI	Tensile Str. PSI	El %	R.A. %
66-091-1A	S.T.	R.T.	115,640	142,800	11.0	16.0
-1B	S.T.	R.T.	120,000	142,800	12.0	20.3
-1F	As Cast	R.T.	110,400	127,200	7.0	17.5
-1G	As Cast	R.-T.	109,680	130,400	11.0	15.3
-1J	ST&Al	1200°F	105,200	129,200	9.0	34.5
66-097-2A	As Cast	R.T.	108,000	130,000	11.0	13.1
-2F	S.T.	R.T.	119,760	146,000	14.0	16.7
66-110-2A	S.T.	R.T.	115,680	143,200	14.0	16.0
-2B	S.T.	R.T.	115,440	142,000	12.0	17.5
-2D*	S.T.	R.T.	130,080	135,600	4.0	5.5
66-173-2A1	S.T.	R.T.	122,400	154,400	11.0	18.2
-2A6	S.T.	R.T.	125,280	159,200	10.0	16.0
66-388-2C	S.T.	R.T.	113,280	143,200	11.0	18.9
-2B	S.T.	R.T.	-	-	-	-
66-400-2C	S.T.	R.T.	110,880	148,000	16.0	18.9
-2B	S.T.	R.T.	-	-	-	-
66-433-2C	S.T.	R.T.	110,400	150,000	16.0	17.5
-2B	S.T.	R.T.	-	-	-	-
66-456-2C	S.T.	R.T.	115,200	152,000	15.0	18.9
-2B	S.T.	R.T.	-	-	-	-
66-485-2C	S.T.	R.T.	110,400	147,600	15.0	19.6
-2B	S.T.	R.T.	-	-	-	-

NOTES:

A1 = 1200°F-48 hr. - air cooled.

*66-110-2D = Residual properties after creep test, 80,000 psi, 1200°F, discontinued after 738 hours with zero creep.

TABLE XXXVIII

ROOM TEMPERATURE
TENSILE PROPERTIES OF TEST BARS CUT FROM
BURST TEST DISC CASTING 66-097-1

Specimen Number	Thermal History	Test Bar Location	Yield Strength at .2% Offset (PSI)	Ultimate Str. (PSI)	Elongation (%)	Red. in Area (%)
A3	AC	Web, near O.D., radial	115,000	131,900	9.0	-
A12	AC	"	112,700	123,300	6.0	-
A6	AC	Web, near I.D., radial	103,920	115,200	8.0	14.5
A13	AC	"	101,760	111,600	8.0	10.8
A9	AC	Hub, radial	100,800	124,800	11.0	18.2
A14	AC	"	101,520	121,600	9.0	13.8
B4	ST	Web, near O.D., radial	117,000	135,600	7.0	-
B5	ST	"	116,000	127,100	4.0	-
B7	ST	Web, near I.D., radial	113,280	130,000	8.0	15.3
B8	ST	"	110,400	134,000	8.0	16.9
B10	ST	Hub, radial	114,960	117,600*	1.0*	5.5*
B11	ST	"	118,080	151,600	13.0	19.6
B16	ST	Hub, Tangential	101,760	116,000	9.0	13.1

Notes: Test bars which list no reduction in area figures are flat tensile specimens.
*Test bar showed defect in cross section believed to be cold shut.
Test speed 0.05"/minute.
AC = As Cast
ST = 2150°F, 2 hrs, air cooled.

Table XXXIX

ROOM TEMPERATURE TENSILE PROPERTIES OF TEST BARS CUT FROM CAST INCO 713LC
SPIN TEST DISCS HEAT TREATED TO CONTROL RESIDUAL STRESS LEVELS

Disc No.	Specimen Location*	Specimen Type	Test Direction	Yield Strength .2% Offset (psi)	Tensile Strength (psi)	Elongation (%)	Reduction in Area (%)
66-485-1	A	Flat	Circum.	117,060	142,800	10.0	--
	B	Flat	Circum.	112,000	128,300	8.0	--
	C	.252 dia.	Circum.	113,280	134,000	9.0	15.3
	D	.252 dia.	Circum.	105,120	122,400	7.0	10.8
	E	.252 dia.	Circum.	106,800	122,800	7.0	13.1
	F	.252 dia.	Circum.	104,880	120,800	7.0	14.5
	G	.252 dia.	Circum.	105,600	120,400	9.0	16.0
	H	.252 dia.	Circum.	110,640	120,000	5.0	13.6
	J	.252 dia.	Circum.	115,200	130,400	8.0	13.1
	K	.252 dia.	Circum.	113,040	123,600	4.0	7.0
	L	.252 dia.	Circum.	106,800	113,200	3.0	10.1
	M	Flat	Radial	113,400	128,000	7.0	--
	Q	.252 dia.	Radial	106,080	120,000	8.0	13.8
	P	.252 dia.	Radial	105,600	114,000	3.0	10.1
66-456-1	A	Flat	Circum.	107,400	130,200	8.0	--
	B	Flat	Circum.	108,900	118,900	2.0**	--
	C	.252 dia.	Circum.	105,600	130,000	6.0**	4.7**
	E	.252 dia.	Circum.	101,520	124,000	8.0	13.8
	G	.252 dia.	Circum.	100,560	116,400	8.0	11.6
	J	.252 dia.	Circum.	101,040	112,800	5.0	10.8
	L	.252 dia.	Circum.	98,880	114,400	8.0	13.8
	M	Flat	Radial	104,100	112,500	3.0	--
	N	Flat	Radial	104,640	119,200	6.0	13.1
	P	.252 dia.	Radial	102,240	111,600	5.0	9.3

NOTES:
66-485-1   Air cooled from 2150°F with ceramic insulator.
66-456-1   Cooled in retort (in furnace) to 1200°F from 2150°F
*See Figure 2   ** Broke out of gauge length.

TABLE XL

RESULTS OF SPIN-TESTS
OF
CAST INCO 713LC DISCS

G.E. Test No.	Abex Disc No.	Max Speed (RPM)	Tangential Stress At Max Speed(PSI)	Estimated Ult. Tang. Stress (PSI)	Percent Of Ult. Tang. Stress	Failure
1	66-400-1	23,800	117,000	121,000	96.7	Burst
2	66-433-1	23,189	111,000	121,000	91.7	No burst**
3	67-268-2*	23,230	111,100	121,000	92.0	No burst**

Note: Normal design criterion for forgings is 70% of ultimate tangential stress.

* Warped 0.080" prior to testing

** Test discontinued: cracks found in bore in 66-433-1, in bore and web in 67-268-2

Thermal History:

2150°F-2 Hrs. - cooled at 12°F/min (Av) to 1200°F - air cool to R.T.
Slow heat to 1200°F - hold 16 hrs. - slow cool to R.T.

TABLE XLI

ANTICIPATED MINIMUM PROPERTY LEVELS FOR A CAST INCO 713LC TURBINE ROTOR DISC*

Property at 1200°F	Anticipated Value
0.2% Yield Strength	90,000 psi
0.02% Yield Strength	75,000 psi
Ultimate Strength	105,000 psi
100 Hour Rupture Life Stress	105,000 psi
Low Cycle Fatigue: Pseudo-Stress for 1000 Cycle Life (1000°F)	198,000 psi
0.2% Creep Stress/100 hours	105,000 psi (400 hours)
Young's Modulus (Approx.)	25×10^6 psi
Density (Physical Property)	0.289 pounds/cu.in.

* Heat treatment is assumed to be 2150°F-2 hr-air cool. An additional
  treatment at 1200°F for 16 hours or more will be beneficial to most
  strength properties with little change in ductility at 1200°F. If
  the 1200°F treatment is not applied, strengthening in service may be
  anticipated if service temperature is 1200°F. Properties are based
  on conservative estimate of heaviest section thickness cast (roughly
  5 inches).

LIST OF REFERENCES

(1) Peterson, A. H., "The Use of Castings in Air Frame Design, " Metal Progress, vol. 62, no. 5, November, 1952.

(2) Papen, G. W., "Castings in Airframe Design", Foundrymen's Society Transactions, vol. 63, 1955.

(3) "Report on Precision Steel Castings for Aircraft Use" Panel on Precision Steel Aircraft Castings of the Materials Advisory Board, National Academy of Sciences, Report No. MAB-106-M, 20 April, 1956.

(4) Simmons, H. E., "Steel Castings for Aircraft Challenge the Foundry Industry", Foundry, vol. 84, no. 7, July, 1956.

(5) Gude, W. G. "Close Control Required to Produce Aircraft and Missile Castings, " Foundry, vol. 85, no. 11, November 1957.

(6) McCreery, L. H., "What the Aircraft Maker Wants in a Steel Casting", Metal Progress, vol. 74, no. 1, July, 1958.

(7) Elizondo, Y. J., "Steel Castings for the Aircraft Industry, " Modern Castings, vol. 35, no. 6, June, 1959.

(8) Langenheim, A. H., "The Foundry Approaches the Space Age", Foundry, vol. 87, October, 1959.

(9) Varga, John Jr., "Review of Certain Ferrous Casting Applications in Aircraft and Missiles, " DMIC Report 120, December 18, 1959.

(10) "Second Progress Report by the Panel on Casting and Powder Metallurgy", Materials Advisory Board, National Academy of Sciences, National Research Council, Report MAB-163-M (1), October, 1960.

(11) "State of the Art on Casting". Third Progress Report by the Panel on Casting and Powder Metallurgy, Materials Advisory Board, National Academy of Sciences National Research Council Report MAB-139-M (C3), June, 1962.

(12) "Recommended Research Programs for Casting", Seventh Progress Report by the Panel on Casting and Powder Metallurgy, Materials Advisory Board, National Academy of Sciences National Research Council Report no. MAB-139-M (C7), September, 1962.

(13) Schuyten, John, "High Integrity Castings for Ordnance Applications", *Metal Progress*, vol. 83, no. 3, March, 1963.

(14) Nereo, G. E., Polich, R. F. and Flemings, M. C., "Unidirectional Solidification of Steel Castings", *Modern Castings*, vol. 47, no. 2 February, 1965.

(15) "Costs Cut in Precision Casting Process", *Materials in Design Engineering*, vol. 54, August, 1961.

(16) Found, George H., "High Precision and Mass Production in the Foundry with Ceramic Mold Process", *Modern Castings*, vol. 46, no. 4, October, 1964.

(17) "Ceramic Shells Solve Problems on Heavy Complex Castings", *Iron Age*, vol. 186, July, 1960.

(18) "The Shaw Process", Copyright 1962, Avnet-Shaw Corp., Div. Avnet Electronics Corp., Plainview, L.I., N.Y.

(19) Wilcox, R.J., and Martini, R. W., "Investment Castings for Advanced Aircraft", *Metal Progress*, vol. 82, no. 3, Sept., 1962.

(20) Stutzman, M. J. and Cunningham, J. W., "The Effects of Melting and Casting Procedures on the Elevated Temperature Properties of Nickel and Cobalt Base Alloys", *Trans. Met. Soc. AIME*, vol. 215, August, 1959.

(21) Damara, F. N., Huntington, J. S. and Machlin, E. S., "Vacuum Induction Melting", *J. Iron and Steel Inst.*, vol. 191, 1959.

(22) Chalmers, B., "Principles of Solidification", John Wiley and Sons, New York, 1964.

(23) Chalmers, B., "Fundamentals of Structure Control by Solidification", Paper presented at AFS T&RI Seminar, Swampscott, Mass., September, 1965.

(24) Wallace, John F., "Grain Refinement of Steels", *Journal of Metals*, May, 1963.

(25) VerSnyder, F. L. and Guard, R. W., "Directional Grain Structures for High Temperature Strength", *Trans. ASM.* vol. 52, 1960.

(26) Pearcy, B.J. and VerSnyder, "A New Development in Gas Turbine Materials-The Properties and Characteristics of PWA 664", Pratt & Whitney Aircraft Report No. 65-007, 21 April, 1965.

(27)   Henzel, J. G., Jr. and Keverian, J., "The Theory and Application of a Digital Computer in Predicting Solidification Patterns", J. Inst. of Metals, May, 1965

(28)   Brockloff, J. E., and Kortovich, C. S., "Research and Development on Mathematical Techniques in Casting", Second Interim Engineering Report, 1 March 1965 - 31 May, 1965, MMP Project Nr. 8-300, Systems Engineering Group, WPAFB.

(29)   Ely, R. J. and Fries, J. E., "High Integrity Steel Castings-Foundry Procedure Development", Trans. AFS, vol. 69, 1961.

(30)   Dunlop, A., "Recent Developments in Precision Casting", British Foundryman, vol. 54, December, 1961.

(31)   Schlinkmann, Paul E., "Investment Casting in Shell Molds", Precision Metal Molding, vol. 17, November, 1959.

(32)   "Ceramic Shell Molding Gets Boost", Steel, vol. 146, May, 1960.

(33)   Dunlop, Adam, "Ceramic Shell Moulds", Metal Industry, vol. 96, April, 1960.

(34)   Rapoport, D. B., "Aerofoil Investment Castings for the Mach 3 Engine", Foundry Trade Journal, vol. 116, no. 2461, Feb., 1964.

(35)   Taylor, L. S., "Investment Casting in Vacuum," Foundry Trade Journal, vol. 109, October, 1960.

(36)   "Vacuum Remelting and Casting", Precision Metal Moulding, vol. 18, May, 1960.

(37)   Rapoport, D., "Recent Developments in Vacuum Melting and Pouring", Foundry, vol. 91, November, 1963.

(38)   Wood, D. R., "Recent Developments in Investment Cast, Nickel-Base, High Temperature Alloys," Foundry Trade J., vol. 115, September, 1963.

(39)   Brown, T. J. And Bulina, J., "A New Higher Temperature Turbine Disc Alloy", High Temperature Materials, John Wiley and Sons, New York, 1959.

(40)   "High Nickel Alloy Developed for Turbine Wheels", Inco Nickel Topics, The International Nickel Co., N.Y., vol. 17, no. 7, 1964.

(41)   Schweikert, W. H., "Properties and Characteristics of a New High-Strength Nickel-Base Alloy", Foundry, December, 1961.

(42)   Decker, R. F., and DeWitt, F. R., "Trends in High Temperature Alloys", Journal of Metals, February 1965.

(43)   Avery, Howard S., Internal reports concerning Project nr. 8-297
       Case XC-1360, The Abex Corporation Research Laboratory,
       Mahwah, New Jersey.

(44)   Alexander, W. O., and Vaughan, N. B., "The Constitution of
       The Nickel-Aluminum System", J. Inst. of Metals, vol. 61, 1937.

(45)   Taylor, A. and Floyd, R. W., "The Constitution of the Nickel-
       Chromium-Aluminum System," J. Inst. of Metals, vol. 81,
       1952-53.

(46)   Floyd, R. A., "The Formation of the Ni_3Al Phase in Nickel-
       Aluminum Alloys", J. Inst. of Metals, vol. 80, 1951-52.

(47)   Wagner, H. J. and Hall, A. M., "Physical Metallurgy of Alloy
       718", SMIC Report 217, June 1, 1965.

(48)   Eiselstein, H. L., "Metallurgy of Columbium Hardened Nickel-
       Chromium-Iron Alloy". Advances in the Technology of Stainless
       Steels and Related Alloys, Special Technical Publication No. 369,
       ASTM, 1965.

(49)   Nordheim, R. and Grant, N. J., "Aging Characteristics of
       Nickel-Chromium Alloys Hardened with Titanium and Aluminum",
       Trans. AIME, vol. 200, 1954.

(50)   Guard, R. W. and Westbrook, J. H., "Alloying Behavior of the
       Ni3Al Phase", Trans. AIME, vol. 1959.

(51)   Silverman, R., and Arbiter, W., and Hodi, F., "Effect of
       Sigma Phase on Co-Cr-Mo Base Alloys", Trans. ASM, vo. 49, 1957.

(52)   Hansen, M. "Constitution of Binary Alloys", McGraw-Hill, N.Y. 1958.

(53)   Wlodek, S. T., "The Structure of IN-100", Trans. ASM, vol. 57, 1964.

(54)   Davis, Sidney O. "Elevated Temperature Tensile and Creep Pro-
       perties of M-252 (Bar), Inconel 700 (Bar), and Inconel 713C
       (Cast)", Tech. Doc. Report No. ML TDR 64-79, AFML, Res. &
       Tech. Div., Air Force Systems Command, WPAFB, July, 1964.

(55)   "Alloy 713LC, Low Carbon Alloy 713LC, Preliminary Data", The
       International Nickel Company, N. Y., July, 1964.

(56)   Wagner, H. J. and Hall, A. M. "Physical Metallurgy of Alloy
       718", DMIC Report 217, June 1, 1965.

(57)   Henning, H. J. and Boulger, F. W., "Superalloy Forgings",
       DMIC Memorandum 86, February 10, 1961.

(58)   General Electric Co., Specification GEC50T53-S7

(59)   "Fracture Toughness Testing and Its Applications", ASTM Special
         Technical Publication No. 381, 1965.

(60)   Fellows, J. A., Cook, Ernshaw, Avery, H. S., "Precision in
         Creep Testing", Trans. AIME, vol. 150, 1942.

(61)   Glover, W. J., "The Effects of a Slow Cool from Solution Treating
         Temperature on the Tensile and Rupture Properties of Cast Rene 41",
         G. E. Co. Materials Information Memorandum, Report No. DM65-416,
         19 Oct. 1965.

(62)   General Electric Co., Specification GEC 50T53-S7

(63)   C. T. Sims: "A Contemporary View of Nickel Base Superalloys",
         Jl. of Metals, Oct. 1966, P. 1119.

(64)   H. J. Wagner and A. M. Hall: "The Physical Metallurgy of Alloy
         718" DMIC Report 217, June 1, 1965, Battelle Memorial Institute.

(65)   C. H. Lund and H. J. Wagner: "Identification of Microconstituents
         in Superalloys", DMIC Memorandum 160, Nov. 1962, Battelle
         Memorial Institute.

(66)   R. A. Gregg and B. J. Piearcy: "Solute Distribution and Eutectic
         Formation in As-Cast Nickel Base Superalloys", Trans. Met.
         Soc. AIME 1964, V230 P. 559.

(67)   H. L. Eiselstein: "Metallurgy of a Columbium-Hardened Nickel-
         Chrome-Iron Alloy", Advances in the Technology of Stainless
         Steels, ASTM, STP No. 369, 1964, P. 62.

(68)   M. Kaufman: "Control of Phases and Mechanical Properties
         in Nickel-Base Alloys of the Rene 41 Type", Trans. Met. Soc
         AIME 1963, V227 P. 405.

(69)   "High Temperature High Strength Nickel Base Alloys", The
         International Nickel Co., Inc., N. Y. C., N. J.

(70)   Schwiekert, Wilber H., "Controlled Grain Size Casting Method",
         U. S. Patent No. 3,158,912, Dec. 1, 1964.

(71)   Larson, H. R., Campbell, R. C., Lloyd, H. W., "Development
         of Low Alloy Steel Compositions Suitable for High Strength Steel
         Castings:, WADCTR 59-63, I & II.

(72)   Schaefer, R. H. and Mott, W. S., "The Fluidity of Cast Alloyed
        Steels and Irons," Report No. 4-M-96, HRC Project 61-A, July, 1945.

(73)   Ollif, I. D., Lumby, R. J. and Kondic, V. "Effect of Casting
        Conditions and Melting Atmosphere on the Fluidity of Air and Vacuum
        Melted Alloys", Foundry Trade J. v. 119, No. 2548, October 7, 1965
        pp. 469-475.

(74)   Hetenyi, M., "Handbook of Experimental Stress Analysis",
        John Wiley & Sons, N. Y. 1950.

(75)   Private Communication, W. Schweikert, General Electric Co.

(76)   Ver Snyder, Fl., et. al., "Directional Solidification in the Precision
        Castings of Gas-Turbine Parts", Modern Castings, vol. 52, no. 6
        December, 1967.

(77)   Piearcey, B. J., et. al., "Correlation of Structure with Properties
        in a Directionally Solidified Nickel-Base Superalloy", Trans. ASM
        vol. 60, no. 4, December, 1967.

APPENDIX I - LETTER OF INQUIRY

The Research Center of the Abex Corporation has recently been awarded an Air Force contract (Contract No. AF 33 (615)-2797) entitled "Manufacturing Process Development for Superalloy Cast Parts". It is the objective of this program "......to develop a manufacturing process for the precision casting of superalloys in larger, more complex configuration with improved strength and corrosion resistance in the temperature range of 1200°F to 2000°F." The alloys Inco 718, Inco 713C(LC), and Rene 41 have been designated by the Air Force for investigation. As subcontractors, the General Electric Company and LTV Vought Aeronautics Division will supply consultation, component designs and extensive reliability testing of the cast components.

As part of this contract, we have been requested by the Air Force to conduct a comprehensive investigation of the aerospace industries, particularly propulsion, airframe and related sub-system manufacturers, relative to their present and possible future utilization of large superalloy castings. In the sense used here, "large" infers castings which are normally beyond the capabilities of current vacuum casting techniques utilizing the lost-wax investment, ceramic shell, etc. processes. It is anticipated that the foundry shipping weight of the proposed castings would approximate 100 lbs. or larger. Airframe components subjected to elevated temperatures and large engine turbine components are two examples of the end products anticipated by this program.

In connection with this investigation, it is our intention to contact a reasonably large number of organizations such as yours in order to obtain a significant cross section of opinion regarding the possible application of large superalloy castings in existing and future designs. The attached questionnaire summarizes the information we need to present a complete picture to the Air Force. It would be greatly appreciated if you would supply us with your answers to these questions as well as any additional comments which may appear pertinent to your particular requirements. If you should feel that the subject matter requires a more thorough treatment than is possible in a written reply, we would be most pleased to visit with you to further discuss the potential and limitations of large superalloy castings in your designs. To keep our records straight, however, we would still appreciate a brief written reply to the enclosed questionnaire, along with notification that you would like to discuss the matter in more detail.

We are also anxious to be advised if there is any other section or division of your organization where there may be application for the subject castings. While we have attempted to contact the majority of manufacturers where application is most likely, it is quite possible that there are areas we have missed.

We will be looking forward to hearing from you and, if it appears appropriate, seeing you to discuss this matter further.

Very truly yours,

R. J. Ely
Manager, Contract R&D

B. A. Heyer
Project Engineer

APPENDIX II - QUESTIONNAIRE

ABEX CORPORATION
RESEARCH CENTER
QUESTIONNAIRE FOR SUPERALLOY CASTING PROGRAM

1. Do you now utilize superalloy castings?
   a. Up to what size?
   b. What alloys?
   c. In what applications?

2. Do you now utilize superalloy forgings?
   a. Up to what size?
   b. What alloys?
   c. In what applications?

3. Can you envision applications for reliable superalloy castings in the weight range of 100 lbs. or higher?
   a. In what applications?
   b. At what service temperatures?
   c. In what environment?

4. If an industrial capability for manufacturing large (100 lb. and larger) superalloy castings was developed, would you envision an improved flexibility in high temperature service design?
   a. Would you consider redesigning existing superalloy forgings to any advantage?
   b. Assuming that reliability consistent with existing requirements could be documented, would you consider large superalloy castins for future designs?

5. Please comment on your opinion of the future of large superalloy castings, assuming that a reliable industrial supply would become available in the future.

APPENDIX III

Industrial Survey Distribution List

Aerojet-General Corporation
Metallurgical Engineering
Department 1184

Aerojet-General Nucleonics

Air Research Manufacturing Co.
Materials & Process Engr. 93-18

Avco Corporation
Lycoming Division

Bell Aerosystems Company
Advanced Manufacturing Engineering

Bell Helicopter Company
Production Engineering

The Boeing Company
Aerospace Division

The Boeing Company
Airplane Division

The Boeing Company
Airplane Division-Wichita Branch

Continental Aviation & Engineering Corp.
Research and Advanced Development

Douglas Aircraft Company
Incorporated Aircraft Division

Douglas Aircraft Company
Incorporated Missile & Space

General Dynamics/Astronautics

General Dynamics/Convair
Manufacturing R&D

General Dynamics/Fort Worth
Applied Mfg. Research & Process Dev.

Grumman Aircraft Eng.,Co.

Hiller Aircraft Company
Engineering Division

Hughes Aircraft Company

Lear Siegler Incorporated

Ling-Temco-Vought Incorporated
Vought Aeronautics Division

Lockheed-Georgia Company

Lockheed Missiles & Space Co.

McDonnell Aircraft Corporation

North American Aviation, Inc.
Producibility Metals

North American Aviation, Inc.
Los Angeles Division

Pratt & Whitney Aircraft Div.
United Aircraft Corporation

Republic Aviation Corporation

Rocketdyne Division
North American Aviation, Inc.

Rohr Aircraft Company

Ryan Aeronautical Company

Sikorsky Aircraft Division
United Aircarft Corporation

TRW Industries

Union Carbide Corporation
Stellite Division

General Dynamics/Pomona
Manufacturing Engineering

General Electric Company
Re-Entry Systems Department

North American Aviation, Inc.
Columbus Division

The Marquardt Corporation

Martin-Marietta Corporation
Orlando Division

Curtiss-Wright Corporation
Wright Aeronautical Division

United Technology Center

Allison Division
General Motors Corporation

Hamilton Standard Division
United Aircraft Corporation

Martin-Marietta Corporation
Denver Division

Lockheed California Company

Beech Aircraft Corporation

DOCUMENT CONTROL DATA - R & D

(Security classification of title, body of abstract and indexing annotation must be entered when the overall report is classified)

1. ORIGINATING ACTIVITY (Corporate author)	2a. REPORT SECURITY CLASSIFICATION
Abex Corporation	Unclassified
Research Center	2b. GROUP
Mahwah, New Jersey 07430	N/A

3. REPORT TITLE

Manufacturing Process For Superalloy Cast Parts
Volume I

4. DESCRIPTIVE NOTES *(Type of report and inclusive dates)*
Final Technical Report, 1 July 1965 through 31 December 1970

5. AUTHOR(S) *(First name, middle initial, last name)*

Heyer, Bruce A.

6. REPORT DATE	7a. TOTAL NO. OF PAGES	7b. NO. OF REFS
15 February 1971	358	77

8a. CONTRACT OR GRANT NO.	9a. ORIGINATOR'S REPORT NUMBER(S)
AF 33(615)-2797	XC-1360-9I
b. PROJECT NO.	
8-297	
c.	9b. OTHER REPORT NO(S) *(Any other numbers that may be assigned this report)*
d.	AFML-TR-71-38 Vol I

10. DISTRIBUTION STATEMENT This document is subject to special export controls and each transmittal to foreign Governments or foreign nationals may be made only with prior approval of the Manufacturing Technology Division (LT), Air Force Materials Laboratory, Wright-Patterson AFB, Ohio 45433.

11. SUPPLEMENTARY NOTES	12. SPONSORING MILITARY ACTIVITY
	Air Force Materials Laboratory
	Air Force Systems Command
	Wright-Patterson AFB, Ohio 45433

13. ABSTRACT

This is Volume I of the final technical engineering report covering Phase I of a two-phase program designed to establish procedures for the manufacture of large, high-integrity, superalloy castings with shipping weights near 100 pounds. Specifically, a main fin beam structural component and a hollow, air-cooled turbine rotor disc were produced during Phase II with Phase I serving as the source of fundamental data required for their manufacture. A literature survey covering the field of high-integrity and superalloy castings is presented, and a survey of the current and future needs of the aerospace industry. Based on foundry characteristics and the mechanical properties and microstructure of separately cast specimens and specimens cut from cast components with section thickness up to 5 inches, Inco 713LC alloy was selected from among Inco 713LC, Inco 718, and Rene 41 alloys for subscale spin testing and for the Phase II components. The methods of manufacturing a series of spin-test discs for evaluation of the alloy and process for the turbine rotor application are presented, together with the procedures adopted for overcoming a serious problem of residual stresses in the cast and heat-treated disc. The testing of the spin-test discs has established that the cast rotor can be designed using the same burst criterion as is currently used for forged discs. The mechanical property minimums to which the air-cooled turbine rotor disc was designed in Phase II are presented.

14. KEY WORDS	LINK A		LINK B		LINK C	
	ROLE	WT	ROLE	WT	ROLE	WT
Superalloy Casting Inco 713LC Alloy Inco 718 Alloy Rene 41 Alloy Subscale Turbine Disc Casting Ceramic Mold Vacuum Casting Exothermic Risers						